

**ANALYSIS OF A BIRD STRIKE ON THE EXTERNAL  
FUEL TANK OF A JET TRAINER AIRCRAFT**

**BİR JET EĞİTİM UÇAĞININ HARİCİ YAKIT  
TANKINA KUŞ ÇARPMASI ANALİZİ**

**ÖZLEM İŞIKDOĞAN**

**PROF. DR. BORA YILDIRIM**

**Tez Danışmanı**

Submitted to  
Graduate School of Science and Engineering of Hacettepe University as  
a Partial Fulfillment to the Requirements  
for the Award of the Degree of Master of Science in  
Mechanical Engineering

2022



# **ABSTRACT**

## **ANALYSIS OF A BIRD STRIKE ON THE EXTERNAL FUEL TANK OF A JET TRAINER AIRCRAFT**

**Özlem IŞIKDOĞAN**

**Master of Science, Department of Mechanical Engineering**

**Supervisor: Prof. Dr. Bora YILDIRIM**

**May 2022, 213 pages**

Bird strike is defined as a collision between a bird and an air vehicle during flight, take-off of landing. According to statistics, a bird strike occurs once every 2000 flights. [1]

A collision with a bird during flight can cause serious damage on aircraft. All forward facing components shall be taken into account i.e. the engine fan blades, inlet, windshield, canopy, radome, forward fuselage skin and the leading edges of wing and empennage. The Aviation authorities require that the bird strike resistance of these components should be proved by certification tests.

The aviation authorities regulations for forward facing components are mainly listed below.

- For windshield and canopy, 4 lb bird impact resistance is required at cruise speed without penetration.
- For wing leading edges, 4 lb bird impact resistance is required at operational speed.
- For empennage leading edges, 8 lb bird impact resistance is required at operational speed.
- For engine and inlet, 4 lb bird impact resistance is required.

The aim of this study is to analyze the effect of bird strike on an external fuel tank of a jet trainer aircraft and contribute an example study to the literature of our country. After theoretical method was mentioned, information was given about numerical methods and compared with each other. After that, a geometry, dimensions and density of bird was defined and analyses were done using cylindrical with hemispherical ends bird geometry using SPH method according to speed and mass given in literature.

The bird strike analysis performed for an external fuel tank of a jet-trainer aircraft. Fuel carrying capacity of the external fuel tank is 1000lb. The cross-section is elliptical. The analysis was carried out using two materials which are Aluminium 2024-T3 and Aluminium 7075-T6. The numerical analysis was carried-out using LS-DYNA program to analyse a 4 lb bird strike. The geometrical model of the impactor is 4lb and the density is  $950\text{kg/m}^3$ . For numerical simulation, the structure was modelled as a shell element by using hypermesh software and the bird was be modelled using SPH method. Using numerical analysis, the stress and displacement distributions, maximum stress and displacement were calculated. As a result, the robustness of the external fuel tank under bird strike was verified.

**Keywords:** Bird, Strike, Bird Strike, External Fuel Tank, Jet Trainer Aircraft, Lagrange, ALE, SPH

# ÖZET

## BİR JET EĞİTİM UÇAĞININ HARİCİ YAKIT TANKINA KUŞ ÇARPMASI ANALİZİ

Özlem IŞIKDOĞAN

Yüksek Lisans, Makina Mühendisliği Bölümü

Tez Danışmanı: Prof. Dr. Bora YILDIRIM

Mayıs 2022, 213 sayfa

Kuş çarpması, kuş ve hava aracının uçuş, kalkış veya iniş sırasında çarpışması olayıdır. İstatistiklere göre, kuş çarpması her 2000 uçuşta bir gerçekleşmektedir.

Uçuş sırasında gerçekleşen kuş çarpması, uçak üzerinde ciddi hasara yol açabilir. Motor fan pervaneleri, hava alığı, ön cam, kanopi, radom, ön gövde kabuğu, kanat hücum kenarı ve kuyruk hücum kenarı gibi öne bakan komponentler dikkate alınmaktadır. Havacılık otoriteleri, bu komponentlerin kuş çarpması dayanıklılığının sertifikasyon testleriyle doğrulanmasını şart koşturmaktadır.

Ön kısma bakan komponentler için havacılık otoriteleri kuralları aşağıda listelenmiştir:

- Ön cam ve kanopi için, seyir hızındayken, penetrasyon olmayacak şekilde, 4lb kuş çarpması dayanıklılığı gerekmektedir
- Kanat hücum kenarı için, operasyonel hızdayken, 4lb kuş çarpması dayanıklılığı gerekmektedir
- Kuyruk hücum kenarı için, operasyonel hızdayken, 8lb kuş çarpması dayanıklılığı gerekmektedir
- Motor ve hava alığı için, 4lb kuş çarpması dayanıklılığı gerekmektedir

Bu çalışmanın amacı, kuş çarpmasının bir jet Eğitim uçağının harici yakıt tankına olan etkisini analiz etmek ve ülkemiz literatürüne katkı sağlamaktır. Teorik metodlara değinilmesini takiben, numerik metodlar ile ilgili bilgi verilmiş ve metodların karşılaştırması yapılmıştır. Daha sonra, kuşun geometrisi, boyutları ve yoğunluğu tanımlanmış ve kuş çarpması analizi, SPH metodu ile, iki ucu küre olan silindirik model kullanılarak, literatürde tanımlanmış olan hız ve kütleyle uygun olarak yapılmıştır.

Kuş çarpması analizi, bir jet eğitim uçağına ait harici yakıt tankı için gerçekleştirilmiştir. Harici yakıt tankının yakıt taşıma kapasitesi 1000lb'dir. Tankın enine kesiti eliptiktir. Analizler, Alüminyum 2024-T3 ve Alüminyum 7075-T6 olmak üzere, iki farklı malzeme kullanılarak gerçekleştirilmiştir. Numerik analizler, 4lb kuş çarpması için, LS\_DYNA programı kullanılarak gerçekleştirilmiştir. Çarpma tertibatının geometric modeli 4lb ve yoğunluğu  $950\text{kg/m}^3$ tür. Numerik simulasyon için; yapı, hypermesh kullanılarak kabuk element şeklinde; kuş ise SPH metodu kullanılarak modellenmiştir.

Numerik analizler kullanılarak, maksimum gerilme ve yer değiştirme hesaplanmıştır. Sonuç olarak, harici yakıt tankının kuş çarpması dayanıklılığı doğrulanmıştır.

**Anahtar Kelimeler:** Kuş, Çarpma, Kuş Çarpması, Harici Yakıt Tankı, Jet Eğitim Uçağı, Lagrange, ALE, SPH

## **ACKNOWLEDGEMENTS**

First of all, I would like to thank my respectable supervisor Prof. Dr. Bora YILDIRIM for his invaluable guidance and support. I completed this study with the help of him.

I want to thank my colleagues Evren Sakarya and Latif Aykut Sümer for their technical support.

Finally, I want to thank my husband and my daughters for their endless love and patience.

Özlem Işıkdoğan

May 2022, Ankara

# TABLE OF CONTENTS

ABSTRACT .....	i
ÖZET.....	iii
ACKNOWLEDGEMENTS .....	v
LIST OF FIGURES.....	viii
LIST OF TABLES .....	xiii
LIST OF SYMBOLS AND ABBREVIATIONS .....	xiv
1 INTRODUCTION .....	15
2 METHODS .....	16
2.1 Theoretical Method.....	16
2.2 Numerical Method .....	17
2.3 Lagrangian Method.....	18
2.4 Eulerian Method .....	18
2.5 Arbitrary Lagrangian – Eulerian Method .....	19
2.6 Smoothed Particle Hydrodynamics .....	19
2.7 Comparison of Methods.....	20
3 NUMERICAL MODELLING OF AN EXTERNAL FUEL TANK .....	21
3.1 Finite Element Modelling of the External Fuel Tank.....	21
4 MATERIAL MODELS .....	24
4.1 Johnson Cook Material Model.....	24
4.2 Piecewise Linear Plasticity Material Model .....	28
5 Bird Models .....	29
5.1 Smoothed Particle Hydrodynamics Bird Model.....	29
6 Energy Ratio.....	30
7 Analysis Results .....	32
8 CONCLUSION .....	201
9 REFERENCES .....	204
10 APPENDIX .....	205



11 CURRICULUM VITAE ..... **Error! Bookmark not defined.**

## LIST OF FIGURES

Figure 1 Soft Body Impact Phases [3].....	16
Figure 2 Typical Pressure Curve for a Soft Body Impact on a Rigid Target Plate[3].....	17
Figure 3 Underformed and Deformed Element in Lagrangian Method .....	18
Figure 4 Underformed and Deformed Element in Eulerian Method.....	18
Figure 5 Undeformed and Deformed Element in ALE Method .....	19
Figure 6 Undeformed and Deformed Element in SPH Method[3].....	19
Figure 7 CAD Model of EFT.....	21
Figure 8 CAD Model of EFT Figure 8 FEM Model of EFT .....	22
Figure 9 Boundaries of the External Fuel Tank.....	22
Figure 10 Rotation and Translation Layout of Boundaries .....	23
Figure 11 Stress Flow for AL 2024 T3.....	27
Figure 12 Stress Flow for AL 7075 T6.....	27
Figure 13 Geometrical Models of Bird.....	29
Figure 14 SPH Dimensions and Model of Soft Body Impactor .....	30
Figure 15 Impactor Positions.....	34
Figure 16 Displacement Results (mm) at 0.5 ms for Impactor Position 1. ....	36
Figure 17 Displacement Results (mm) at 1.0 ms for Impactor Position 1 .....	37
Figure 18 Displacement Results (mm) at 1.5 ms for Impactor Position 1 .....	38
Figure 19 Displacement Results (mm) at 2.0 ms for Impactor Position 1 .....	39
Figure 20 Displacement Results (mm) at 2.5 ms for Impactor Position 1 .....	40
Figure 21 Displacement Results (mm) at 3.0 ms for Impactor Position 1 .....	41
Figure 22 Displacement Results (mm) at 3.5 ms for Impactor Position 1 .....	42
Figure 23 Displacement Results (mm) at 4.0 ms for Impactor Position 1 .....	43
Figure 24 Displacement Results (mm) at 4.5 ms for Impactor Position 1 .....	44
Figure 25 Displacement Results (mm) at 5.0 ms for Impactor Position 1 .....	45
Figure 26 Von Mises Stress Results (MPa) at 0.5 ms for Impactor Position 1.....	46
Figure 27 Von Mises Stress Results (MPa) at 1.0 ms for Impactor Position 1.....	47
Figure 28 Von Mises Stress Results (MPa) at 1.5 ms for Impactor Position 1.....	48
Figure 29 Von Mises Stress Results (MPa) at 2.0 ms for Impactor Position 1.....	49
Figure 30 Von Mises Stress Results (MPa) at 2.5 ms for Impactor Position 1.....	50
Figure 31 Von Mises Stress Results (MPa) at 3.0 ms for Impactor Position 1.....	51
Figure 32 Von Mises Stress Results (MPa) at 3.5 ms for Impactor Position 1.....	52
Figure 33 Von Mises Stress Results (MPa) at 4.0 ms for Impactor Position 1.....	53
Figure 34 Von Mises Stress Results (MPa) at 4.5 ms for Impactor Position 1.....	54
Figure 35 Von Mises Stress Results (MPa) at 3.0 ms for Impactor Position 1.....	55
Figure 36 Energy Variation of Position 1 .....	57
Figure 37 Energy Ratio of Position 1 .....	58
Figure 38 Hourglass, Damping and Sliding Energies Variation of Case 1 .....	59
Figure 39 Bird Impact at 4 ms for Case 1.....	59
Figure 40 Hourglass, Damping and Sliding Energies Variation of Case 2 .....	60
Figure 41 Bird Impact at 4 ms for Case 2.....	60
Figure 42 Hourglass, Damping and Sliding Energies Variation of Case 3 .....	61
Figure 43 Bird Impact at 4 ms for Case 3.....	61
Figure 44 Hourglass, Damping and Sliding Energies Variation of Case 4 .....	62
Figure 45 Bird Impact at 4 ms for Case 4.....	62
Figure 46 Displacement Results (mm) at 0.5 ms for Impactor Position 2 .....	63
Figure 47 Displacement Results (mm) at 1.0 ms for Impactor Position 2 .....	64
Figure 48 Displacement Results (mm) at 1.5 ms for Impactor Position 2 .....	65

Figure 49 Displacement Results (mm) at 2.0 ms for Impactor Position 2 .....	66
Figure 50 Displacement Results (mm) at 2.5 ms for Impactor Position 2 .....	67
Figure 51 Displacement Results (mm) at 3.0 ms for Impactor Position 2 .....	68
Figure 52 Displacement Results (mm) at 3.5 ms for Impactor Position 2 .....	69
Figure 53 Displacement Results (mm) at 4.0 ms for Impactor Position 2 .....	70
Figure 54 Displacement Results (mm) at 4.5 ms for Impactor Position 2 .....	71
Figure 55 Displacement Results (mm) at 5.0 ms for Impactor Position 2 .....	72
Figure 56 Von Mises Stress Results (MPa) at 0.5 ms for Impactor Position 2.....	73
Figure 57 Von Mises Stress Results (MPa) at 1.0 ms for Impactor Position 2.....	74
Figure 58 Von Mises Stress Results (MPa) at 1.5 ms for Impactor Position 2.....	75
Figure 59 Von Mises Stress Results (MPa) at 2.0 ms for Impactor Position 2.....	76
Figure 60 Von Mises Stress Results (MPa) at 2.5 ms for Impactor Position 2.....	77
Figure 61 Von Mises Stress Results (MPa) at 3.0 ms for Impactor Position 2.....	78
Figure 62 Von Mises Stress Results (MPa) at 3.5 ms for Impactor Position 2.....	79
Figure 63 Von Mises Stress Results (MPa) at 4.0 ms for Impactor Position 2.....	80
Figure 64 Von Mises Stress Results (MPa) at 4.5 ms for Impactor Position 2.....	81
Figure 65 Von Mises Stress Results (MPa) at 5.0 ms for Impactor Position 2.....	82
Figure 66 Energy Variation of Position 2.....	84
Figure 67 Energy Ratio of Position 2 .....	85
Figure 68 Hourglass, Damping and Sliding Energies Variation of Case 5 .....	86
Figure 69 Bird Impact at 4 ms for Case 5.....	86
Figure 70 Hourglass, Damping and Sliding Energies Variation of Case 6 .....	87
Figure 71 Bird Impact at 4 ms for Case 6.....	87
Figure 72 Hourglass, Damping and Sliding Energies Variation of Case 7 .....	88
Figure 73 Bird Impact at 4 ms for Case 7.....	88
Figure 74 Hourglass, Damping and Sliding Energies Variation of Case 8 .....	89
Figure 75 Bird Impact at 4 ms for Case 8.....	89
Figure 76 Displacement Results (mm) at 0.5 ms for Impactor Position 3 .....	90
Figure 77 Displacement Results (mm) at 1.0 ms for Impactor Position 3 .....	91
Figure 78 Displacement Results (mm) at 1.5 ms for Impactor Position 3 .....	92
Figure 79 Displacement Results (mm) at 2.0 ms for Impactor Position 3 .....	93
Figure 80 Displacement Results (mm) at 2.5 ms for Impactor Position 3 .....	94
Figure 81 Displacement Results (mm) at 3.0 ms for Impactor Position 3 .....	95
Figure 82 Displacement Results (mm) at 3.5 ms for Impactor Position 3 .....	96
Figure 83 Displacement Results (mm) at 4.0 ms for Impactor Position 3 .....	97
Figure 84 Displacement Results (mm) at 4.5 ms for Impactor Position 3 .....	98
Figure 85 Displacement Results (mm) at 5.0 ms for Impactor Position 3 .....	99
Figure 86 Von Mises Stress Results (MPa) at 0.5 ms for Impactor Position 3.....	100
Figure 87 Von Mises Stress Results (MPa) at 1.0 ms for Impactor Position 3.....	101
Figure 88 Von Mises Stress Results (MPa) at 1.5 ms for Impactor Position 3.....	102
Figure 89 Von Mises Stress Results (MPa) at 2.0 ms for Impactor Position 3.....	103
Figure 90 Von Mises Stress Results (MPa) at 2.5 ms for Impactor Position 3.....	104
Figure 91 Von Mises Stress Results (MPa) at 3.0 ms for Impactor Position 3.....	105
Figure 92 Von Mises Stress Results (MPa) at 3.5 ms for Impactor Position 3.....	106
Figure 93 Von Mises Stress Results (MPa) at 4.0 ms for Impactor Position 3.....	107
Figure 94 Von Mises Stress Results (MPa) at 4.5 ms for Impactor Position 3.....	108
Figure 95 Von Mises Stress Results (MPa) at 5.0 ms for Impactor Position 3.....	109
Figure 96 Energy Variation of Position 3.....	111
Figure 97 Energy Ratio of Position 3 .....	113

Figure 98 Hourglass, Damping and Sliding Energies Variation of Case 9 .....	114
Figure 99 Bird Impact at 4 ms for Case 9.....	114
Figure 100 Hourglass, Damping and Sliding Energies Variation of Case 10 .....	115
Figure 101 Bird Impact at 4 ms for Case 10.....	115
Figure 102 Hourglass, Damping and Sliding Energies Variation of Case 11 .....	116
Figure 103 Bird Impact at 4 ms for Case 11.....	116
Figure 104 Hourglass, Damping and Sliding Energies Variation of Case 12 .....	117
Figure 105 Bird Impact at 4 ms for Case 12.....	117
Figure 106 Displacement Results (mm) at 0.5 ms for Impactor Position 4 .....	118
Figure 107 Displacement Results (mm) at 1.0 ms for Impactor Position 4 .....	119
Figure 108 Displacement Results (mm) at 1.5 ms for Impactor Position 4 .....	120
Figure 109 Displacement Results (mm) at 2.0 ms for Impactor Position 4 .....	121
Figure 110 Displacement Results (mm) at 2.5 ms for Impactor Position 4 .....	122
Figure 111 Displacement Results (mm) at 3.0 ms for Impactor Position 4 .....	123
Figure 112 Displacement Results (mm) at 3.5 ms for Impactor Position 4 .....	124
Figure 113 Displacement Results (mm) at 4.0 ms for Impactor Position 4 .....	125
Figure 114 Displacement Results (mm) at 4.5 ms for Impactor Position 4 .....	126
Figure 115 Displacement Results (mm) at 5.0 ms for Impactor Position 4 .....	127
Figure 116 Von Mises Stress Results (MPa) at 0.5 ms for Impactor Position 4.....	128
Figure 117 Von Mises Stress Results (MPa) at 1.0 ms for Impactor Position 4.....	129
Figure 118 Von Mises Stress Results (MPa) at 1.5 ms for Impactor Position 4.....	130
Figure 119 Von Mises Stress Results (MPa) at 2.0 ms for Impactor Position 4.....	131
Figure 120 Von Mises Stress Results (MPa) at 2.5 ms for Impactor Position 4.....	132
Figure 121 Von Mises Stress Results (MPa) at 3.0 ms for Impactor Position 4.....	133
Figure 122 Von Mises Stress Results (MPa) at 3.5 ms for Impactor Position 4.....	134
Figure 123 Von Mises Stress Results (MPa) at 4.0 ms for Impactor Position 4.....	135
Figure 124 Von Mises Stress Results (MPa) at 4.5 ms for Impactor Position 4.....	136
Figure 125 Von Mises Stress Results (MPa) at 5.0 ms for Impactor Position 4.....	137
Figure 126 Energy Variation of Position 4.....	139
Figure 127 Energy Ratio of Position 4 .....	140
Figure 128 Hourglass, Damping and Sliding Energies Variation of Case 13 .....	141
Figure 129 Bird Impact at 4 ms for Case 13.....	141
Figure 130 Hourglass, Damping and Sliding Energies Variation of Case 14 .....	142
Figure 131 Bird Impact at 4 ms for Case 14.....	142
Figure 132 Hourglass, Damping and Sliding Energies Variation of Case 15 .....	143
Figure 133 Bird Impact at 4 ms for Case 15.....	143
Figure 134 Hourglass, Damping and Sliding Energies Variation of Case 16 .....	144
Figure 135 Bird Impact at 4 ms for Case 16.....	144
Figure 136 Displacement Results (mm) at 0.5 ms for Impactor Position 5 .....	145
Figure 137 Displacement Results (mm) at 1.0 ms for Impactor Position 5 .....	146
Figure 138 Displacement Results (mm) at 1.5 ms for Impactor Position 5 .....	147
Figure 139 Displacement Results (mm) at 2.0 ms for Impactor Position 5 .....	148
Figure 140 Displacement Results (mm) at 2.5 ms for Impactor Position 5 .....	149
Figure 141 Displacement Results (mm) at 3.0 ms for Impactor Position 5 .....	150
Figure 142 Displacement Results (mm) at 3.5 ms for Impactor Position 5 .....	151
Figure 143 Displacement Results (mm) at 4.0 ms for Impactor Position 5 .....	152
Figure 144 Displacement Results (mm) at 4.5 ms for Impactor Position 5 .....	153
Figure 145 Displacement Results (mm) at 5.0 ms for Impactor Position 5 .....	154
Figure 146 Von Mises Stress Results (MPa) at 0.5 ms for Impactor Position 5.....	156

Figure 147 Von Misses Stress Results (MPa) at 1.0 ms for Impactor Position 5.....	157
Figure 148 Von Misses Stress Results (MPa) at 1.5 ms for Impactor Position 5.....	158
Figure 149 Von Misses Stress Results (MPa) at 2.0 ms for Impactor Position 5.....	159
Figure 150 Von Misses Stress Results (MPa) at 2.5 ms for Impactor Position 5.....	160
Figure 151 Von Misses Stress Results (MPa) at 3.0 ms for Impactor Position 5.....	161
Figure 152 Von Misses Stress Results (MPa) at 3.5 ms for Impactor Position 5.....	162
Figure 153 Von Misses Stress Results (MPa) at 4.0 ms for Impactor Position 5.....	163
Figure 154 Von Misses Stress Results (MPa) at 4.5 ms for Impactor Position 5.....	164
Figure 155 Von Misses Stress Results (MPa) at 5.0 ms for Impactor Position 5.....	165
Figure 156 Energy Variation of Position 5.....	167
Figure 157 Energy Ratio of Position 5 .....	168
Figure 158 Hourglass, Damping and Sliding Energies Variation of Case 17 .....	169
Figure 159 Bird Impact at 4 ms for Case 17.....	169
Figure 160 Hourglass, Damping and Sliding Energies Variation of Case 18 .....	170
Figure 161 Bird Impact at 4 ms for Case 18.....	170
Figure 162 Hourglass, Damping and Sliding Energies Variation of Case 19 .....	171
Figure 163 Bird Impact at 4 ms for Case 19.....	171
Figure 164 Hourglass, Damping and Sliding Energies Variation of Case 20 .....	172
Figure 165 Bird Impact at 4 ms for Case 20.....	172
Figure 166 Displacement Results (mm) at 0.5 ms for Impactor Position 6 .....	173
Figure 167 Displacement Results (mm) at 1.0 ms for Impactor Position 6 .....	174
Figure 168 Displacement Results (mm) at 1.5 ms for Impactor Position 6 .....	175
Figure 169 Displacement Results (mm) at 2.0 ms for Impactor Position 6 .....	176
Figure 170 Displacement Results (mm) at 2.5 ms for Impactor Position 6 .....	177
Figure 171 Displacement Results (mm) at 3.0 ms for Impactor Position 6 .....	178
Figure 172 Displacement Results (mm) at 3.5 ms for Impactor Position 6 .....	179
Figure 173 Displacement Results (mm) at 4.0 ms for Impactor Position 6 .....	180
Figure 174 Displacement Results (mm) at 4.5 ms for Impactor Position 6 .....	181
Figure 175 Displacement Results (mm) at 5.0 ms for Impactor Position 6 .....	182
Figure 176 Von Misses Stress Results (MPa) at 0.5 ms for Impactor Position 6.....	183
Figure 177 Von Misses Stress Results (MPa) at 1.0 ms for Impactor Position 6.....	184
Figure 178 Von Misses Stress Results (MPa) at 1.5 ms for Impactor Position 6.....	185
Figure 179 Von Misses Stress Results (MPa) at 2.0 ms for Impactor Position 6.....	186
Figure 180 Von Misses Stress Results (MPa) at 2.5 ms for Impactor Position 6.....	187
Figure 181 Von Misses Stress Results (MPa) at 3.0 ms for Impactor Position 6.....	188
Figure 182 Von Misses Stress Results (MPa) at 3.5 ms for Impactor Position 6.....	189
Figure 183 Von Misses Stress Results (MPa) at 4.0 ms for Impactor Position 6.....	190
Figure 184 Von Misses Stress Results (MPa) at 4.5 ms for Impactor Position 6.....	191
Figure 185 Von Misses Stress Results (MPa) at 5.0 ms for Impactor Position 6.....	192
Figure 186 Energy Variation of Position 6.....	194
Figure 187 Energy Ratio of Position 6 .....	195
Figure 188 Hourglass, Damping and Sliding Energies Variation of Case 21 .....	196
Figure 189 Bird Impact at 4 ms for Case 21.....	196
Figure 190 Hourglass, Damping and Sliding Energies Variation of Case 22 .....	197
Figure 191 Bird Impact at 4 ms for Case 22.....	197
Figure 192 Hourglass, Damping and Sliding Energies Variation of Case 23 .....	198
Figure 193 Bird Impact at 4 ms for Case 23.....	198
Figure 194 Hourglass, Damping and Sliding Energies Variation of Case 24 .....	199
Figure 195 Bird Impact at 4 ms for Case 24.....	199

Figure 196 FEM Model of External Fuel Tank ..... 202

## LIST OF TABLES

Table 1 The units consistent with LS-Dyna software.....	23
Table 2 Parameters of Johnson Cook Material Model for AL 2024 T3 and AL 7075 T6 ..	25
Table 3 Material Card of Johnson Cook Material Model for AL 2024 T3 .....	25
Table 4 Material Card of Johnson Cook Material Model for AL 7075 T6 .....	26
Table 5 Material Card of Piecewise Linear Plasticity Material Model for AL 2024 T3 .....	28
Table 6 Material Card of Piecewise Linear Plasticity Material Model for AL 7075 T6.....	28
Table 7 Material Card of SPH Bird Model.....	30
Table 8 Cases of This Study .....	33

## LIST OF SYMBOLS AND ABBREVIATIONS

### Symbols

$\sigma_y$	Equivalent stress
$A$	Initial yield stress
$B$	Hardening modulus
$n$	Work hardening exponent
$C$	Strain rate dependency
$\dot{\varepsilon}^*$	Normalized plastic strain rate
$\bar{\varepsilon}^p$	Effective plastic strain
$\varepsilon^*$	Strain Rate
$\sigma^*$	Ratio of Pressure divided by the Effective Stress.
$\sigma_{eff}$	Effective Stress
$\varepsilon^p$	Effective Plastic Strain
$\bar{\varepsilon}^f$	Failure Strain
$\rho_0$	Density of Soft Body Impactor
$u_0$	Impact Velocity
$u_s$	Shock Velocity

### Abbreviations

CPU	Central Processing Unit
EFT	External Fuel Tank
SPH	Smoothed Particle Hydrodynamic
ALE	Arbitrary Lagrangian-Eulerian



# 1 INTRODUCTION

Air vehicles are at the risk of bird strike during flight, take-off and landing; and as a result of these collisions, catastrophic damages may occur. Since the beginning of aviation, the importance of birds strike has been realized and international aviation standards have been established as a precaution.[2]

Forward facing components of the aircraft, such as; wing leading edge, empennage leading edge, windshield, canopy, nose radome are required to be impact resistant against bird strike.

While bird strike analyses were carried out using real bird before, nowadays analyses are carried out in computer environment. After the bird strike resistance of air vehicle is confirmed with the help of bird strike numerical analyses, the experimental compliances have been performed. With this way, expensive and time consuming repetitive experiments are eliminated.

Any leakage on the external fuel tank may cause fire, the loss of aircraft and death of the pilot.

In this thesis work, effects of a 4lb bird strike on an external fuel tank of a jet trainer aircraft were investigated. The post processes of the analyses were carried out with Hypermesh software and impact analyses were performed using LS\_Dyna software. The structure was modelled as shell elements. Smoothed Particle Hydrodynamics method was used for soft body impact analysis. Six different impactor positions were analyzed for two different materials and two different material models. Using numerical analysis, stress distribution, displacement distribution, the maximum stress and deformation were be calculated. As a result, the robustness of the external fuel tank was verified due to the regulations of aviation authorities.

## 2 METHODS

### 2.1 Theoretical Method

The theoretical model is based on the impact behavior consisting of four main cases;

- a) initial shock at contact
- b) impact shock decay
- c) steady flow
- d) pressure decay

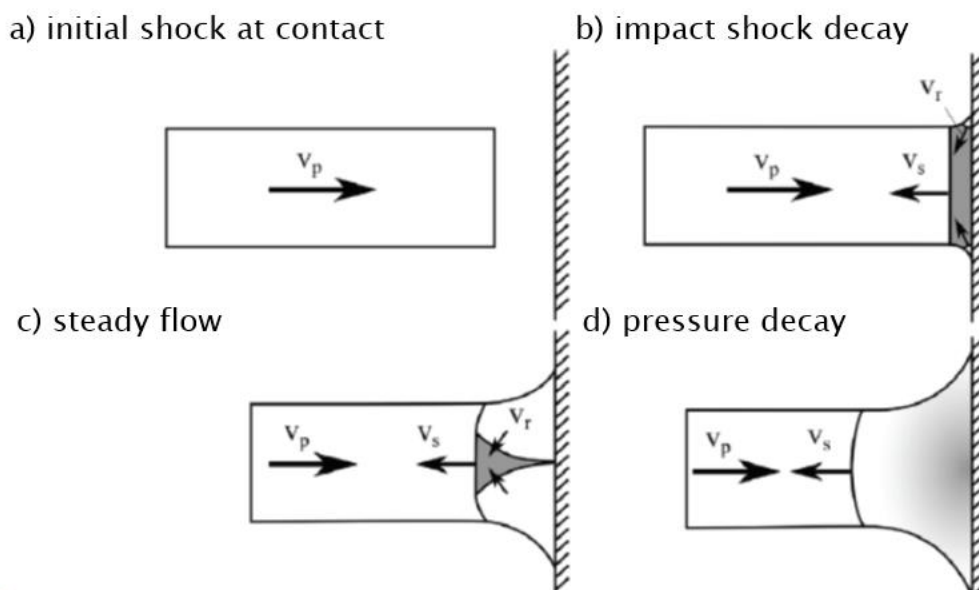


Figure 1 Soft Body Impact Phases [3]

- $V_r$  : Radial Velocity
- $V_0$  : Impact Velocity
- $V_s$  : Shock Velocity

A typical pressure curve for such a soft body impact on a rigid target plate is shown below:

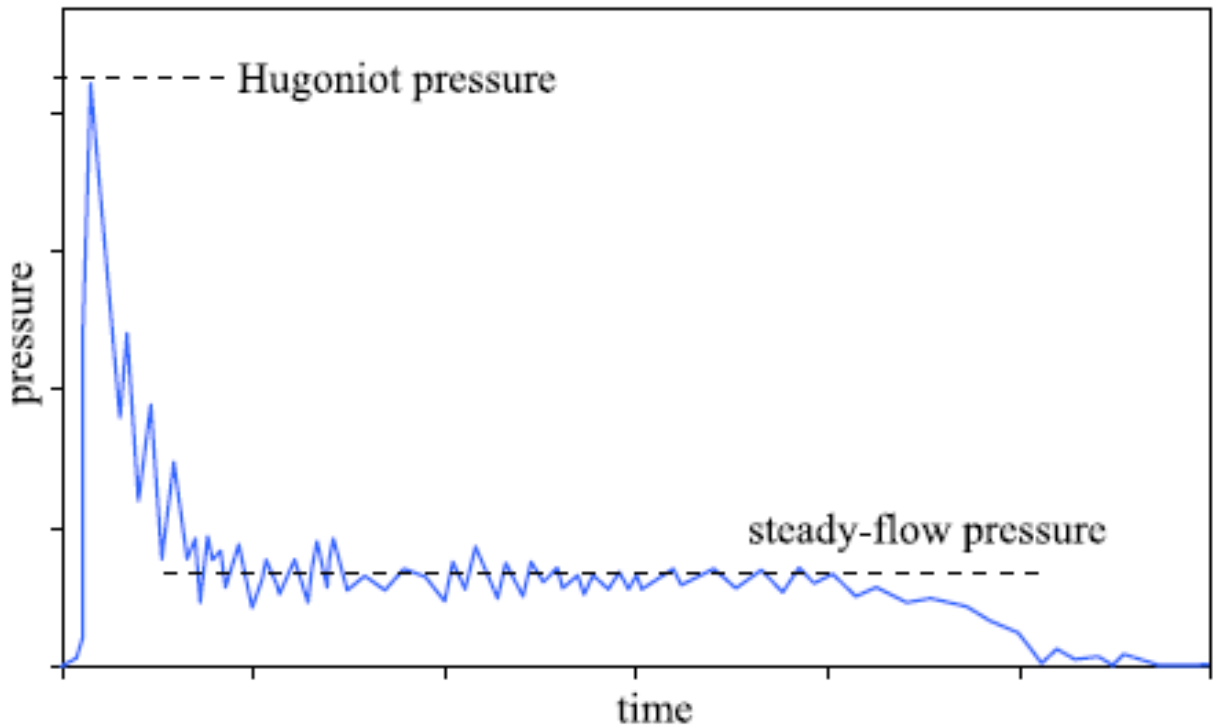


Figure 2 Typical Pressure Curve for a Soft Body Impact on a Rigid Target Plate[3]

We can calculate the max pressure and the steady-flow pressure by using these formulas;

- The initial pressure peak in the contact point:

$$P_H = \rho_0 u_0 u_s \quad (2.1)$$

- The steady-flow pressure  $P_s$  can be estimated by the Bernoulli relationship:

$$P_s = \frac{1}{2} \rho_0 u_0^2 \quad (2.2)$$

$\rho_0$  : density of soft body impactor

$u_0$  : impact velocity

$u_s$  : shock velocity

## 2.2 Numerical Method

The finite element analysis methods used for numerical modelling of bird strike are mainly;

- Lagrangian Method,
- Eulerian Method,
- Arbitrary Lagrangian-Eulerian (ALE) Method,
- Smoothed Particle Hydrodynamic (SPH) Method.

### 2.3 Lagrangian Method

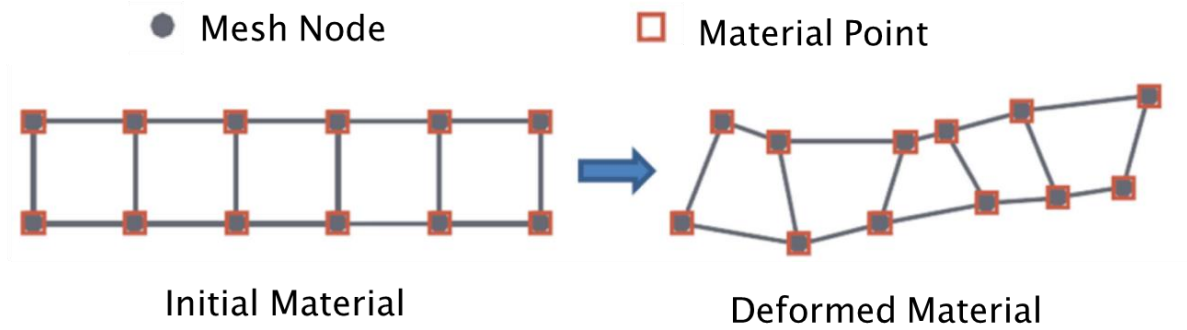


*Figure 3 Underformed and Deformed Element in Lagrangian Method*

The nodes of the mesh are fixed to the material and therefore each node of the mesh follows the material under motion and deformation.

### 2.4 Eulerian Method

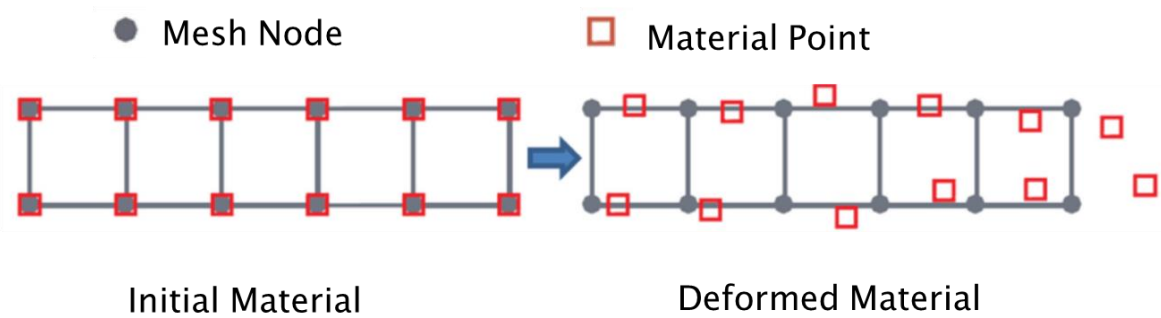


*Figure 4 Underformed and Deformed Element in Eulerian Method*

The nodes of the mesh remains fixed therefore the material flows through the mesh under motion and deformation.

## 2.5 Arbitrary Lagrangian – Eulerian Method

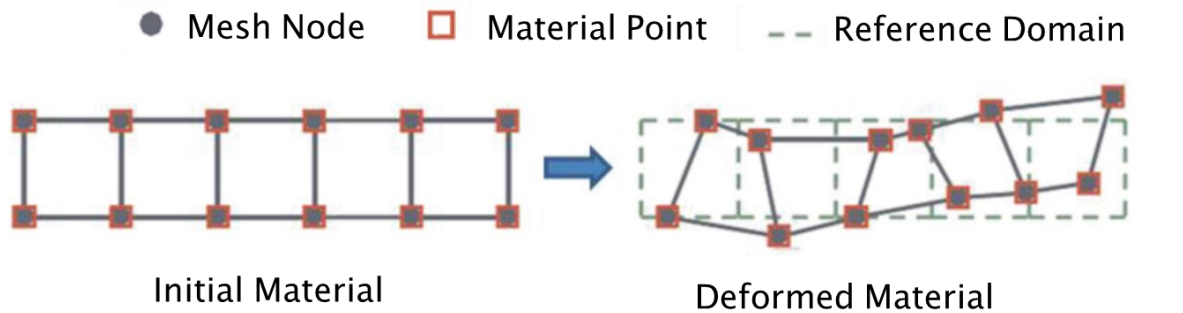


Figure 5 Undeformed and Deformed Element in ALE Method

The ALE method is similar to the Eulerian method, but the surrounding Eulerian box can move and stretch if needed and is not fixed in space [4].

## 2.6 Smoothed Particle Hydrodynamics

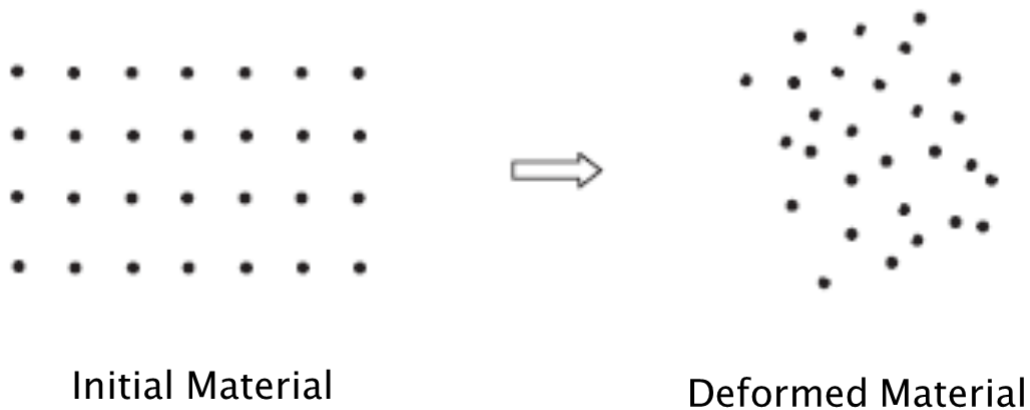


Figure 6 Undeformed and Deformed Element in SPH Method[3]

It is a meshless Lagrangian method. The fluid is modelled by particles which are independent from each other.[5]

## 2.7 Comparison of Methods

The advantages of the Lagrangian Method are:

- Simple model generation,
- Low CPU time,
- Clearly defined impactor boundary.

The disadvantages are:

- Severe mesh distortion,
- Element erosion may remove mass from the simulation.

The advantages of the Eulerian Method are:

- No mesh distortion,
- Numerically stable simulations.

The disadvantages are:

- Model generation and result visualization are more complex,
- No clear impactor boundary,
- Fine mesh is necessary,
- High computational cost.

The advantages of the SPH Method are

- No mesh distortion,
- Numerically stable simulations.
- Lower computational cost than Eulerian model

The disadvantages are:

- Model generation is more complex,
- No clear impactor boundary,
- Higher CPU time than Lagrangian model.

### 3 NUMERICAL MODELLING OF AN EXTERNAL FUEL TANK

External fuel tank of a jet trainer aircraft shall be considered as a forward facing component because of its location on the A/C. The main function of an external fuel tank is fuel storage. Since the EFT is installed outside of the aircraft, robustness against bird strike must be demonstrated. Any impact on EFT can cause very serious effects of the A/C.

In this study, bird strike analysis of the external fuel tank of a jet trainer aircraft is going to be carried out.

The model is created using CATIA V5 R28 software.

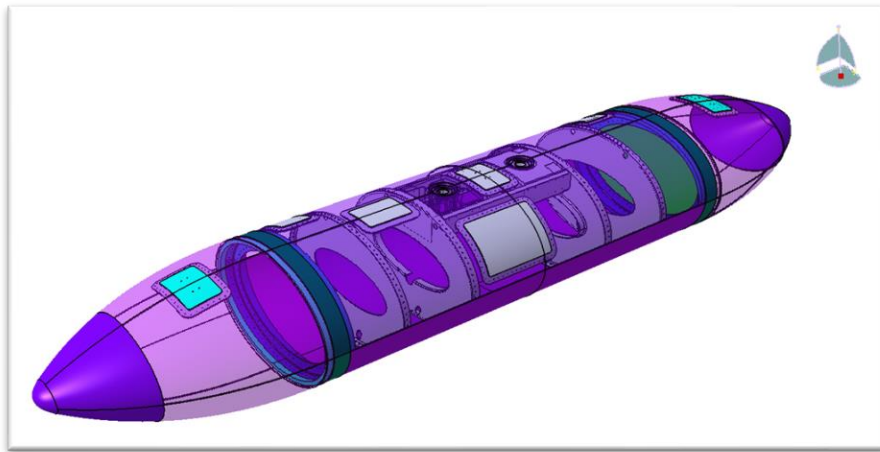


*Figure 7 CAD Model of EFT*

#### 3.1 Finite Element Modelling of the External Fuel Tank

Mesh model is created using Hypermesh software. First, CAD model is imported to the Hypermesh Program and using mid-surface command, each component is converted to the surface. After that, the model is arranged and each component becomes in contact with each other. The FEM model consists of 393862 nodes and 391032 elements as shown in Figure 8.

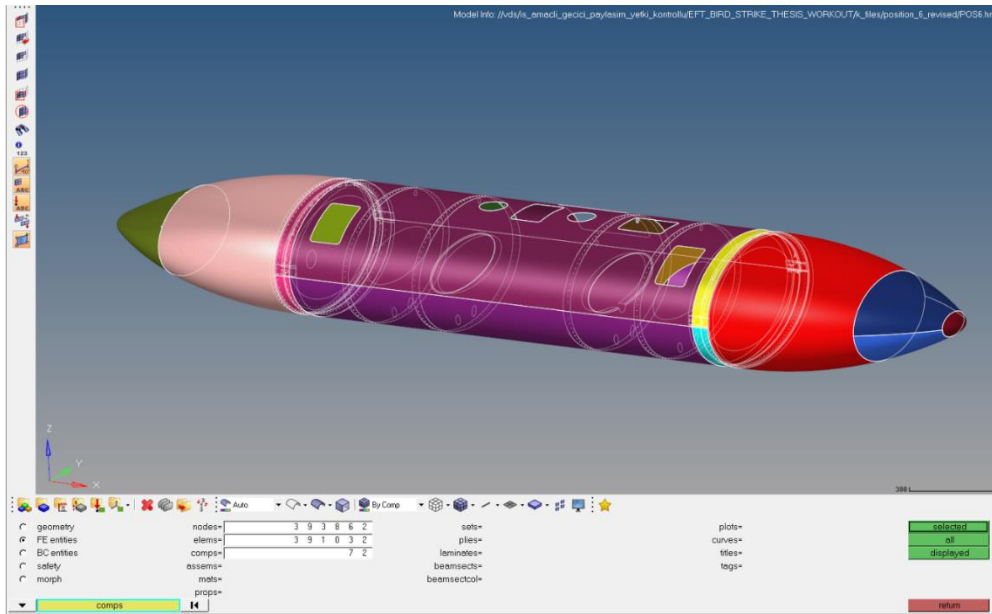


Figure 8 CAD Model of EFT Figure 8 FEM Model of EFT

Mesh model is uploaded to LS-DYNA Program and the boundary conditions are defined with the help of this software. EFT is installed to the aircraft from two points. Figure 9 shows the boundaries of EFT.

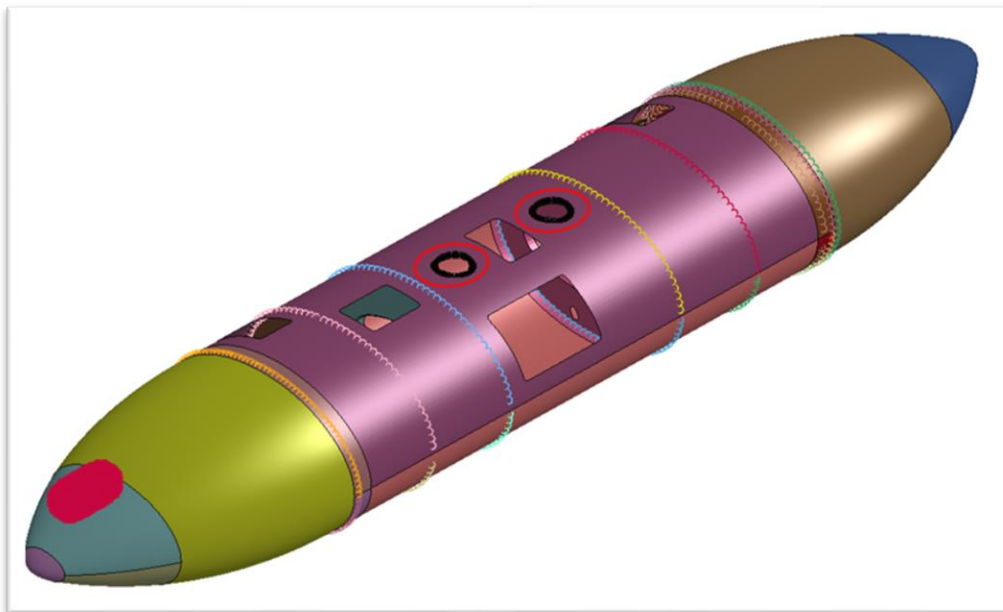


Figure 9 Boundaries of the External Fuel Tank



As shown in Figure 10, translation is fixed and rotation is free at the boundaries of EFT.

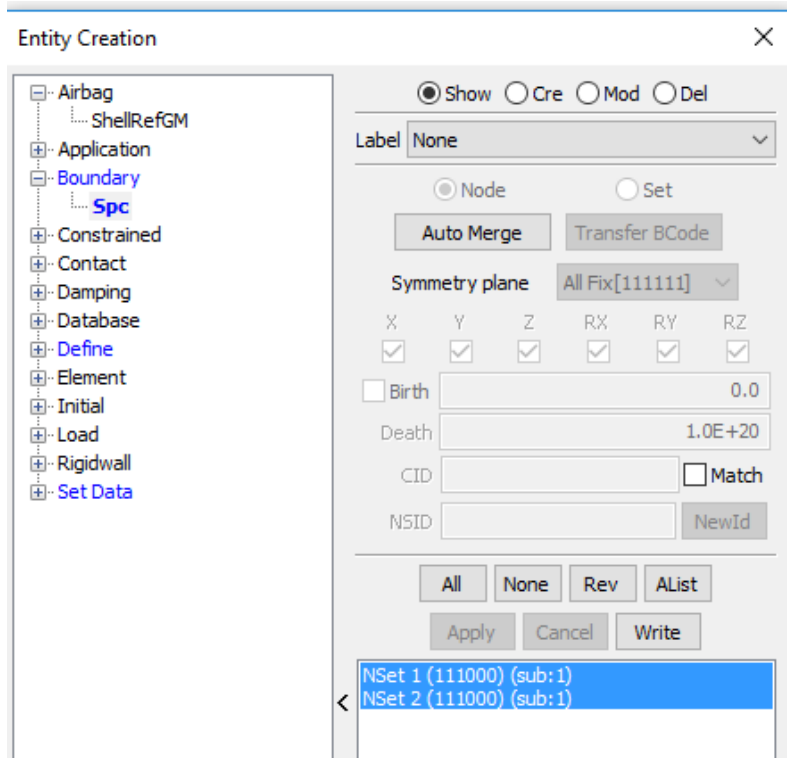


Figure 10 Rotation and Translation Layout of Boundaries

The units consistent with LS-Dyna software is shown in Table 1. In this study, g, mm, ms, N and MPa is used.

Table 1 The units consistent with LS-Dyna software

MASS	LENGTH	TIME	FORCE	STRESS	ENERGY	DENSITY	YOUNG'S	GRAVITY
kg	m	s	N	Pa	J	7.83e+03	2.07E+11	9.806
kg	cm	s	1.0e-02 N			7.83e-03	2.07E+09	9.806e+02
kg	cm	ms	1.0e+04 N			7.83e-03	2.07E+03	9.806e-04
kg	cm	us	1.0e+10 N			7.83e-03	2.07E-03	9.806e-10
kg	mm	ms	kN	GPa	kN-mm	7.83e-06	2.07E+02	9.806e-03
g	cm	s	dyne	dyne/cm <sup>2</sup>	erg	7.83e+00	2.07E+12	9.806e+02
g	cm	us	1.0e+07 N	Mbar	1.0e+07 N-cm	7.83e+00	2.07E+00	9.806e-10
g	mm	s	1.0e-06 N	Pa		7.83e-03	2.07E+11	9.806e+03
g	mm	ms	N	MPa	N-mm	7.83e-03	2.07E+05	9.806e-03
ton	mm	s	N	MPa	N-mm	7.83e-09	2.07E+05	9.806e+03
lbf-s <sup>2</sup> /in	in	s	lbf	psi	lbf-in	7.33e-04	3.00E+07	386
slug	ft	s	lbf	psf	lbf-ft	1.52e+01	4.32E+09	32.17
kgf-s <sup>2</sup> /mm	mm	s	kgf	kgf/mm <sup>2</sup>	kgf-mm	7.98e-10	2.11E+04	9.806e+03
kg	mm	s	mN	1.0e+03 Pa		7.83e-06	2.07E+08	9.806e+03
g	cm	ms	1.0e+1 N	1.0e+05 Pa		7.83e+00	2.07E+06	9.806e-04

## 4 MATERIAL MODELS

In this study, two different metallic materials, Al 2024-T3 and Al 7075-T6, are decided to be used.

“Johnson Cook” and “Piecewise Linear Plasticity” are used for metallic materials.

### 4.1 Johnson Cook Material Model

During bird striking impact, aluminum parts experience high rate deformation. In Ls-Dyna, Johnson-Cook material model can be used to model the high rate deformation of many materials including metals.

Johnson Cook Material model is a strain, temperature dependent visco-plastic material model that takes high strain rate process into account. In this study, Simplified Johnson Cook Material model is used which ignores temperature changes.

Flow stress equation of Johnson Cook Material model is shown in Eq.4.1:

$$\sigma_y = (A + B\bar{\epsilon}^p)^n (1 + C \ln \dot{\epsilon}^*) \quad (4.1)$$

Where;

$\sigma_y$  : Equivalent stress

$A$  : Initial yield stress

$B$  : Hardening modulus

$n$  : Work hardening exponent

$C$  : Strain rate dependency

$\dot{\epsilon}^*$  : Normalized plastic strain rate

$\bar{\epsilon}^p$  : Effective plastic strain

Parameters of Johnson Cook Material Model are given for AL 2024 T3 and AL 7075 T6 in Table 2.

Table 2 Parameters of Johnson Cook Material Model for AL 2024 T3 and AL 7075 T6

Johnson Cook Parameters	AL 2024 T3	AL 7075 T6
A	369	546
B	684	678
C	0.083	0.024
n	0.73	0.71
D1	0.13	-0.068
D2	0.13	0.451
D3	1.5	-0.952
D4	0.011	0.036
D5	0	0.697

Table 3 and Table 4 shows the material cards of Johnson Cook Material Model for AL 2024-T3 and AL 7075-T6.

Table 3 Material Card of Johnson Cook Material Model for AL 2024 T3

TITLE								
AA2024-T3 MATERIAL MODEL								
1	<b>MID</b>	<b>RO</b>	<b>G</b>	<b>E</b>	<b>PR</b>	<b>DIF</b>	<b>VP</b>	<b>RATEOP</b>
	100	2.700e-009	2.800e+004	7.308e+004	0.3300000	0.0	0.0	3.0
2	<b>A</b>	<b>B</b>	<b>N</b>	<b>C</b>	<b>M</b>	<b>TM</b>	<b>TR</b>	<b>EPSO</b>
	369.00000	684.00000	0.7300000	0.0083000	1.7000000	900.00000	300.00000	1.0000000
3	<b>CP</b>	<b>PC</b>	<b>SPALL</b>	<b>II</b>	<b>D1</b>	<b>D2</b>	<b>D3</b>	<b>D4</b>
	9.100e+008	-1500.0000	2.0	0.0	0.1300000	0.1300000	1.5000000	0.0110000
4	<b>D5</b>	<b>C2/P</b>	<b>EROD</b>	<b>EFMIN</b>				
	0.0	0.0	0	0.0				

Table 4 Material Card of Johnson Cook Material Model for AL 7075 T6

TITLE								
AA7075-T6 MATERIAL MODEL								
1	<b>MID</b>	<b>RO</b>	<b>G</b>	<b>E</b>	<b>PR</b>	<b>DTF</b>	<b>VP</b>	<b>RATEOP</b>
	200	2.700e-009	2.800e+004	7.308e+004	0.3300000	0.0	0.0	3.0
2	<b>A</b>	<b>B</b>	<b>N</b>	<b>C</b>	<b>M</b>	<b>TM</b>	<b>IR</b>	<b>EPSO</b>
	546.00000	678.00000	0.7100000	0.0240000	1.7000000	900.00000	300.00000	1.0000000
3	<b>CP</b>	<b>PC</b>	<b>SPALL</b>	<b>IT</b>	<b>D1</b>	<b>D2</b>	<b>D3</b>	<b>D4</b>
	9.100e+008	-1500.0000	2.0	0.0	-0.0680000	0.4510000	-0.9520000	0.0360000
4	<b>D5</b>	<b>C2/P</b>	<b>EROD</b>	<b>EFMIN</b>				
	0.6970000	0.0	0	0.0				

Johnson Cook parameters given in Table 2 are defined in Johnson Cook Material Cards. D1, D2,D3, D4 and D5 are failure parameters. D5 is taken as 0 since temperature effect is not taken into account.

Failure strain is given as:

$$\varepsilon^f = [D_1 + D_2 \exp D_3 \sigma^*][1 + D_4 \ln \varepsilon^*][1 + D_5 T] \quad (4.2)$$

In this equation,  $\varepsilon^*$  is strain rate and  $\sigma^*$  is the ratio of pressure divided by the effective stress ( $\sigma_{eff}$ ).

In Johnson Cook approach, failure occurs when the failure parameter D1 equals 1. This failure parameter is given by;

$$D = \frac{\varepsilon^p}{\bar{\varepsilon}^f} \quad (4.2)$$

In this equation,  $\varepsilon^p$  is effective plastic strain and  $\bar{\varepsilon}^f$  is the failure strain.

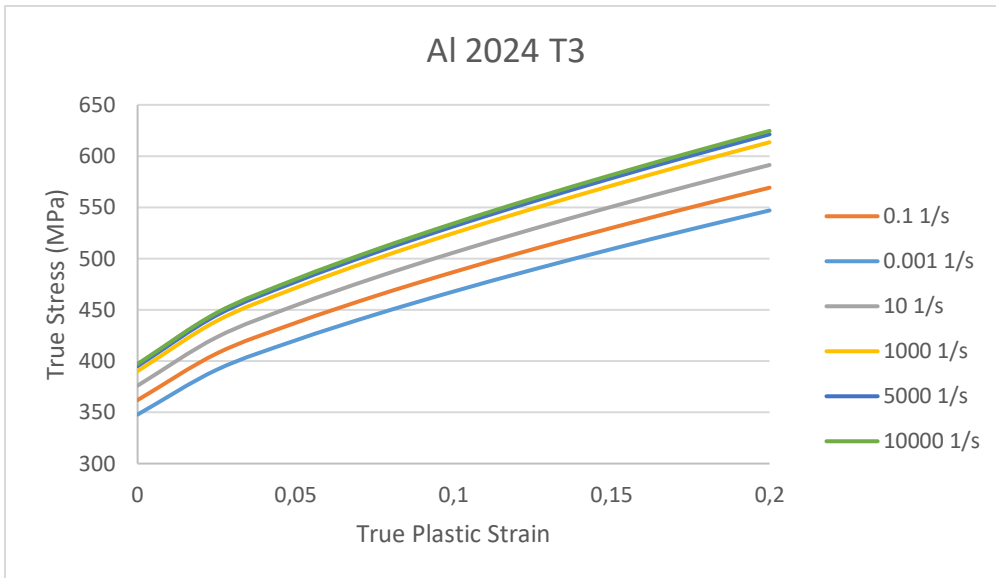


Figure 11 Stress Flow for AL 2024 T3

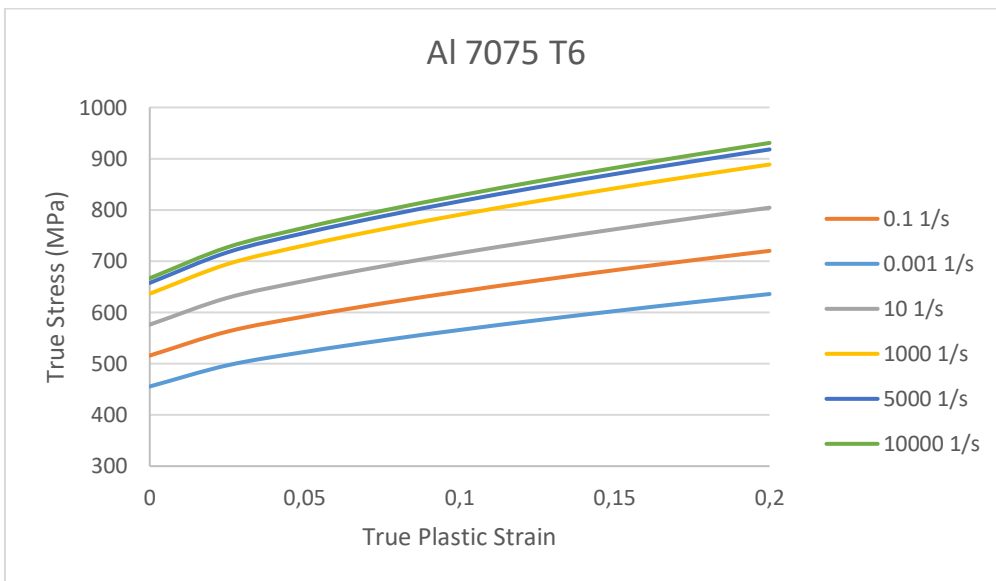


Figure 12 Stress Flow for AL 7075 T6

True stress- true plastic strain curves, which are obtained using Johnson Cook Equation, are shown in Figure 11 and Figure 12. Since aluminum alloys are strain rate dependent materials, calculations are made with different strain rates. The Johnson Cook parameter “C” controls strain rate factor. The strain rate causes greater stress changes on Al 7075-T6 which has larger ‘C’ than Al 2024 T3.

## 4.2 Piecewise Linear Plasticity Material Model

In piecewise material model, the plastic behavior of the material is directly defined to the material card [6].

Density (RO), modulus of elasticity (E), poison's ratio (PR), tangent modulus (ETAN), yield stress on the material card (SIGY), failure strain (FAIL), Cowper\_Symond strain rate parameters (C and P), effective plastic strain values (EPS1, EPS2, EPS3, EPS4, EPS5, EPS6, EPS7, EPS8) and equivalent stress values (ES1, ES2, ES3, ES4, ES5, ES6, ES7, ES8) is defined at the material card.

Table 5 Material Card of Piecewise Linear Plasticity Material Model for AL 2024 T3

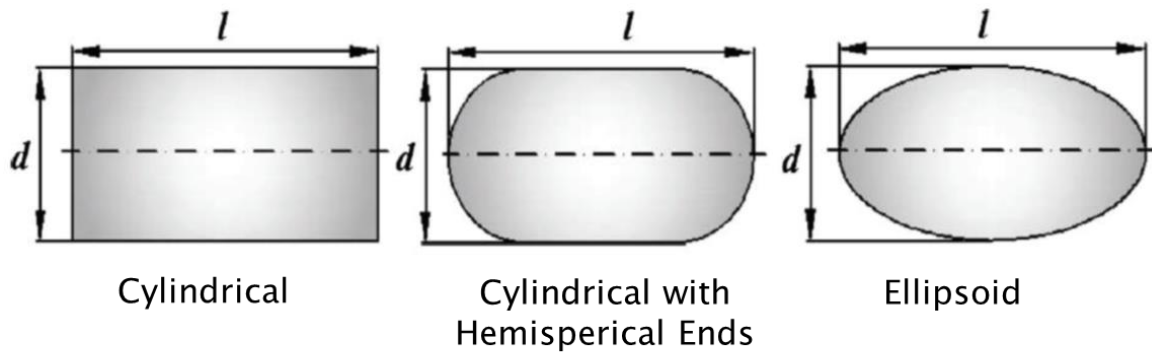
TITLE								
AL_2024_REFERENCED_MAT_MODEL_AS IN THESIS_								
1	<u>MID</u>	<u>RO</u>	<u>E</u>	<u>PR</u>	<u>SIGY</u>	<u>ETAN</u>	<u>FAIL</u>	<u>TDEL</u>
	1	2.768e-009	7.308e+004	0.3300000	0.0	0.0	1.000e+021	0.0
2	<u>C</u>	<u>P</u>	<u>LCSS</u>	<u>LCSR</u>	<u>VP</u>			
	0.0	0.0	16	0	0.0			
3	<u>EPS1</u>	<u>EPS2</u>	<u>EPS3</u>	<u>EPS4</u>	<u>EPS5</u>	<u>EPS6</u>	<u>EPS7</u>	<u>EPS8</u>
	0.0	0.0	0.0	0.0	0.0	0.0	0.0	0.0
4	<u>ES1</u>	<u>ES2</u>	<u>ES3</u>	<u>ES4</u>	<u>ES5</u>	<u>ES6</u>	<u>ES7</u>	<u>ES8</u>
	0.0	0.0	0.0	0.0	0.0	0.0	0.0	0.0

Table 6 Material Card of Piecewise Linear Plasticity Material Model for AL 7075 T6

TITLE								
AL_7075_REFERENCED_MAT_MODEL_AS IN THESIS_								
1	<u>MID</u>	<u>RO</u>	<u>E</u>	<u>PR</u>	<u>SIGY</u>	<u>ETAN</u>	<u>FAIL</u>	<u>TDEL</u>
	2	2.796e-009	7.102e+004	0.3300000	0.0	0.0	1.000e+021	0.0
2	<u>C</u>	<u>P</u>	<u>LCSS</u>	<u>LCSR</u>	<u>VP</u>			
	0.0	0.0	17	0	0.0			
3	<u>EPS1</u>	<u>EPS2</u>	<u>EPS3</u>	<u>EPS4</u>	<u>EPS5</u>	<u>EPS6</u>	<u>EPS7</u>	<u>EPS8</u>
	0.0	0.0	0.0	0.0	0.0	0.0	0.0	0.0
4	<u>ES1</u>	<u>ES2</u>	<u>ES3</u>	<u>ES4</u>	<u>ES5</u>	<u>ES6</u>	<u>ES7</u>	<u>ES8</u>
	0.0	0.0	0.0	0.0	0.0	0.0	0.0	0.0

## 5 Bird Models

Generally, three different geometric bird models are accepted in literature to simulate the bird strike. Figure 13 shows geometric models of impactor.



*Figure 13 Geometrical Models of Bird*

### 5.1 Smoothed Particle Hydrodynamics Bird Model

Soft body impactor is modeled with smoothed particle hydrodynamics method. The first step of creating SPH soft body impactor is to create the solid model in LS Dyna software. Then, this solid model is converted to SPH model. After that, the solid model is deleted and SPH model is obtained.

SPH bird model is created as a cylinder with hemi-spherical ends and SPH particles are defined in a set of points.

For this study, most common bird geometry modelling technique cylinder with hemispherical end caps is chosen as seen in Figure 14 since it shows better correlation performances with experimental results from literature and the bird is modelled as the hemispherical-ended cylinder geometry. [7]

Figure 14 shows SPH dimensions and model of soft body impactor. The dimensions and weight of the soft body impactor are standardized in FAA Regulations. In this study, 4 lb bird model is used. Bird impact speed is taken as 350 KTAS (approx.180 m/s).

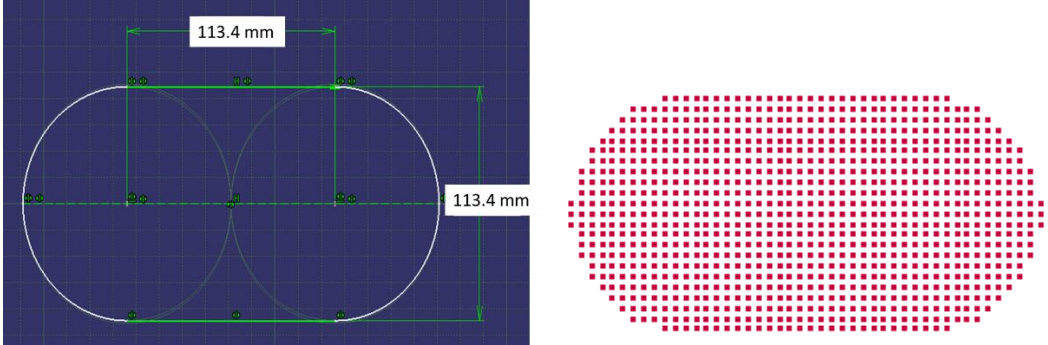


Figure 14 SPH Dimensions and Model of Soft Body Impactor

Table 7 Material Card of SPH Bird Model

TITLE								
SMOOTHED PARTICLE HYDRODYNAMICS FOR BIRD MATERIAL								
1	MID	RO	PC	MU	TEROD	CEROD	YM	PR
	7024	9.500e-010	-0.0997400	0.0	1.1000000	0.8000000	0.0	0.0

### 6 Energy Ratio

Energy checks are performed in order to be ensure that spurious results are not obtained. The sum of energies should be equal to the sum of the initial energies at any instant during impact as given in Eq 6.1;

$$E_K + E_I + E_S + E_H + E_{rw} + E_{damp} = E_K^0 + E_I^0 + W_{Ext} \quad (6.1)$$

Where;

$E_K$  : Kinetic energy

$E_I$  :Internal energy



$E_S$  :Sliding interface (contact) energy

$E_H$  :Hourglass energy

$E_{rw}$  :Rigid wall energy

$E_{damp}$  :Damping energy

The total energy is the sum of these energies as shown in Eq 6.2;

$$E_K + E_I + E_S + E_H + E_{rw} + E_{damp} = E_T \quad (6.2)$$

Internal energy is the energy related with elastic strain energy and work done in permanent deformation. The acceptable limit for maximum internal energy ratio shall be 1.0.

Kinetic energy is work done due to motion of nodes and elements with certain velocity. The acceptable limit for maximum internal energy ratio shall be 1.0.

External work is the work done under applied force, pressure, velocity, displacement or acceleration.

Sliding energy is the work done by sliding interfaces during impact. When friction is included in a contact definition, positive contact is expected. In the absence of friction, small contact energy is acceptable (10% of peak energy).

Hourglass modes are nonphysical modes of deformation which occur in under-integrated elements (zero stress and strain). Hourglass energy takes away from physical energy of the system. This nonphysical energy should be relatively small compared to peak energy for each part of the model [8]. The acceptable limit for maximum hourglass energy ratio shall be 0.1.

The hourglass energy, damping energy and sliding energy cause increase of the total energy during analysis.

For under integrated shell elements, forces and displacements may exist for each mode of the element, like sum of all these forces and displacements give null strain and stress on the integration point of the element. This problem only exists for under integrated elements. Using fully integrated and small elements helps minimization of hourglass energy.

Energy ratio is the ratio of total energy to the initial total energy and external work. Acceptable limits for energy ratio are between 0.9 to 1.1 [8].

## **7 Analysis Results**

24 different cases were compared on this study, which are shown in Table 8. Six different impactor positions were studied with the combination of two different material models which are Johnson Cook material model (MAT\_15) and Piecewise Linear Plasticity material model (MAT\_24) and two different material types which are Al 2024-T3 and Al 7075-T6. Figure 15 shows impactor positions of these cases.

Table 8 Cases of This Study

Case	Material	Material Model	Position
1	AL 2024-T3	Johnson Cook (MAT_015)	1
2	AL 7075-T6	Johnson Cook (MAT_015)	1
3	AL 2024-T3	Piecewise Linear Plasticity (MAT_024)	1
4	AL 7075-T6	Piecewise Linear Plasticity (MAT_024)	1
5	AL 2024-T3	Johnson Cook (MAT_015)	2
6	AL 7075-T6	Johnson Cook (MAT_015)	2
7	AL 2024-T3	Piecewise Linear Plasticity (MAT_024)	2
8	AL 7075-T6	Piecewise Linear Plasticity (MAT_024)	2
9	AL 2024-T3	Johnson Cook (MAT_015)	3
10	AL 7075-T6	Johnson Cook (MAT_015)	3
11	AL 2024-T3	Piecewise Linear Plasticity (MAT_024)	3
12	AL 7075-T6	Piecewise Linear Plasticity (MAT_024)	3
13	AL 2024-T3	Johnson Cook (MAT_015)	4
14	AL 7075-T6	Johnson Cook (MAT_015)	4
15	AL 2024-T3	Piecewise Linear Plasticity (MAT_024)	4
16	AL 7075-T6	Piecewise Linear Plasticity (MAT_024)	4
17	AL 2024-T3	Johnson Cook (MAT_015)	5
18	AL 7075-T6	Johnson Cook (MAT_015)	5
19	AL 2024-T3	Piecewise Linear Plasticity (MAT_024)	5
20	AL 7075-T6	Piecewise Linear Plasticity (MAT_024)	5
21	AL 2024-T3	Johnson Cook (MAT_015)	6
22	AL 7075-T6	Johnson Cook (MAT_015)	6
23	AL 2024-T3	Piecewise Linear Plasticity (MAT_024)	6
24	AL 7075-T6	Piecewise Linear Plasticity (MAT_024)	6

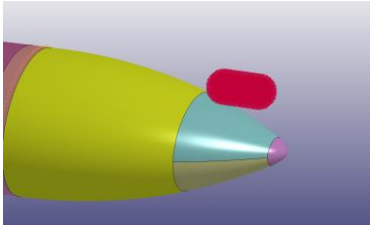
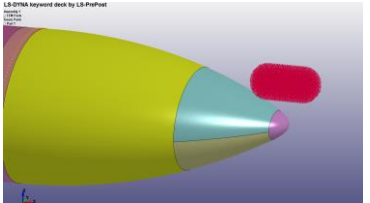
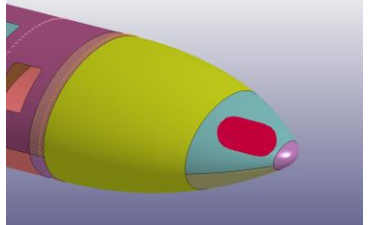
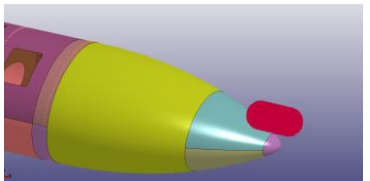
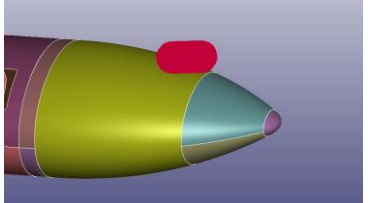
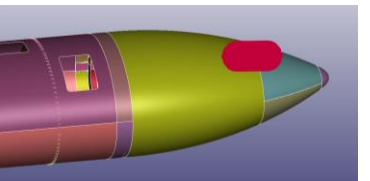
POSITION NO	ISOMETRIC VIEW OF POSITIONS
1	
2	
3	
4	
5	
6	

Figure 15 Impactor Positions

If a penetration occurs during bird strike, this causes fuel leakage, which is a serious threat to the survivability of the aircraft. Because of this reason, the design criteria of the external fuel tank was decided to be impact resistant without penetration.

### **Analysis Results for Position 1**

An overview of the impact simulation for the position 1 was given for the general understanding. The time history was presented as a series of time step plots with explanations. The plots in Figure 16 to Figure 35 show the simulation run in several steps. Total simulation time was set to 5 ms and plots are saved in the intervals of 0.5 ms.

Displacement results at 0.5 ms for impactor position 1 is shown in Figure 16.

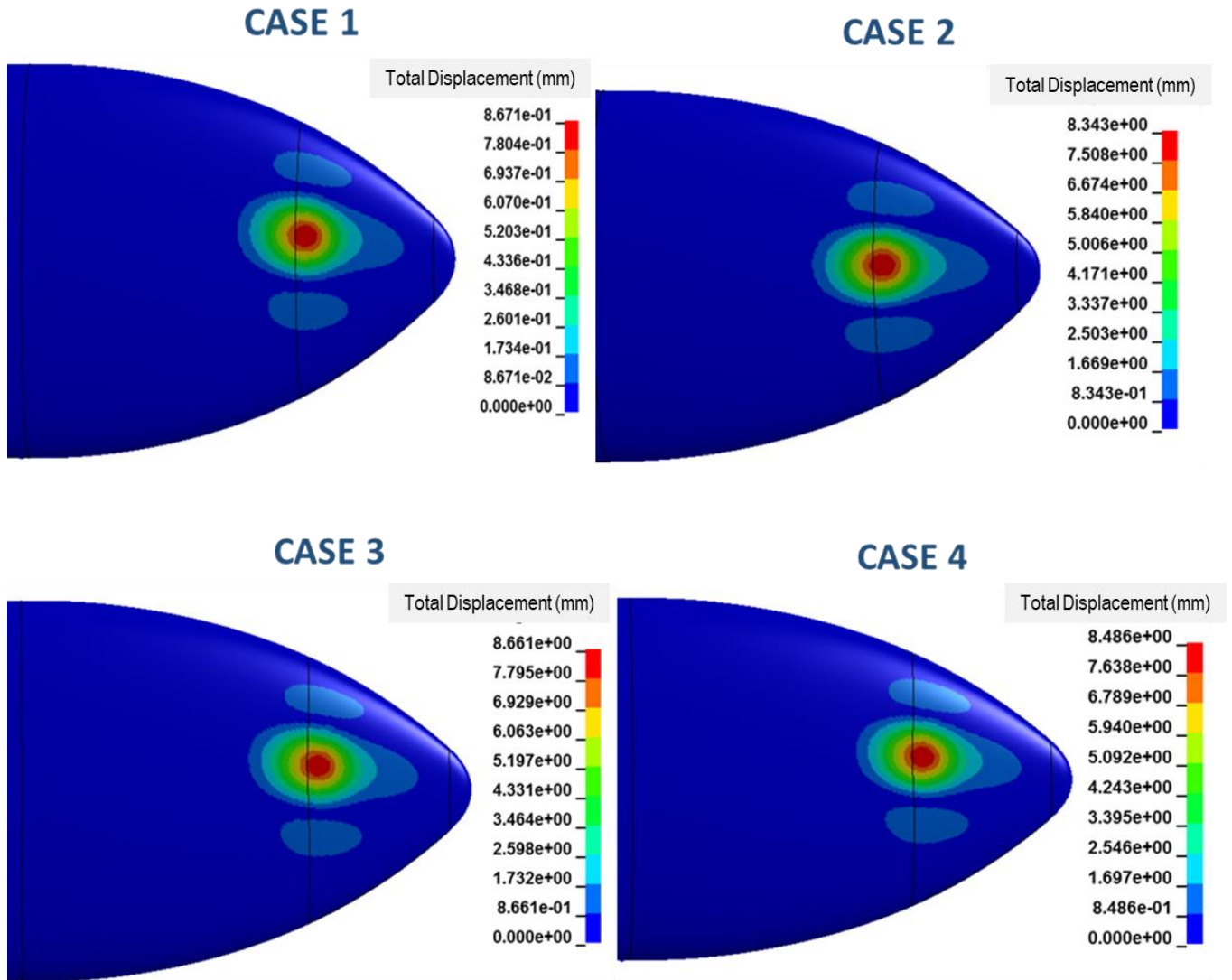


Figure 16 Displacement Results (mm) at 0.5 ms for Impactor Position 1.

Displacements on Al 7075 -T6 and Al 2024-T3 are similar. Displacement values according to Piecewise Linear Plasticity material model are also similar to Johnson Cook Material model.

Displacement results at 1.0 ms for impactor position 1 is shown in Figure 17.

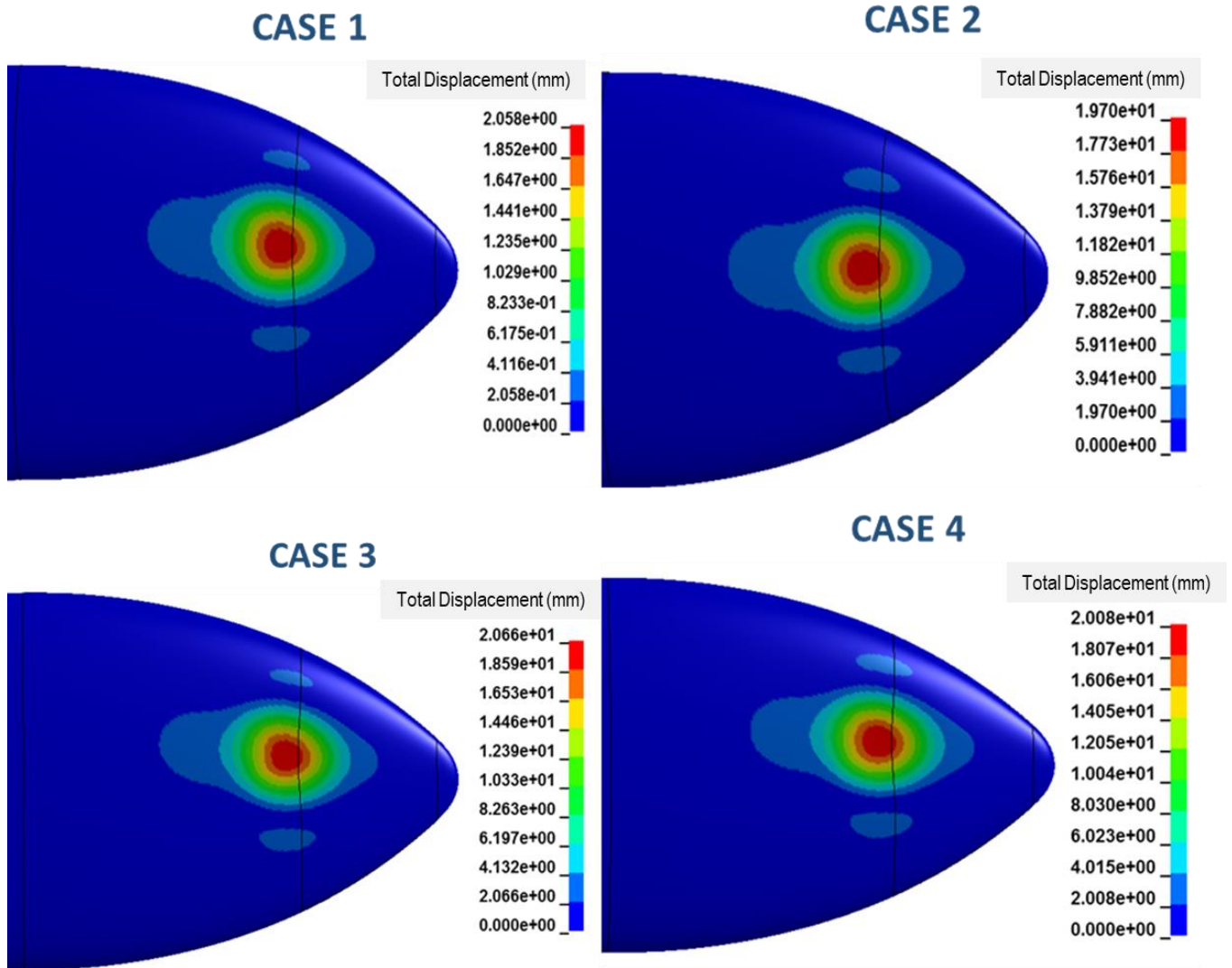


Figure 17 Displacement Results (mm) at 1.0 ms for Impactor Position 1

Displacements on Al 7075 -T6 and Al 2024-T3 are similar. Displacement values according to Piecewise Linear Plasticity material model are also similar to Johnson Cook Material model.

Displacement results at 1.5 ms for impactor position 1 is shown in Figure 18.

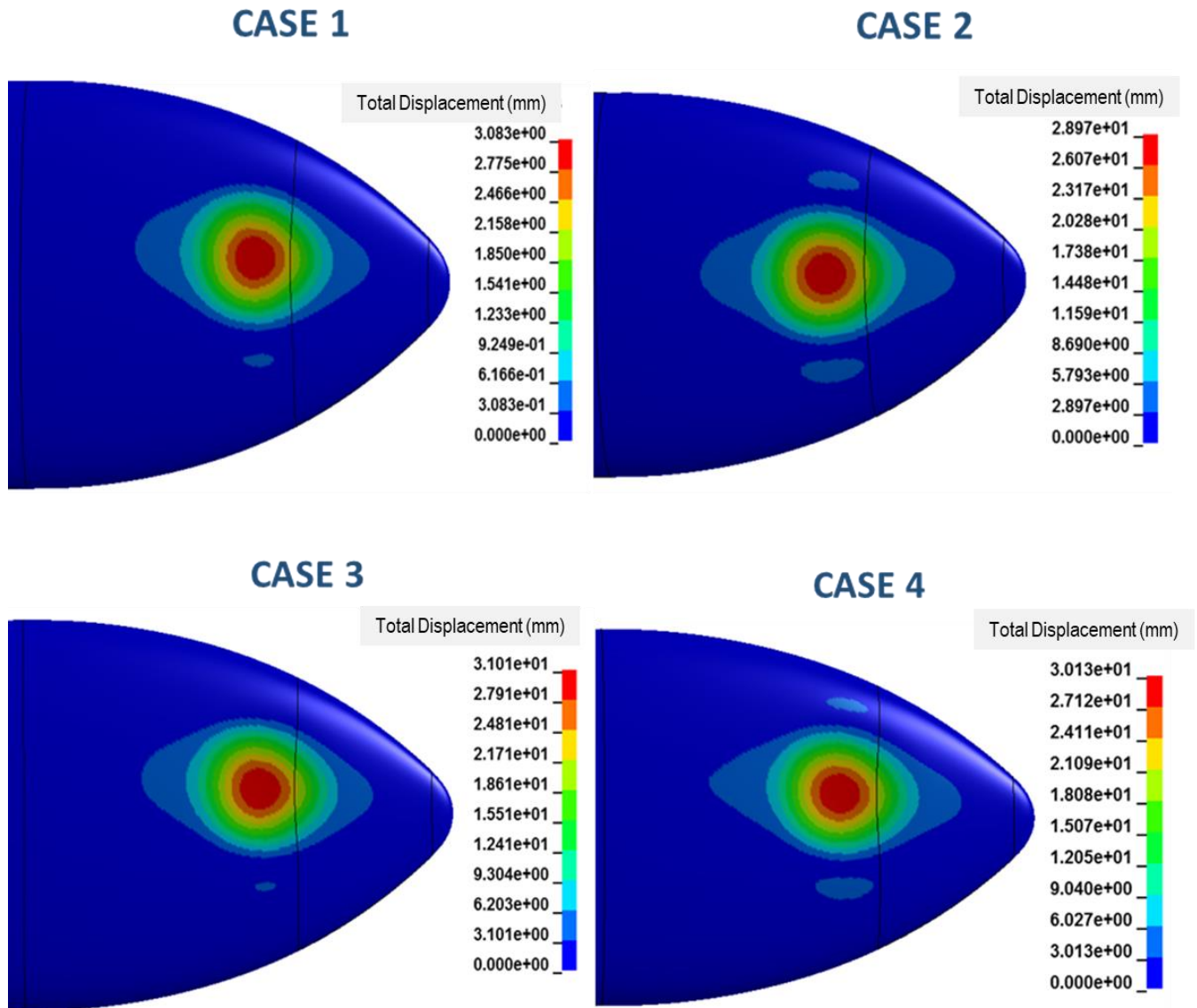


Figure 18 Displacement Results (mm) at 1.5 ms for Impactor Position 1

Displacements on Al 7075 -T6 and Al 2024-T3 are similar. Displacement values according to Piecewise Linear Plasticity material model are also similar to Johnson Cook Material model.

Displacement results at 2.0 ms for impactor position 1 is shown in Figure 19.



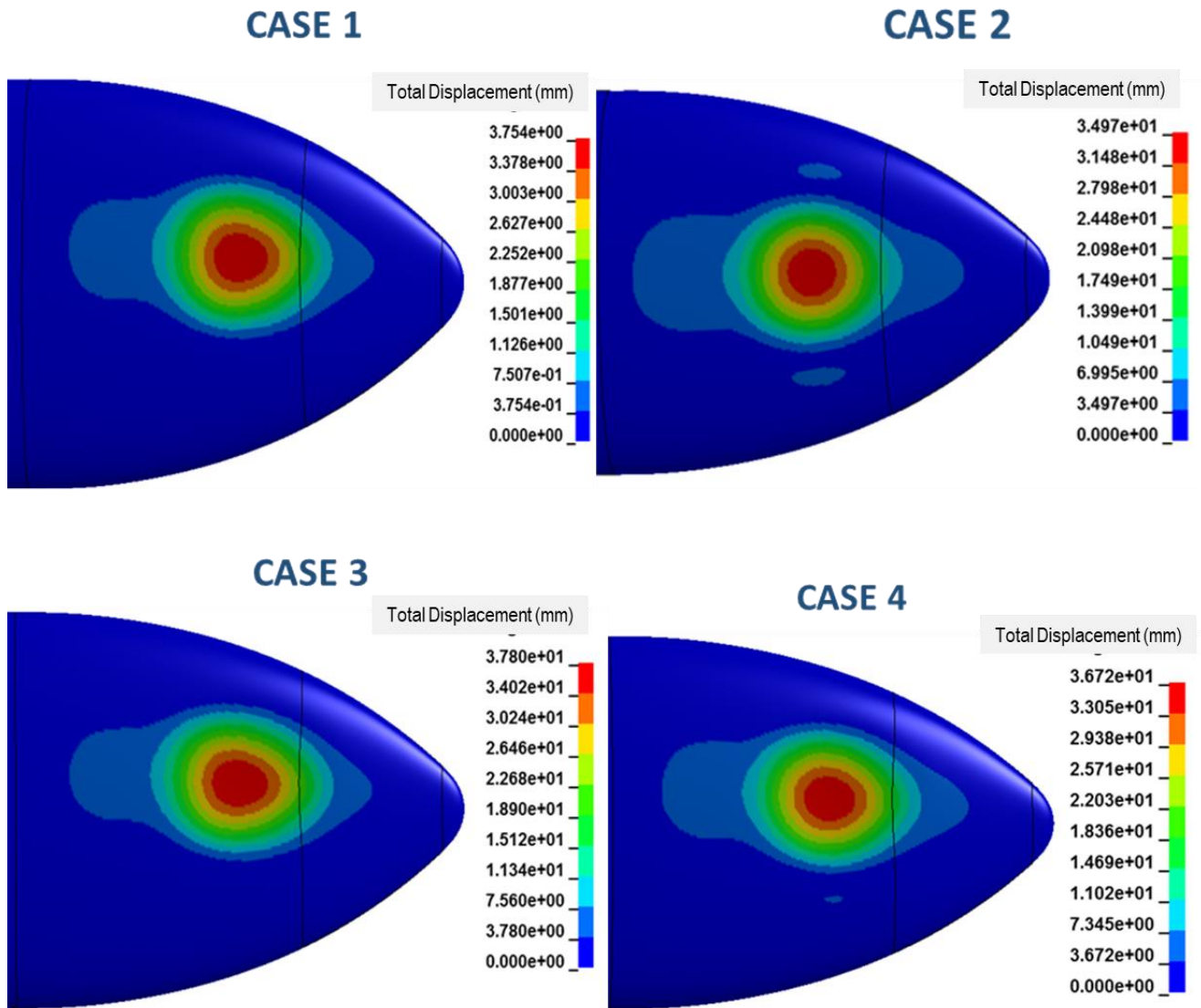


Figure 19 Displacement Results (mm) at 2.0 ms for Impactor Position 1

Displacements on Al 7075 -T6 and Al 2024-T3 are similar. Displacement values according to Piecewise Linear Plasticity material model are also similar to Johnson Cook Material model.

Displacement results at 2.5 ms for impactor position 1 is shown in Figure 20.

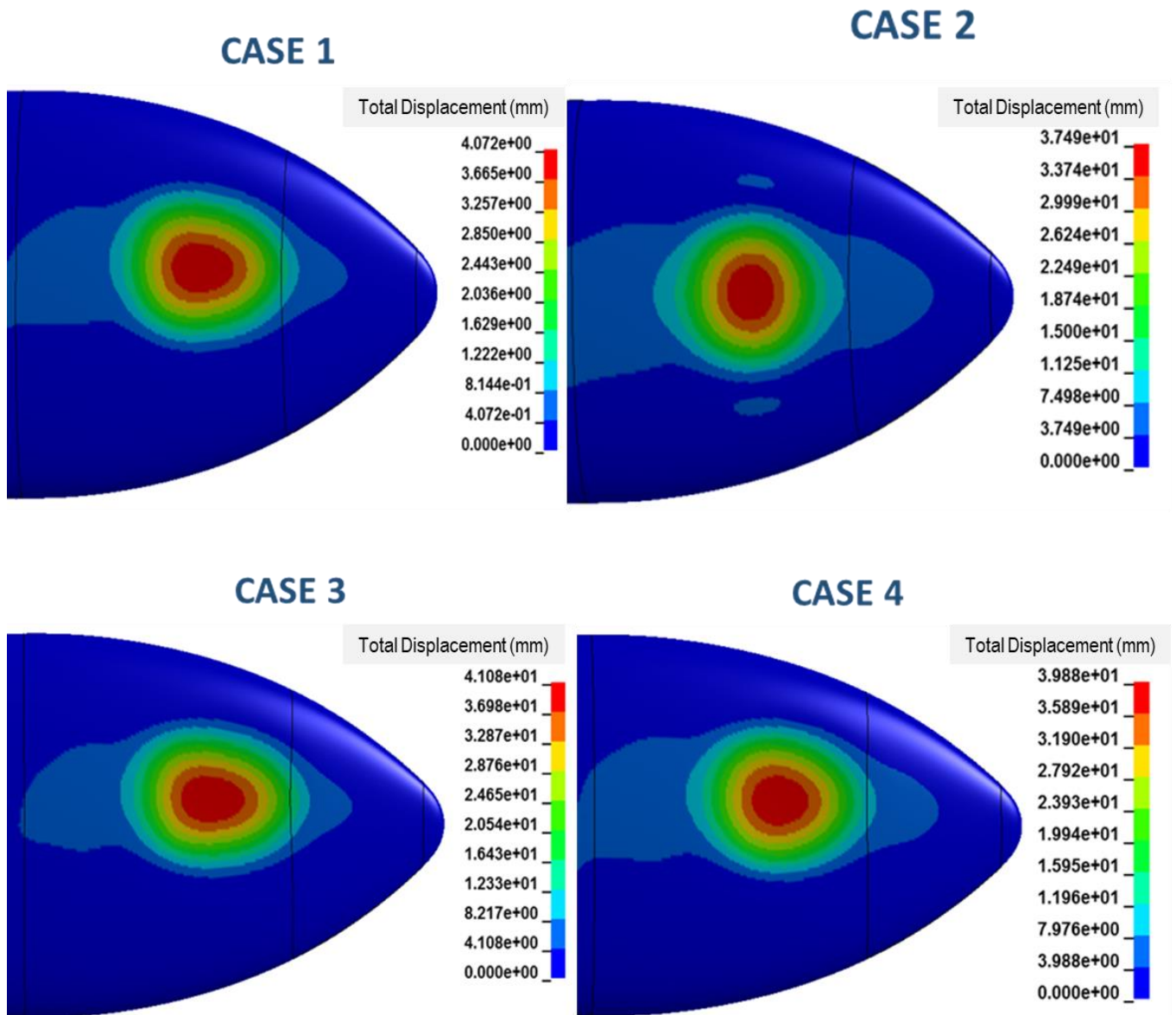


Figure 20 Displacement Results (mm) at 2.5 ms for Impactor Position 1

Displacements on Al 7075 -T6 and Al 2024-T3 are similar. Displacement values according to Piecewise Linear Plasticity material model are also similar to Johnson Cook Material model.

Displacement results at 3.0 ms for impactor position 1 is shown in Figure 21.

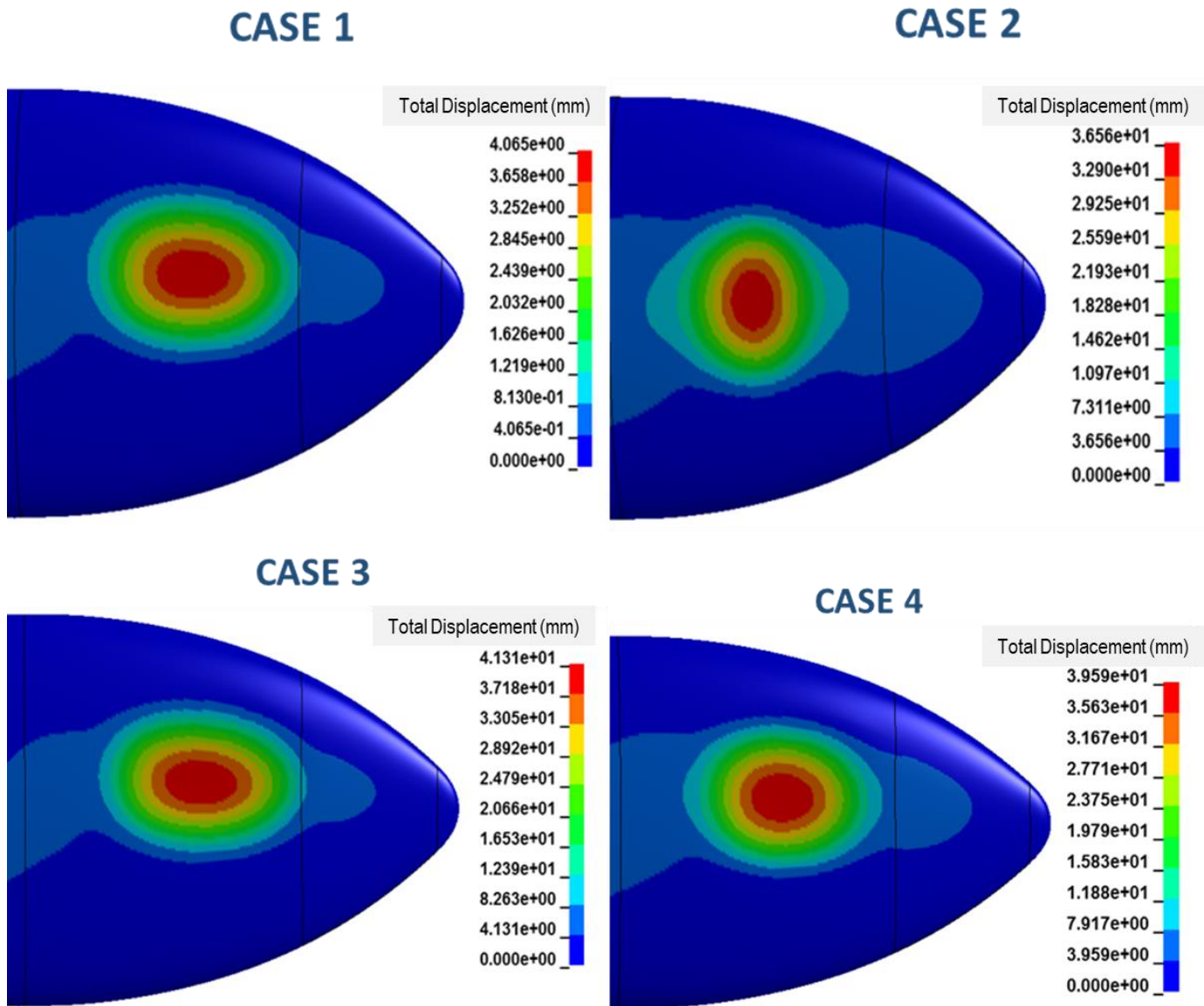


Figure 21 Displacement Results (mm) at 3.0 ms for Impactor Position 1

Displacements on Al 7075 -T6 and Al 2024-T3 are similar. Displacement values according to Piecewise Linear Plasticity material model are also similar to Johnson Cook Material model

Displacement results at 3.5 ms for impactor position 1 is shown in Figure 22.

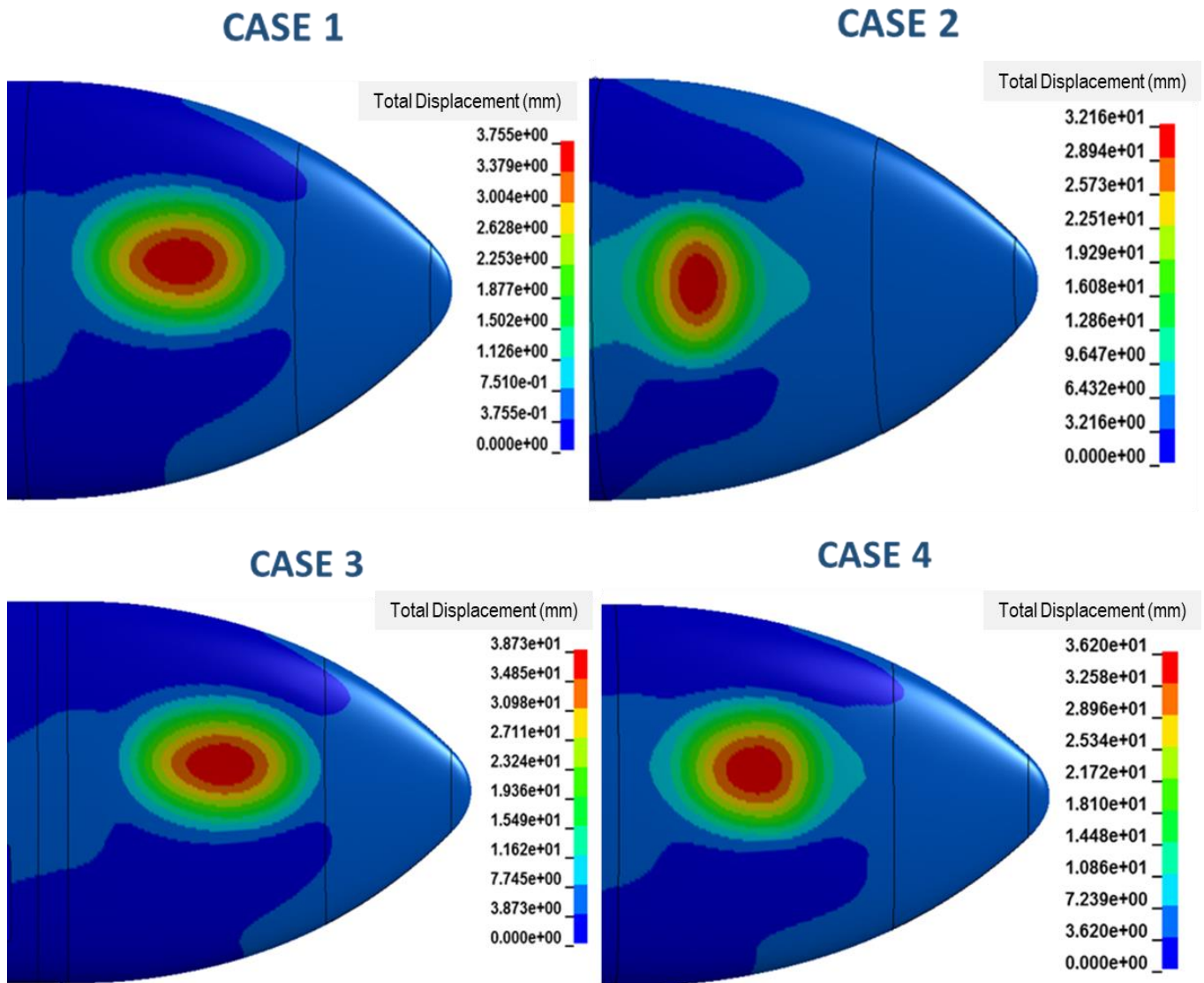


Figure 22 Displacement Results (mm) at 3.5 ms for Impactor Position 1

Displacements on Al 7075 -T6 and Al 2024-T3 are similar. Displacement values according to Piecewise Linear Plasticity material model are also similar to Johnson Cook Material model.

Displacement results at 4.0 ms for impactor position 1 is shown in Figure 23.

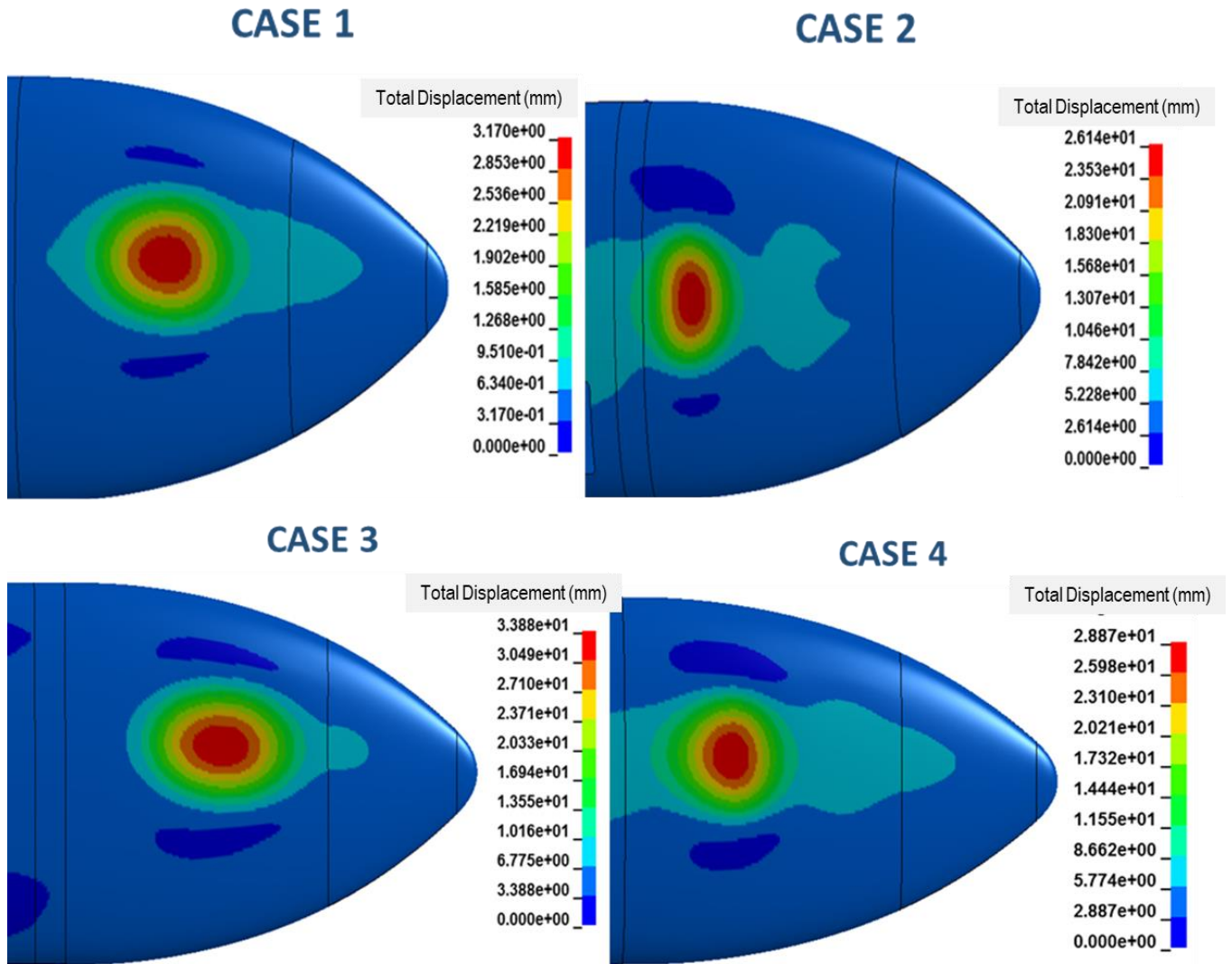


Figure 23 Displacement Results (mm) at 4.0 ms for Impactor Position 1

Displacements on Al 7075 -T6 and Al 2024-T3 are similar. Displacement values according to Piecewise Linear Plasticity material model are also similar to Johnson Cook Material model.

Displacement results at 4.5 ms for impactor position 1 is shown in Figure 24.

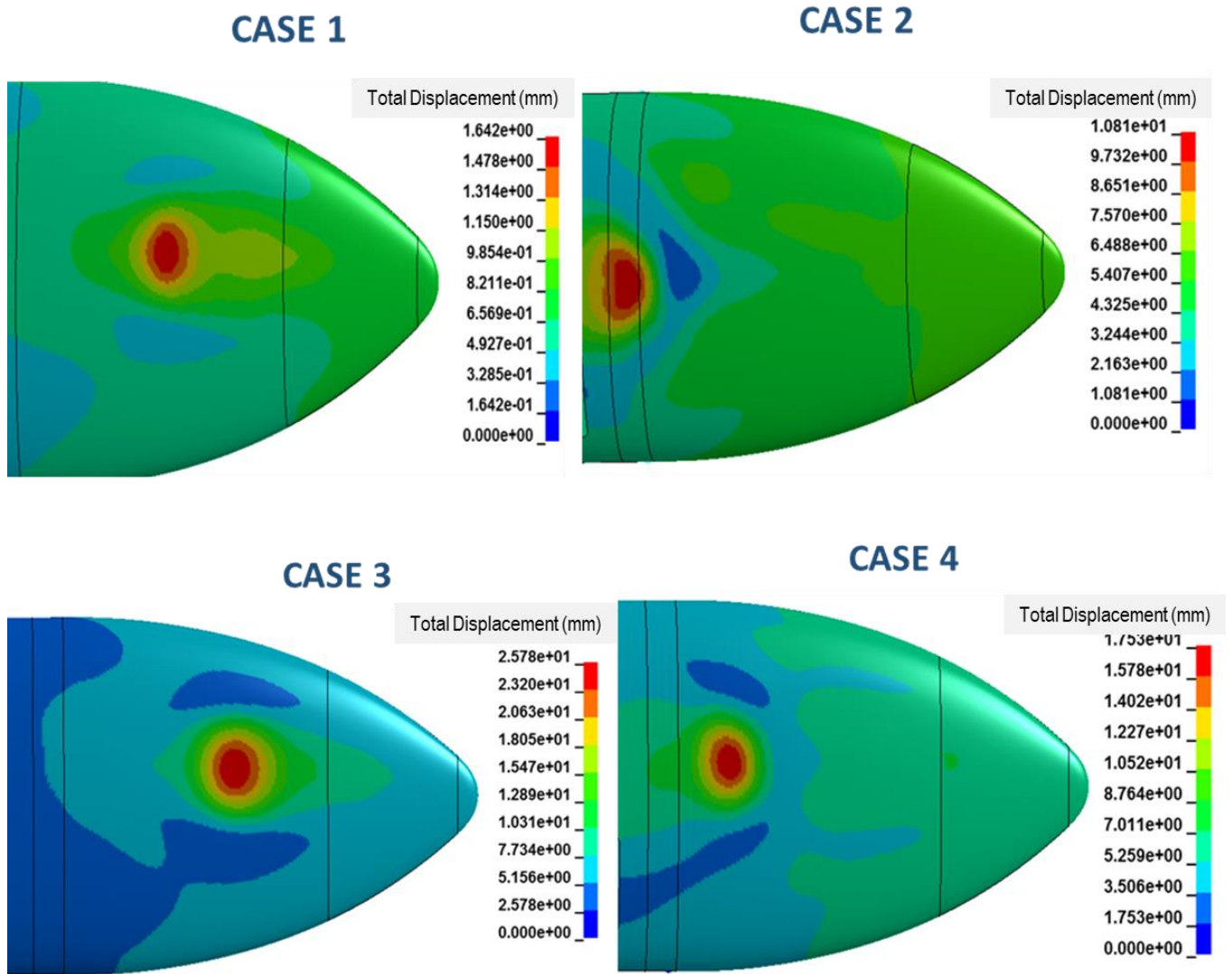


Figure 24 Displacement Results (mm) at 4.5 ms for Impactor Position 1

Displacements on Al 7075 -T6 and Al 2024-T3 are similar. Displacement values according to Piecewise Linear Plasticity material model are also similar to Johnson Cook Material model. Impact ended in 4.5 ms.

Displacement results at 5.0 ms for impactor position 1 is shown in Figure 25.

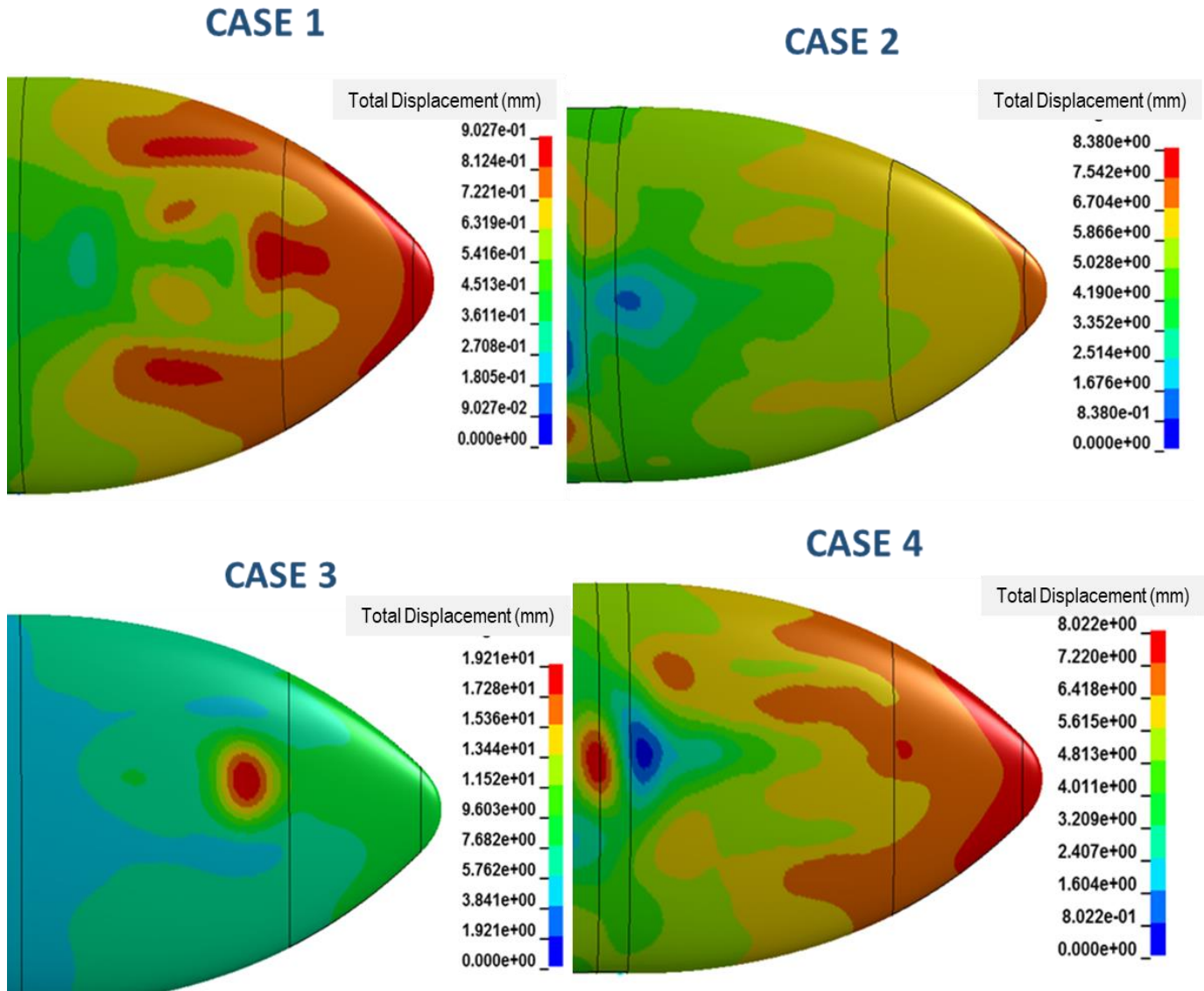


Figure 25 Displacement Results (mm) at 5.0 ms for Impactor Position 1

For position 1, displacements on Al 7075 -T6 and Al 2024-T3 are similar. Displacement values according to Piecewise Linear Plasticity material model are also similar to Johnson Cook Material model which is an expected result because of low strain rates. Impact ended in 4.5 ms.

After impact, screen shots were taken at 0.5ms intervals and the stresses were compared. Since the contact of the bird ended before 5 ms in general, the images were limited to this time period.

Von Misses Stress results at 0.5 ms for impactor position 1 is shown in Figure 26.

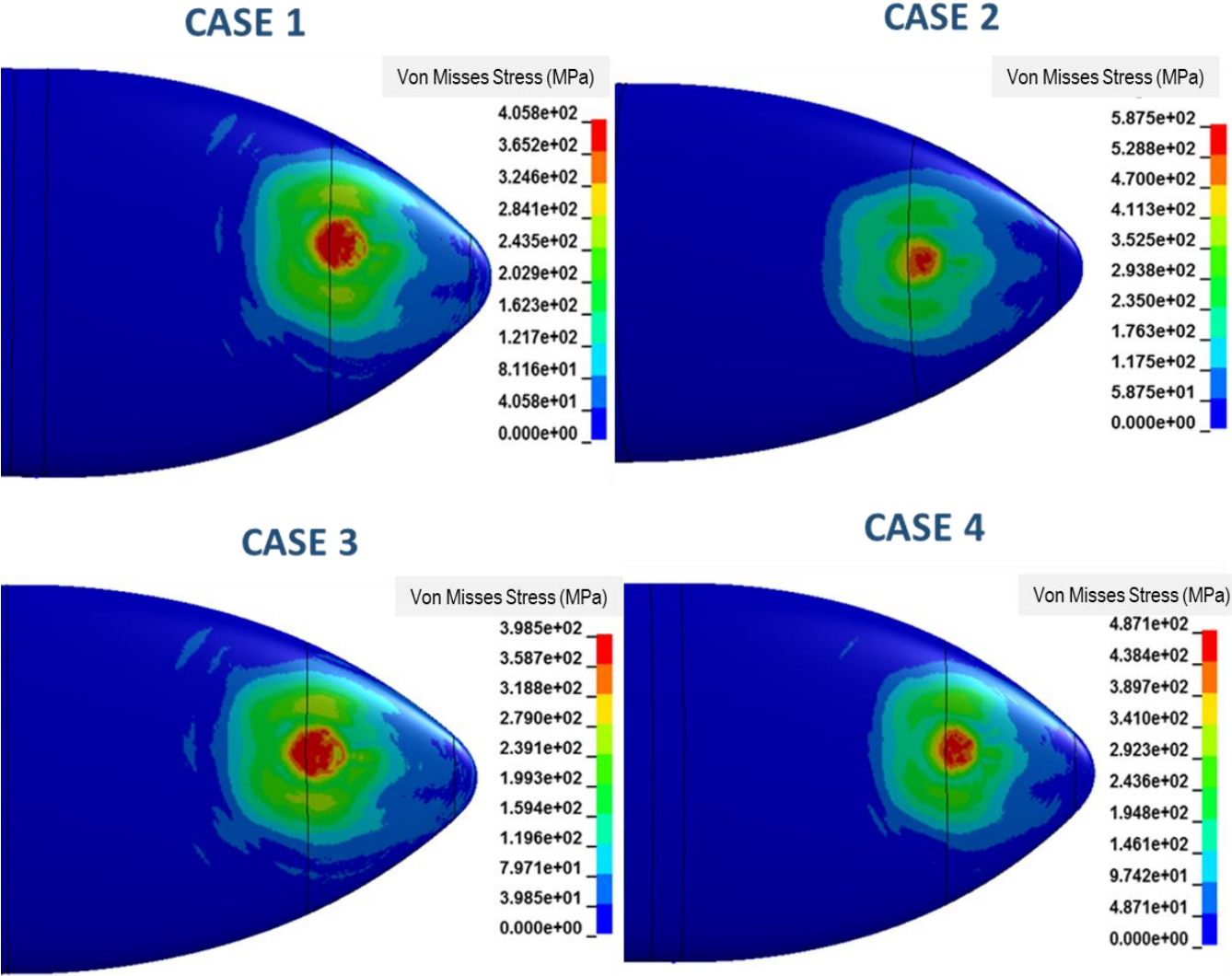


Figure 26 Von Misses Stress Results (MPa) at 0.5 ms for Impactor Position 1



The plastic deformation began at 0.5ms as shown in Figure 26. There was no tearing or penetration on the skin of EFT. The stress distributions and effective stresses on skin are similar for Piecewise Linear Plasticity material model and Johnson Cook Material model.

Von Misses Stress results at 1.0 ms for impactor position 1 is shown in Figure 27.

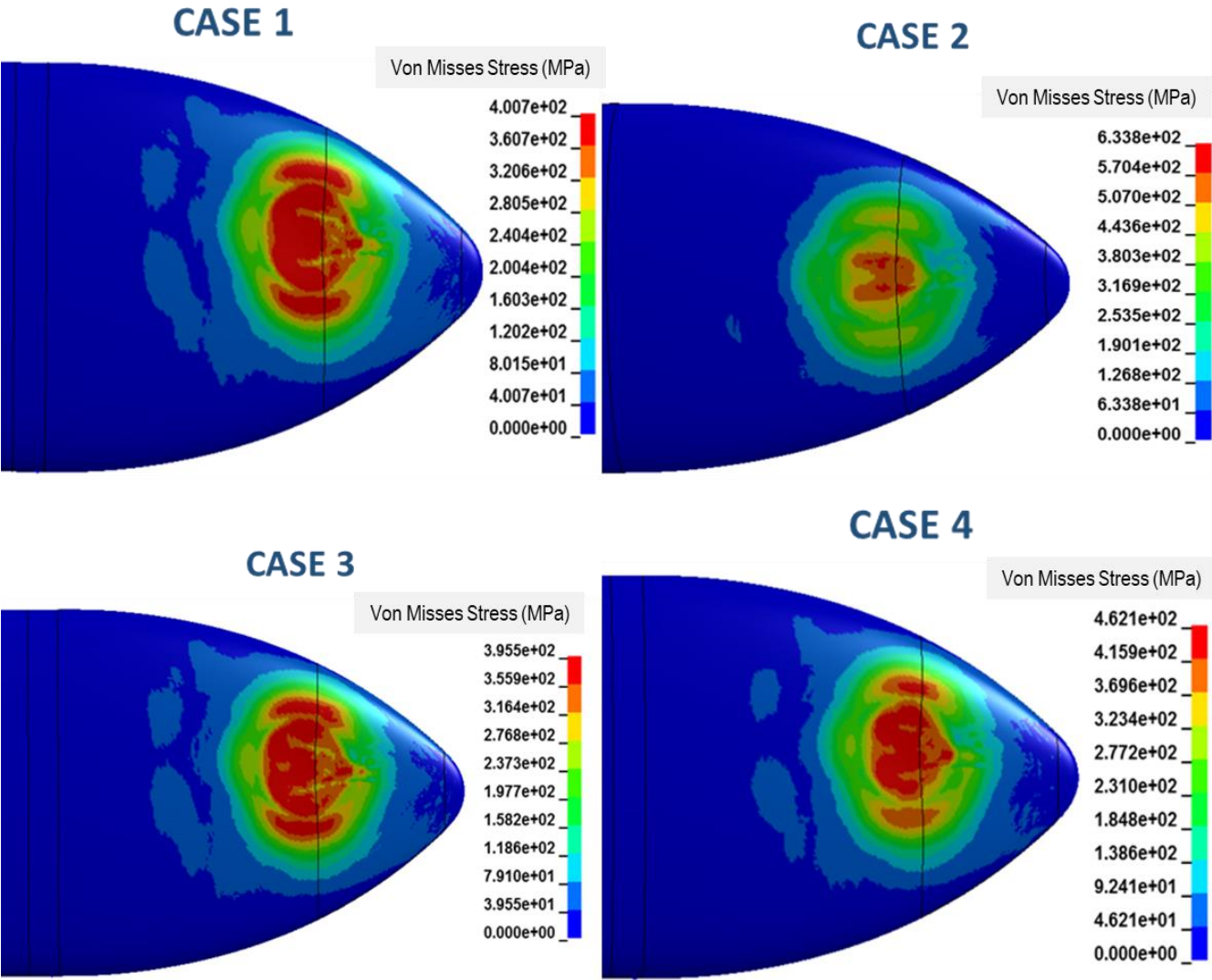


Figure 27 Von Misses Stress Results (MPa) at 1.0 ms for Impactor Position 1

There was no tearing or penetration on the skin of EFT. The stress distributions and effective stresses on skin are similar for Piecewise Linear Plasticity material model and Johnson Cook Material model.

Von Misses Stress results at 1.5 ms for impactor position 1 is shown in Figure 28.

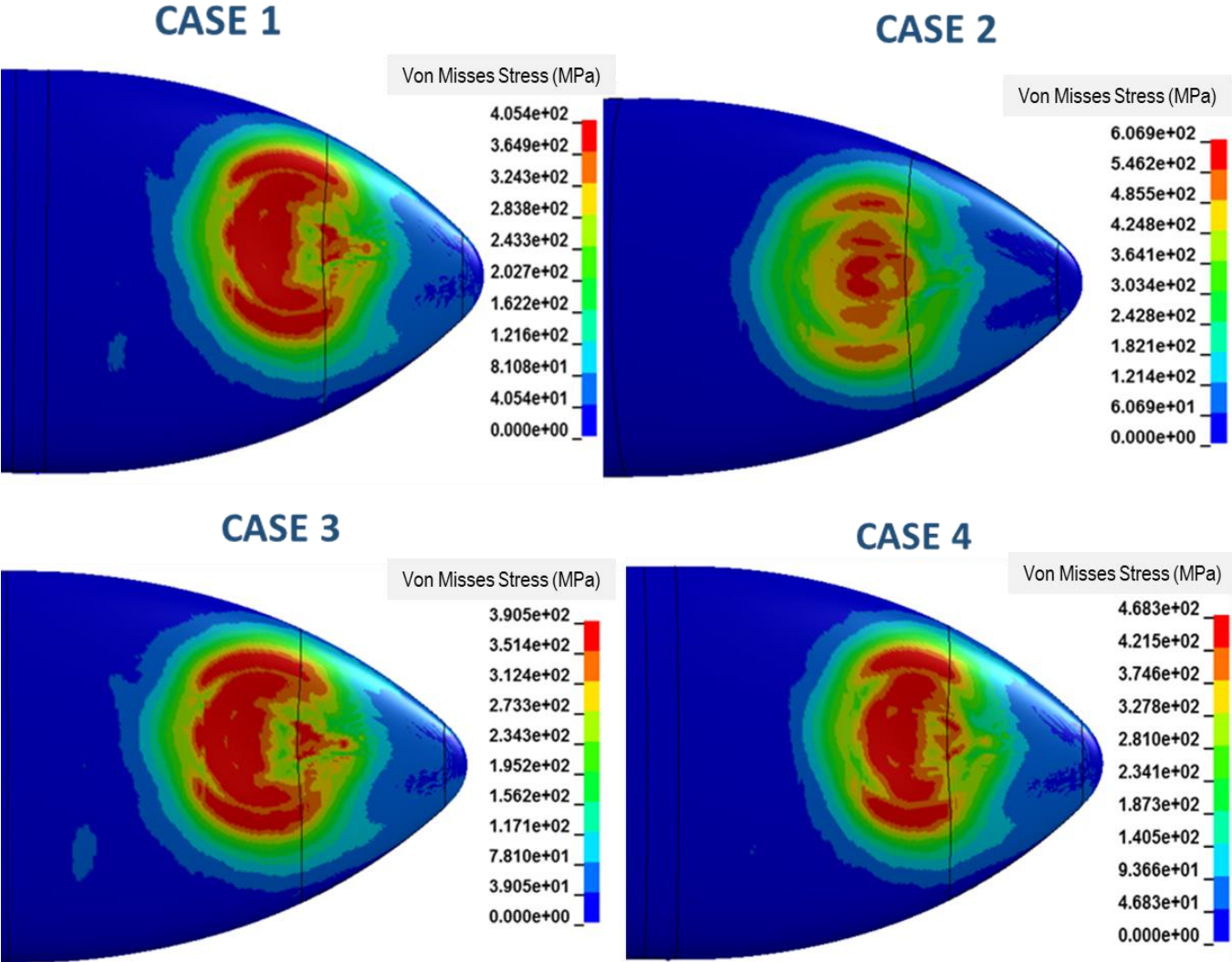


Figure 28 Von Misses Stress Results (MPa) at 1.5 ms for Impactor Position 1

There was no tearing or penetration on the skin of EFT. The stress distributions and effective stresses on skin are similar for Piecewise Linear Plasticity material model and Johnson Cook Material model.

Von Misses Stress results at 2.0 ms for impactor position 1 is shown in Figure 29.

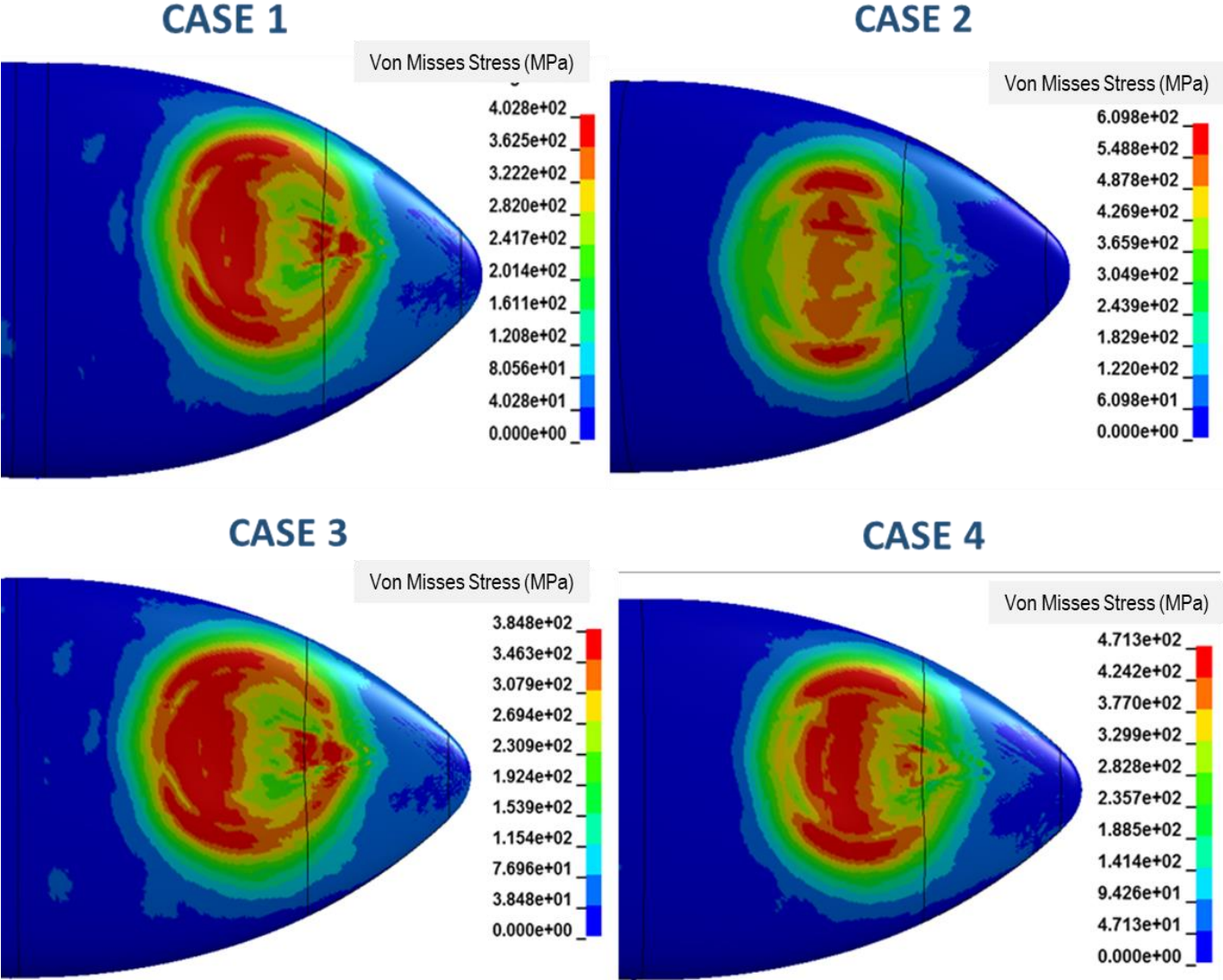


Figure 29 Von Misses Stress Results (MPa) at 2.0 ms for Impactor Position 1

There was no tearing or penetration on the skin of EFT. The stress distributions and effective stresses on skin are similar for Piecewise Linear Plasticity material model and Johnson Cook Material model.

Von Misses Stress results at 2.5 ms for impactor position 1 is shown in Figure 30.

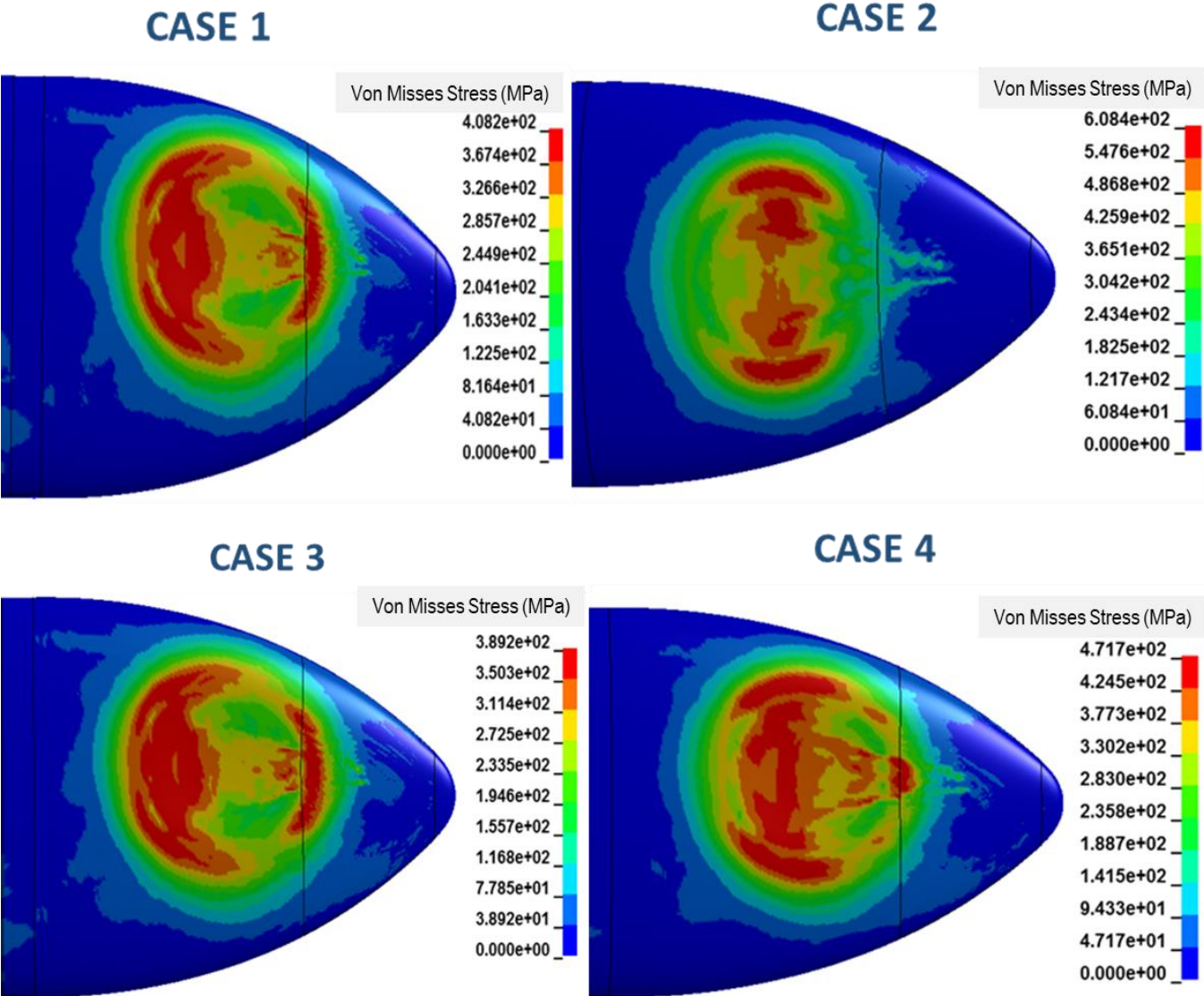


Figure 30 Von Misses Stress Results (MPa) at 2.5 ms for Impactor Position 1

There was no tearing or penetration on the skin of EFT. The stress distributions and effective stresses on skin are similar for Piecewise Linear Plasticity material model and Johnson Cook Material model.

Von Misses Stress results at 3.0 ms for impactor position 1 is shown in Figure 31.

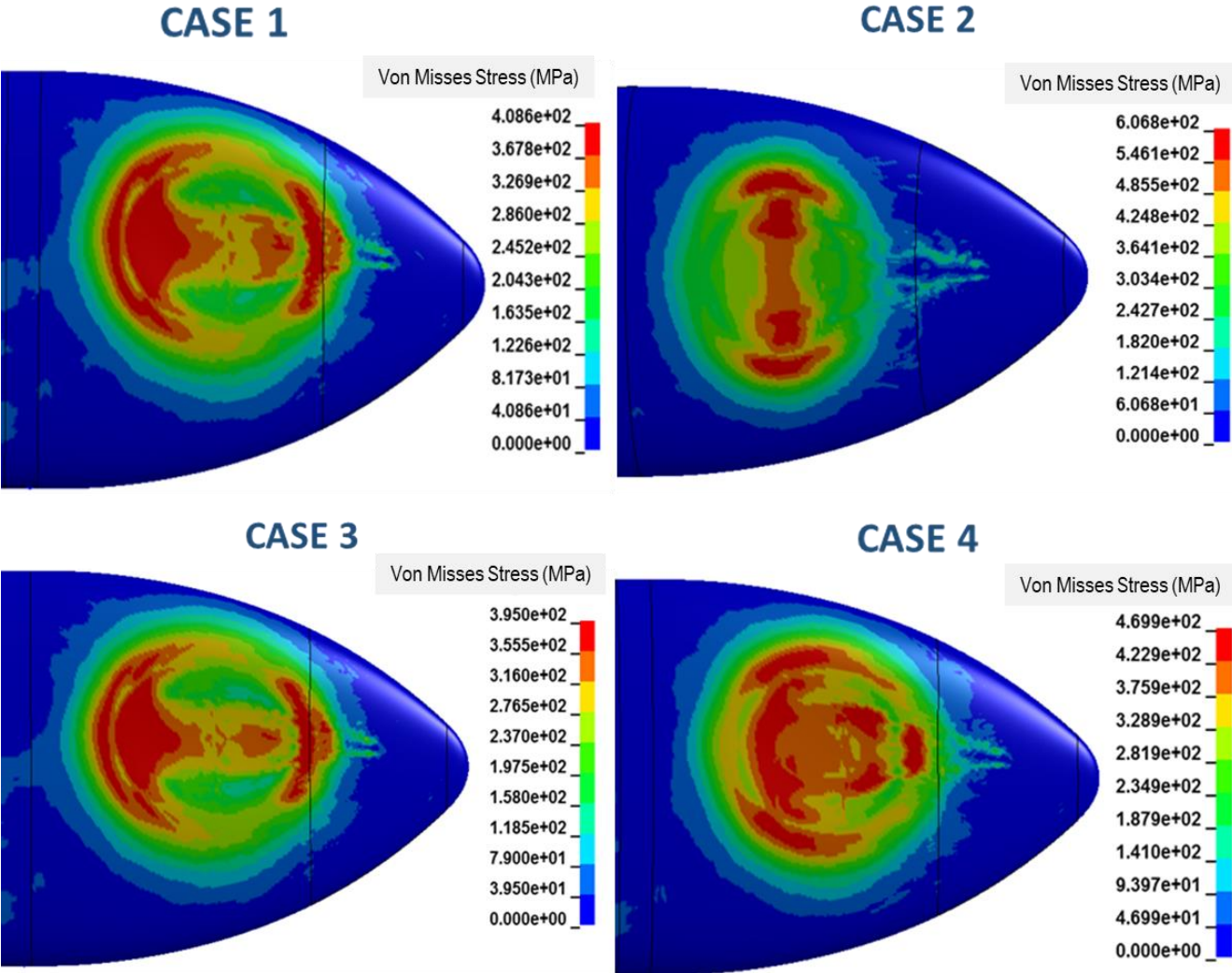


Figure 31 Von Misses Stress Results (MPa) at 3.0 ms for Impactor Position 1

There was no tearing or penetration on the skin of EFT. The stress distributions and effective stresses on skin are similar for Piecewise Linear Plasticity material model and Johnson Cook Material model.

Von Misses Stress results at 3.5 ms for impactor position 1 is shown in Figure 32.

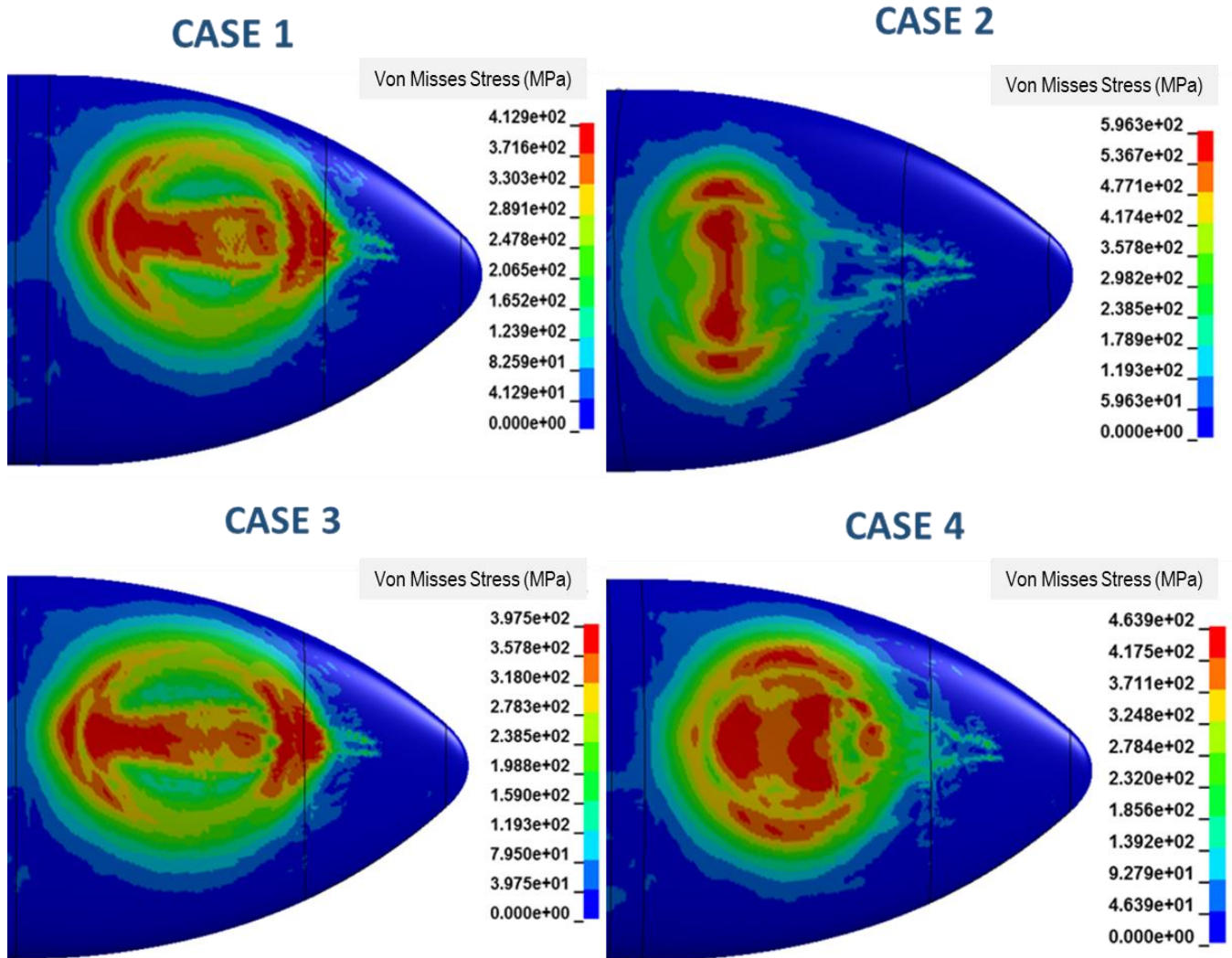


Figure 32 Von Misses Stress Results (MPa) at 3.5 ms for Impactor Position 1

There was no tearing or penetration on the skin of EFT. The stress distributions and effective stresses on skin are similar for Piecewise Linear Plasticity material model and Johnson Cook Material model.

Von Misses Stress results at 4.0 ms for impactor position 1 is shown in Figure 33.

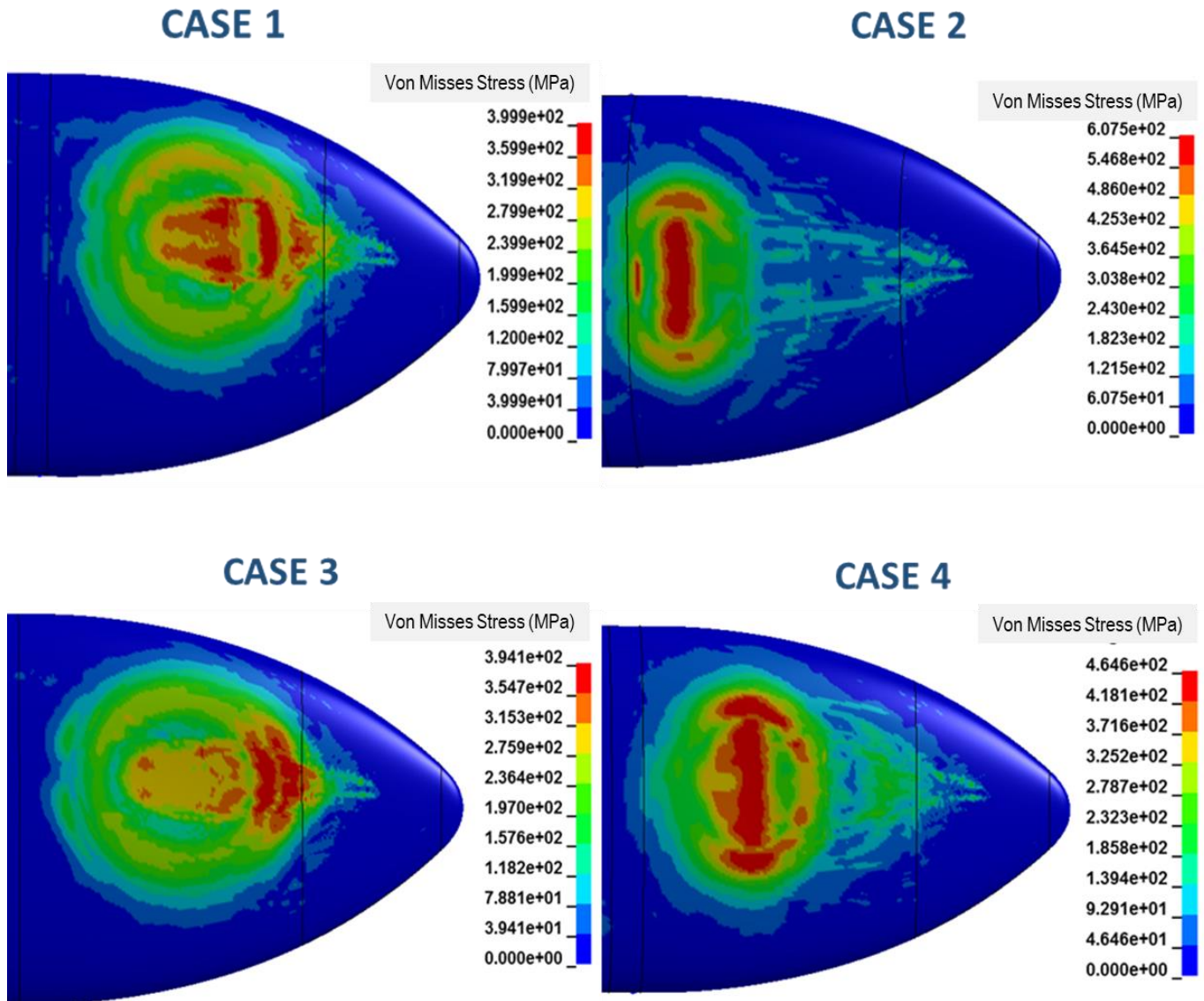


Figure 33 Von Misses Stress Results (MPa) at 4.0 ms for Impactor Position 1

There was no tearing or penetration on the skin of EFT. The stress distributions and effective stresses on skin are similar for Piecewise Linear Plasticity material model and Johnson Cook Material model.

Von Misses Stress results at 4.5 ms for impactor position 1 is shown in Figure 34.

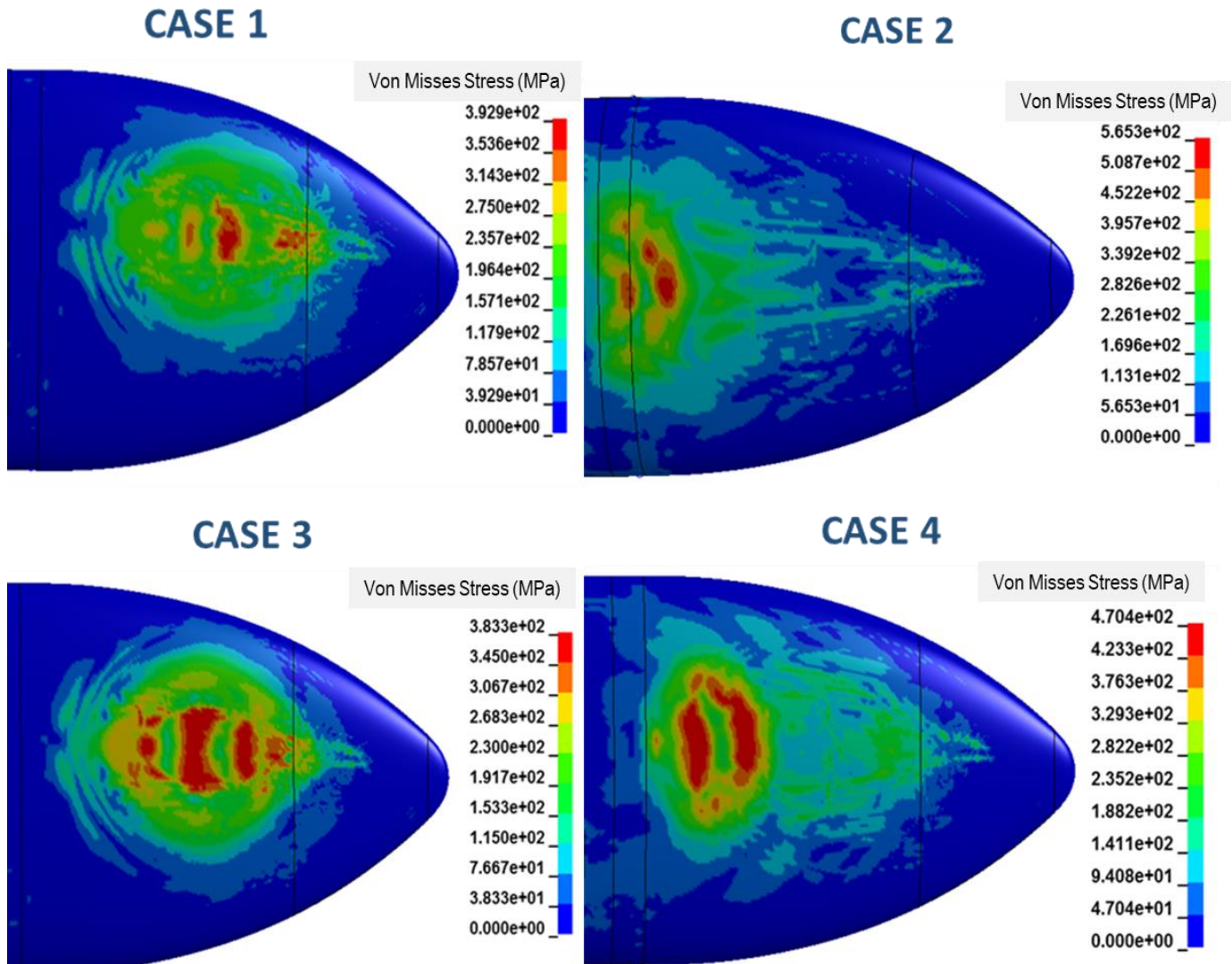


Figure 34 Von Misses Stress Results (MPa) at 4.5 ms for Impactor Position 1

There was no tearing or penetration on the skin of EFT. The stress distributions and effective stresses on skin are similar for Piecewise Linear Plasticity material model and Johnson Cook Material model. Impact ended in 4.5 ms.

Von Misses Stress results at 5.0 ms for impactor position 1 is shown in Figure 35.



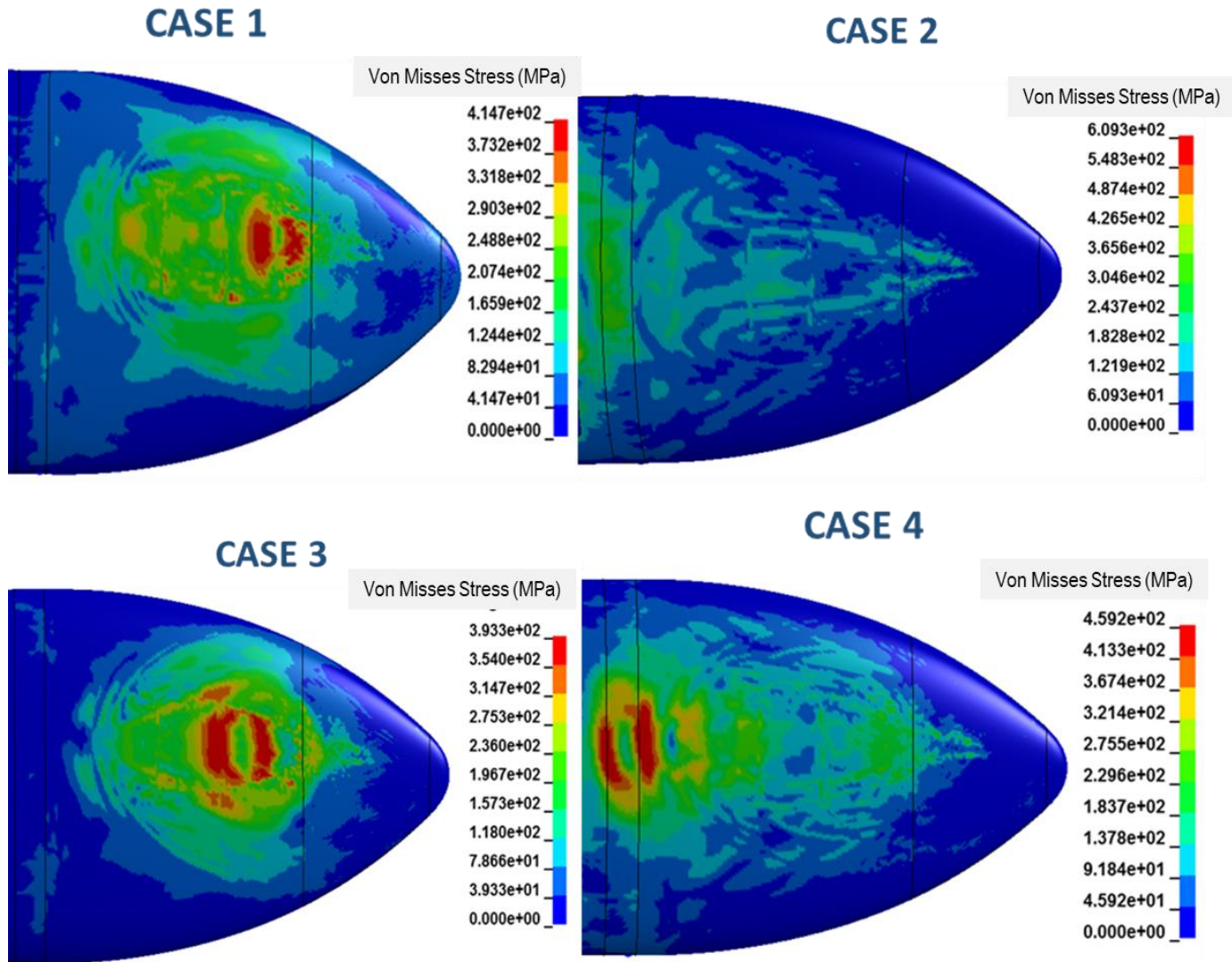


Figure 35 Von Misses Stress Results (MPa) at 3.0 ms for Impactor Position 1

There was no tearing or penetration on the skin of EFT. The stress distributions and effective stresses on skin are similar for Piecewise Linear Plasticity material model and Johnson Cook Material model. Impact ended in 4.5 ms.

The stresses and displacements on EFT skin are shown in Figure 16 to Figure 35. The plastic deformation began at 0.5ms as shown in Figure 26. There was no tearing or penetration on the skin of EFT. The stress distributions and effective stresses on skin are similar for Piecewise Linear Plasticity material model and Johnson Cook Material model.

Maximum stress on EFT skin was 415 MPa for Case 1, 634MPa for Case 2, 399MPa for Case 3, 487MPa for Case 4.

Energy variations for Position 1 (for case 1,2,3 and 4) is given in Figure 36. While kinetic energy decreased, internal energy increased almost linearly. Total energy remained almost constant, which is the ideal result.

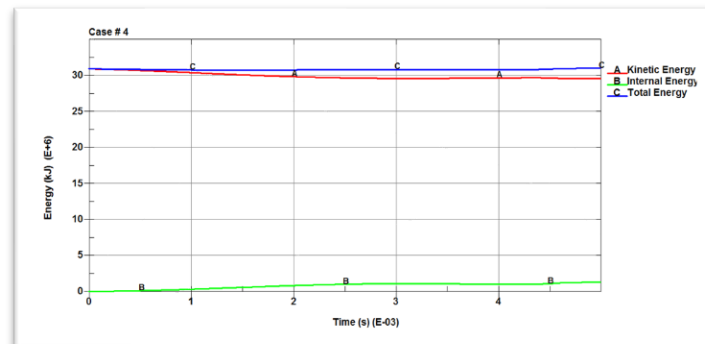
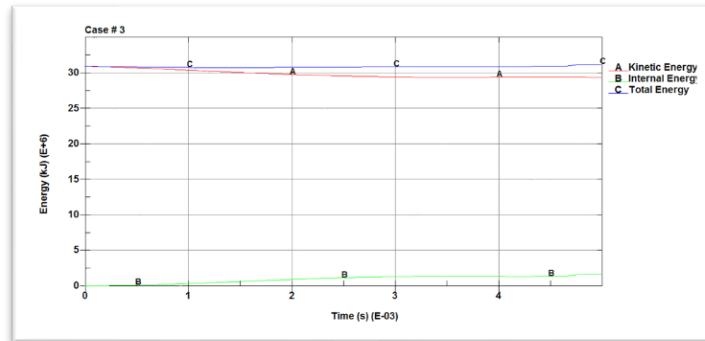
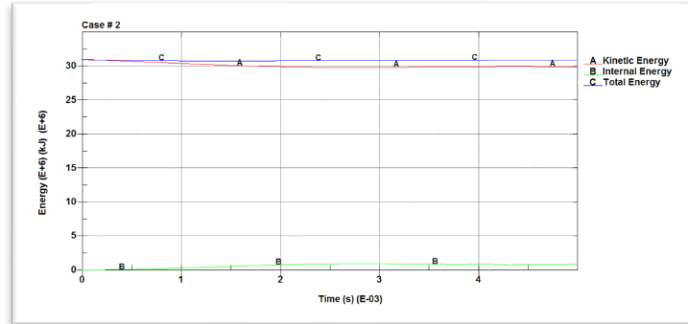
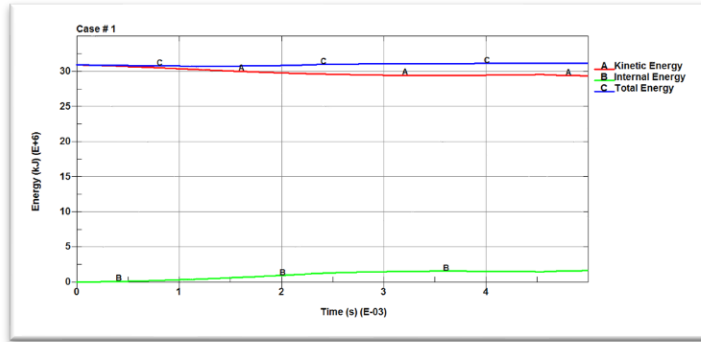


Figure 36 Energy Variation of Position 1

Energy ratios for Position 1 (for case 1,2,3 and 4) is given in Figure 37. Energy ratios for position 1 remained within the acceptable limits as shown.

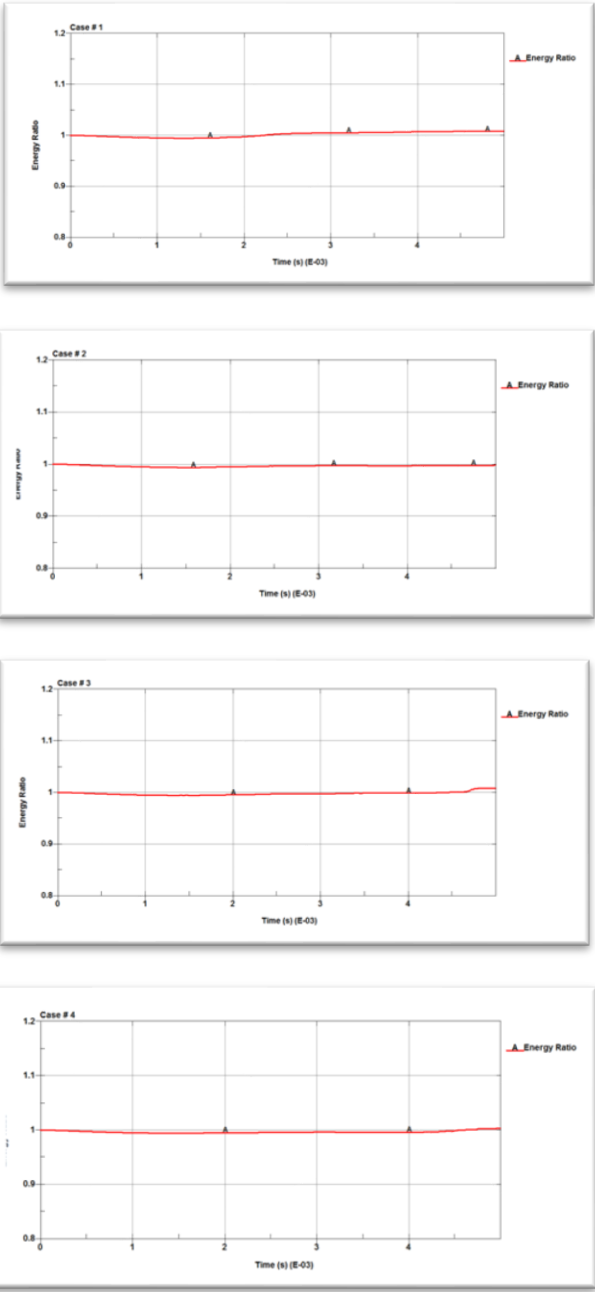


Figure 37 Energy Ratio of Position 1

Hourglass energy, damping energy and sliding energy for case 1 is given in Figure 38. Impact ended in 4.5 ms. Hourglass energy remained 0 for 4.5 ms. For sliding energy, peak did not occur.

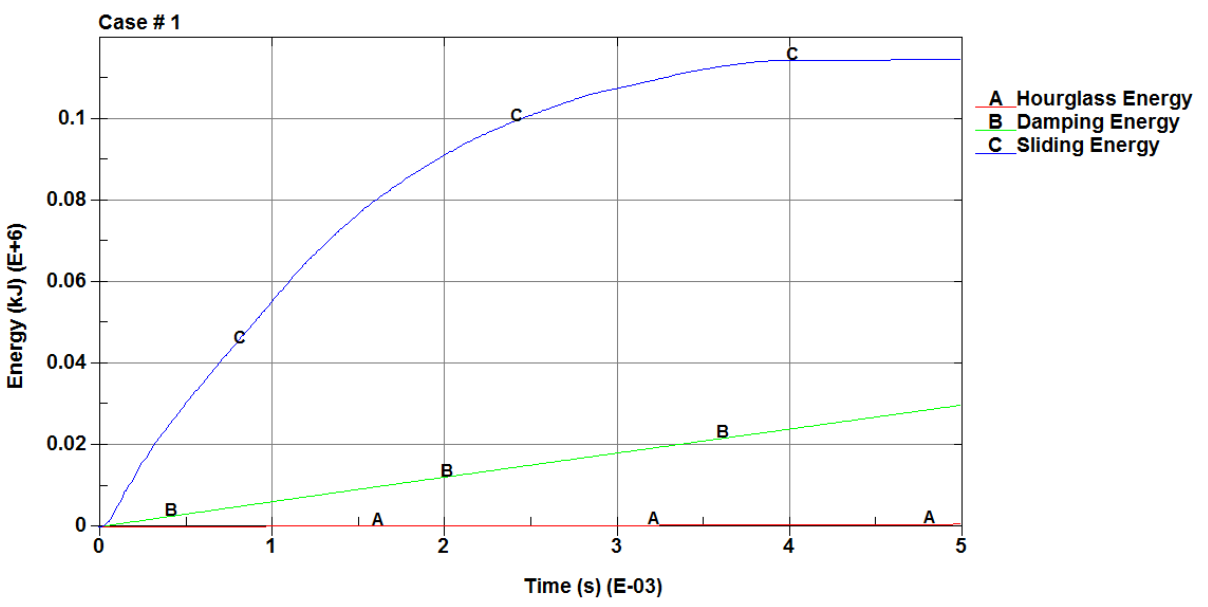


Figure 38 Hourglass, Damping and Sliding Energies Variation of Case 1

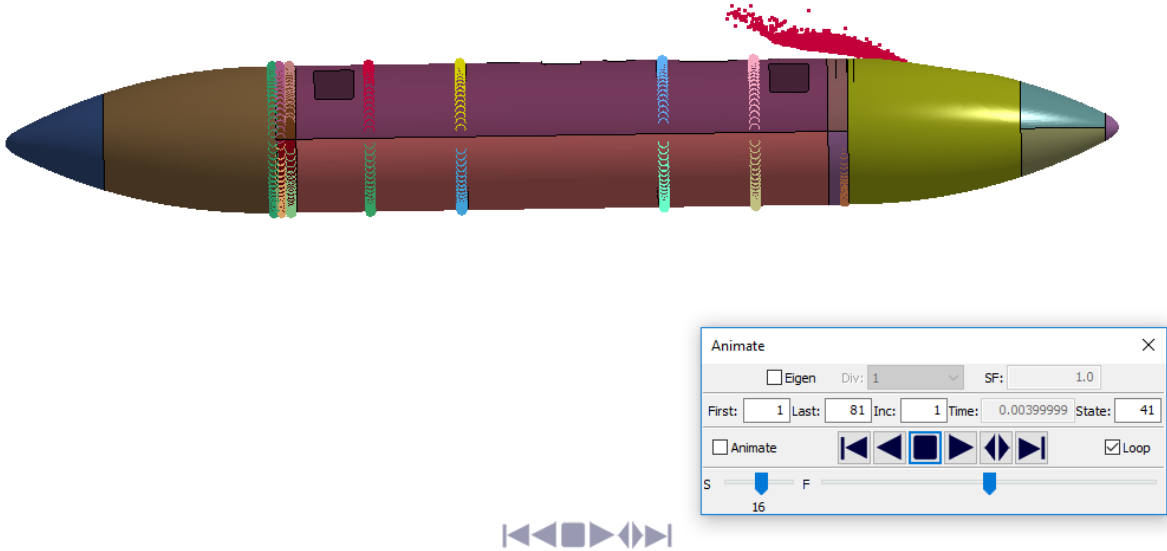


Figure 39 Bird Impact at 4 ms for Case 1

Hourglass energy, damping energy and sliding energy for case 2 is given in Figure 40. Impact ended in 4.0 ms. Hourglass energy remained 0 for 4.0 ms. For sliding energy, peak occurred after the contact between impactor and target ended.

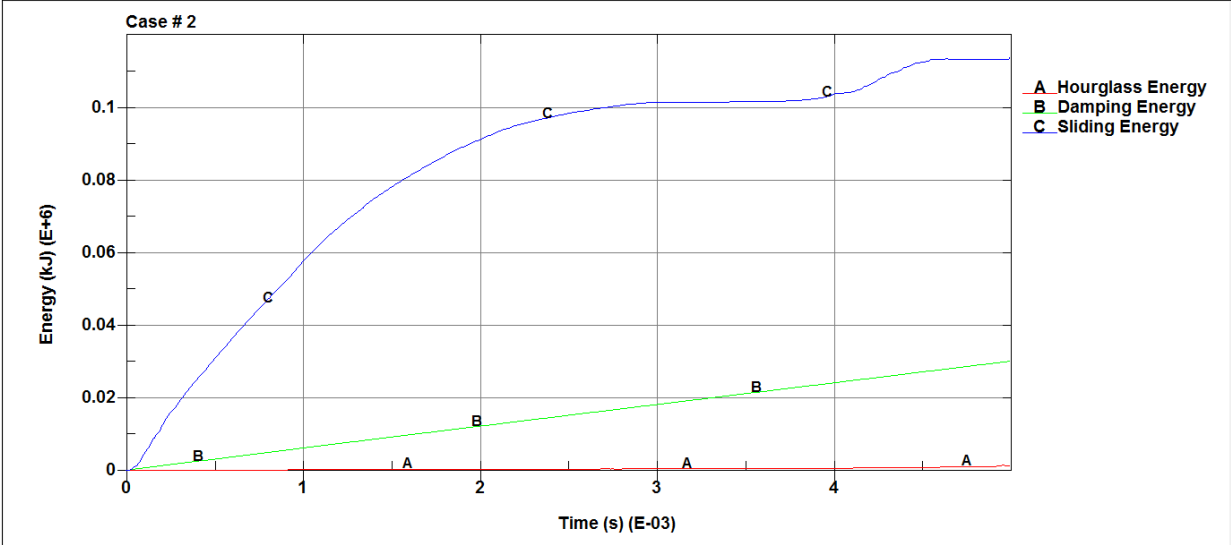


Figure 40 Hourglass, Damping and Sliding Energies Variation of Case 2

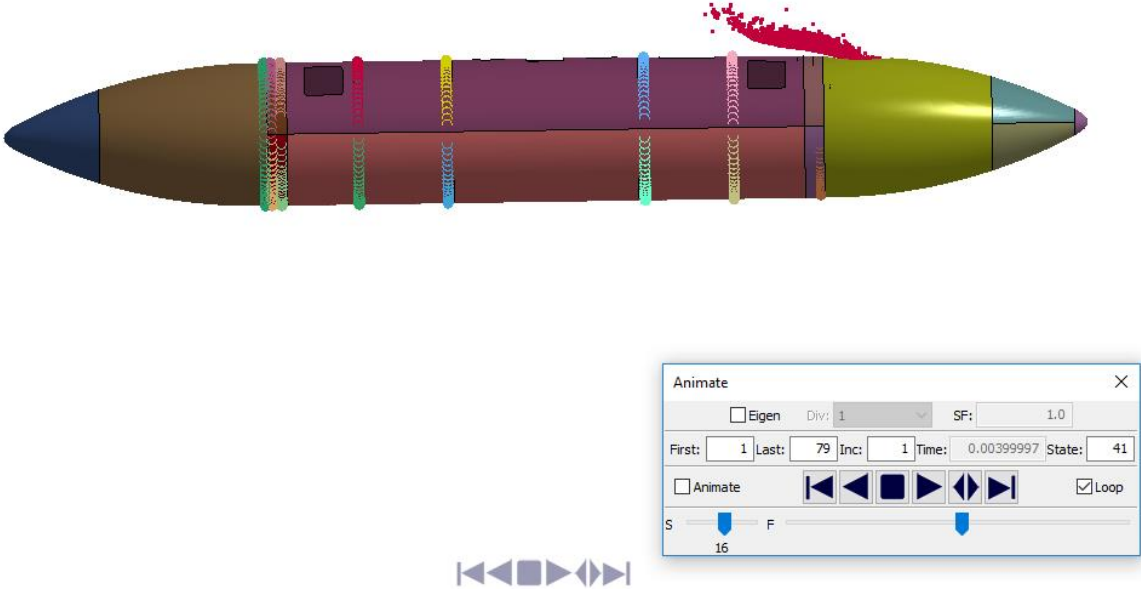


Figure 41 Bird Impact at 4 ms for Case 2

Hourglass energy, damping energy and sliding energy for case 3 is given in Figure 42. Impact ended in 4.4 ms. Hourglass energy remained 0 for 4.4 ms. For sliding energy, peak did not occur.

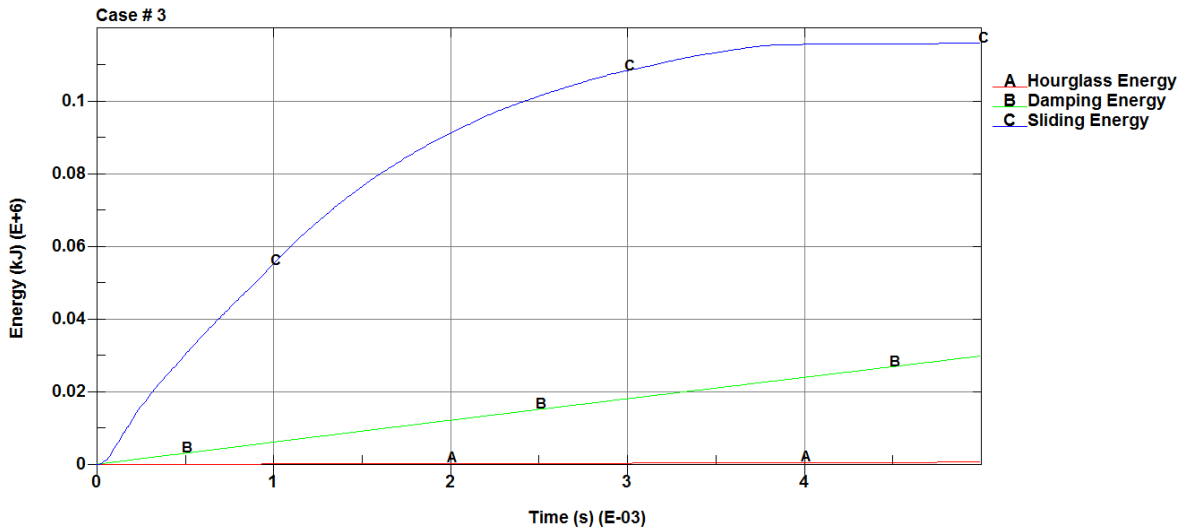


Figure 42 Hourglass, Damping and Sliding Energies Variation of Case 3

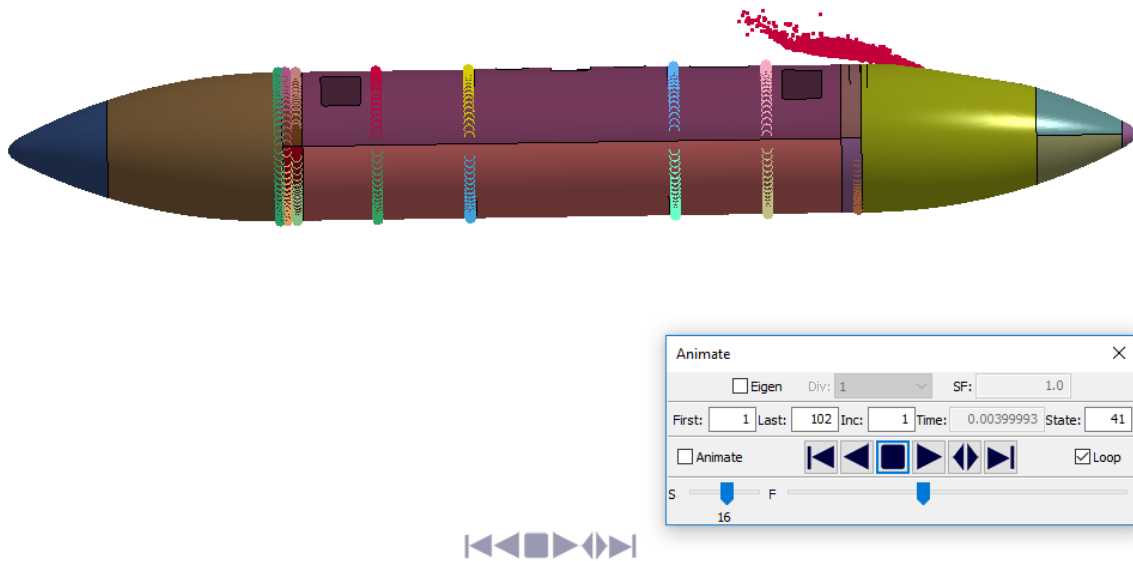


Figure 43 Bird Impact at 4 ms for Case 3

Hourglass energy, damping energy and sliding energy for case 4 is given in Figure 44. Impact ended in 4.5 ms. Hourglass energy remained 0 for 4.5 ms. For sliding energy, peak did not occur.

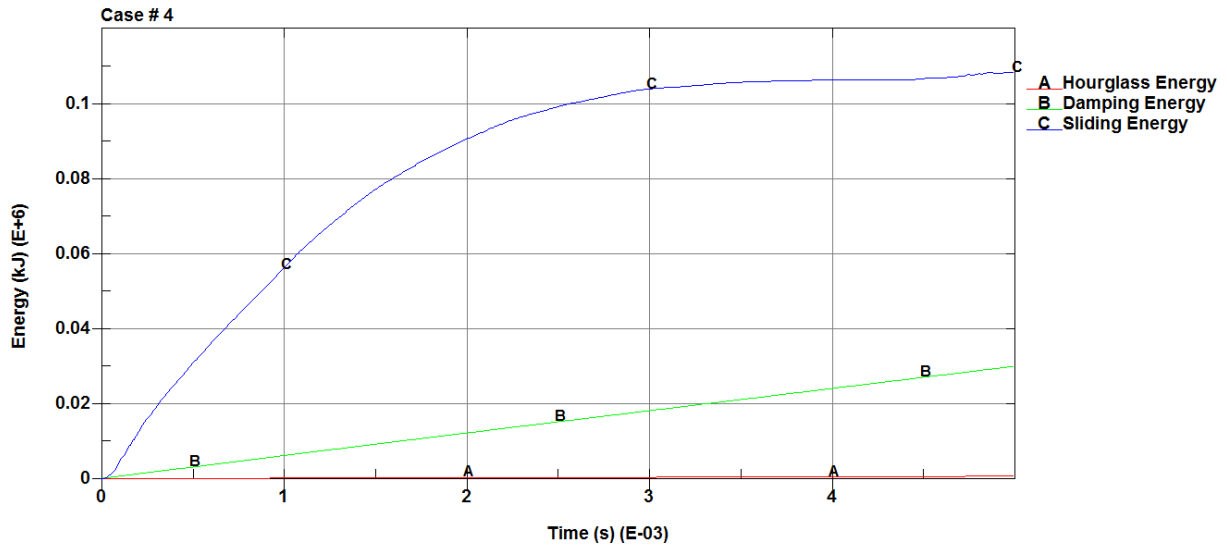


Figure 44 Hourglass, Damping and Sliding Energies Variation of Case 4

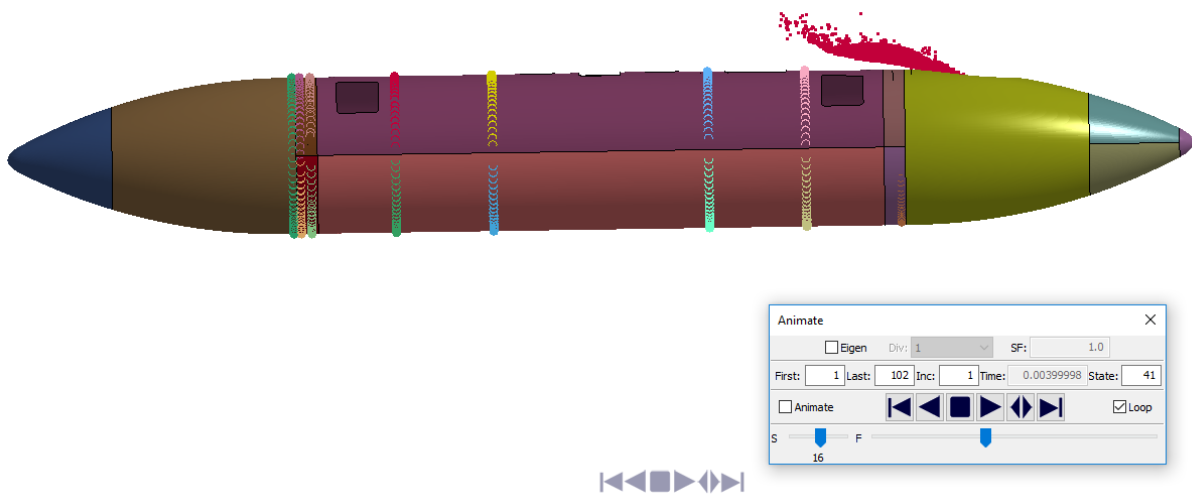


Figure 45 Bird Impact at 4 ms for Case 4

## **Analysis Results for Position 2**

An overview of the impact simulation for the position 2 was given for the general understanding. The time history was presented as a series of time step plots with explanations. The plots in Figure 46 to Figure 65 show the simulation run in several steps. Total simulation time was set to 5 ms and plots were saved in the intervals of 0.5ms.



Displacement results at 0.5 ms for impactor position 2 is shown in Figure 46.

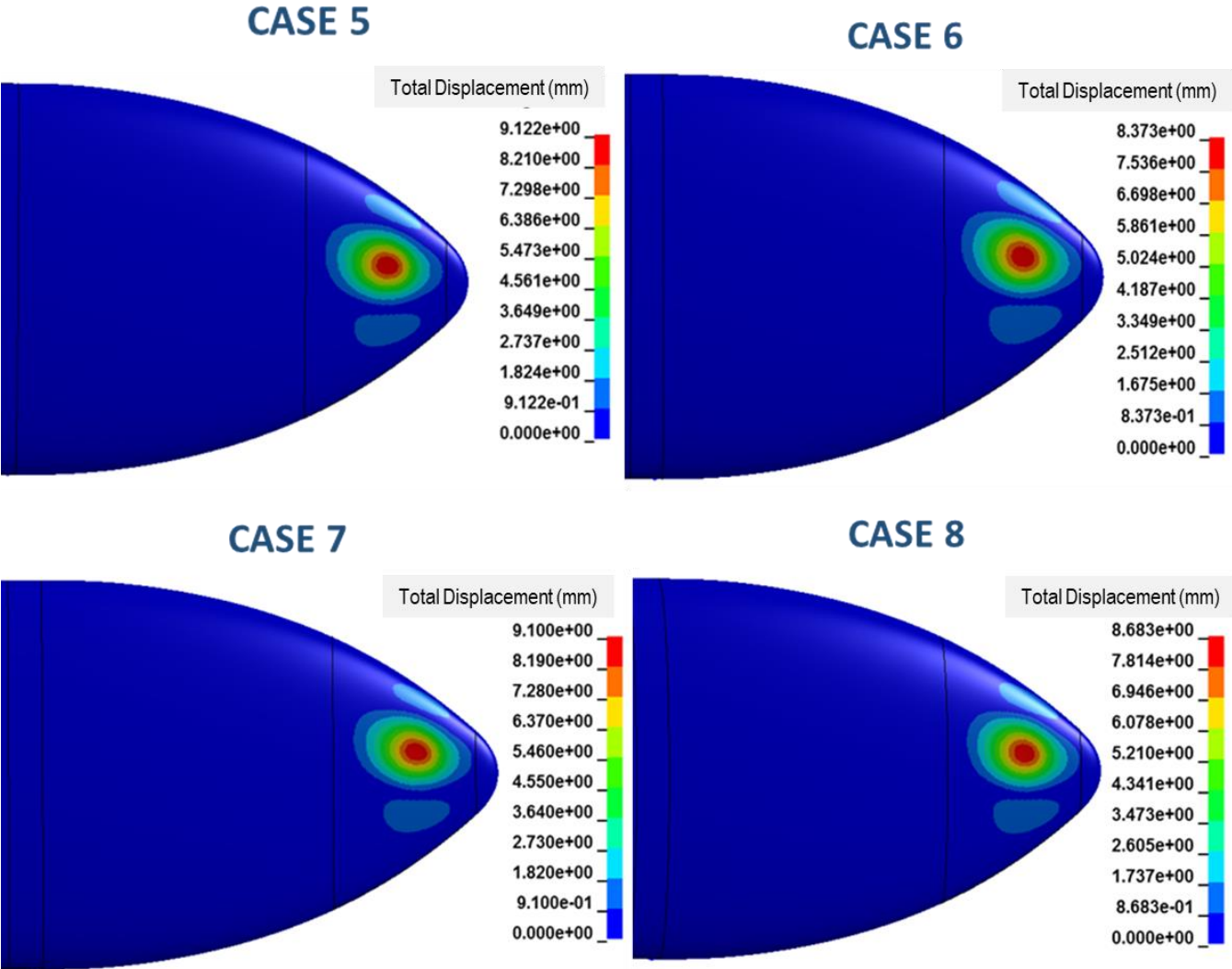


Figure 46 Displacement Results (mm) at 0.5 ms for Impactor Position 2

Displacements on Al 7075 -T6 and Al 2024-T3 are similar. Displacement values according to Piecewise Linear Plasticity material model are also similar to Johnson Cook Material model.

Displacement results at 1.0 ms for impactor position 2 is shown in Figure 47.

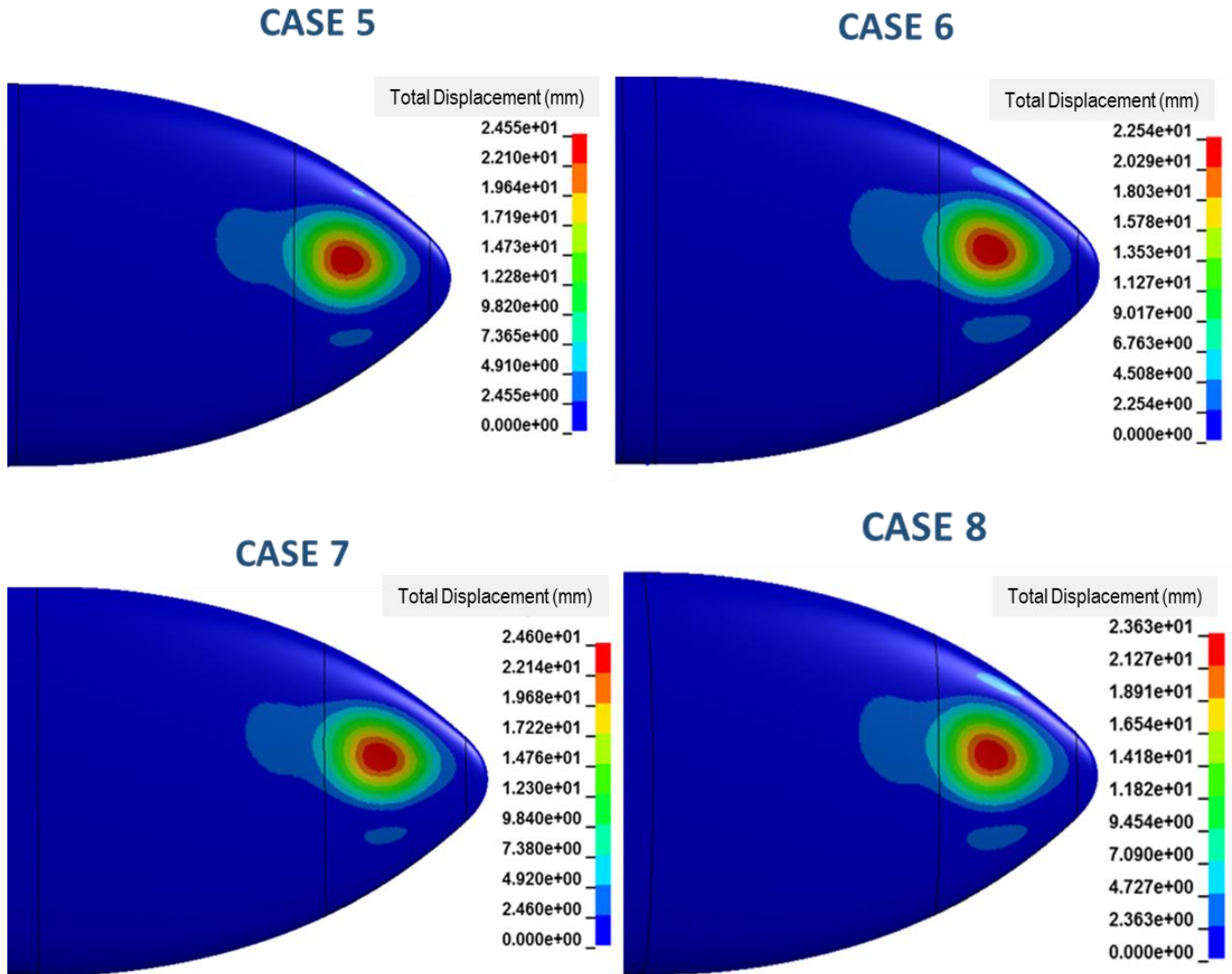


Figure 47 Displacement Results (mm) at 1.0 ms for Impactor Position 2

Displacements on Al 7075 -T6 and Al 2024-T3 are similar. Displacement values according to Piecewise Linear Plasticity material model are also similar to Johnson Cook Material model.

Displacement results at 1.5 ms for impactor position 2 is shown in Figure 48.

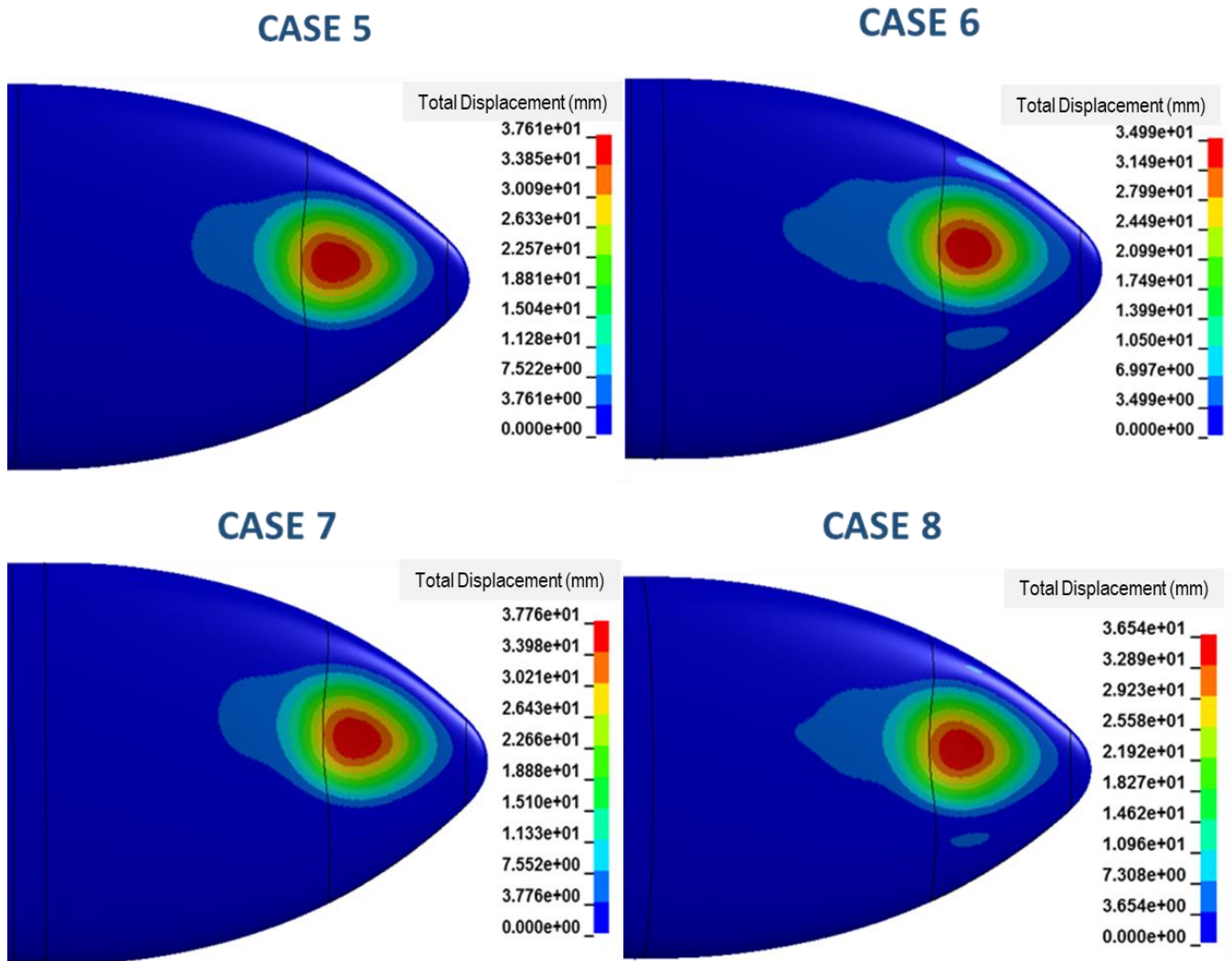


Figure 48 Displacement Results (mm) at 1.5 ms for Impactor Position 2

Displacements on Al 7075 -T6 and Al 2024-T3 are similar. Displacement values according to Piecewise Linear Plasticity material model are also similar to Johnson Cook Material model.

Displacement results at 2.0 ms for impactor position 2 is shown in Figure 49.

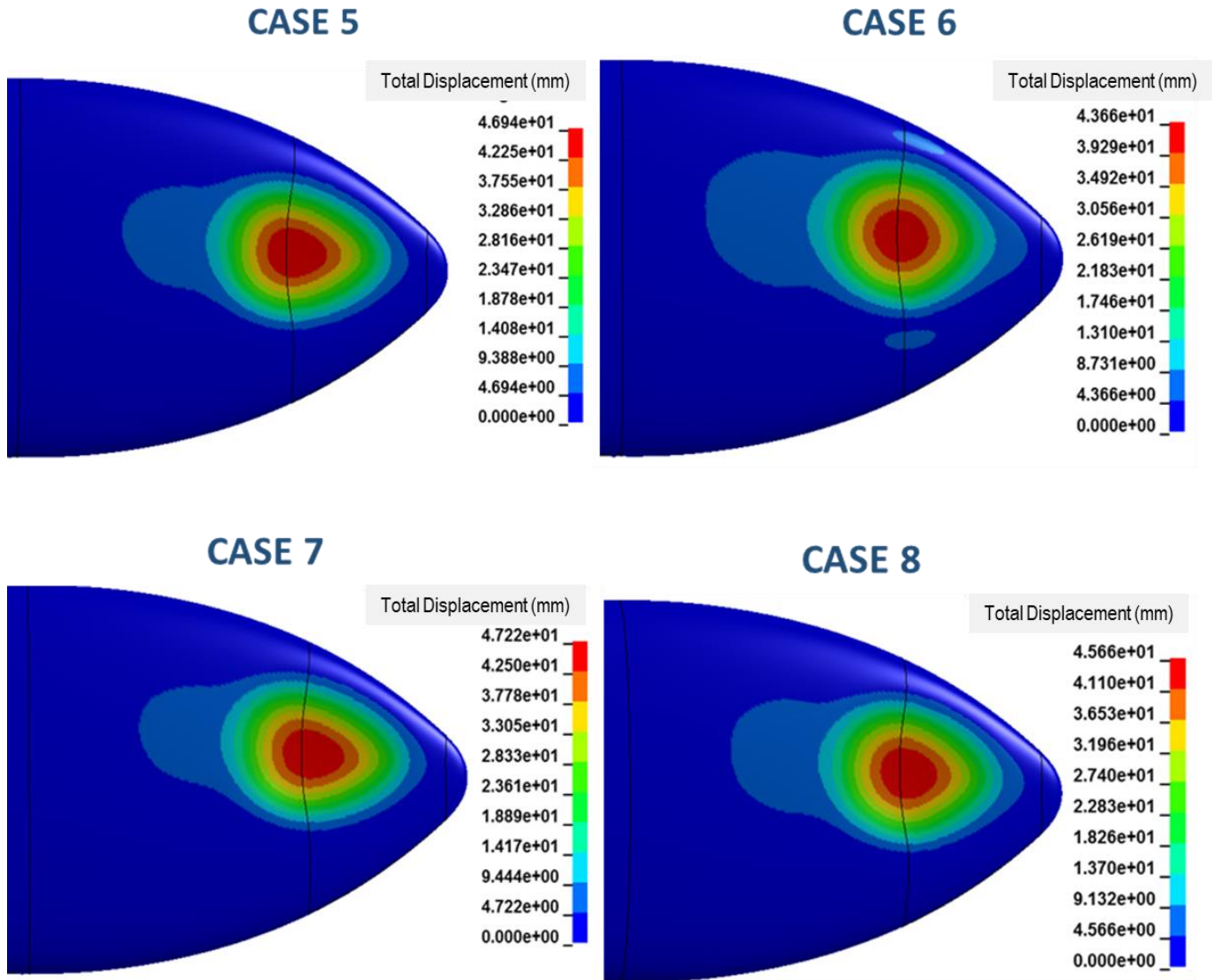


Figure 49 Displacement Results (mm) at 2.0 ms for Impactor Position 2

Displacements on Al 7075 -T6 and Al 2024-T3 are similar. Displacement values according to Piecewise Linear Plasticity material model are also similar to Johnson Cook Material model.

Displacement results at 2.5 ms for impactor position 2 is shown in Figure 50.

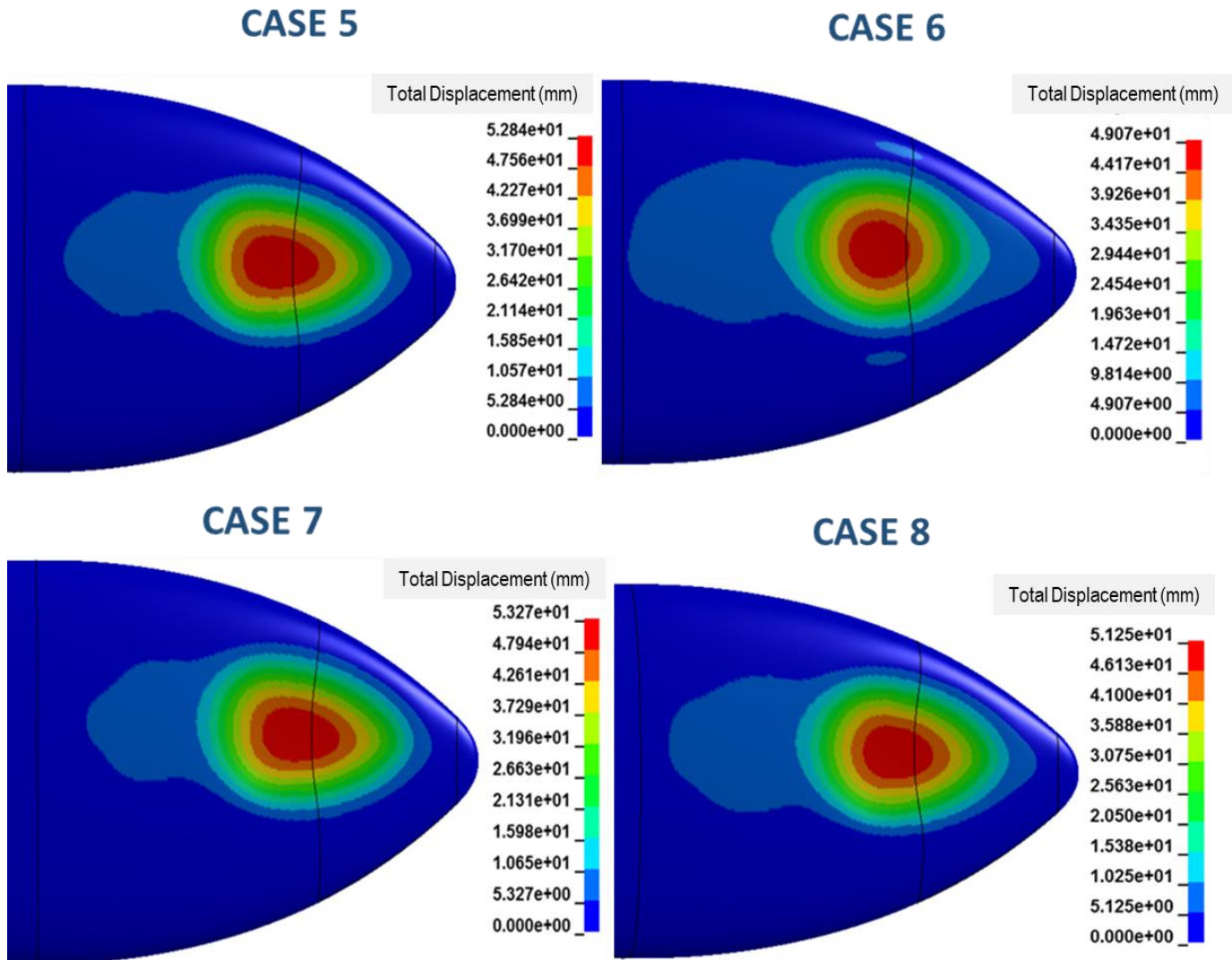


Figure 50 Displacement Results (mm) at 2.5 ms for Impactor Position 2

Displacements on Al 7075 -T6 and Al 2024-T3 are similar. Displacement values according to Piecewise Linear Plasticity material model are also similar to Johnson Cook Material model.

Displacement results at 3.0 ms for impactor position 2 is shown in Figure 51.

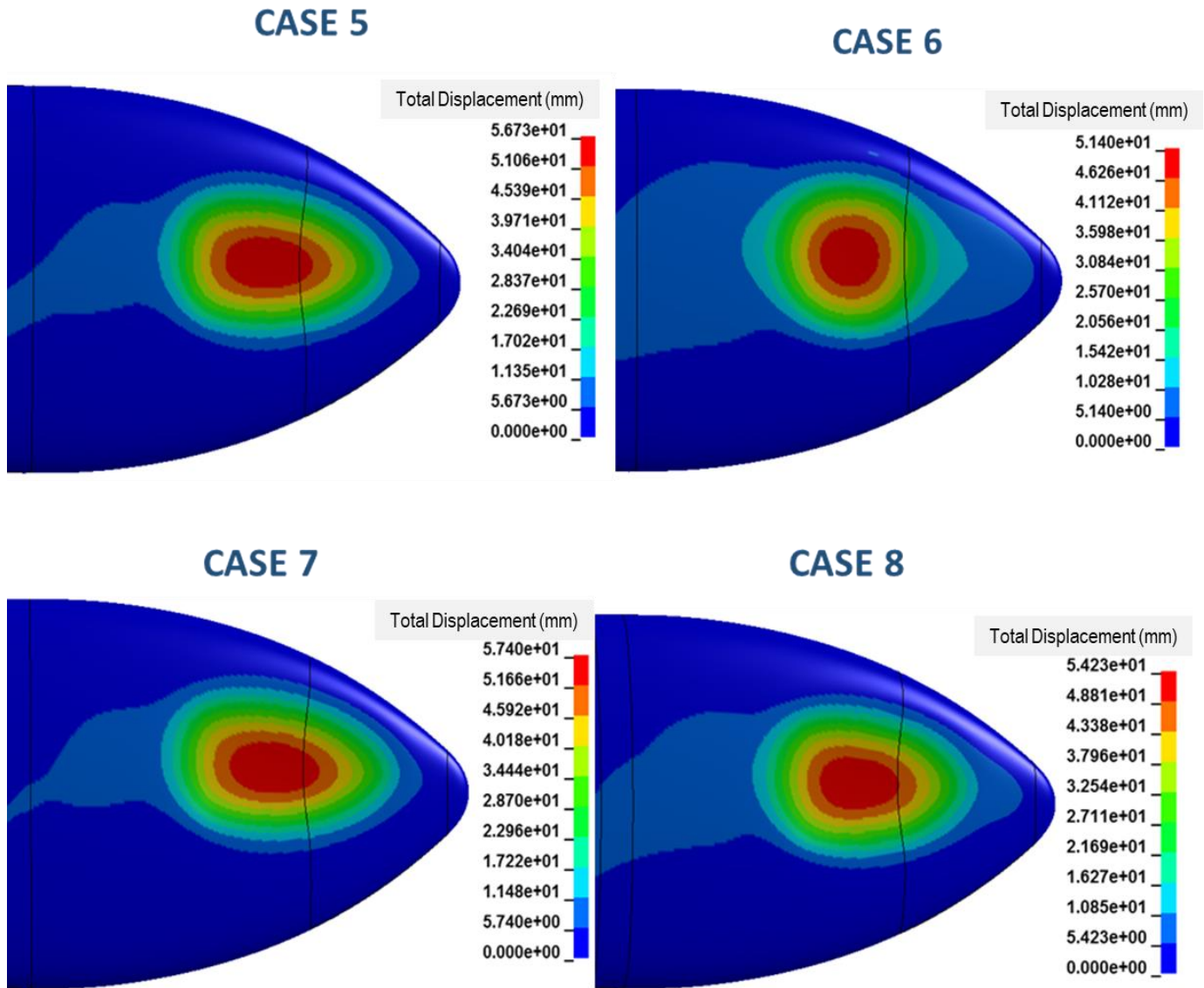


Figure 51 Displacement Results (mm) at 3.0 ms for Impactor Position 2

Displacements on Al 7075 -T6 and Al 2024-T3 are similar. Displacement values according to Piecewise Linear Plasticity material model are also similar to Johnson Cook Material model.

Displacement results at 3.5 ms for impactor position 2 is shown in Figure 52.

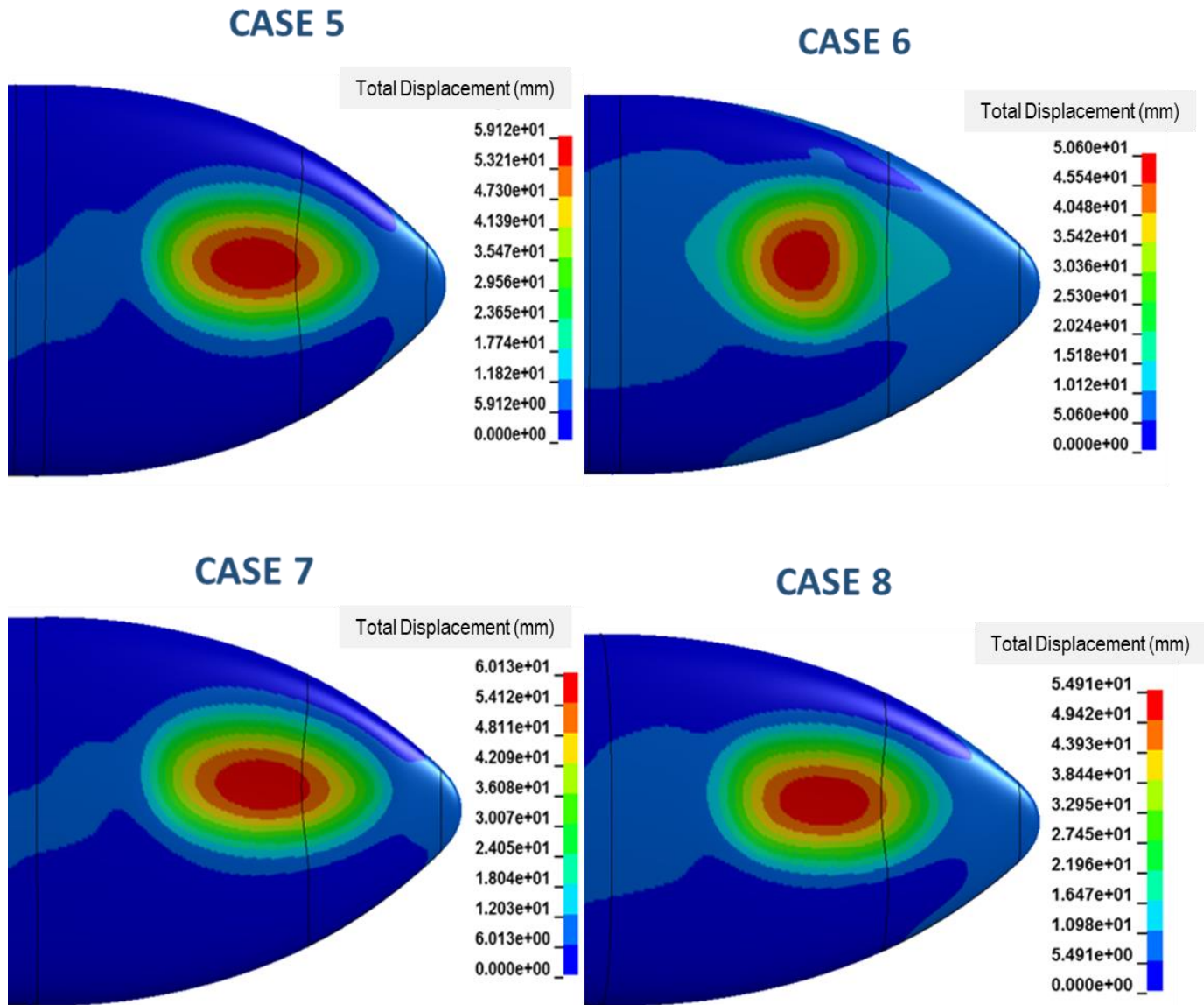


Figure 52 Displacement Results (mm) at 3.5 ms for Impactor Position 2

Displacements on Al 7075 -T6 and Al 2024-T3 are similar. Displacement values according to Piecewise Linear Plasticity material model are also similar to Johnson Cook Material model.

Displacement results at 4.0 ms for impactor position 2 is shown in Figure 53.

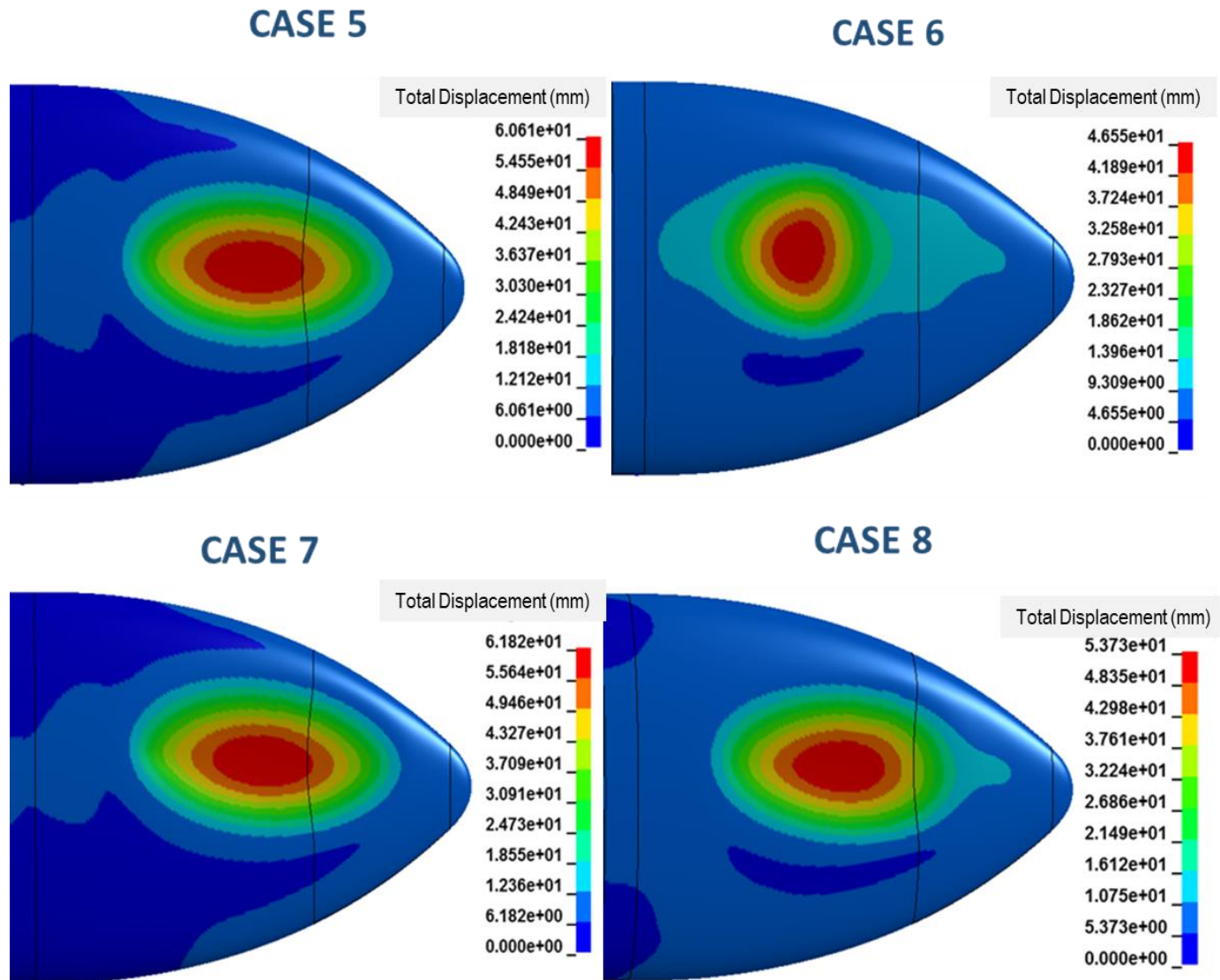


Figure 53 Displacement Results (mm) at 4.0 ms for Impactor Position 2

Displacements on Al 7075 -T6 and Al 2024-T3 are similar. Displacement values according to Piecewise Linear Plasticity material model are also similar to Johnson Cook Material model.

Displacement results at 4.5 ms for impactor position 2 is shown in Figure 54.



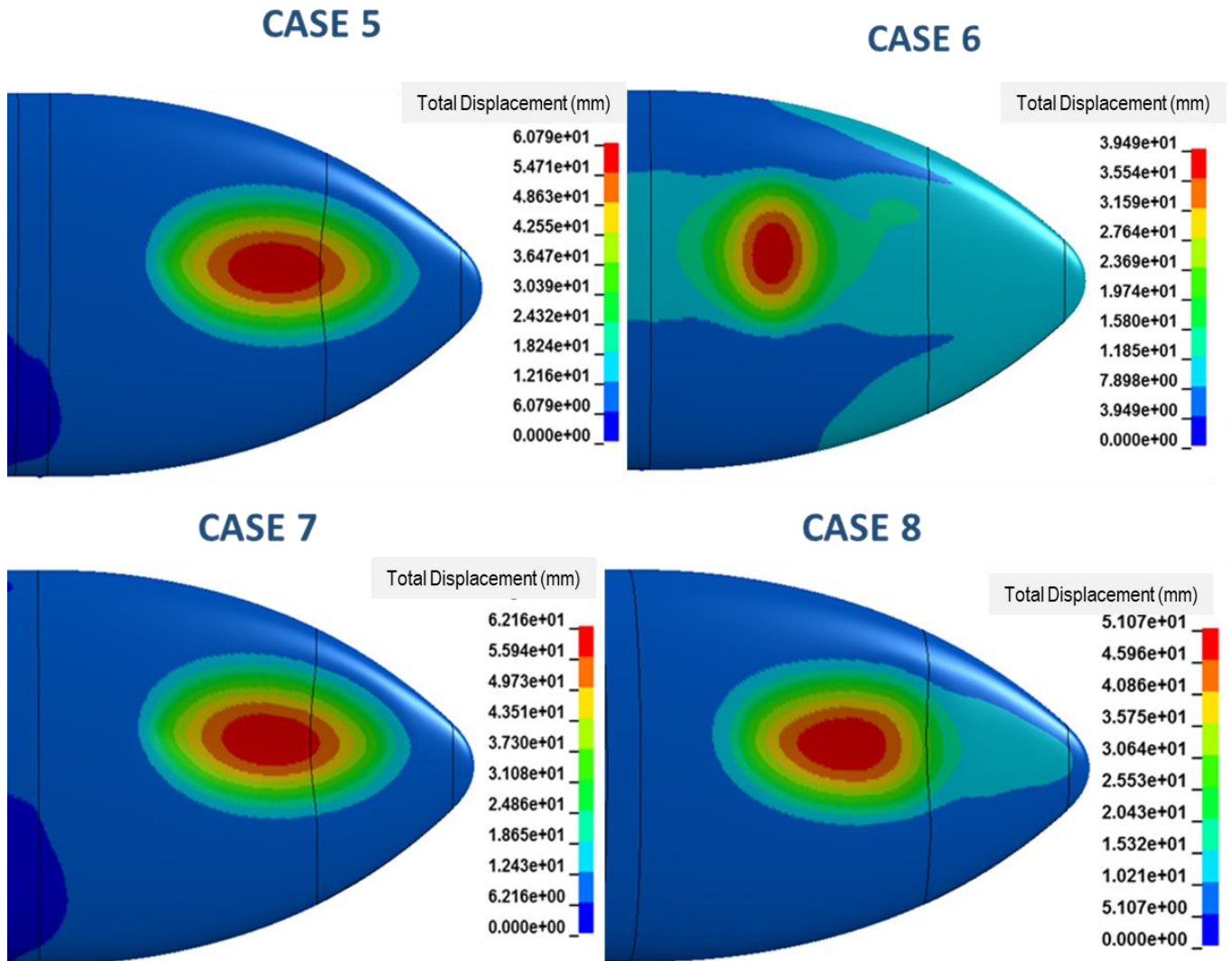


Figure 54 Displacement Results (mm) at 4.5 ms for Impactor Position 2

Displacements on Al 7075 -T6 and Al 2024-T3 are similar. Displacement values according to Piecewise Linear Plasticity material model are also similar to Johnson Cook Material model.

Displacement results at 5.0 ms for impactor position 2 is shown in Figure 55.

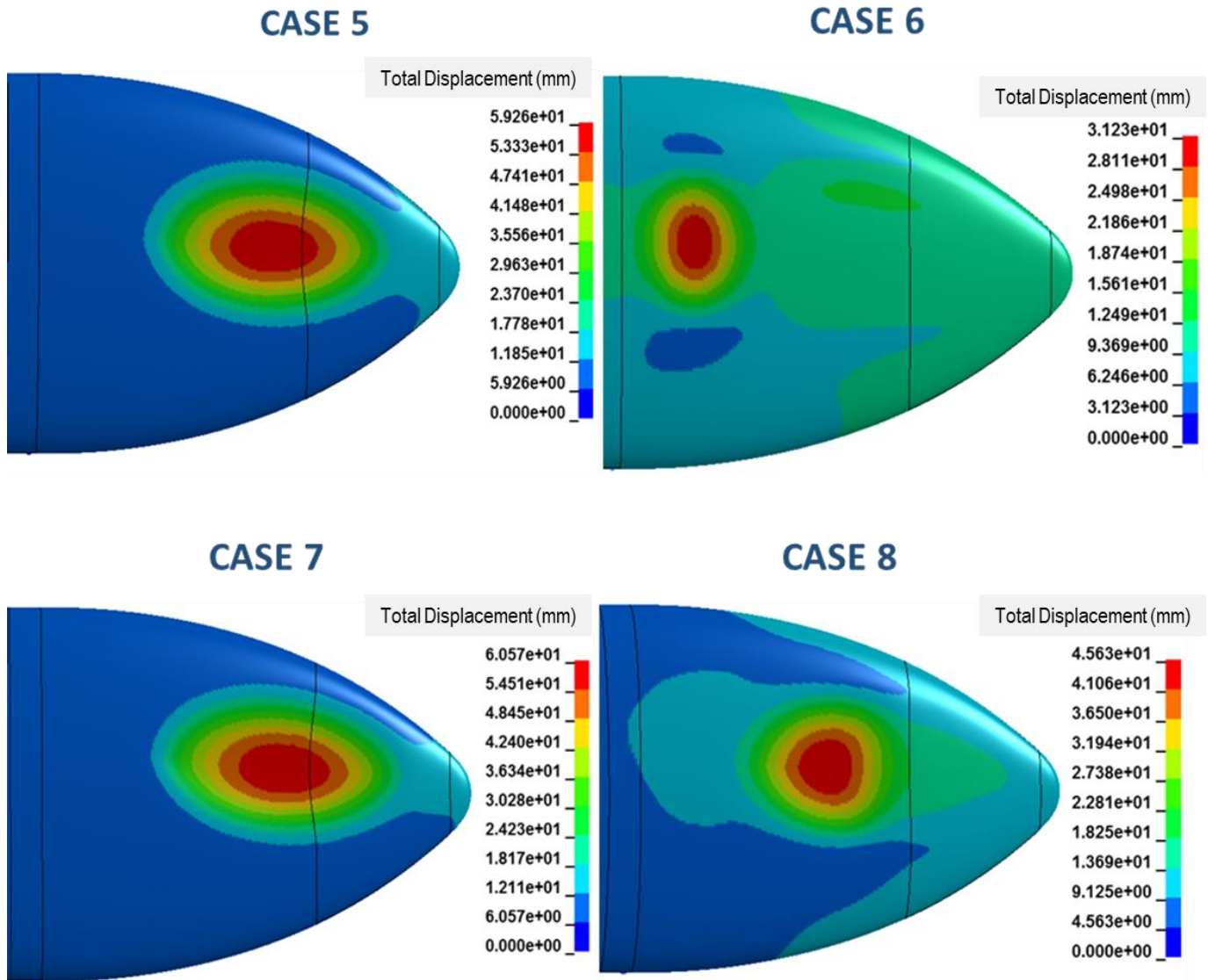


Figure 55 Displacement Results (mm) at 5.0 ms for Impactor Position 2

Displacements on Al 7075 -T6 and Al 2024-T3 are similar. Displacement values according to Piecewise Linear Plasticity material model are also similar to Johnson Cook Material model which is an expected result because of low strain rates. Impact ended in 5.0 ms.

For position 2, displacements on Al 7075 -T6 and Al 2024-T3 are similar. Displacement values according to Piecewise Linear Plasticity material model are also similar to Johnson Cook Material model.

After impact, screen shots were taken at 0.5ms intervals and the stresses were compared. Since the contact of the bird ended before 5 ms in general, the images were limited to this time period.

Von Misses Stress results at 0.5 ms for impactor position 2 is shown in Figure 56.

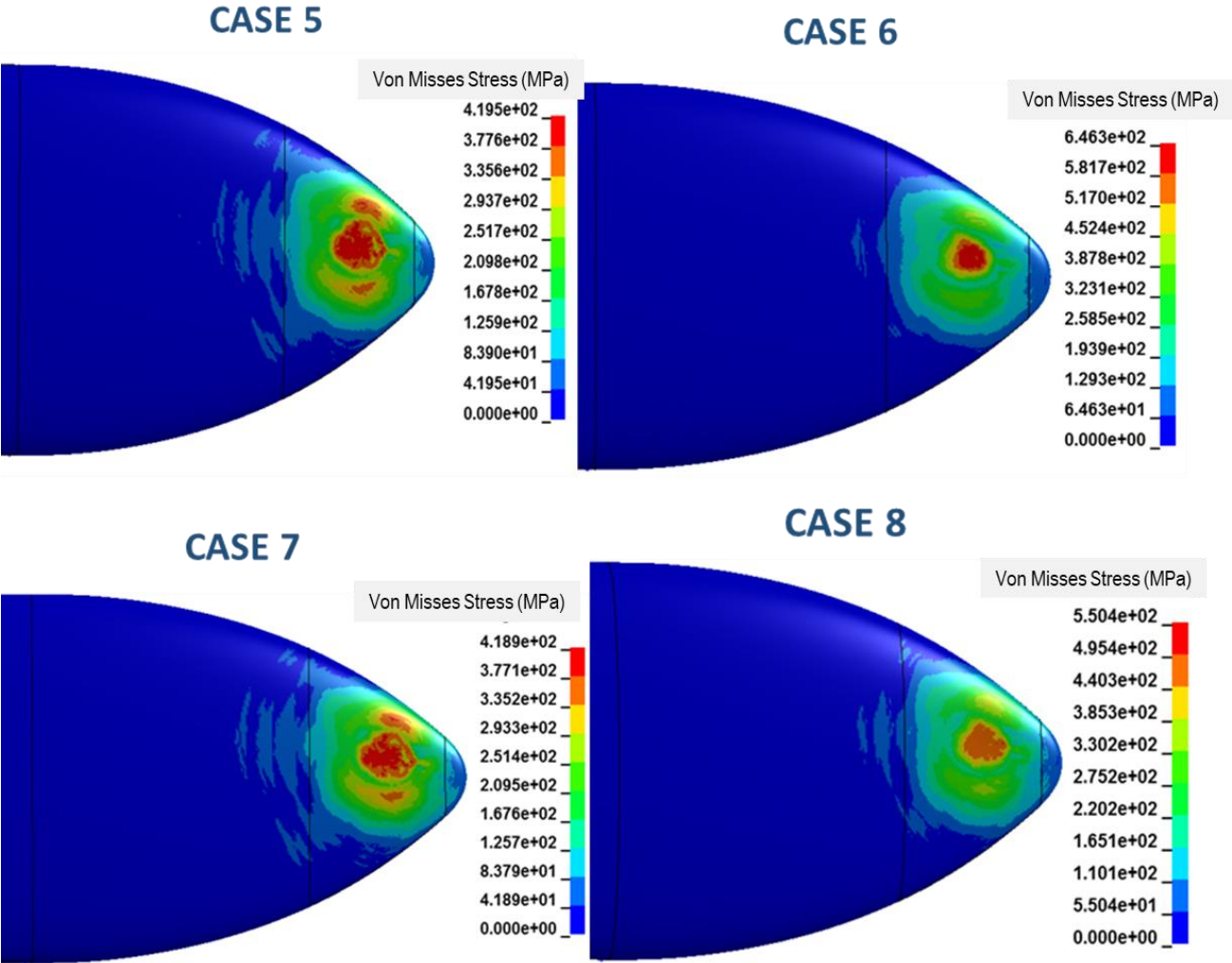


Figure 56 Von Misses Stress Results (MPa) at 0.5 ms for Impactor Position 2

EFT skin began to deform plastically at 0.5ms as shown in Figure 56. Tearing or penetration did not occur on the skin of EFT. The stress distributions and effective stresses on skin are similar for Piecewise Linear Plasticity material model and Johnson Cook Material model.

Von Misses Stress results at 1.0 ms for impactor position 2 is shown in Figure 57.

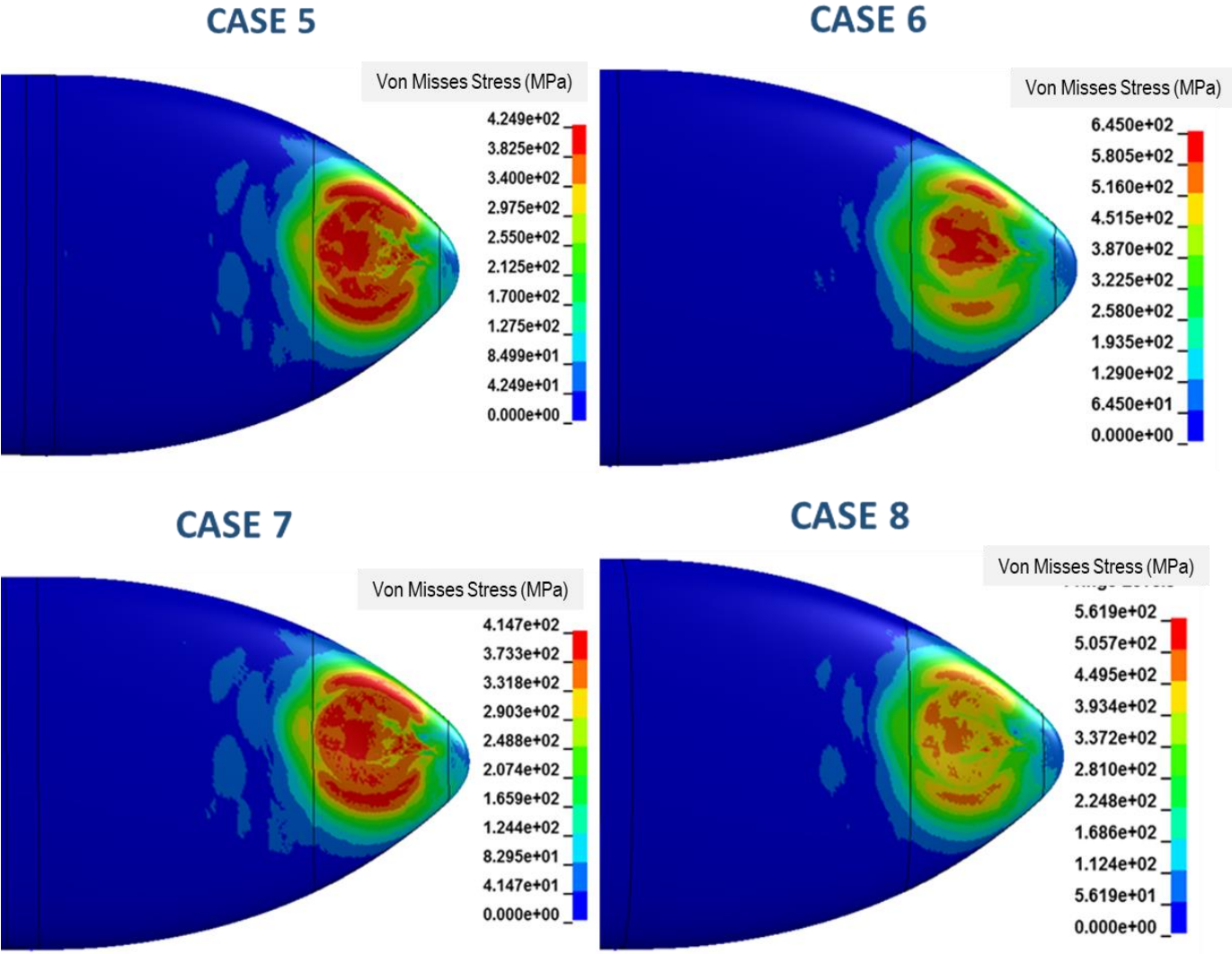


Figure 57 Von Misses Stress Results (MPa) at 1.0 ms for Impactor Position 2

Tearing or penetration did not occur on the skin of EFT. The stress distributions and effective stresses on skin are similar for Piecewise Linear Plasticity material model and Johnson Cook Material model.

Von Misses Stress results at 1.5 ms for impactor position 2 is shown in Figure 58.

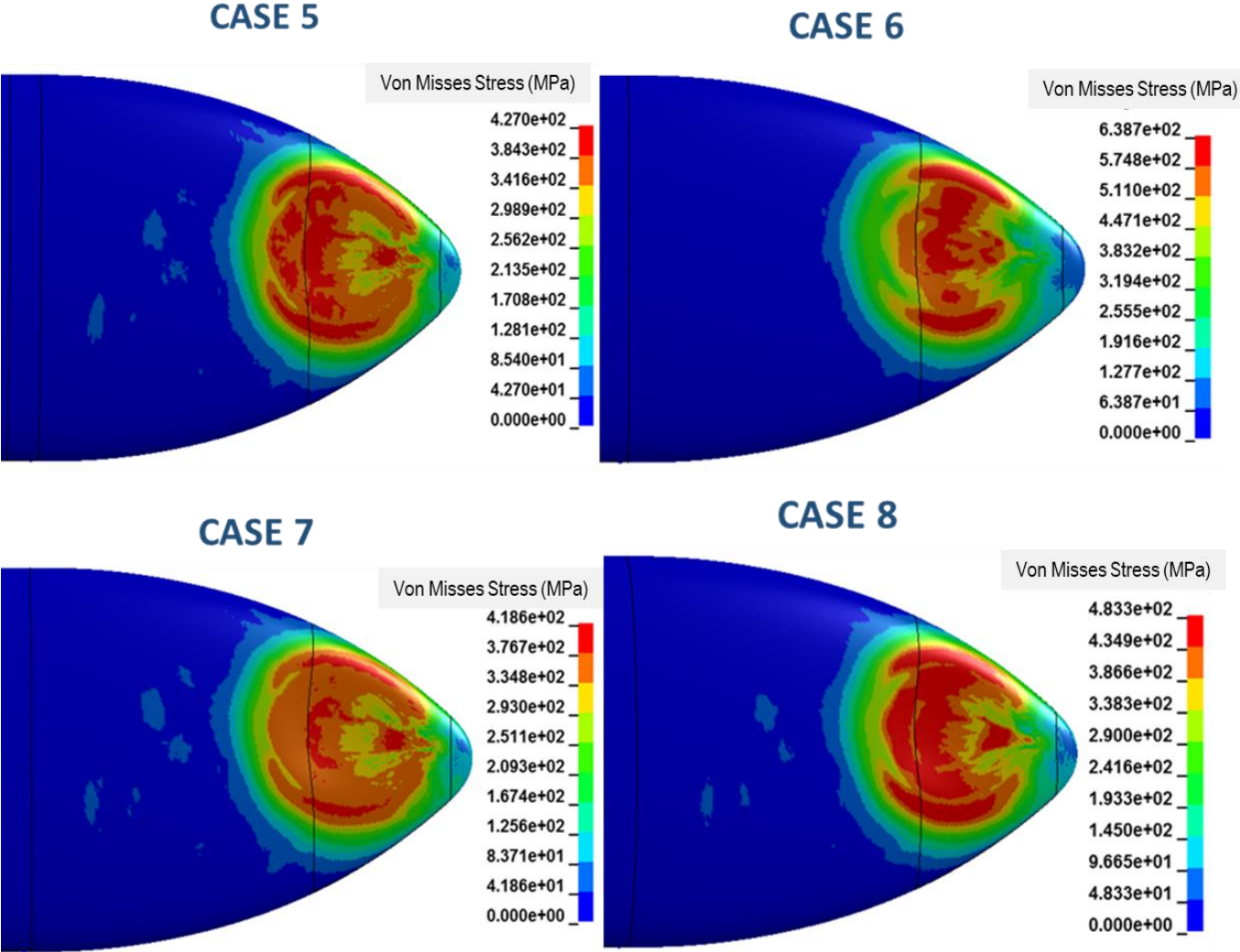


Figure 58 Von Misses Stress Results (MPa) at 1.5 ms for Impactor Position 2

Tearing or penetration did not occur on the skin of EFT. The stress distributions and effective stresses on skin are similar for Piecewise Linear Plasticity material model and Johnson Cook Material model.

Von Misses Stress results at 2.0 ms for impactor position 2 is shown in Figure 59.

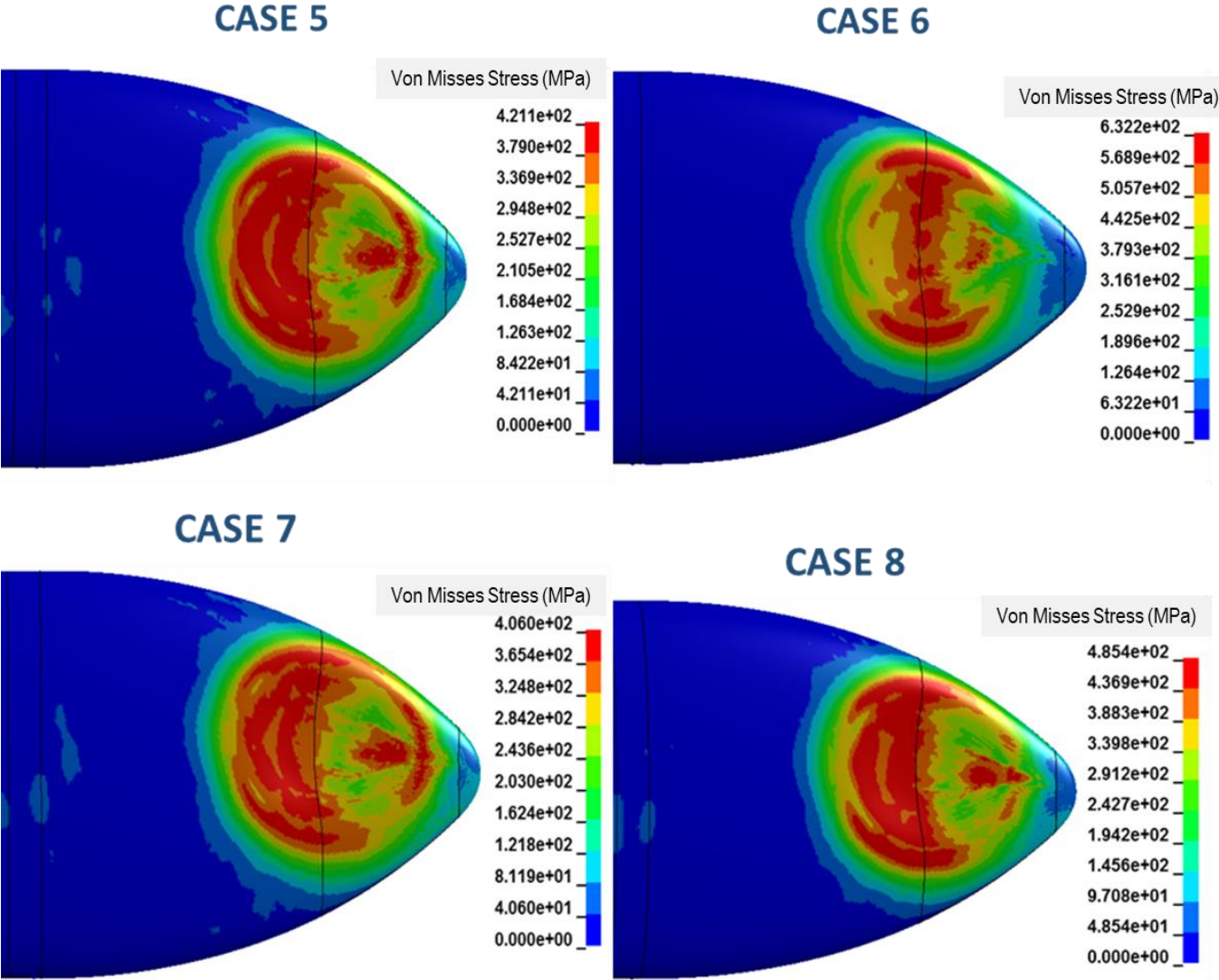


Figure 59 Von Misses Stress Results (MPa) at 2.0 ms for Impactor Position 2

Tearing or penetration did not occur on the skin of EFT. The stress distributions and effective stresses on skin are similar for Piecewise Linear Plasticity material model and Johnson Cook Material model.

Von Misses Stress results at 2.5 ms for impactor position 2 is shown in Figure 60.

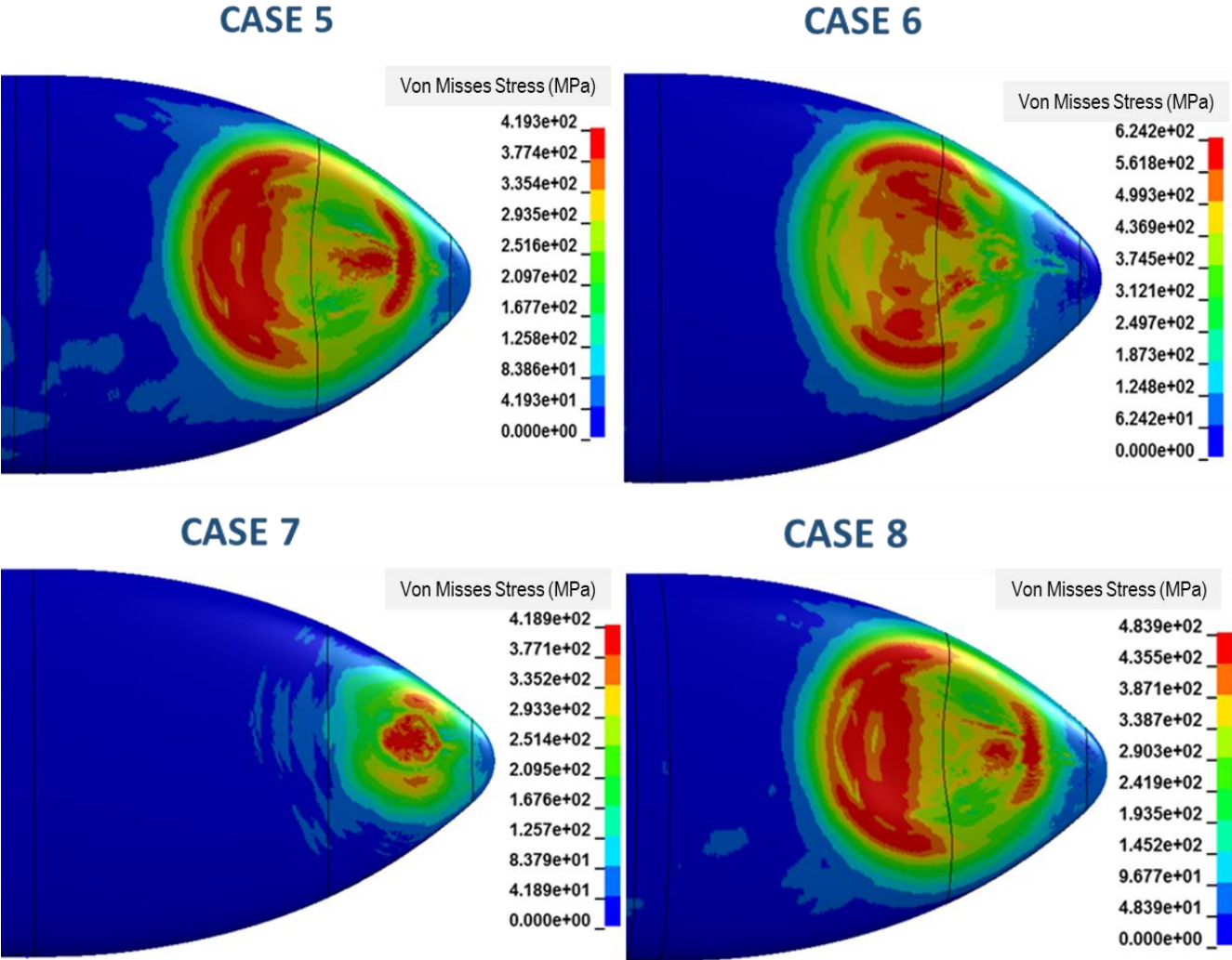


Figure 60 Von Misses Stress Results (MPa) at 2.5 ms for Impactor Position 2

Tearing or penetration did not occur on the skin of EFT. The stress distributions and effective stresses on skin are similar for Piecewise Linear Plasticity material model and Johnson Cook Material model.

Von Misses Stress results at 3.0 ms for impactor position 2 is shown in Figure 61.

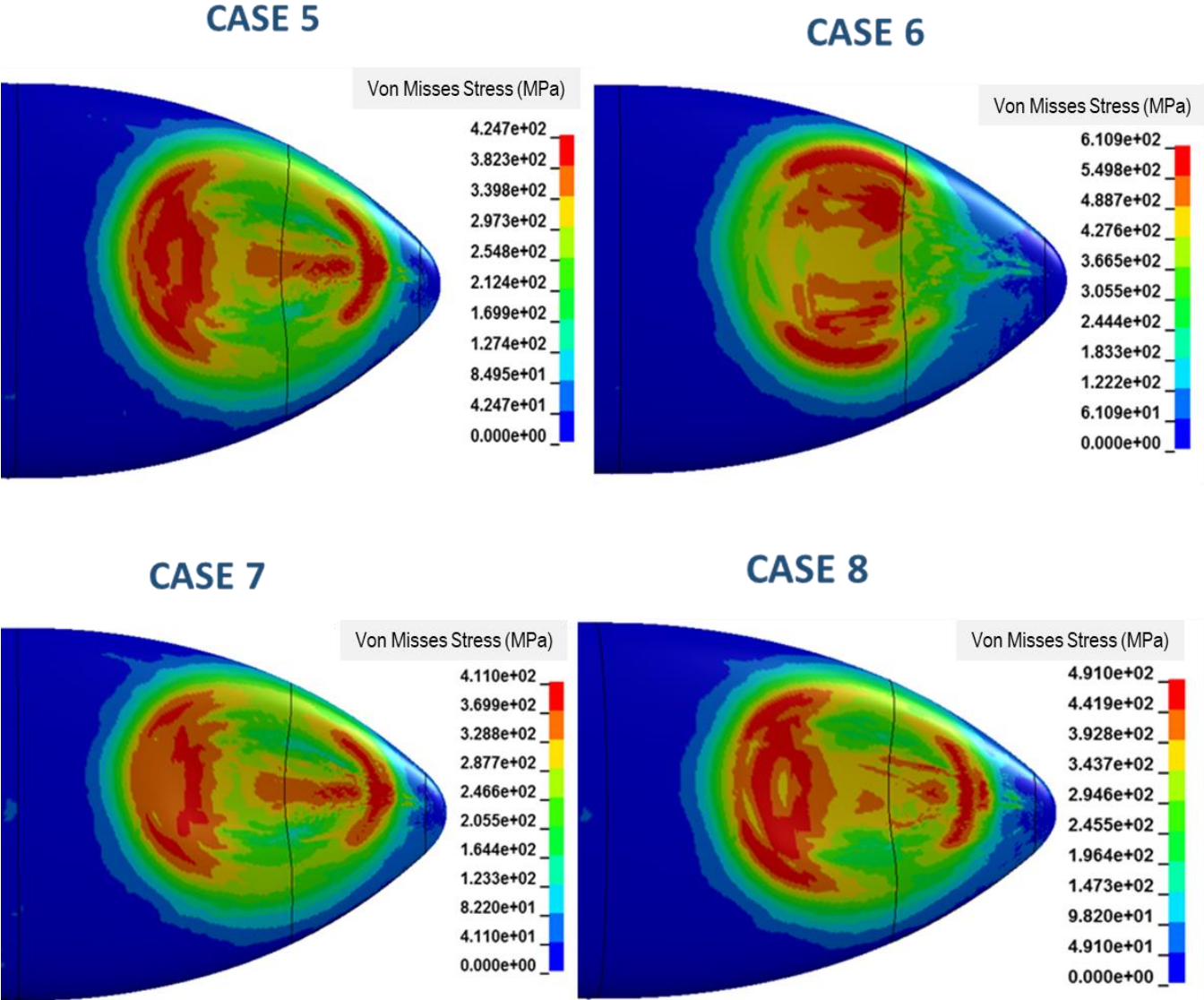


Figure 61 Von Misses Stress Results (MPa) at 3.0 ms for Impactor Position 2



Tearing or penetration did not occur on the skin of EFT. The stress distributions and effective stresses on skin are similar for Piecewise Linear Plasticity material model and Johnson Cook Material model.

Von Misses Stress results at 3.5 ms for impactor position 2 is shown in Figure 62.

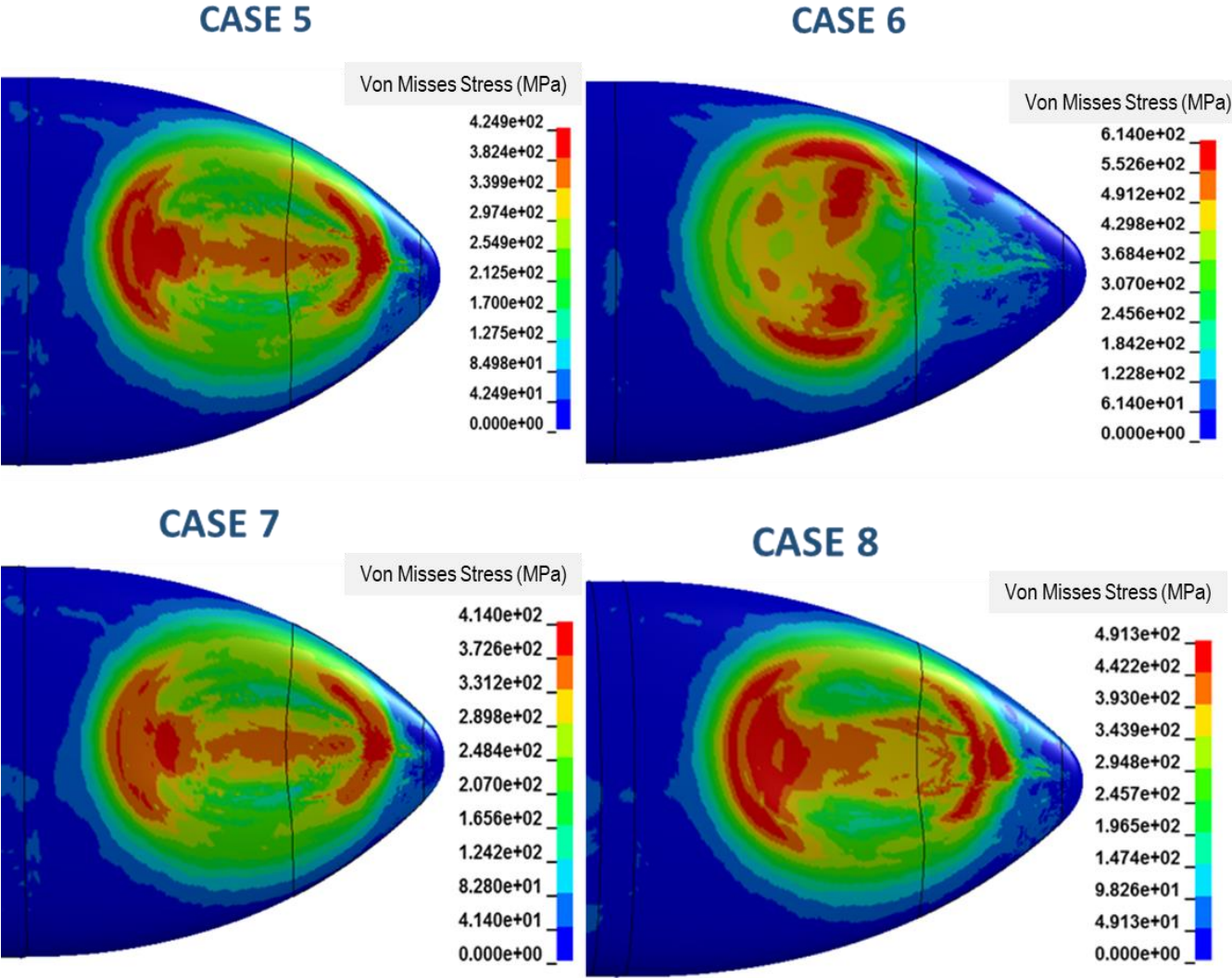


Figure 62 Von Misses Stress Results (MPa) at 3.5 ms for Impactor Position 2

Tearing or penetration did not occur on the skin of EFT. The stress distributions and effective stresses on skin are similar for Piecewise Linear Plasticity material model and Johnson Cook Material model.

Von Misses Stress results at 4.0 ms for impactor position 2 is shown in Figure 63.

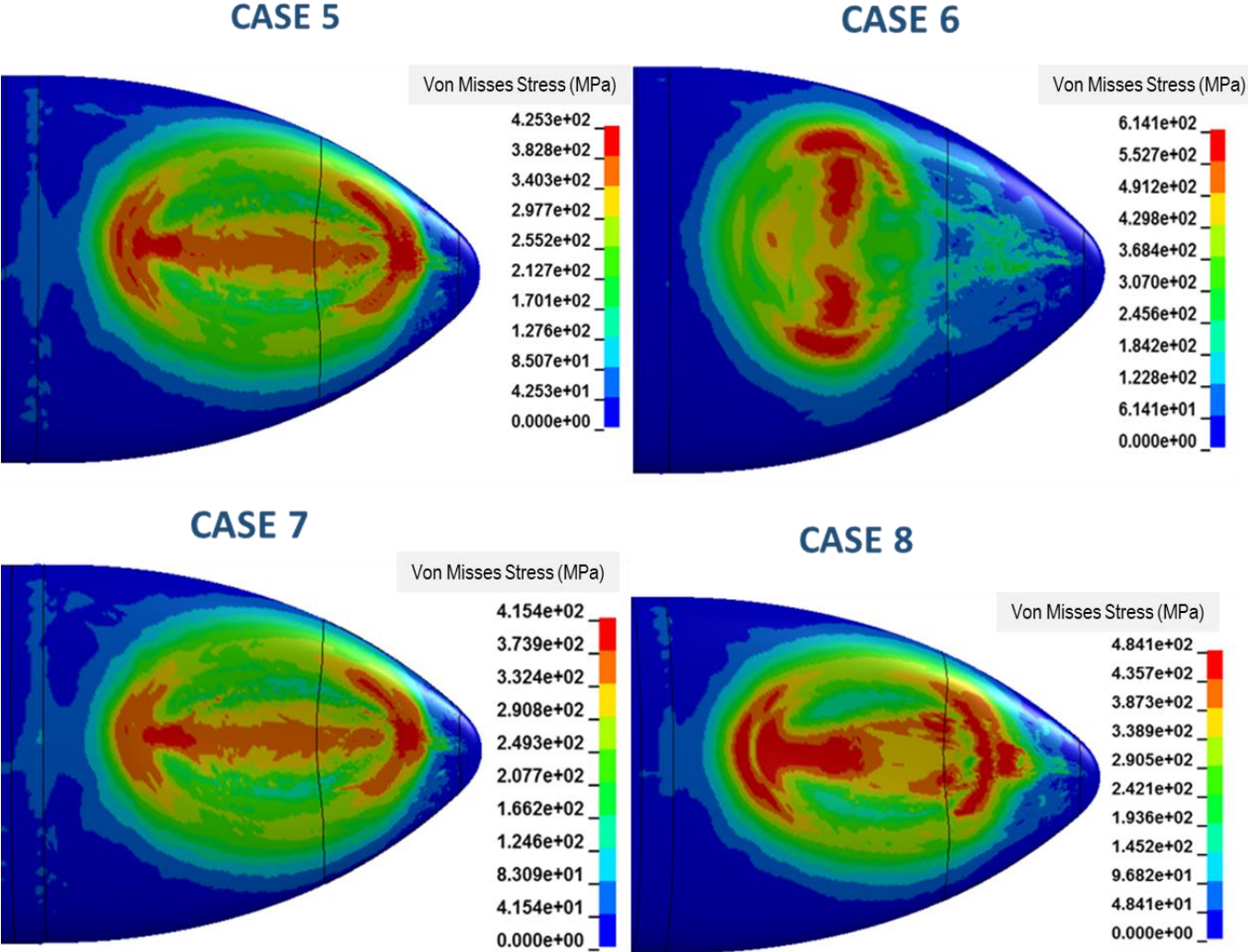


Figure 63 Von Misses Stress Results (MPa) at 4.0 ms for Impactor Position 2

Tearing or penetration did not occur on the skin of EFT. The stress distributions and effective stresses on skin are similar for Piecewise Linear Plasticity material model and Johnson Cook Material model.

Von Misses Stress results at 4.5 ms for impactor position 2 is shown in Figure 64.

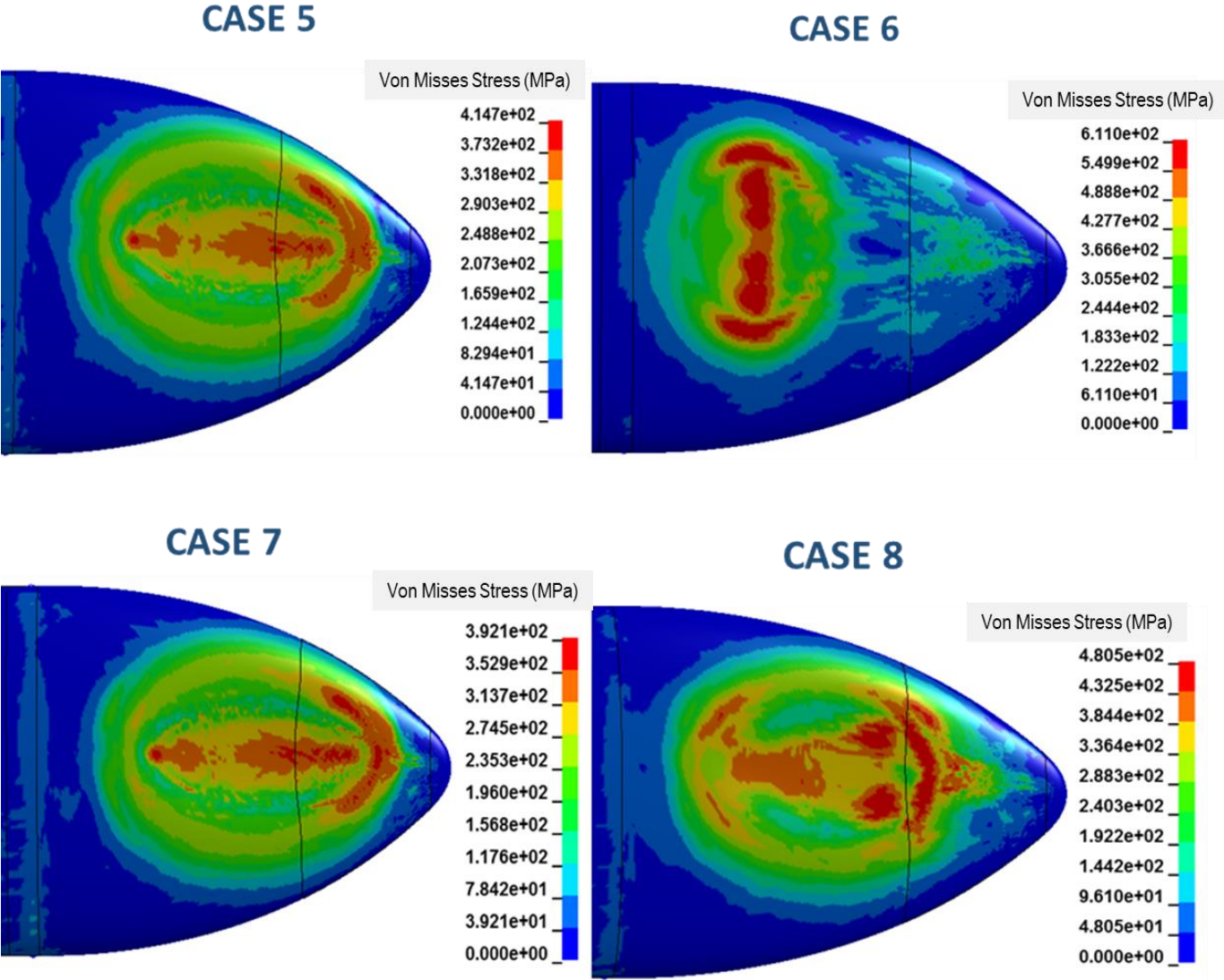


Figure 64 Von Misses Stress Results (MPa) at 4.5 ms for Impactor Position 2

Tearing or penetration did not occur on the skin of EFT. The stress distributions and effective stresses on skin are similar for Piecewise Linear Plasticity material model and Johnson Cook Material model.

Von Misses Stress results at 5.0 ms for impactor position 2 is shown in Figure 65.

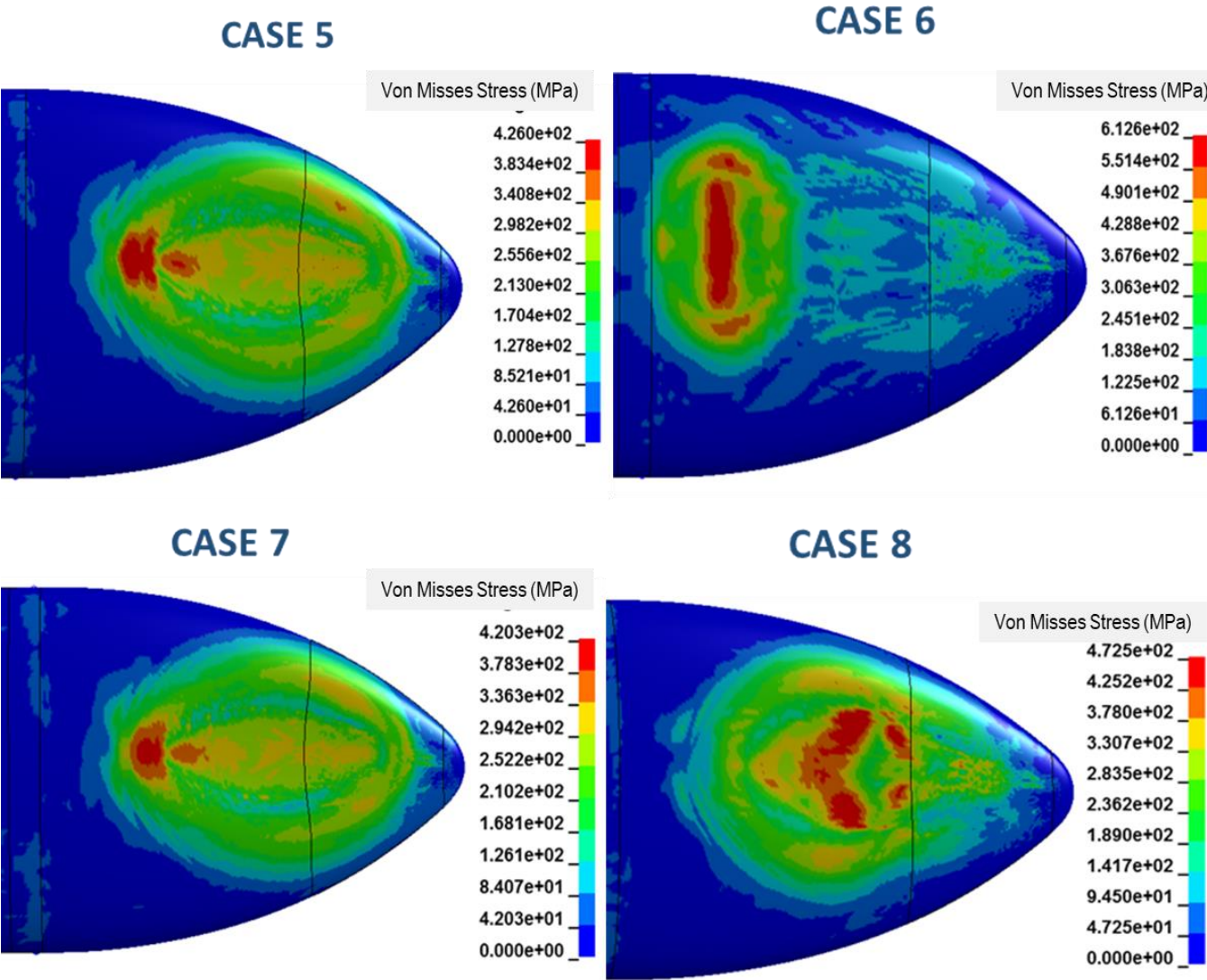


Figure 65 Von Misses Stress Results (MPa) at 5.0 ms for Impactor Position 2

Tearing or penetration did not occur on the skin of EFT. The stress distributions and effective stresses on skin are similar for Piecewise Linear Plasticity material model and Johnson Cook Material model. Impact ended at 5.0 ms.

The stresses and displacements on EFT skin are shown in Figure 46 to Figure 65. EFT skin began to deform plastically at 0.5ms as shown in Figure 56. Tearing or penetration did not occur on the skin of EFT. The stress distributions and effective stresses on skin are similar for Piecewise Linear Plasticity material model and Johnson Cook Material model.

Maximum stress on EFT skin was 427MPa for Case 5, 646MPa for Case 6, 420MPa for Case 7, 562 MPa for Case 8.

Energy variations for Position 2 (for case 5,6,7 and 8) is given in Figure 66. While kinetic energy decreased, internal energy increased. For position 2, total energy increased slightly.

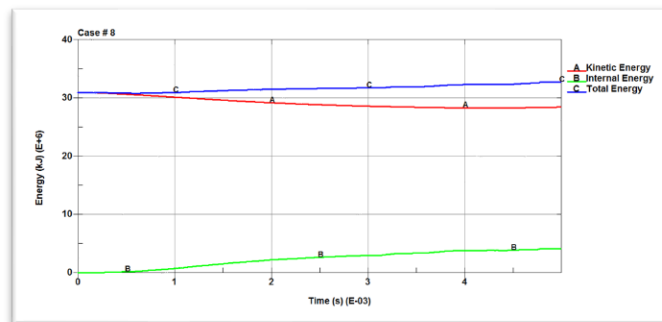
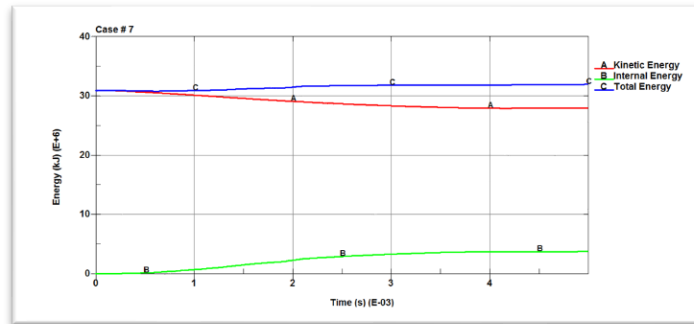
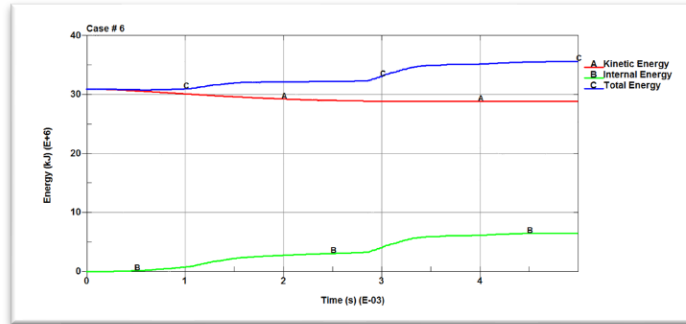
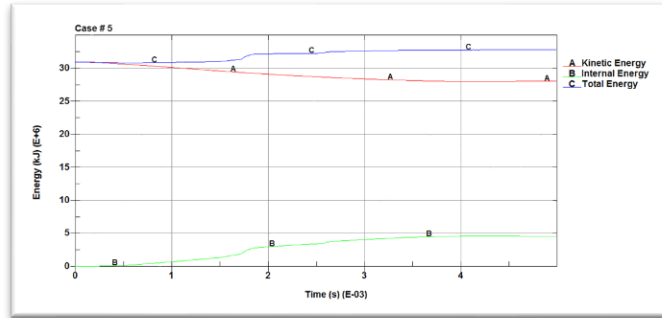


Figure 66 Energy Variation of Position 2

Energy ratios for Position 2 is given in Figure 67. Energy ratios for position 2 remained within the acceptable limits as shown.

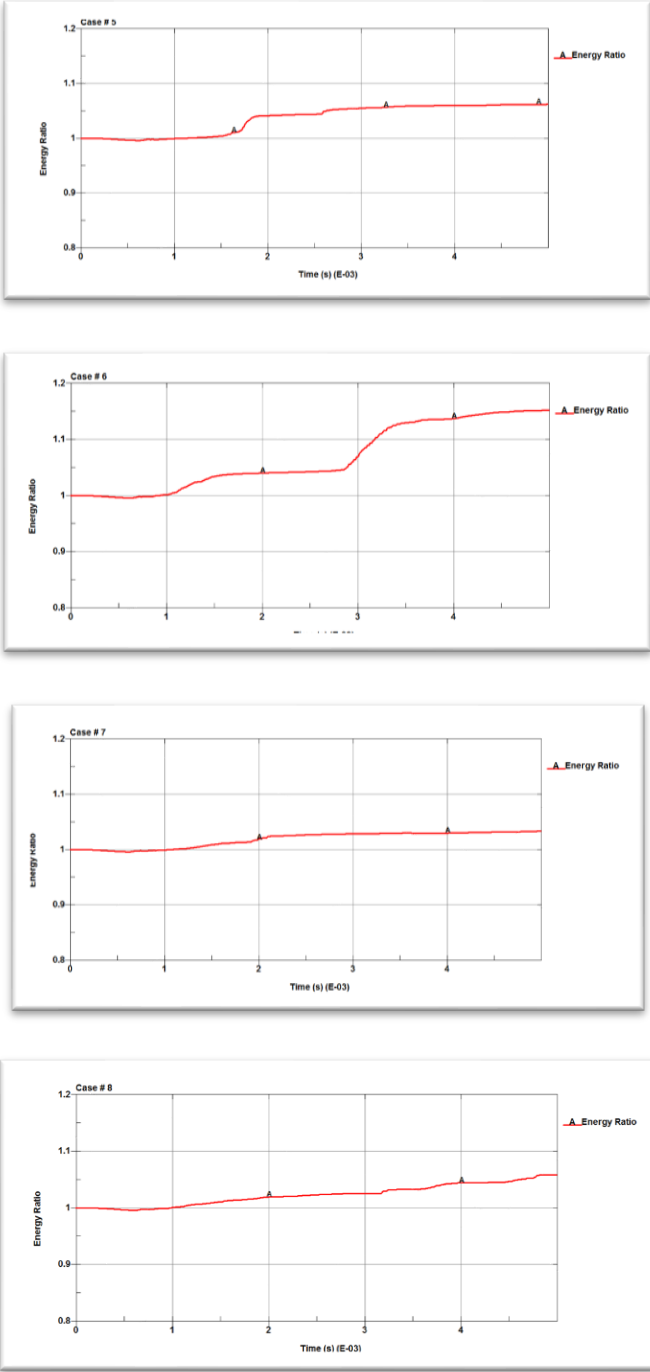


Figure 67 Energy Ratio of Position 2

Hourglass energy, damping energy and sliding energy for case 5 is given in Figure 68. Impact ended in 5.0 ms. Hourglass energy remained almost 0 for 5.0 ms. For sliding energy, peak did not occur.

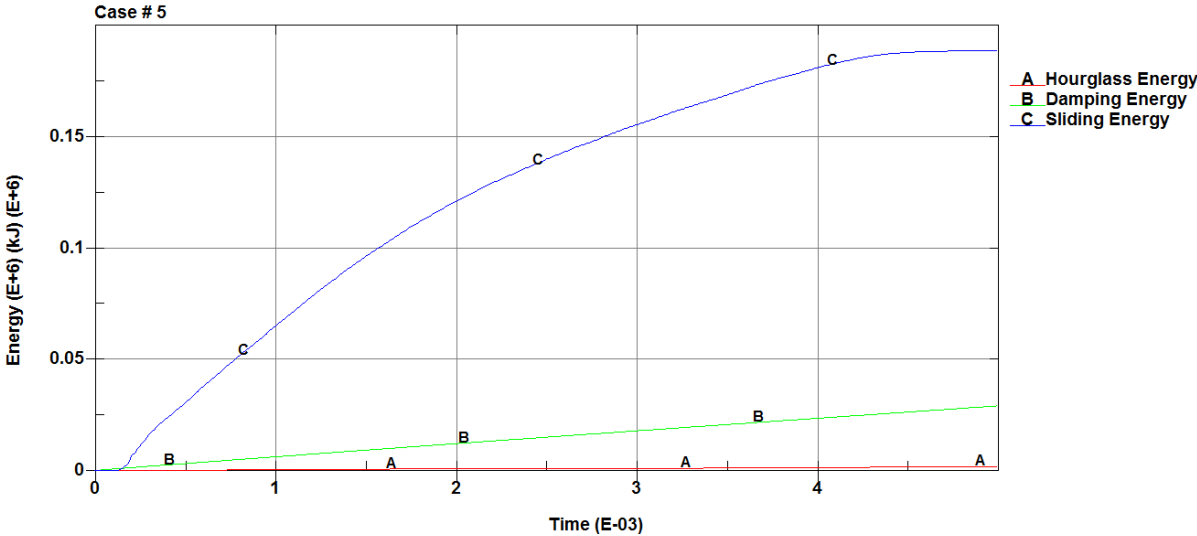


Figure 68 Hourglass, Damping and Sliding Energies Variation of Case 5

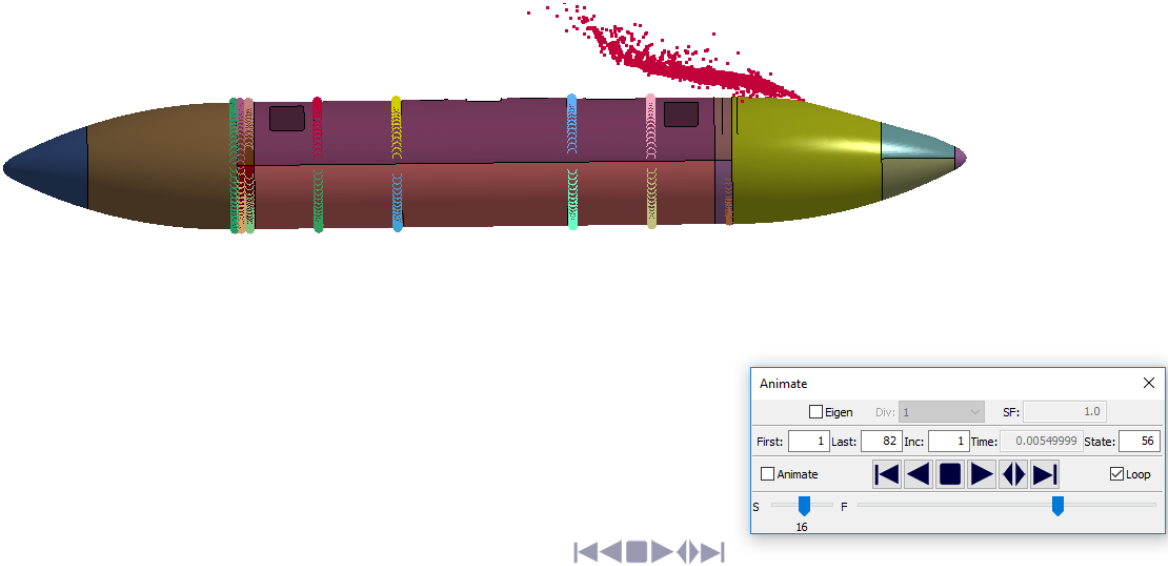


Figure 69 Bird Impact at 4 ms for Case 5



Hourglass energy, damping energy and sliding energy for case 6 is given in Figure 70. Impact ended in 5.0 ms. Hourglass energy remained almost 0 for 5.0 ms. For sliding energy, peak did not occur.

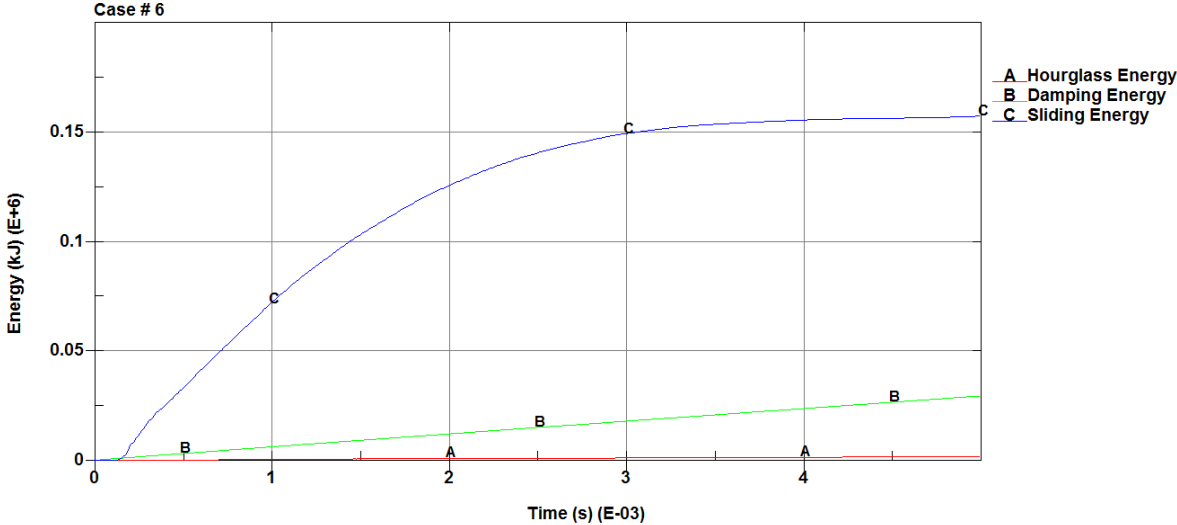


Figure 70 Hourglass, Damping and Sliding Energies Variation of Case 6

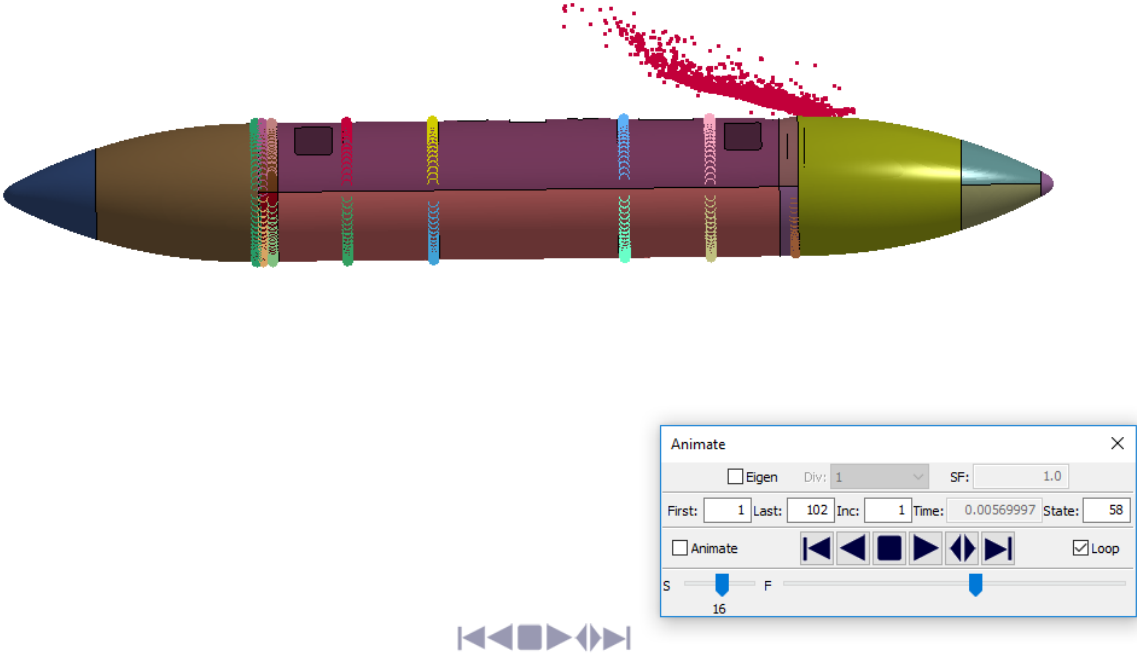


Figure 71 Bird Impact at 4 ms for Case 6

Hourglass energy, damping energy and sliding energy for case 7 is given in Figure 72. Impact ended in 5.0 ms. Hourglass energy remained almost 0 for 5.0 ms. For sliding energy, peak did not occur.

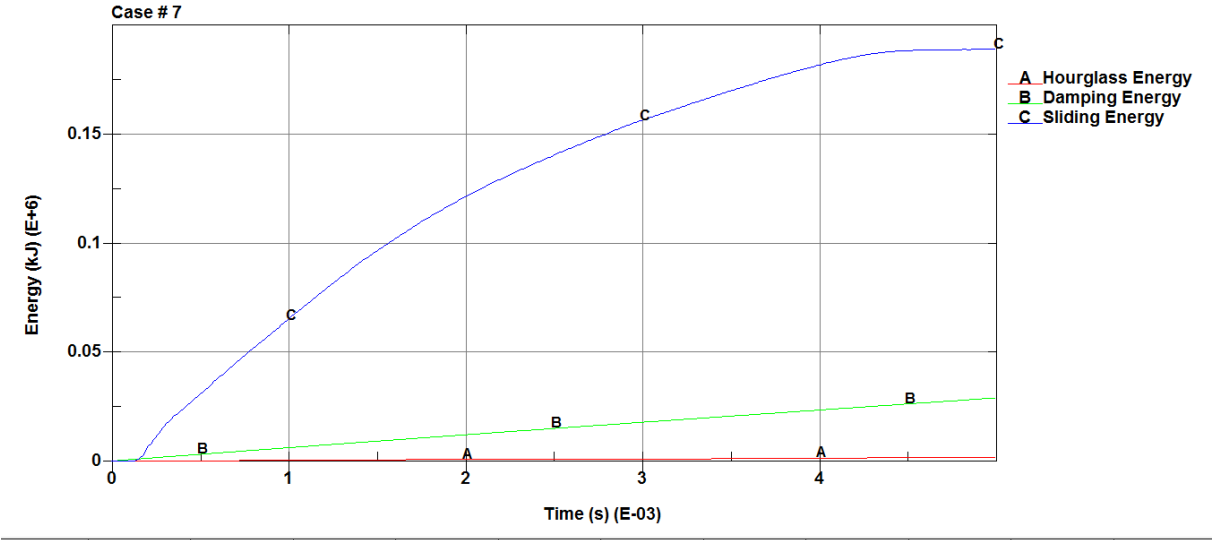


Figure 72 Hourglass, Damping and Sliding Energies Variation of Case 7

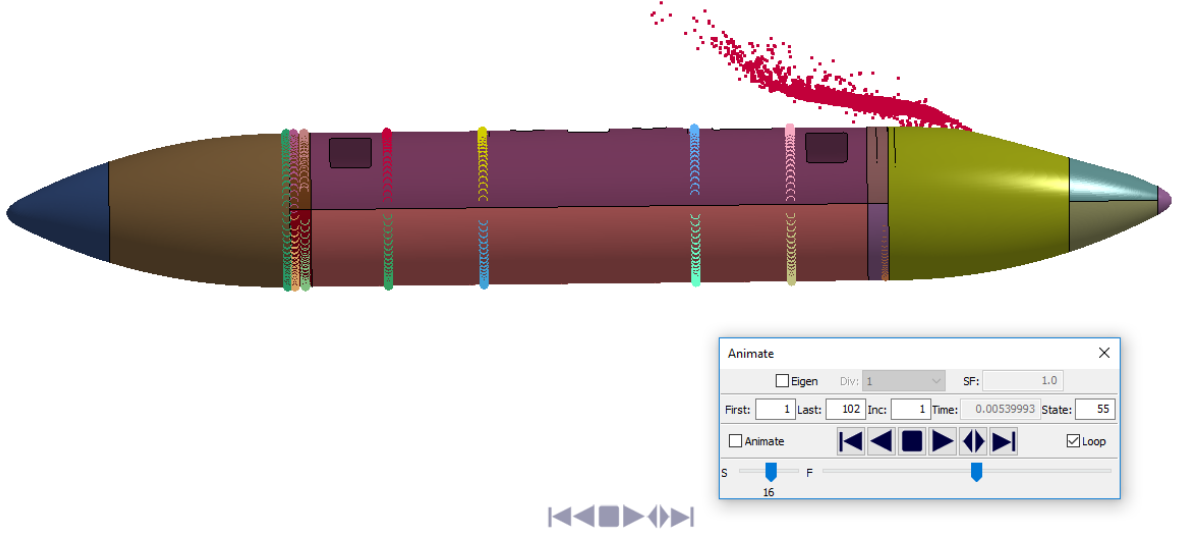


Figure 73 Bird Impact at 4 ms for Case 7

Hourglass energy, damping energy and sliding energy for case 8 is given in Figure 74. Impact ended in 5.0 ms. Hourglass energy remained almost 0 for 5.0 ms. For sliding energy, peak did not occur.

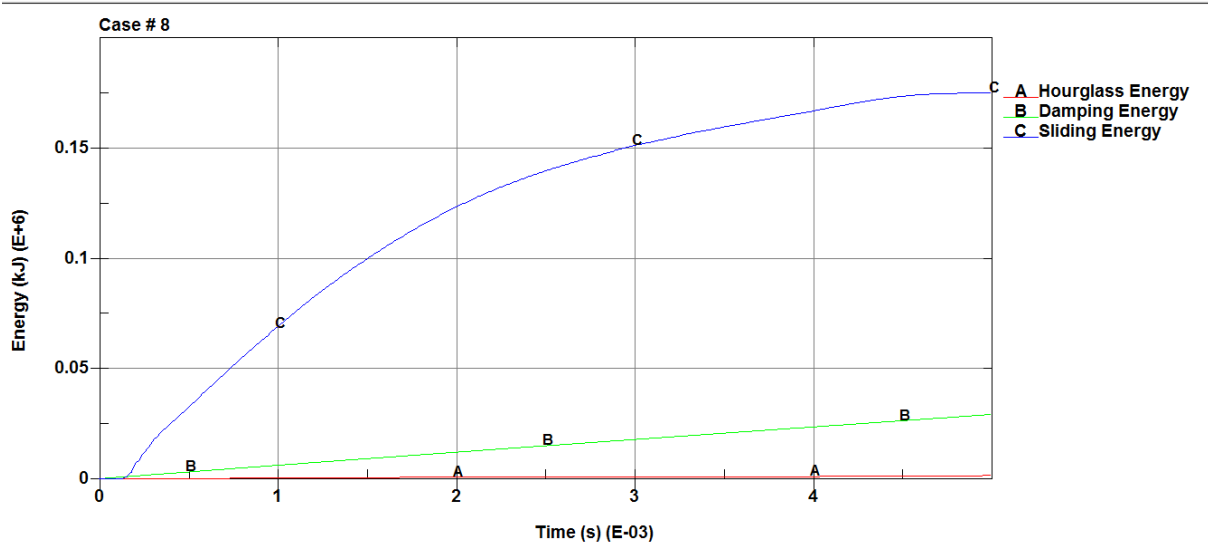


Figure 74 Hourglass, Damping and Sliding Energies Variation of Case 8

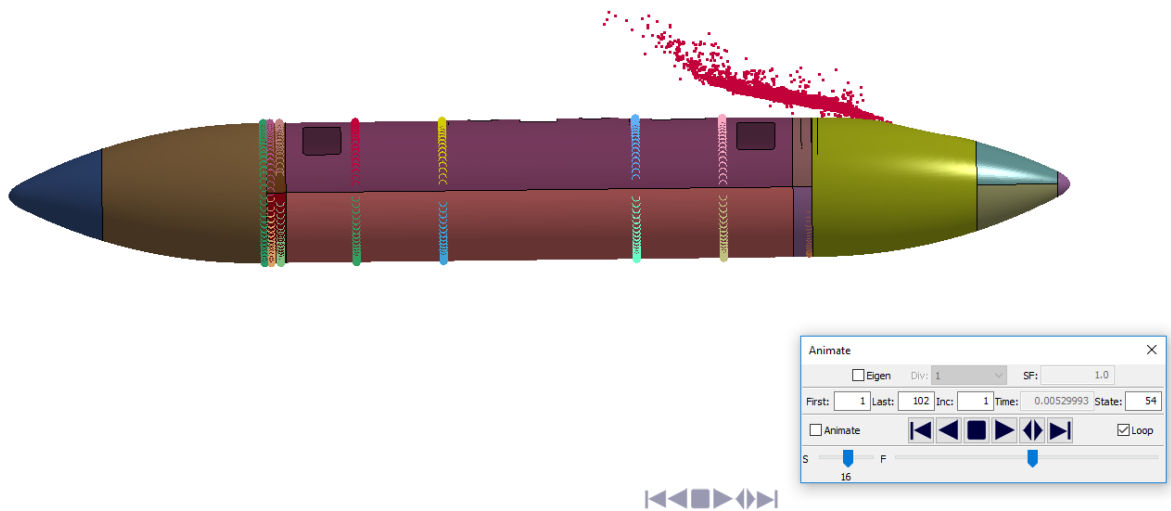


Figure 75 Bird Impact at 4 ms for Case 8

### **Analysis Results for Position 3**

An overview of the impact simulation for the position 3 was given for the general understanding. The time history was presented as a series of time step plots with explanations. The plots in Figure 76 to Figure 95 show the simulation run in several steps. Total simulation time was set to 5 ms and plots were saved in the intervals of 0.5ms.

Displacement results at 0.5 ms for impactor position 3 is shown in Figure 76.

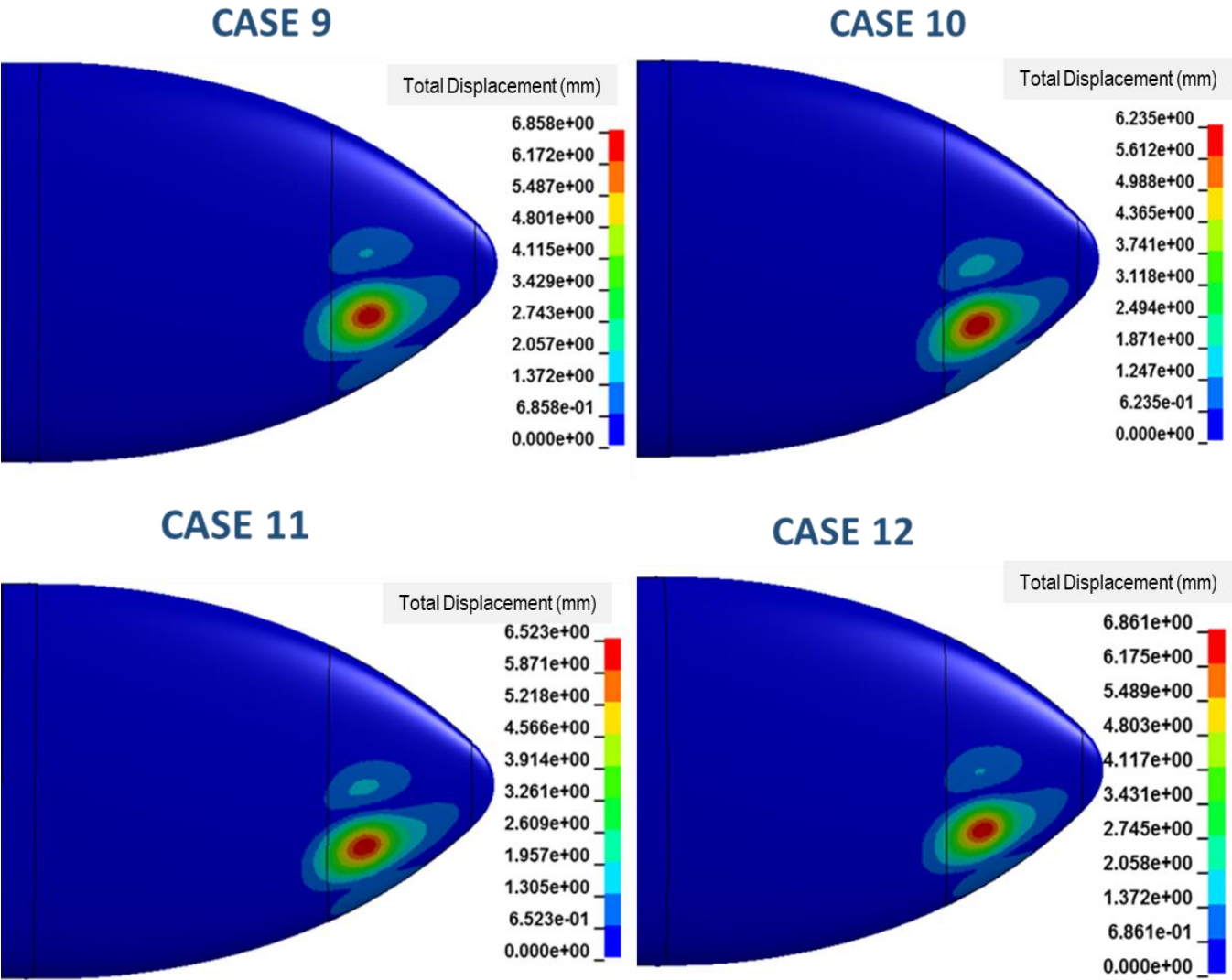


Figure 76 Displacement Results (mm) at 0.5 ms for Impactor Position 3

Displacements on Al 7075 -T6 and Al 2024-T3 are similar. Displacement values according to Piecewise Linear Plasticity material model are also similar to Johnson Cook Material model.

Displacement results at 1.0 ms for impactor position 3 is shown in Figure 77.

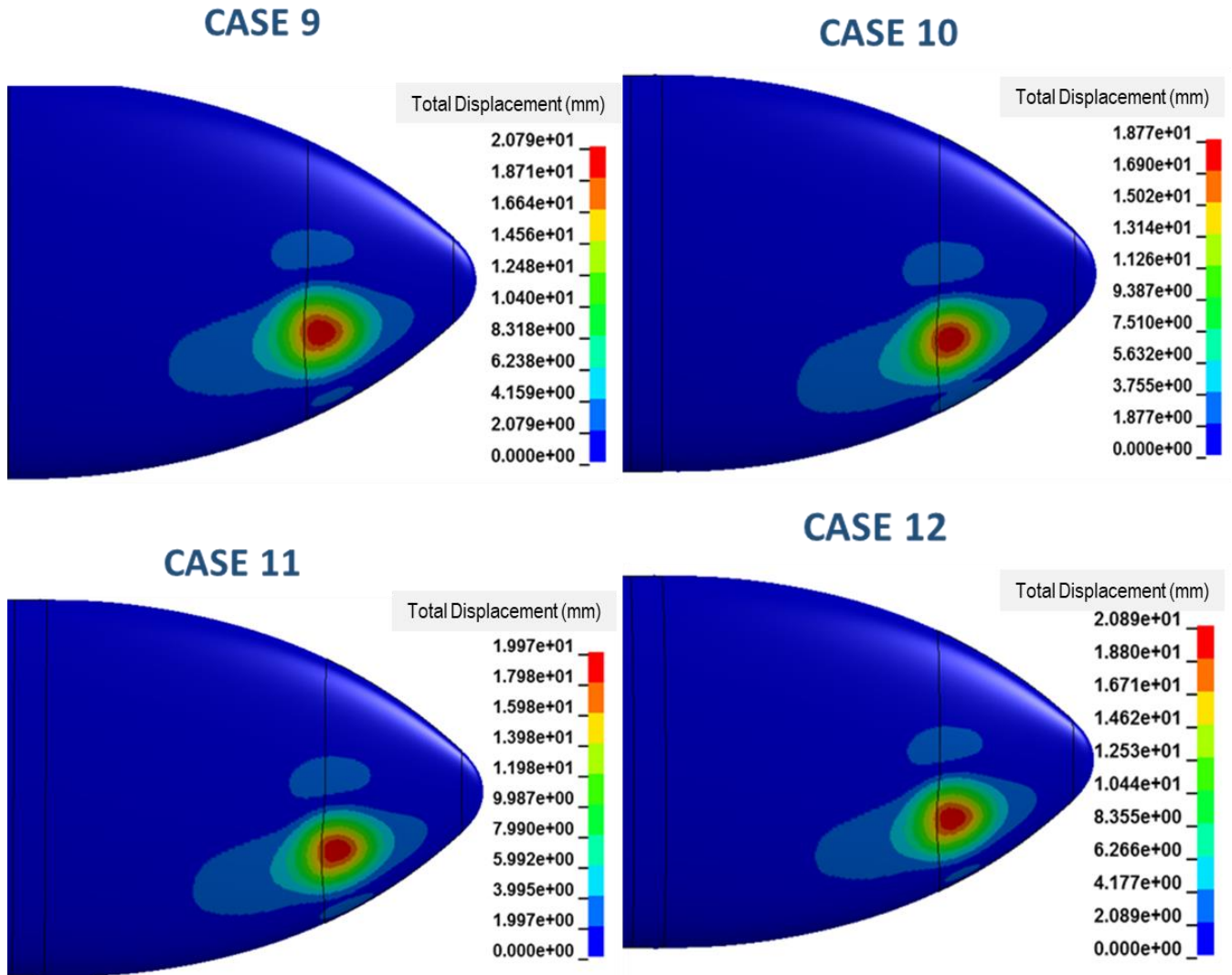


Figure 77 Displacement Results (mm) at 1.0 ms for Impactor Position 3

Displacements on Al 7075 -T6 and Al 2024-T3 are similar. Displacement values according to Piecewise Linear Plasticity material model are also similar to Johnson Cook Material model.

Displacement results at 1.5 ms for impactor position 3 is shown in Figure 78.

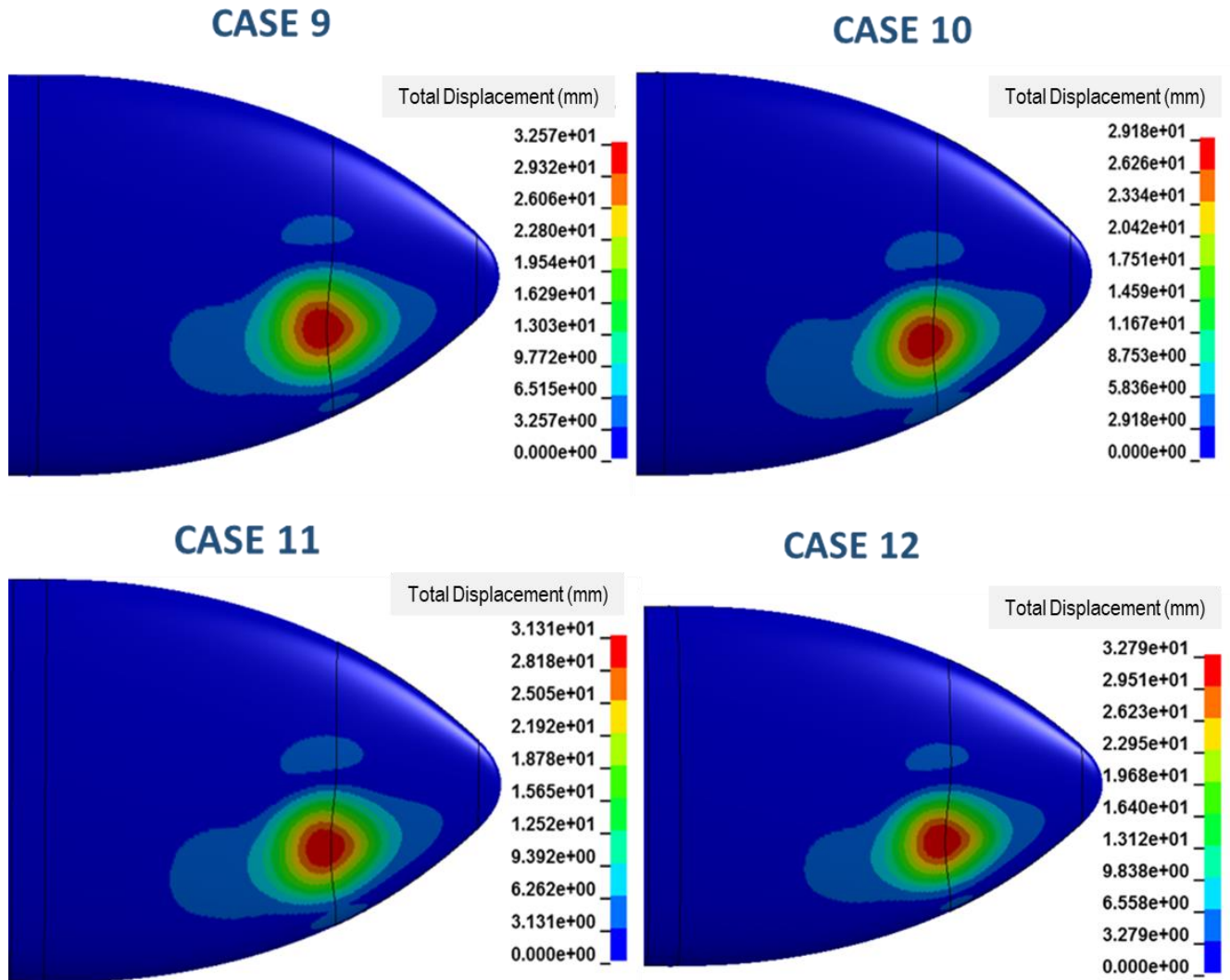


Figure 78 Displacement Results (mm) at 1.5 ms for Impactor Position 3

Displacements on Al 7075 -T6 and Al 2024-T3 are similar. Displacement values according to Piecewise Linear Plasticity material model are also similar to Johnson Cook Material model.

Displacement results at 2.0 ms for impactor position 3 is shown in Figure 79.

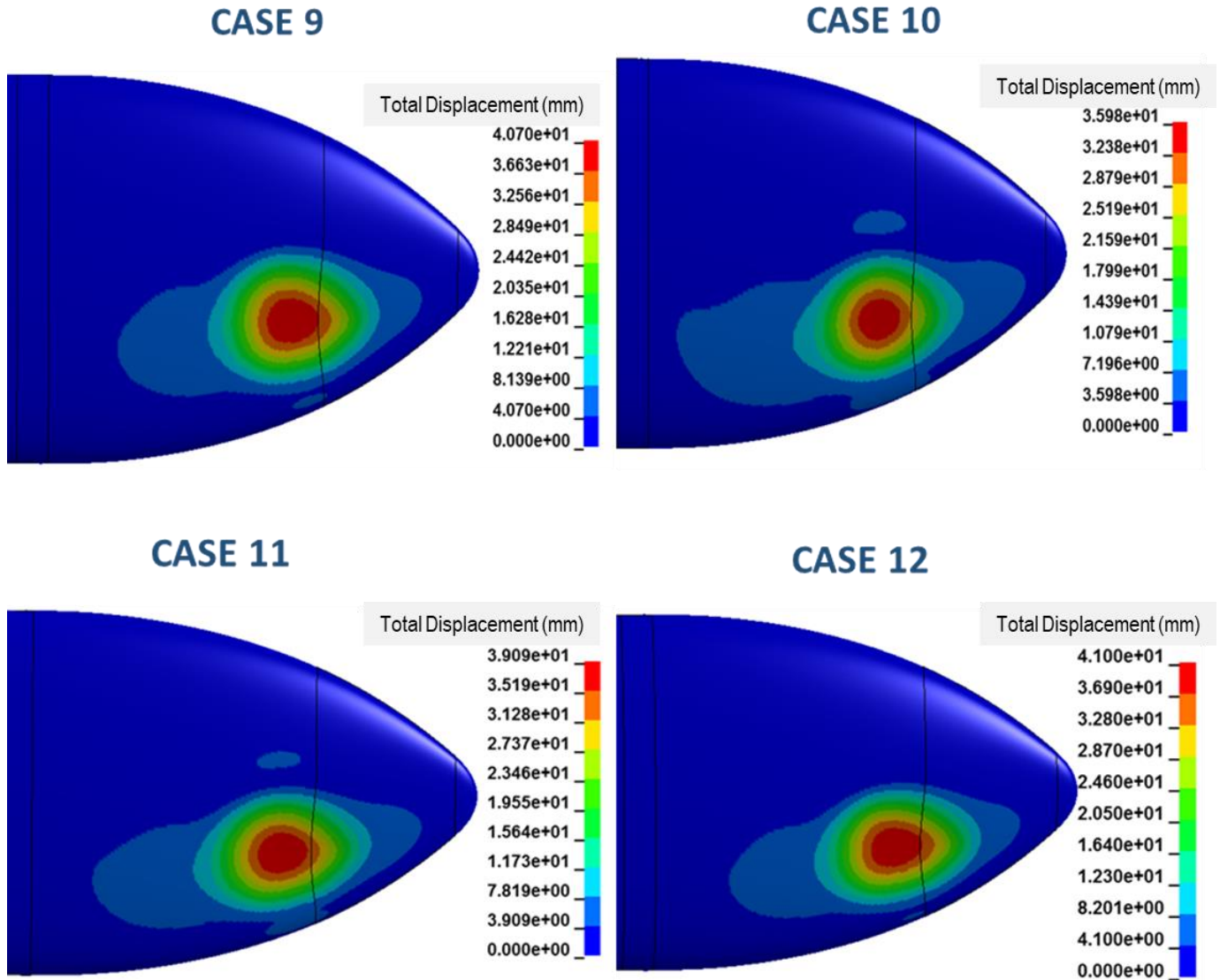


Figure 79 Displacement Results (mm) at 2.0 ms for Impactor Position 3

Displacements on Al 7075 -T6 and Al 2024-T3 are similar. Displacement values according to Piecewise Linear Plasticity material model are also similar to Johnson Cook Material model.

Displacement results at 2.5 ms for impactor position 3 is shown in Figure 80.

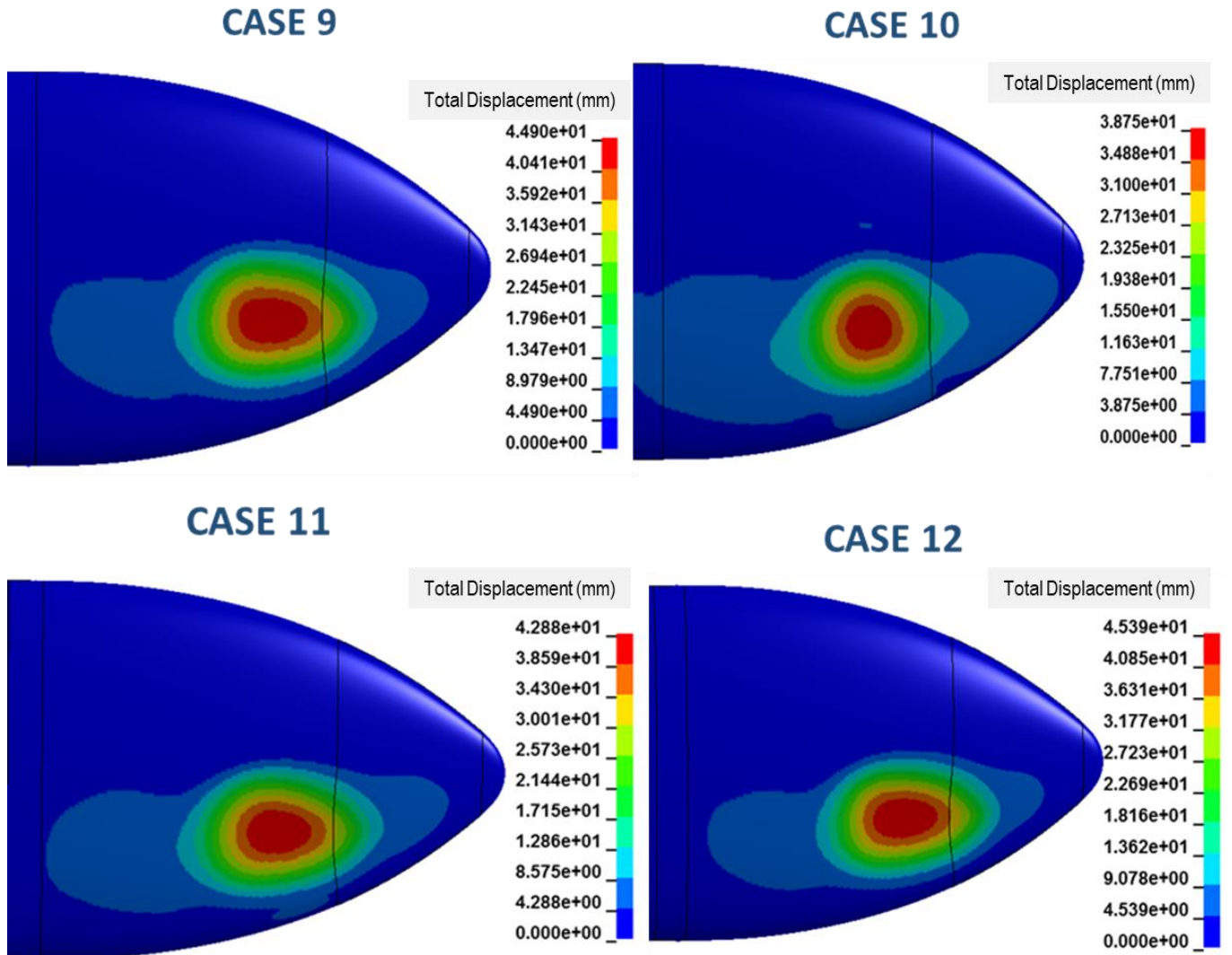


Figure 80 Displacement Results (mm) at 2.5 ms for Impactor Position 3

Displacements on Al 7075 -T6 and Al 2024-T3 are similar. Displacement values according to Piecewise Linear Plasticity material model are also similar to Johnson Cook Material model.

Displacement results at 3.0 ms for impactor position 3 is shown in Figure 81.



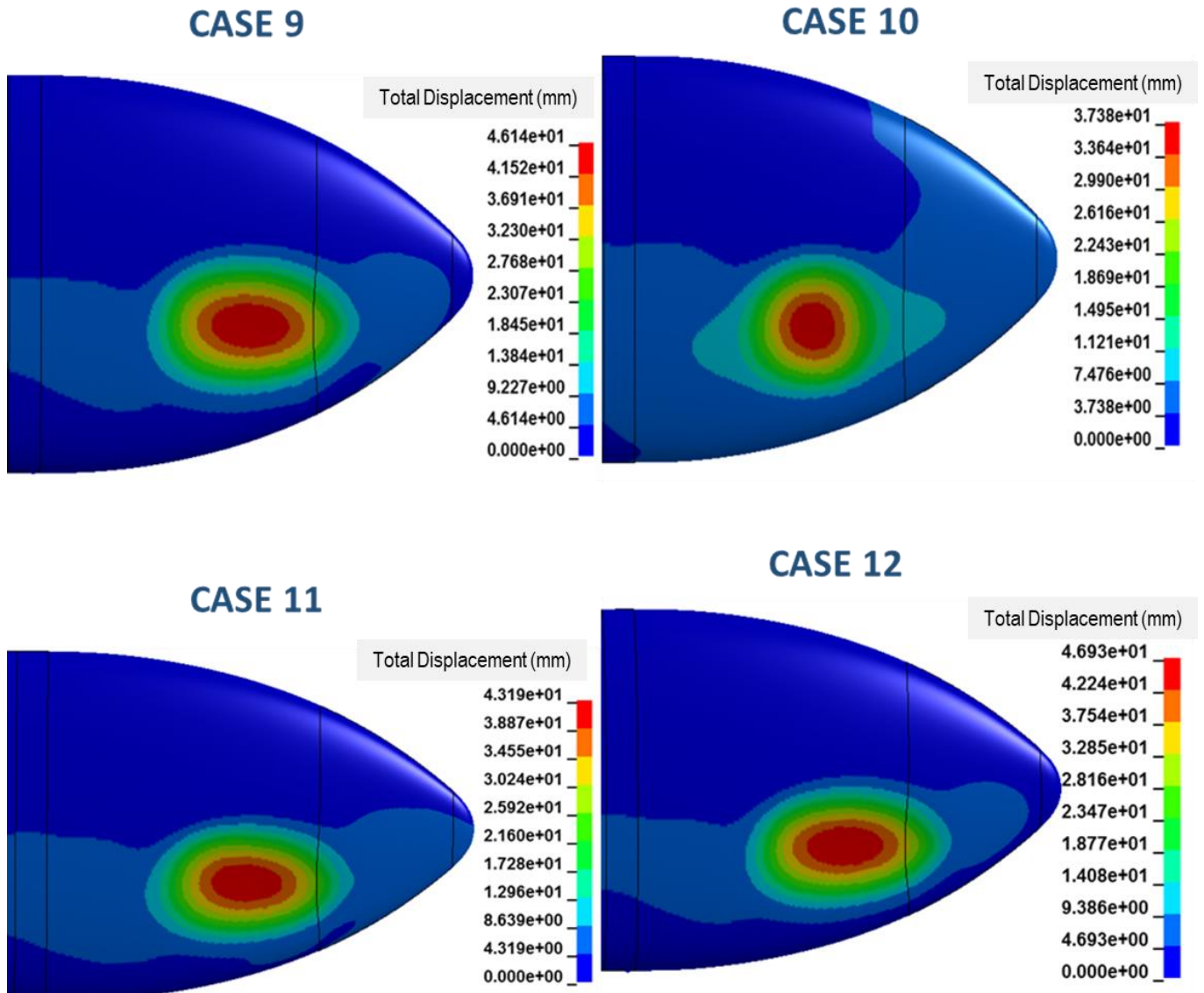


Figure 81 Displacement Results (mm) at 3.0 ms for Impactor Position 3

Displacements on Al 7075 -T6 and Al 2024-T3 are similar. Displacement values according to Piecewise Linear Plasticity material model are also similar to Johnson Cook Material model.

Displacement results at 3.5 ms for impactor position 3 is shown in Figure 82.

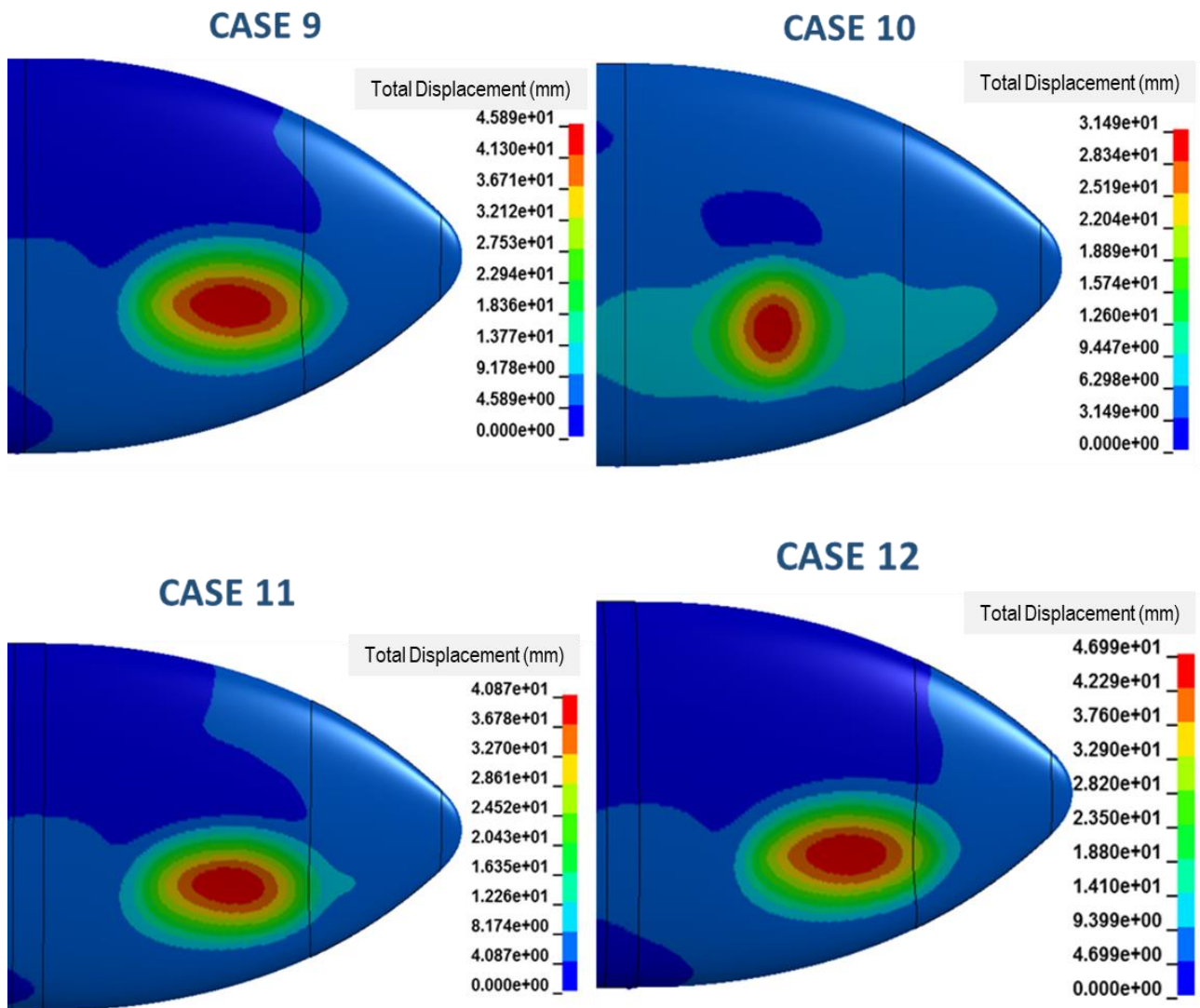


Figure 82 Displacement Results (mm) at 3.5 ms for Impactor Position 3

Displacements on Al 7075 -T6 and Al 2024-T3 are similar. Displacement values according to Piecewise Linear Plasticity material model are also similar to Johnson Cook Material model.

Displacement results at 4.0 ms for impactor position 3 is shown in Figure 83.

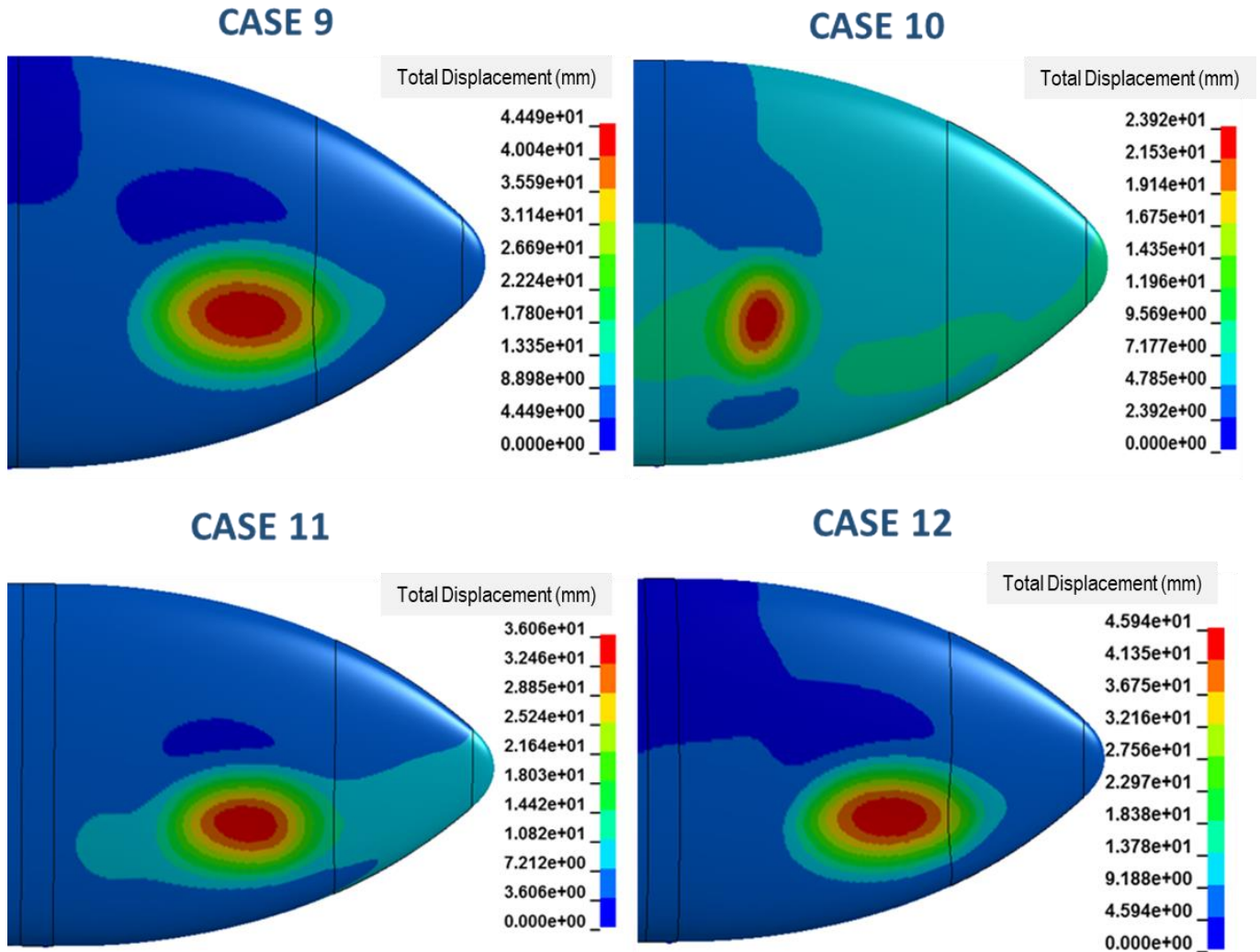


Figure 83 Displacement Results (mm) at 4.0 ms for Impactor Position 3

Displacements on Al 7075 -T6 and Al 2024-T3 are similar. Displacement values according to Piecewise Linear Plasticity material model are also similar to Johnson Cook Material model.

Displacement results at 4.5 ms for impactor position 3 is shown in Figure 84.

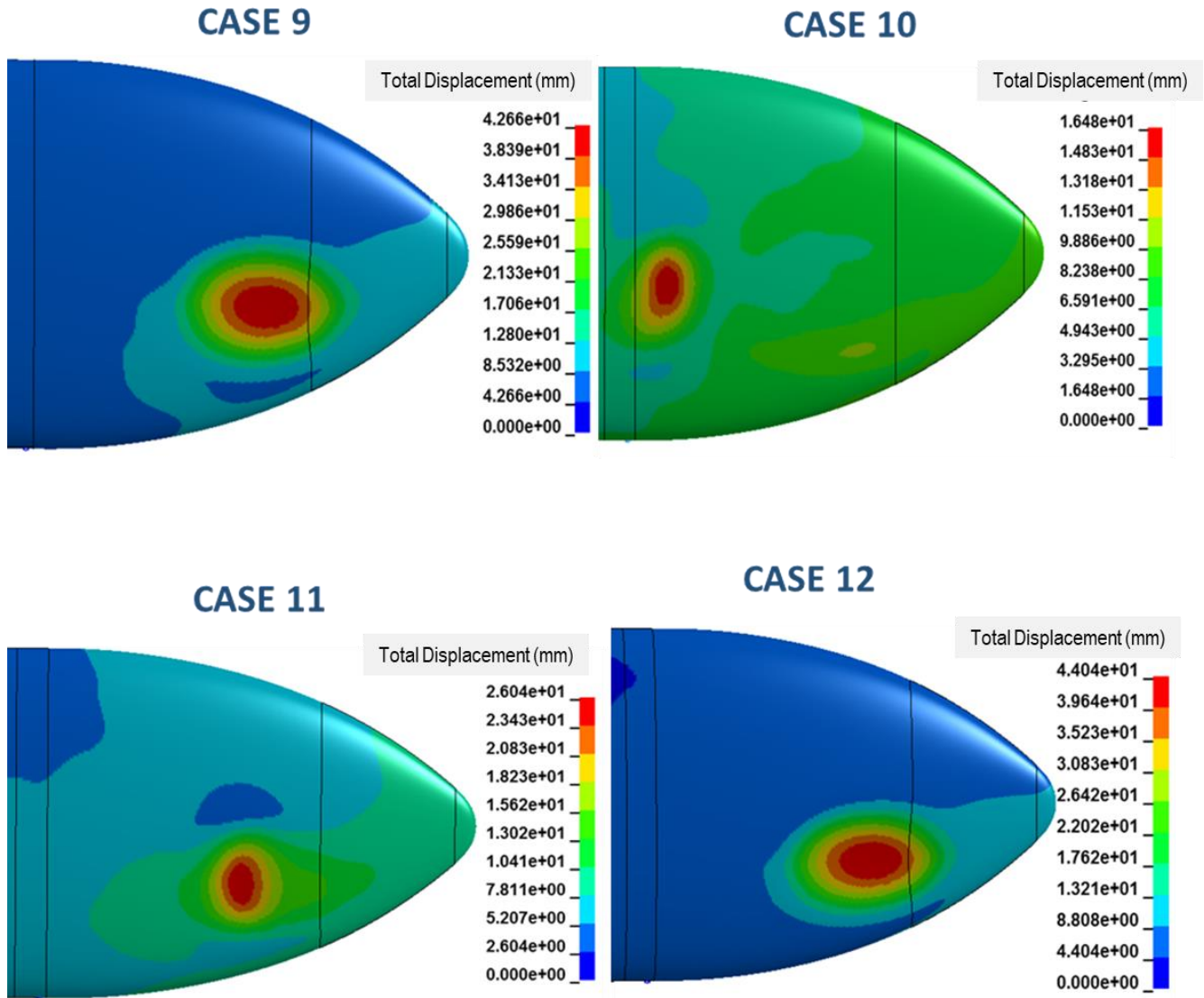


Figure 84 Displacement Results (mm) at 4.5 ms for Impactor Position 3

Displacements on Al 7075 -T6 and Al 2024-T3 are similar. Displacement values according to Piecewise Linear Plasticity material model are also similar to Johnson Cook Material model. Impact ended in 4.4 ms.

Displacement results at 5.0 ms for impactor position 3 is shown in Figure 85.

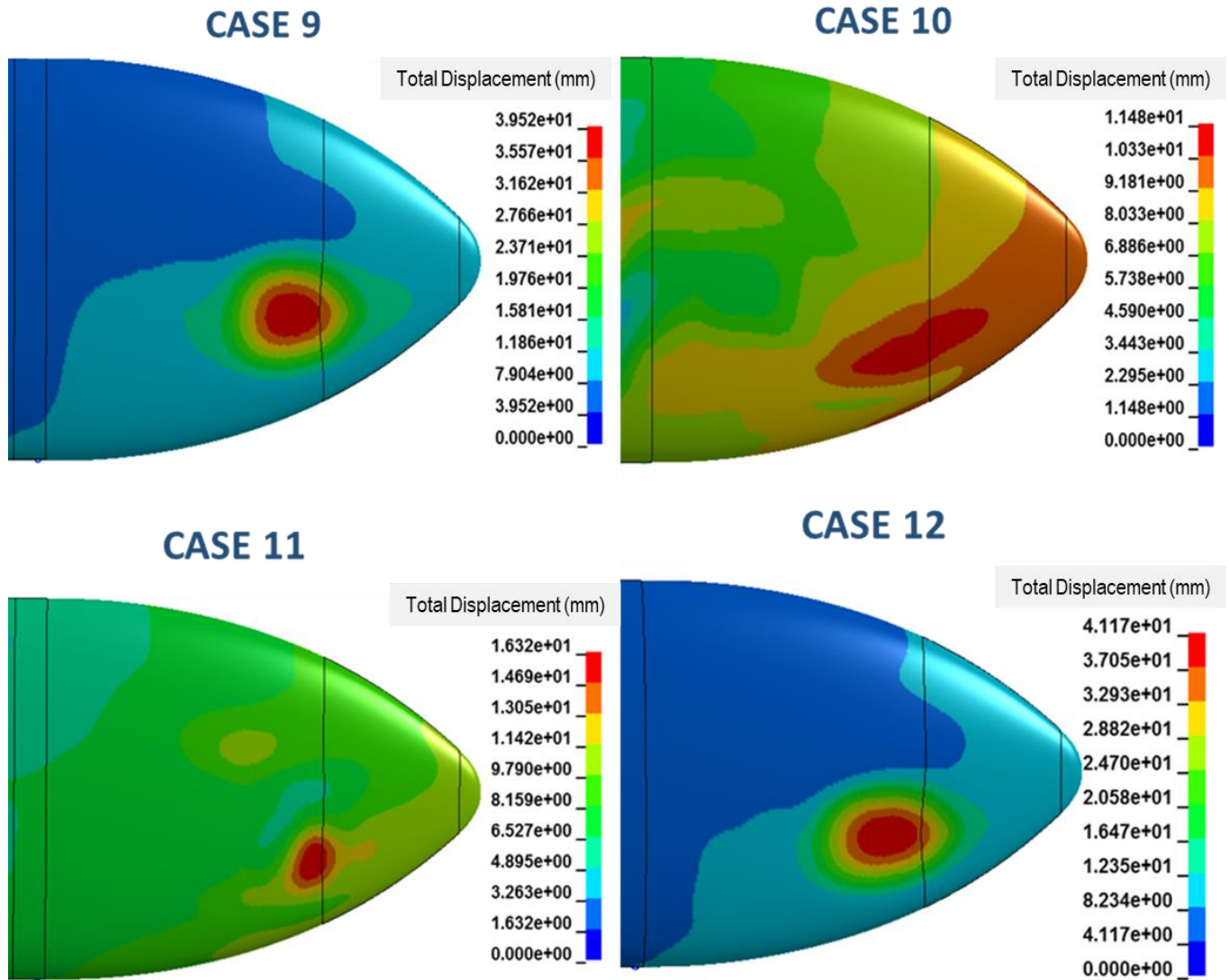


Figure 85 Displacement Results (mm) at 5.0 ms for Impactor Position 3

Displacements on Al 7075 -T6 and Al 2024-T3 are similar. Displacement values according to Piecewise Linear Plasticity material model are also similar to Johnson Cook Material model which is an expected result because of low strain rates. Impact ended in 4.4 ms.

For position 3, displacements on Al 7075 -T6 and Al 2024-T3 are similar. Displacement values according to Piecewise Linear Plasticity material model are also similar to Johnson Cook Material model.

After impact, screen shots were taken at 0.5ms intervals and the stresses are compared. Since the contact of the bird ended before 5 ms in general, the images were limited to this time period.

Von Misses Stress results at 0.5 ms for impactor position 3 is shown in Figure 86.

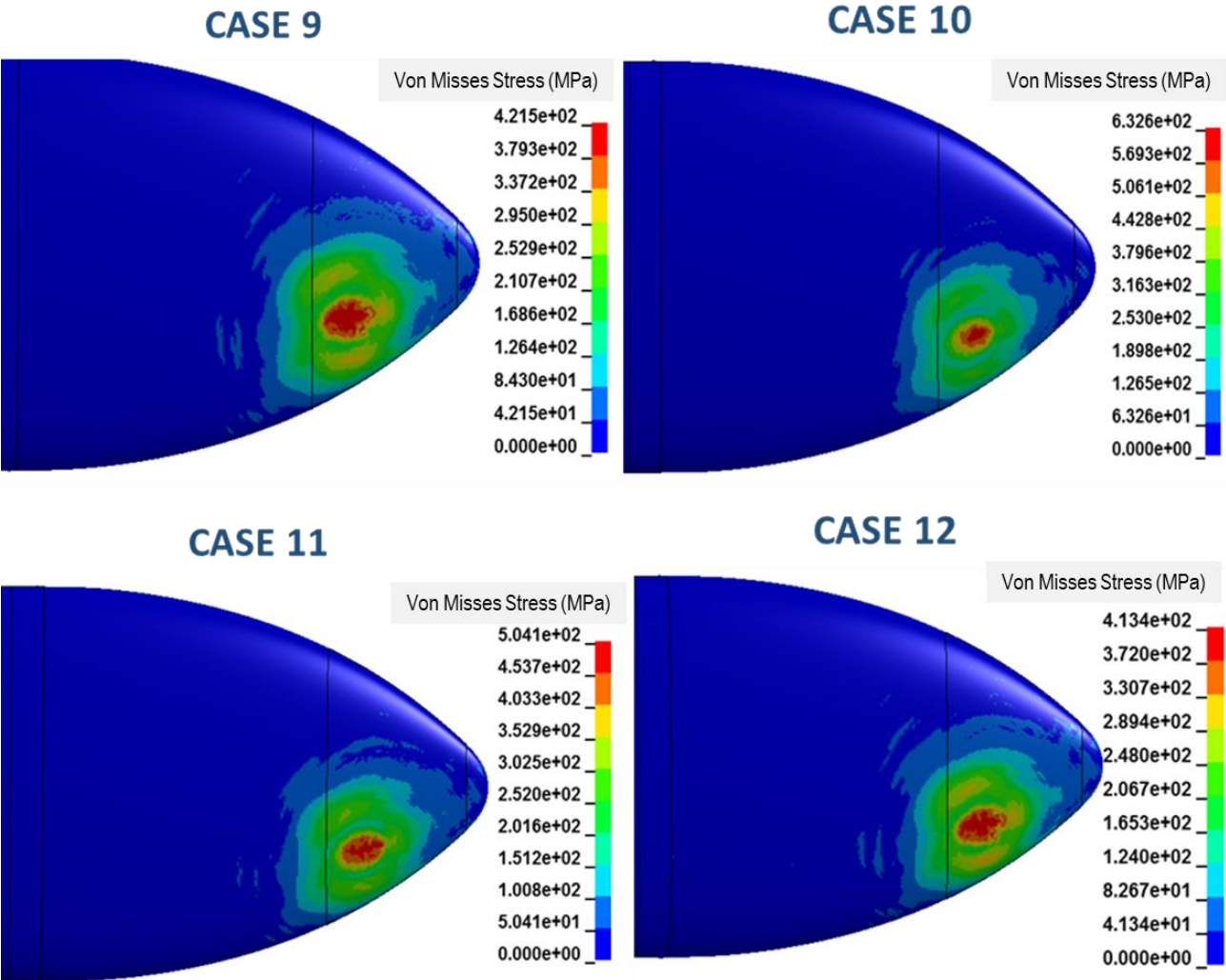


Figure 86 Von Misses Stress Results (MPa) at 0.5 ms for Impactor Position 3

The plastic deformation began at 0.5ms as shown in Figure 86. There was no tear up or penetration on the skin of EFT. The stress distributions and effective stresses on skin are similar for Piecewise Linear Plasticity material model and Johnson Cook Material model.

Von Misses Stress results at 1.0 ms for impactor position 3 is shown in Figure 87.

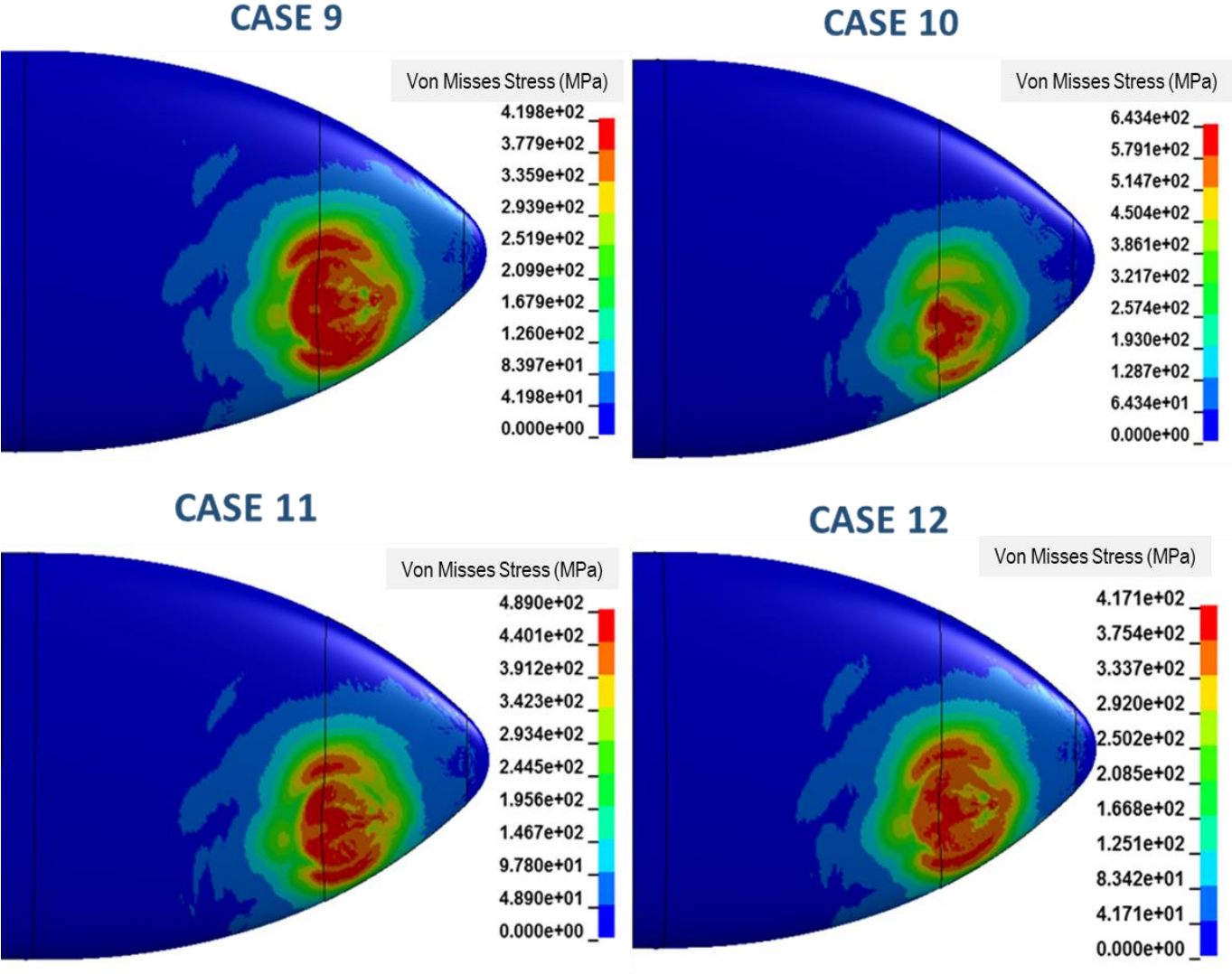


Figure 87 Von Misses Stress Results (MPa) at 1.0 ms for Impactor Position 3

There was no tear up or penetration on the skin of EFT. The stress distributions and effective stresses on skin are similar for Piecewise Linear Plasticity material model and Johnson Cook Material model.

Von Misses Stress results at 1.5 ms for impactor position 3 is shown in Figure 88.

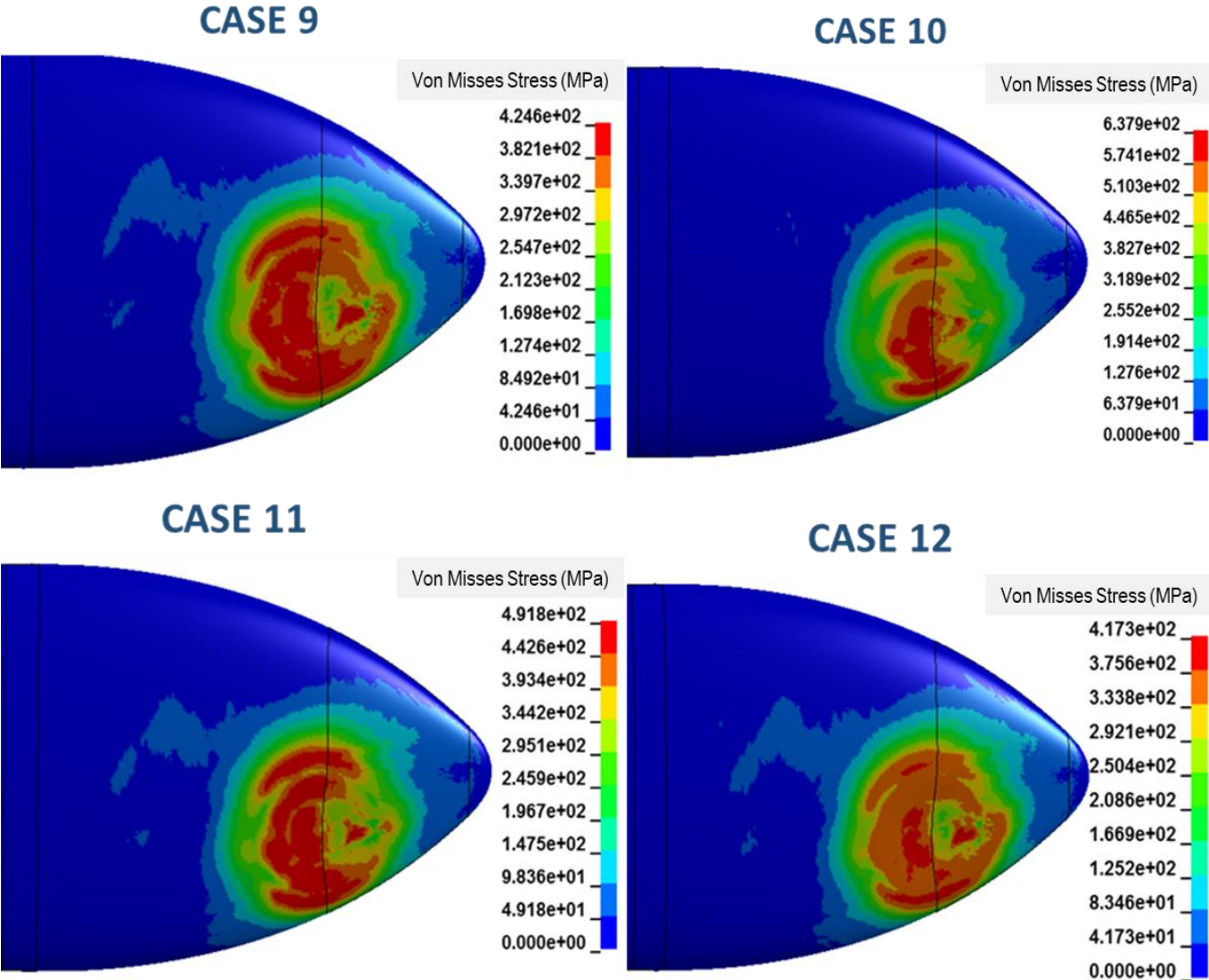


Figure 88 Von Misses Stress Results (MPa) at 1.5 ms for Impactor Position 3



There was no tear up or penetration on the skin of EFT. The stress distributions and effective stresses on skin are similar for Piecewise Linear Plasticity material model and Johnson Cook Material model.

Von Misses Stress results at 2.0 ms for impactor position 3 is shown in Figure 89.

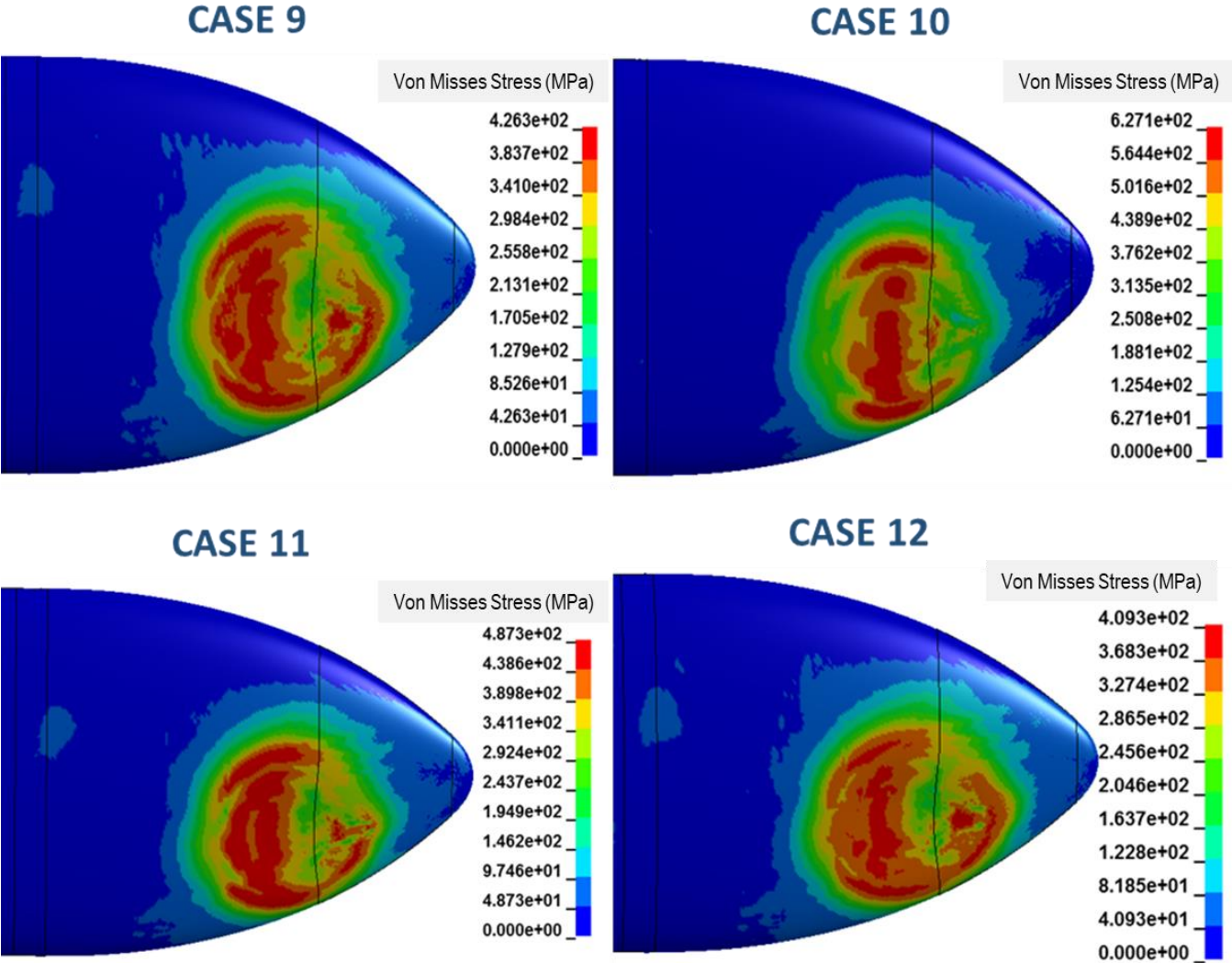


Figure 89 Von Misses Stress Results (MPa) at 2.0 ms for Impactor Position 3

There was no tear up or penetration on the skin of EFT. The stress distributions and effective stresses on skin are similar for Piecewise Linear Plasticity material model and Johnson Cook Material model.

Von Misses Stress results at 2.5 ms for impactor position 3 is shown in Figure 90.

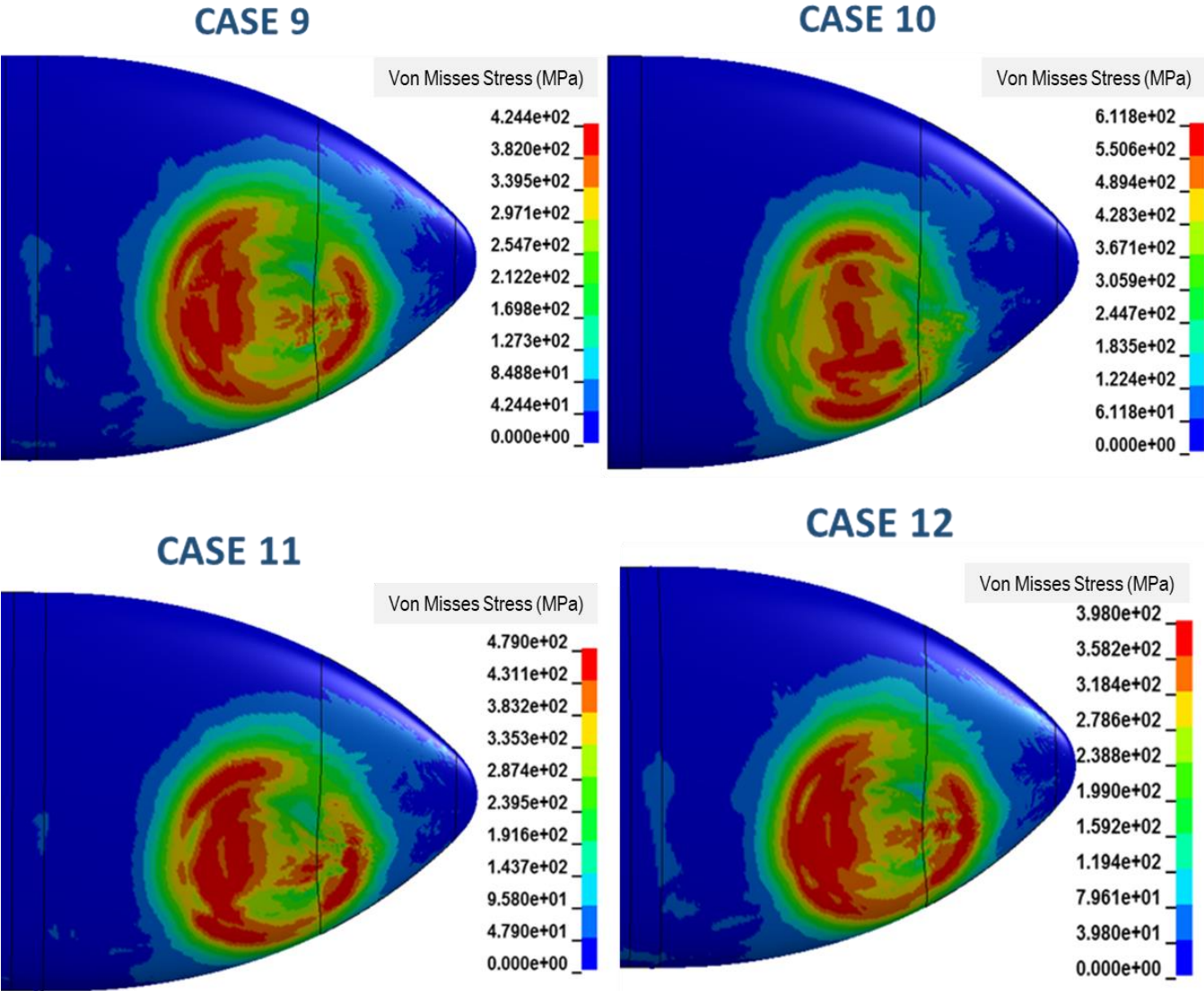


Figure 90 Von Misses Stress Results (MPa) at 2.5 ms for Impactor Position 3

There was no tear up or penetration on the skin of EFT. The stress distributions and effective stresses on skin are similar for Piecewise Linear Plasticity material model and Johnson Cook Material model.

Von Misses Stress results at 3.0 ms for impactor position 3 is shown in Figure 91.

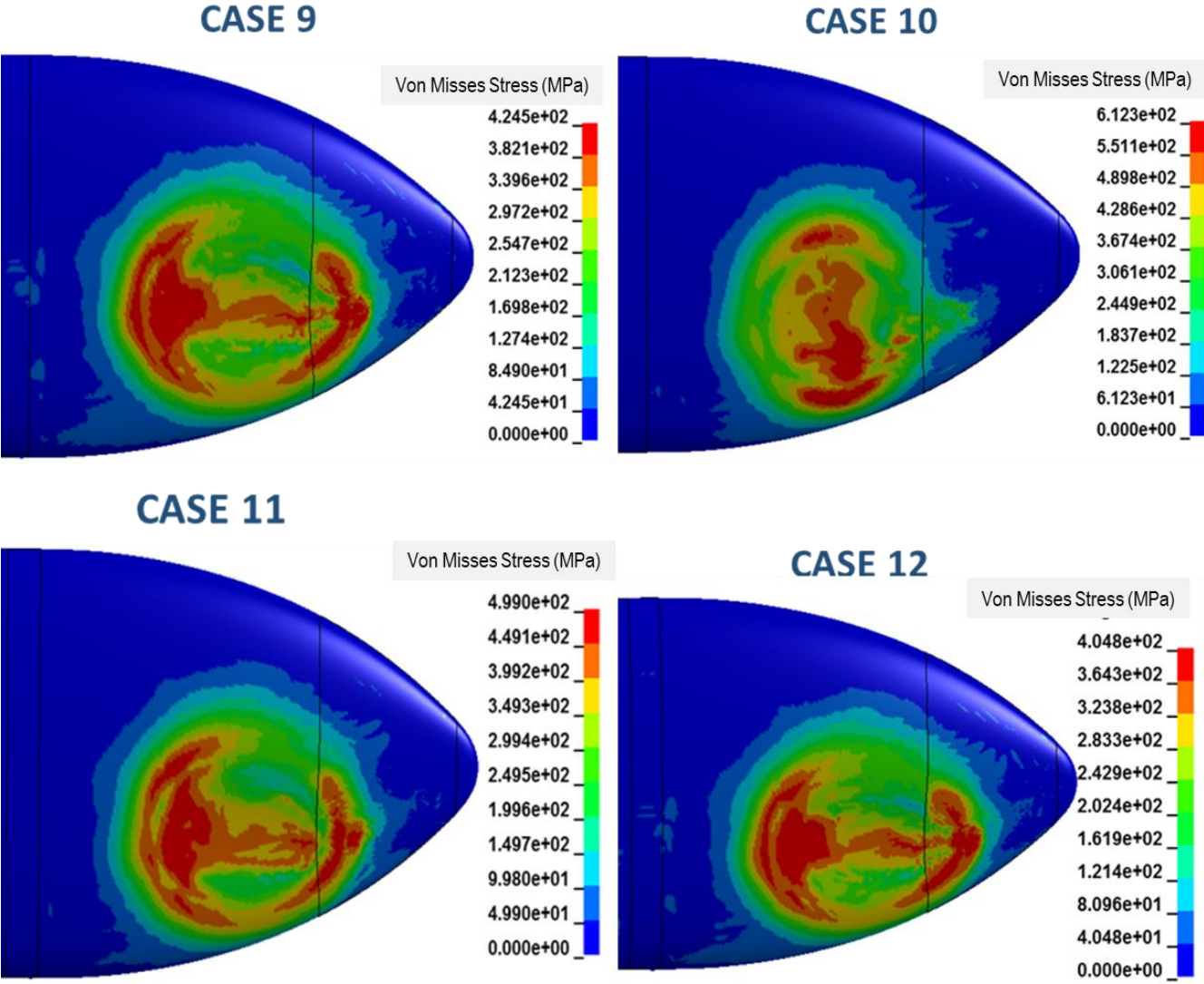


Figure 91 Von Misses Stress Results (MPa) at 3.0 ms for Impactor Position 3

There was no tear up or penetration on the skin of EFT. The stress distributions and effective stresses on skin are similar for Piecewise Linear Plasticity material model and Johnson Cook Material model.

Von Misses Stress results at 3.5 ms for impactor position 3 is shown in Figure 92.

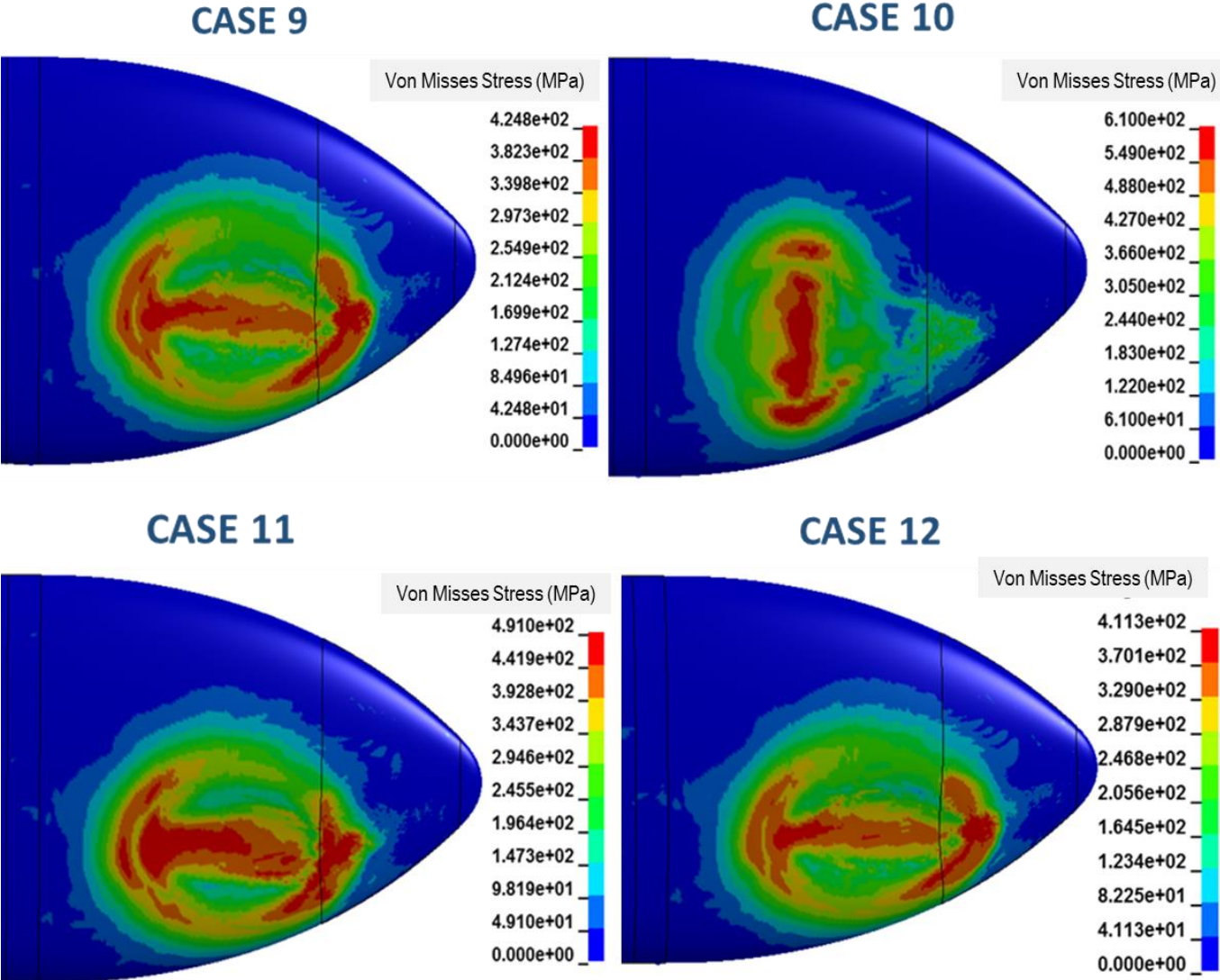


Figure 92 Von Misses Stress Results (MPa) at 3.5 ms for Impactor Position 3

There was no tear up or penetration on the skin of EFT. The stress distributions and effective stresses on skin are similar for Piecewise Linear Plasticity material model and Johnson Cook Material model.

Von Misses Stress results at 4.0 ms for impactor position 3 is shown in Figure 93.

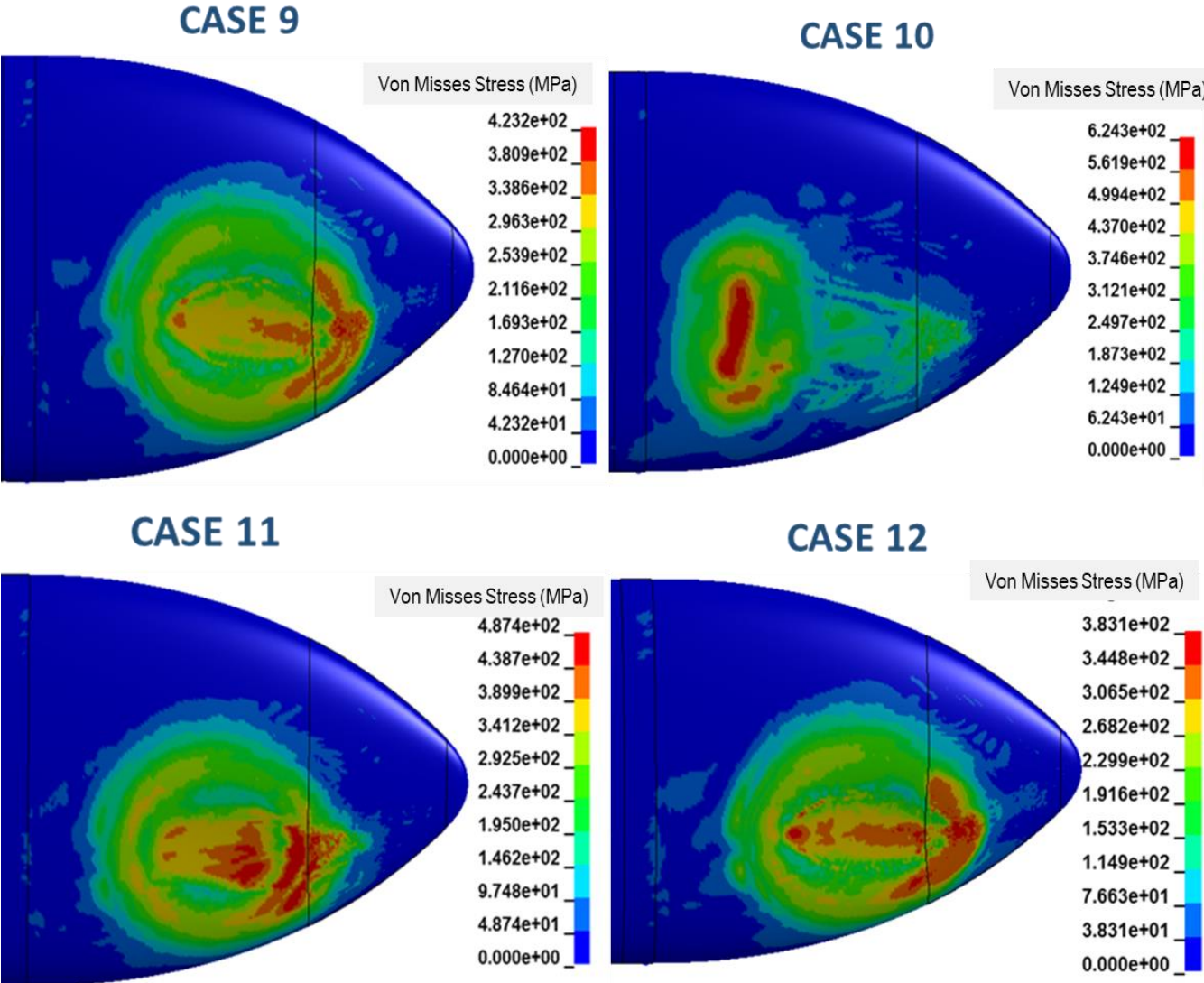


Figure 93 Von Misses Stress Results (MPa) at 4.0 ms for Impactor Position 3

There was no tear up or penetration on the skin of EFT. The stress distributions and effective stresses on skin are similar for Piecewise Linear Plasticity material model and Johnson Cook Material model.

Von Misses Stress results at 4.5 ms for impactor position 3 is shown in Figure 94.

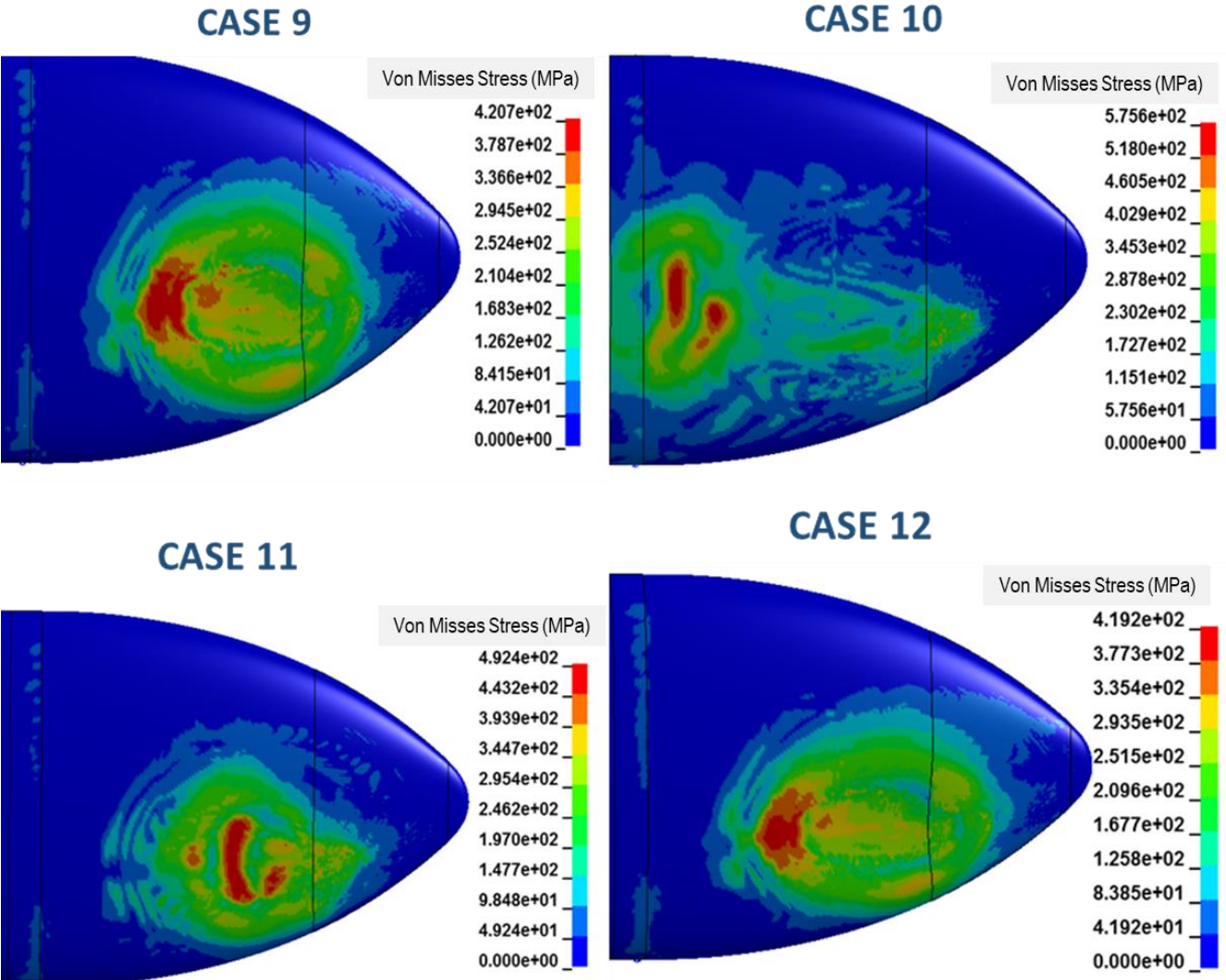


Figure 94 Von Misses Stress Results (MPa) at 4.5 ms for Impactor Position 3

There was no tear up or penetration on the skin of EFT. The stress distributions and effective stresses on skin are similar for Piecewise Linear Plasticity material model and Johnson Cook Material model. Impact ended in 4.4 ms.

Von Misses Stress results at 5.0 ms for impactor position 3 is shown in Figure 95.

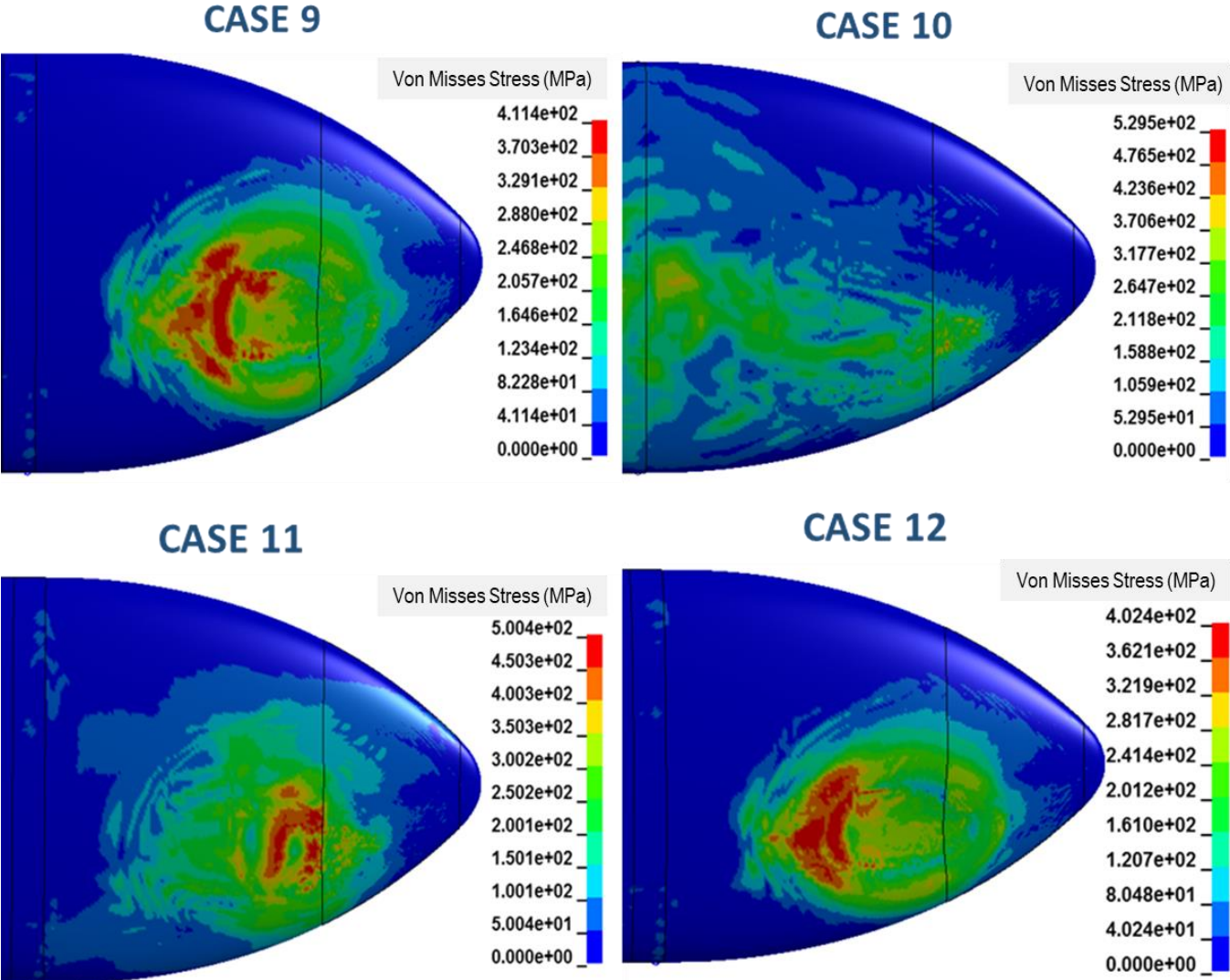


Figure 95 Von Misses Stress Results (MPa) at 5.0 ms for Impactor Position 3

There was no tear up or penetration on the skin of EFT. The stress distributions and effective stresses on skin are similar for Piecewise Linear Plasticity material model and Johnson Cook Material model. Impact ended in 4.4 ms.

The stresses and displacements on EFT skin are shown in Figure 76 to Figure 95. The plastic deformation began at 0.5ms as shown in Figure 86. There was no tear up or penetration on the skin of EFT. The stress distributions and effective stresses on skin are similar for Piecewise Linear Plasticity material model and Johnson Cook Material model.

Maximum stress on EFT skin was 436 MPa for Case 9, 643 MPa for Case 10, 504 MPa for Case 11, 419 MPa for Case 12.

Energy variations for Position 3 is given in Figure 96. While kinetic energy decreased, internal energy increased. For case 9, case 11 and case 12, total energy remained almost constant. For case 10, total energy increased after 4ms. This is because of the peak which occurred after the contact between impactor and target ended.



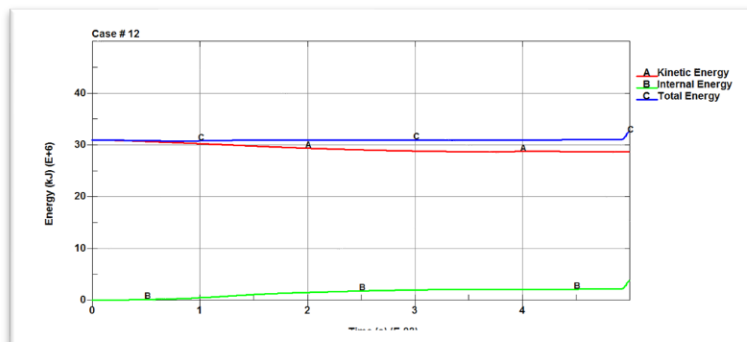
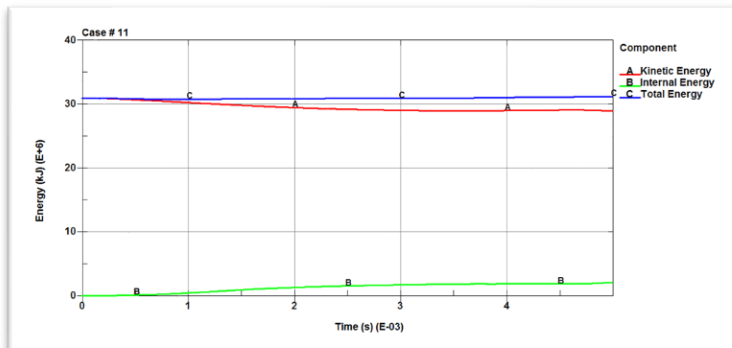
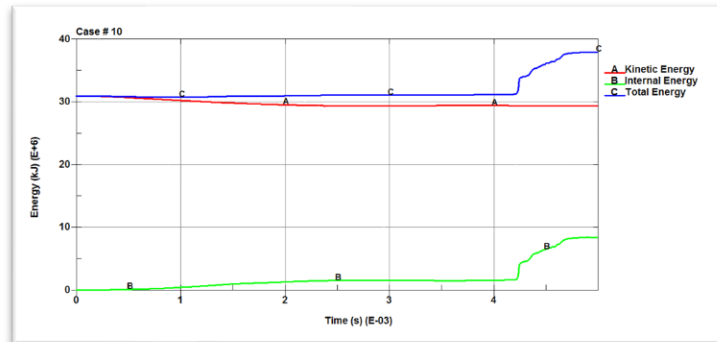
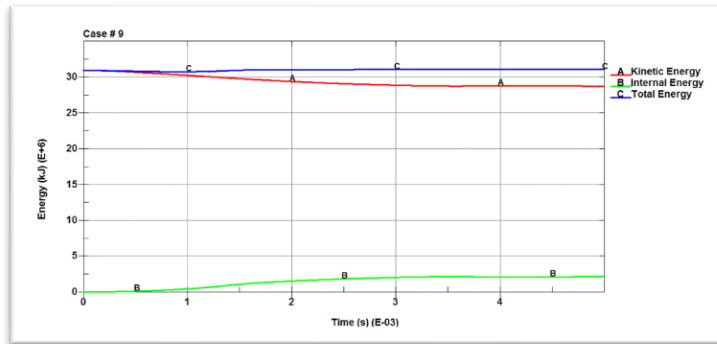


Figure 96 Energy Variation of Position 3

Energy ratios for Position 3 is given in Figure 97. Energy ratios for position 3 remained within the acceptable limits as shown for 4ms. For case 10, Energy ratio increased after 4ms. However, since the contact between impactor and target ended after 4 ms, these increase should not be taken into account.

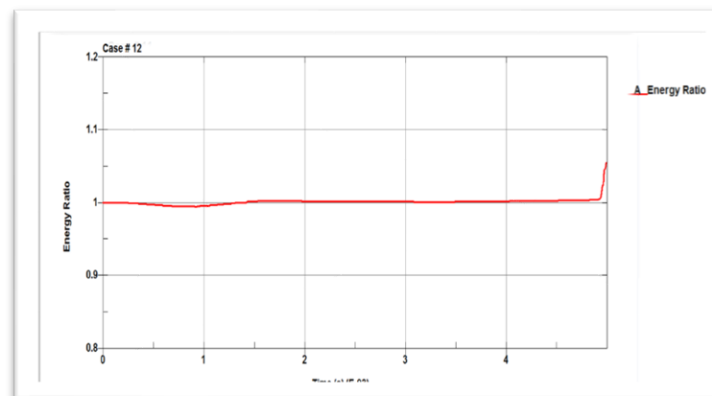
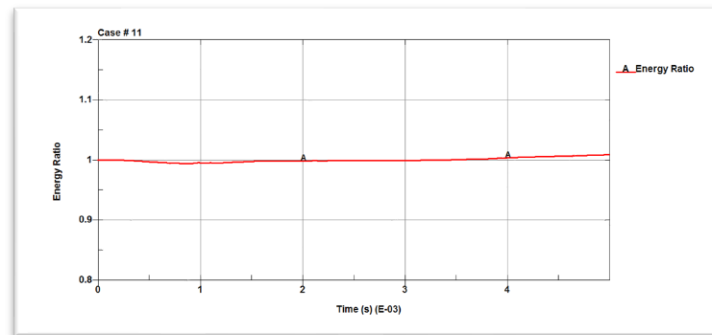
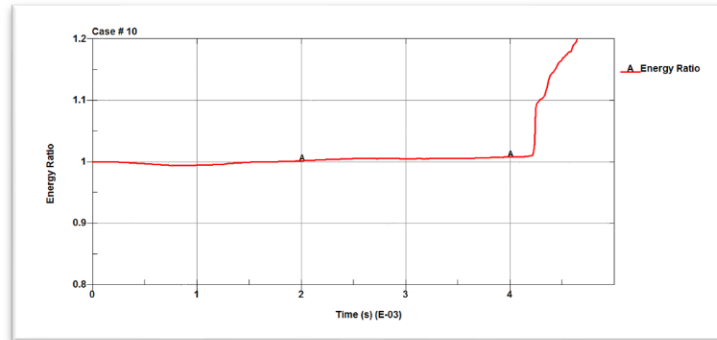
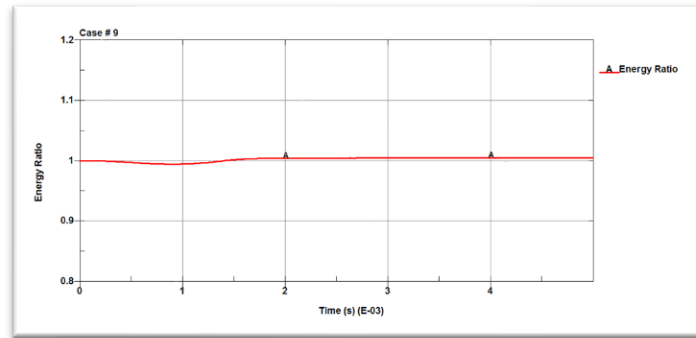


Figure 97 Energy Ratio of Position 3

Hourglass energy, damping energy and sliding energy for case 9 is given in Figure 98. Impact ended in 4.4 ms. Hourglass energy remained almost 0 for 4.4 ms. For sliding energy, peak did not occur.

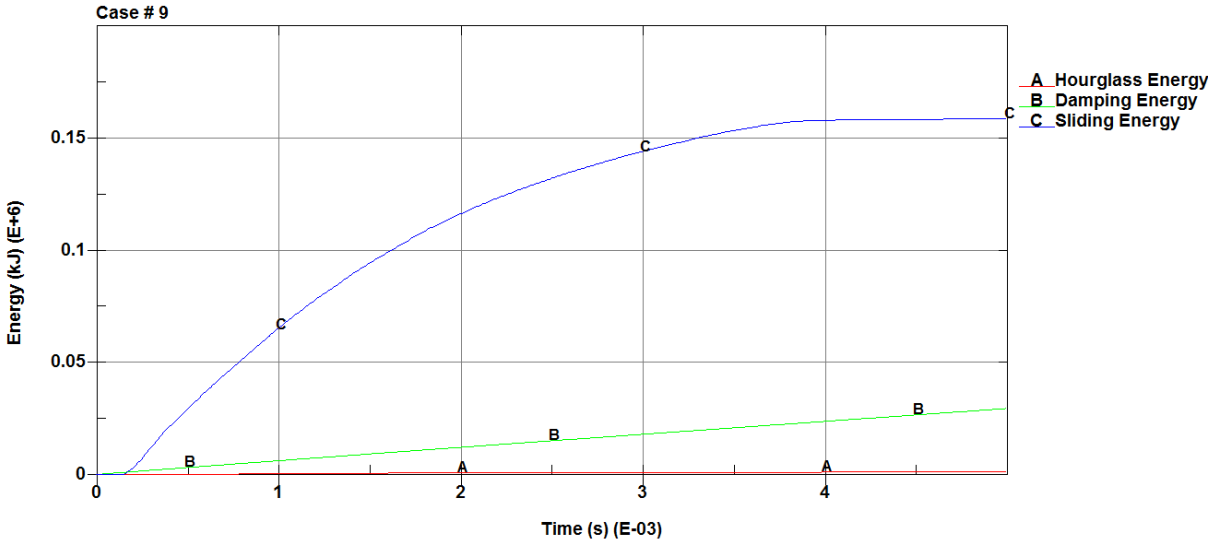


Figure 98 Hourglass, Damping and Sliding Energies Variation of Case 9

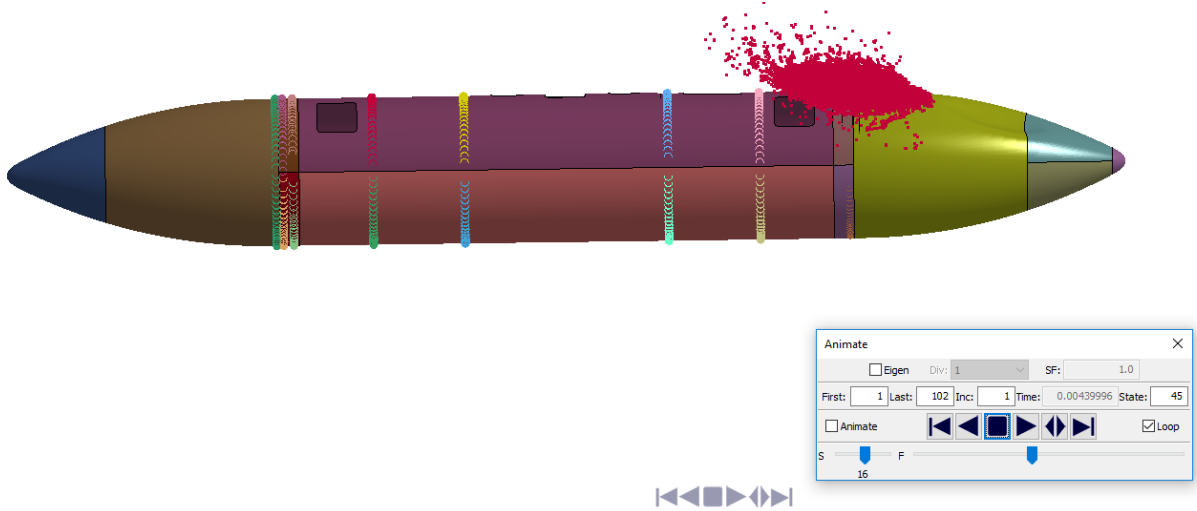


Figure 99 Bird Impact at 4 ms for Case 9

Hourglass energy, damping energy and sliding energy for case 10 is given in Figure 100. Impact ended in 4.4 ms. Hourglass energy remained almost 0 for 4.4 ms. For sliding energy, peak

occurred after the contact between impactor and target ended; however the increase is in the acceptable limit.

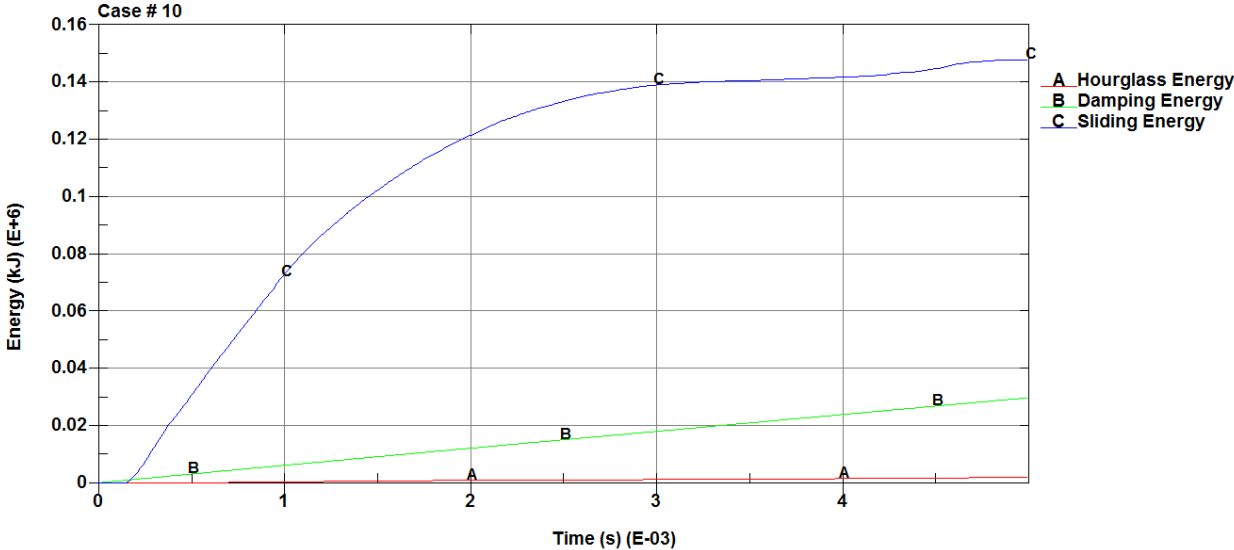


Figure 100 Hourglass, Damping and Sliding Energies Variation of Case 10

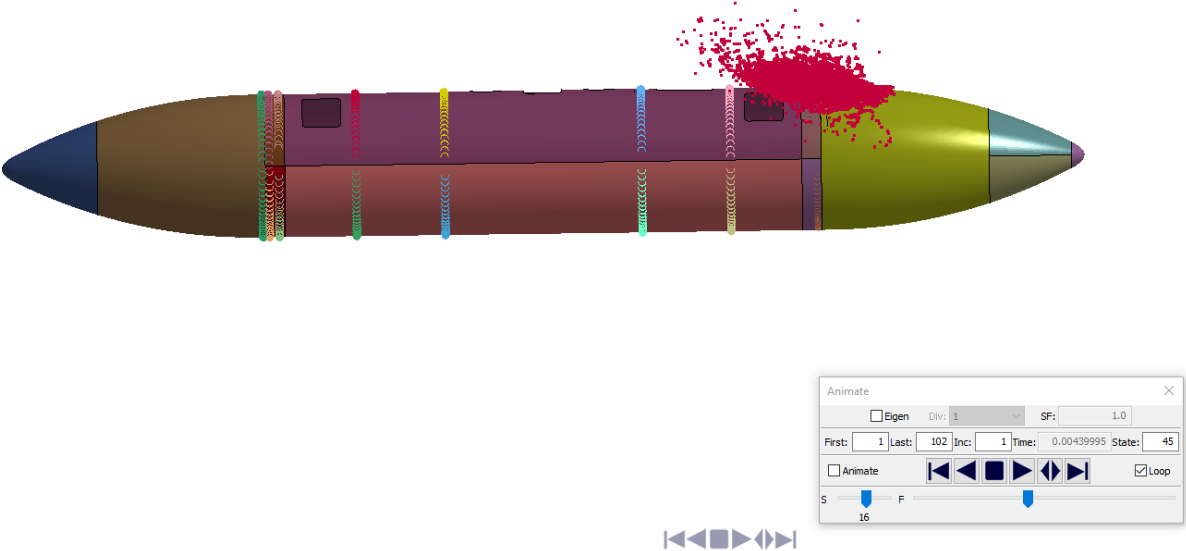


Figure 101 Bird Impact at 4 ms for Case 10

Hourglass energy, damping energy and sliding energy for case 11 is given in Figure 101. Impact ended in 4.3 ms. Hourglass energy remained almost 0 for 4.3 ms. For sliding energy, peak did not occur.

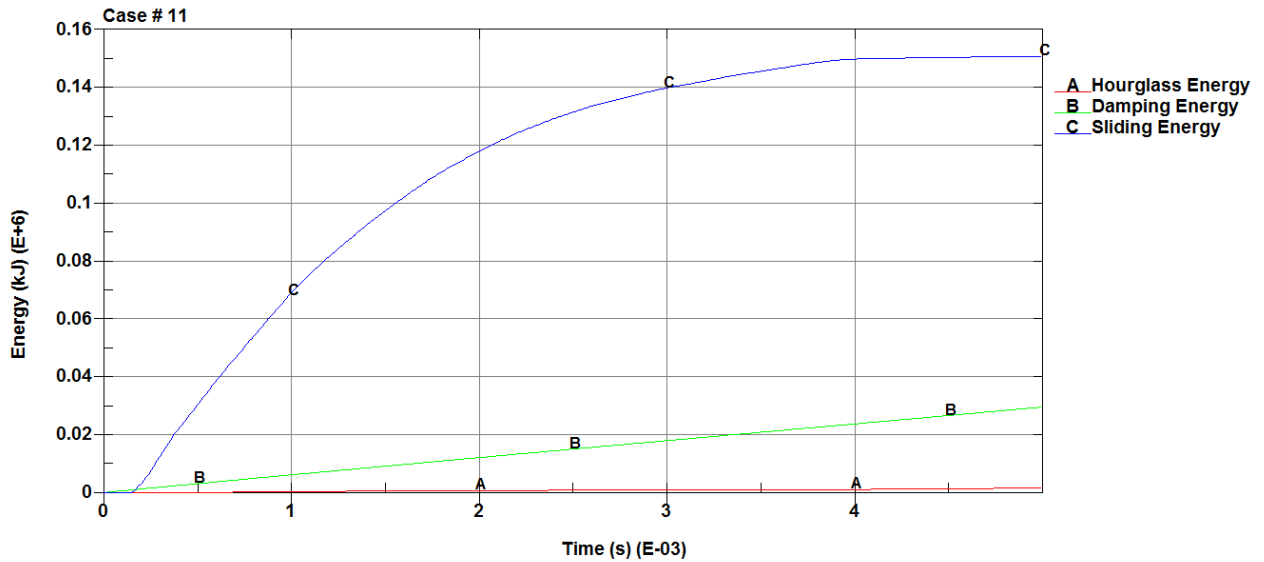


Figure 102 Hourglass, Damping and Sliding Energies Variation of Case 11

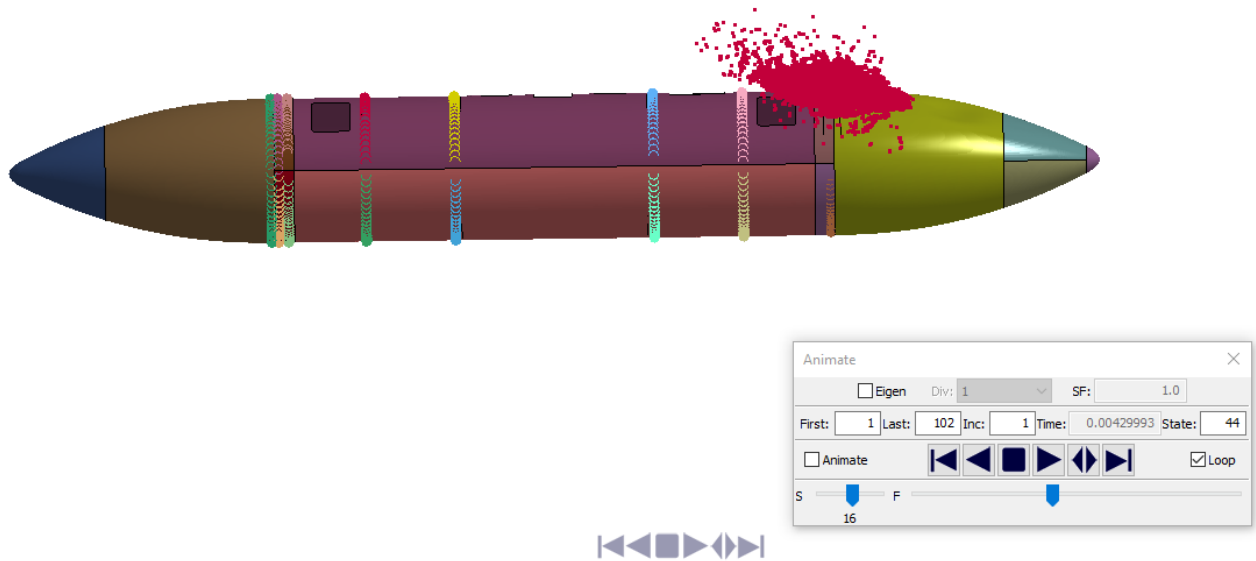


Figure 103 Bird Impact at 4 ms for Case 11

Hourglass energy, damping energy and sliding energy for case 12 is given in Figure 104. Impact ended in 4.4 ms. Hourglass energy remained almost 0 for 4.4 ms. For sliding energy, peak did not occur.

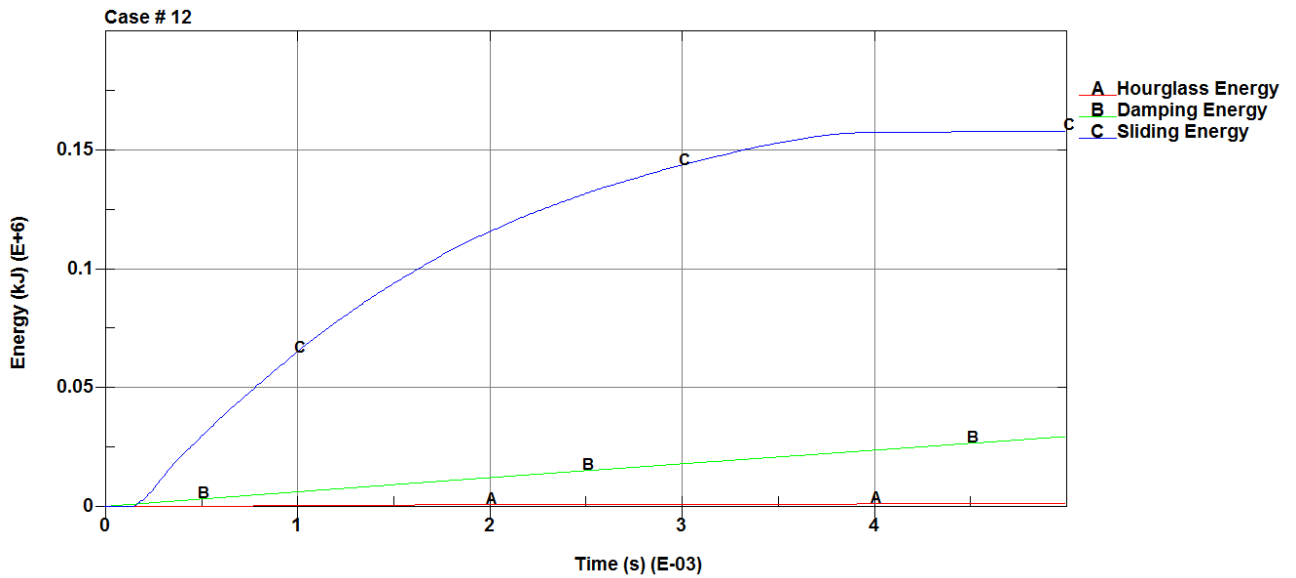


Figure 104 Hourglass, Damping and Sliding Energies Variation of Case 12

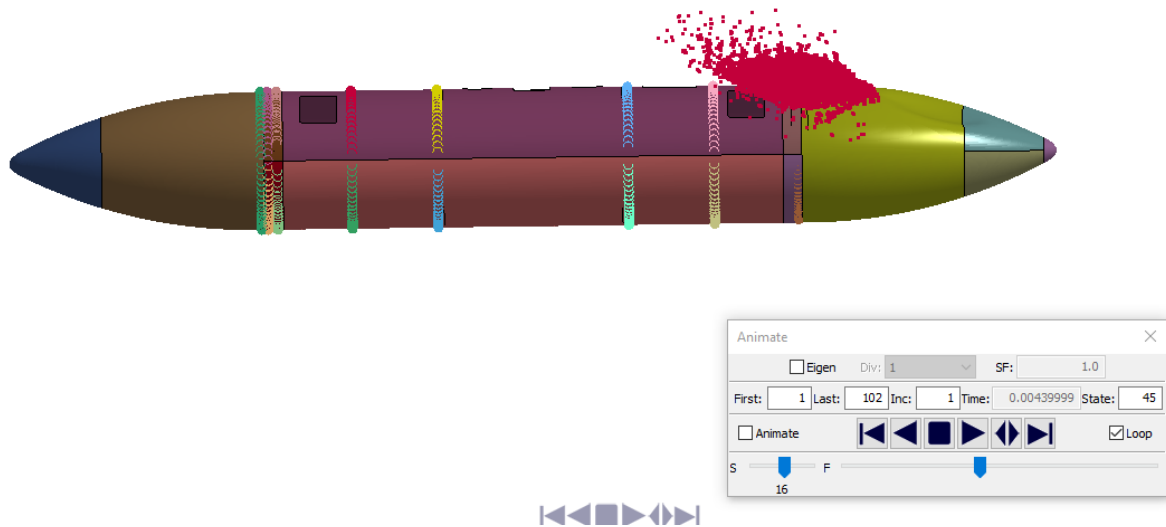


Figure 105 Bird Impact at 4 ms for Case 12

### **Analysis Results for Position 4**

An overview of the impact simulation for the position 4 was given for the general understanding. The time history was presented as a series of time step plots with explanations. The plots in Figure 106 to Figure 125 show the simulation run in several steps. Total simulation time was set to 5 ms and plots are saved in the intervals of 0.5ms.

Displacement results at 0.5 ms for impactor position 4 is shown in Figure 106.

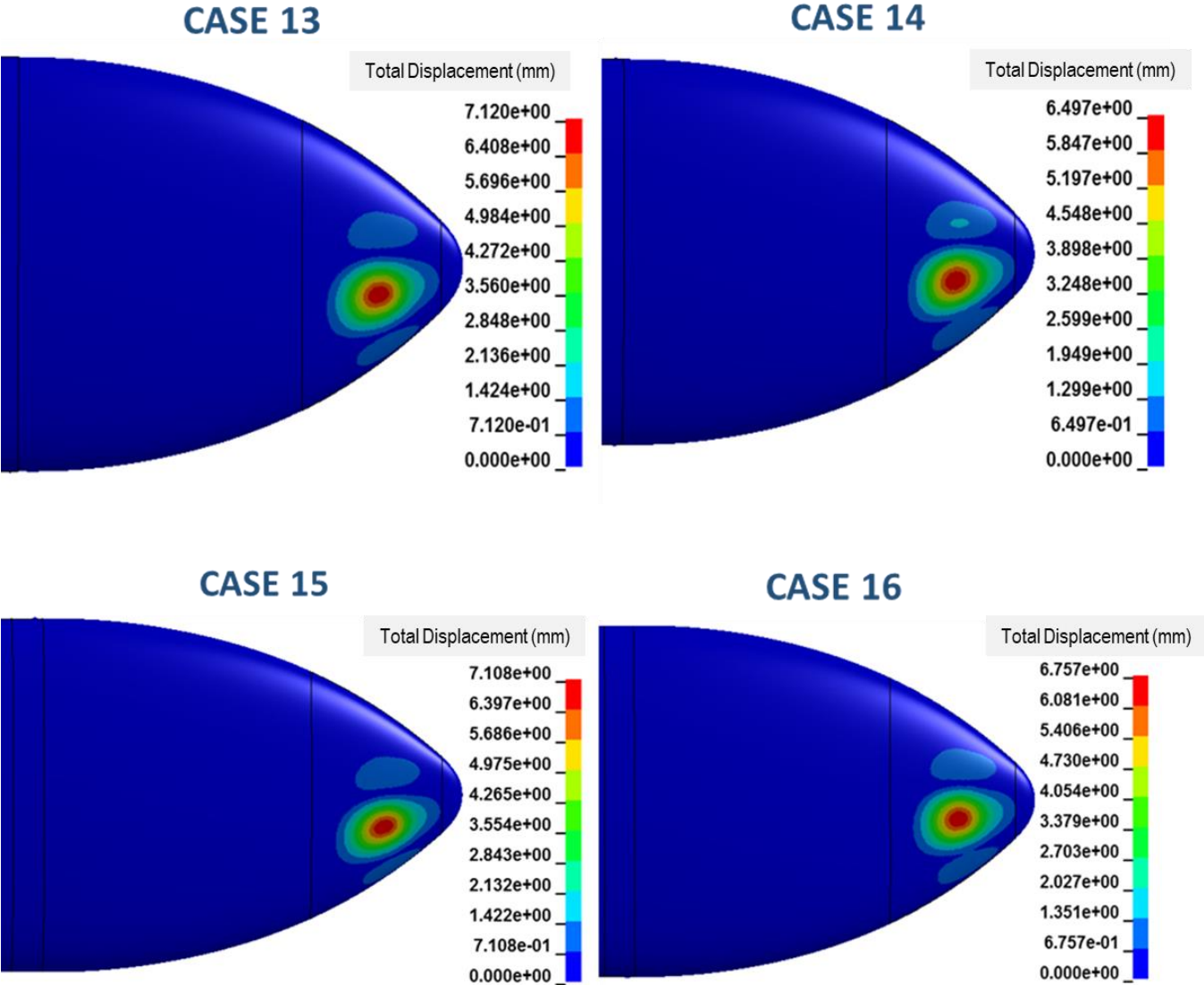


Figure 106 Displacement Results (mm) at 0.5 ms for Impactor Position 4

Displacements on Al 7075 -T6 and Al 2024-T3 are similar. Displacement values according to Piecewise Linear Plasticity material model are also similar to Johnson Cook Material model.

Displacement results at 1.0 ms for impactor position 4 is shown in Figure 107.



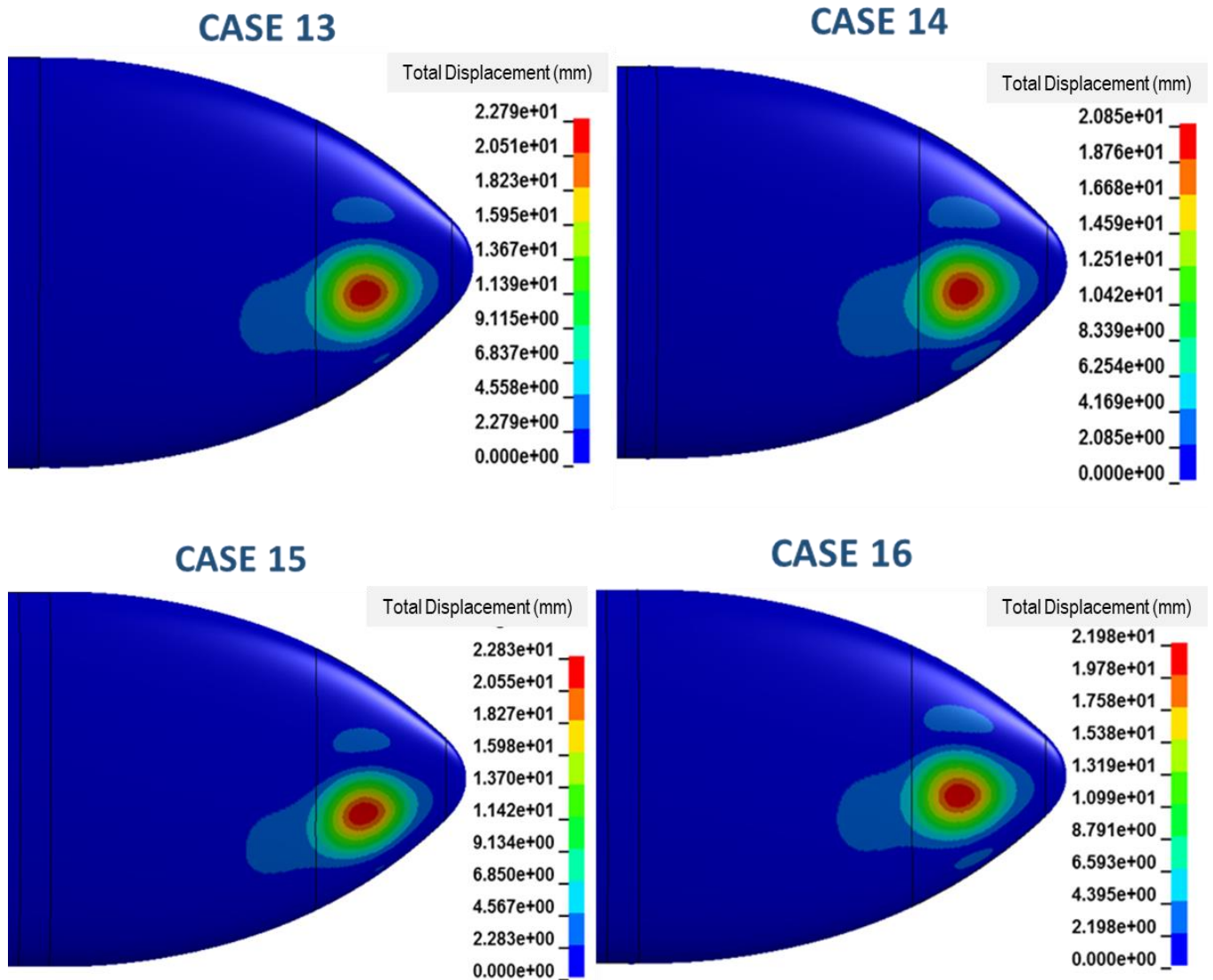


Figure 107 Displacement Results (mm) at 1.0 ms for Impactor Position 4

Displacements on Al 7075 -T6 and Al 2024-T3 are similar. Displacement values according to Piecewise Linear Plasticity material model are also similar to Johnson Cook Material model.

Displacement results at 1.5 ms for impactor position 4 is shown in Figure 108.

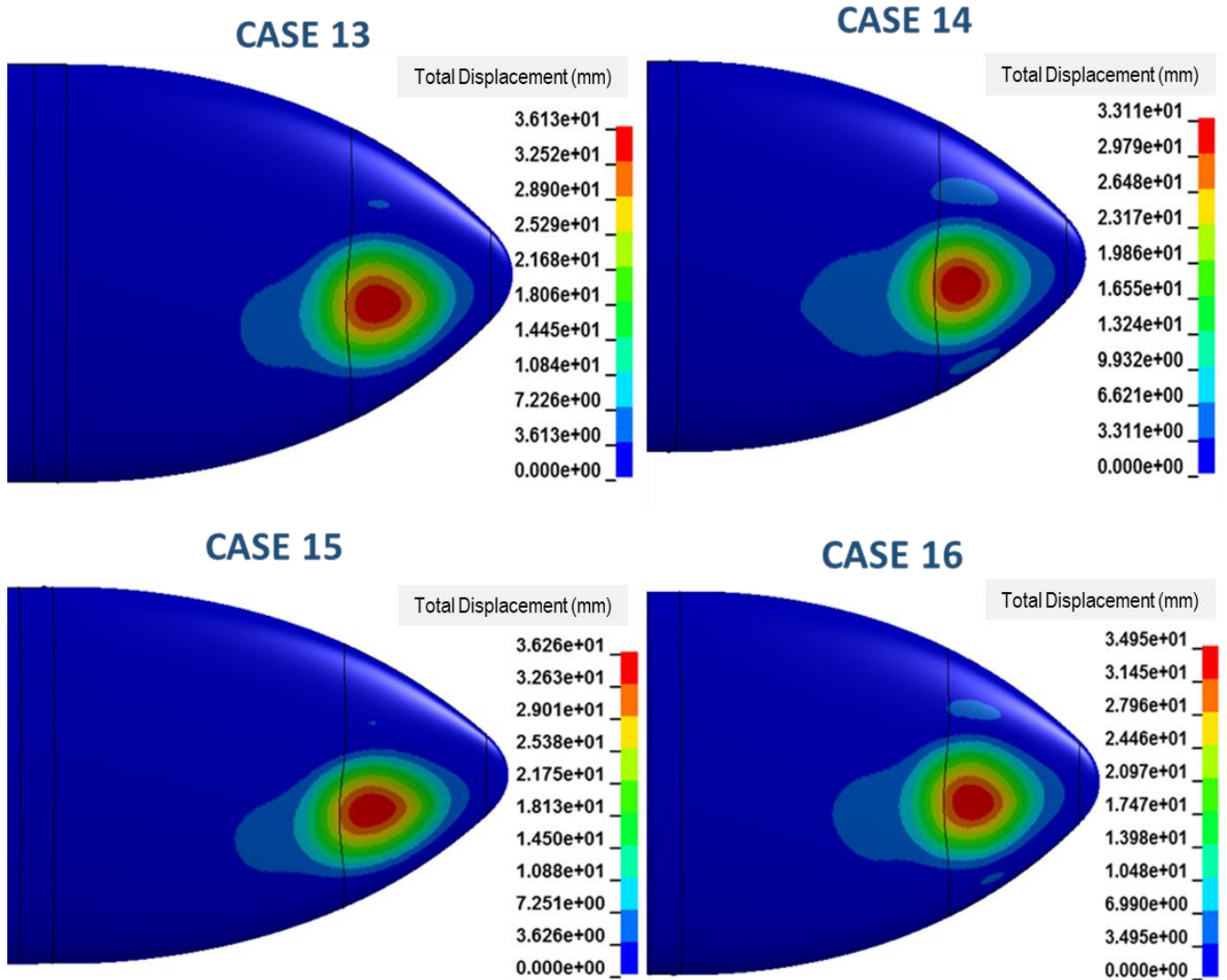


Figure 108 Displacement Results (mm) at 1.5 ms for Impactor Position 4

Displacements on Al 7075 -T6 and Al 2024-T3 are similar. Displacement values according to Piecewise Linear Plasticity material model are also similar to Johnson Cook Material model.

Displacement results at 2.0 ms for impactor position 4 is shown in Figure 109.

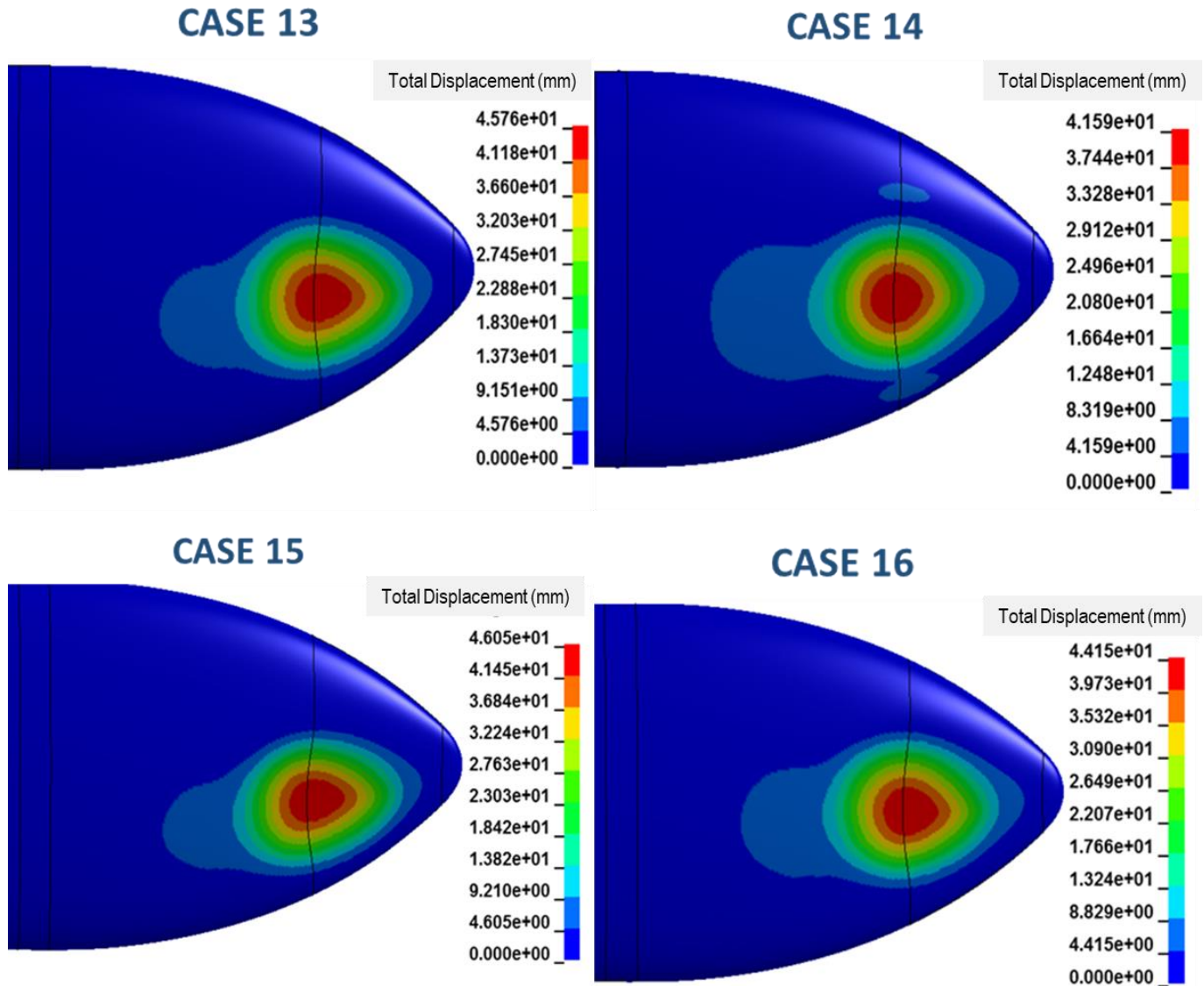


Figure 109 Displacement Results (mm) at 2.0 ms for Impactor Position 4

Displacements on Al 7075 -T6 and Al 2024-T3 are similar. Displacement values according to Piecewise Linear Plasticity material model are also similar to Johnson Cook Material model.

Displacement results at 2.5 ms for impactor position 4 is shown in Figure 110.

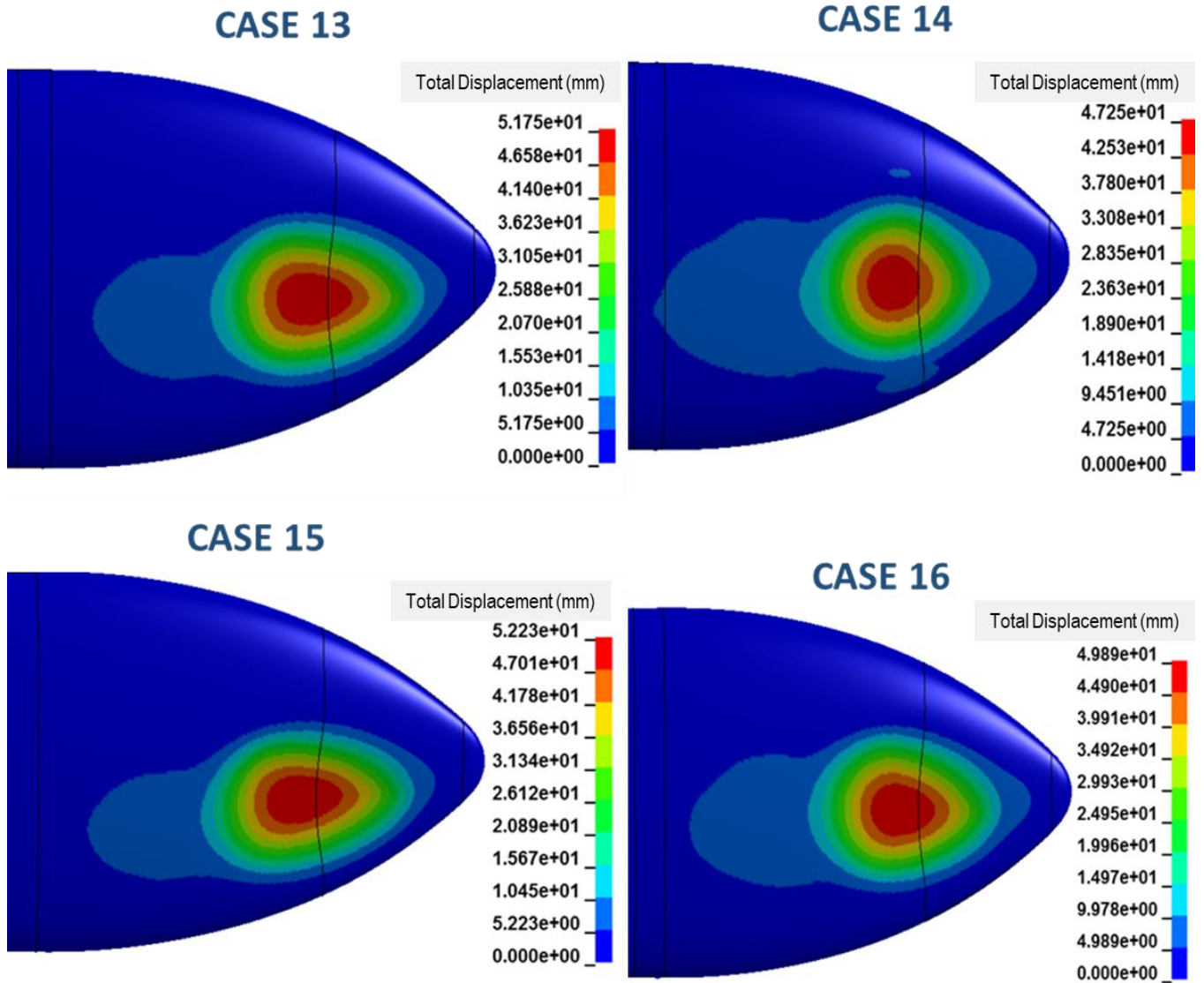


Figure 110 Displacement Results (mm) at 2.5 ms for Impactor Position 4

Displacements on Al 7075 -T6 and Al 2024-T3 are similar. Displacement values according to Piecewise Linear Plasticity material model are also similar to Johnson Cook Material model.

Displacement results at 3.0 ms for impactor position 4 is shown in Figure 111.

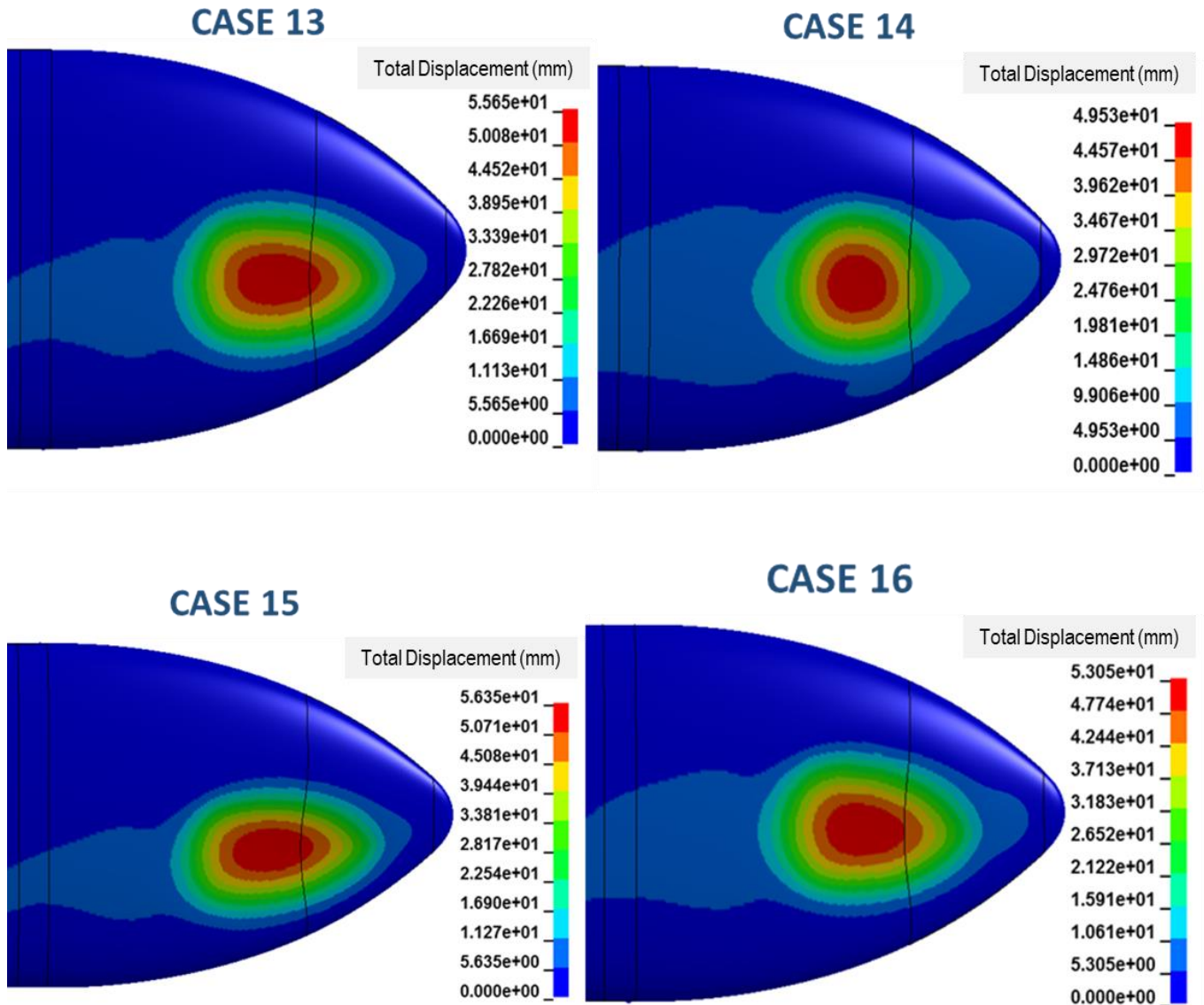


Figure 111 Displacement Results (mm) at 3.0 ms for Impactor Position 4

Displacements on Al 7075 -T6 and Al 2024-T3 are similar. Displacement values according to Piecewise Linear Plasticity material model are also similar to Johnson Cook Material model.

Displacement results at 3.5 ms for impactor position 4 is shown in Figure 112.

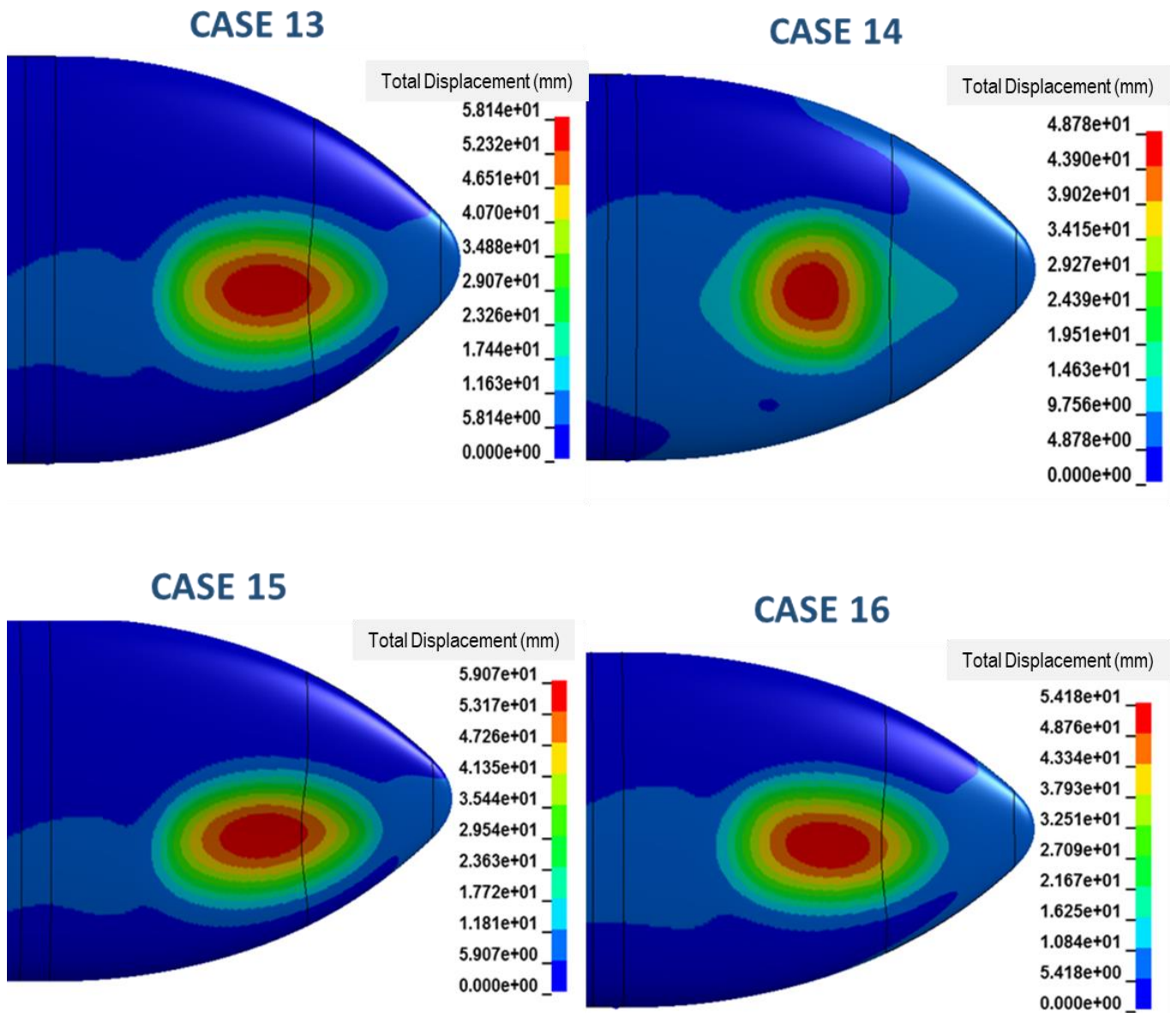


Figure 112 Displacement Results (mm) at 3.5 ms for Impactor Position 4

Displacements on Al 7075 -T6 and Al 2024-T3 are similar. Displacement values according to Piecewise Linear Plasticity material model are also similar to Johnson Cook Material model.

Displacement results at 4.0 ms for impactor position 4 is shown in Figure 113.

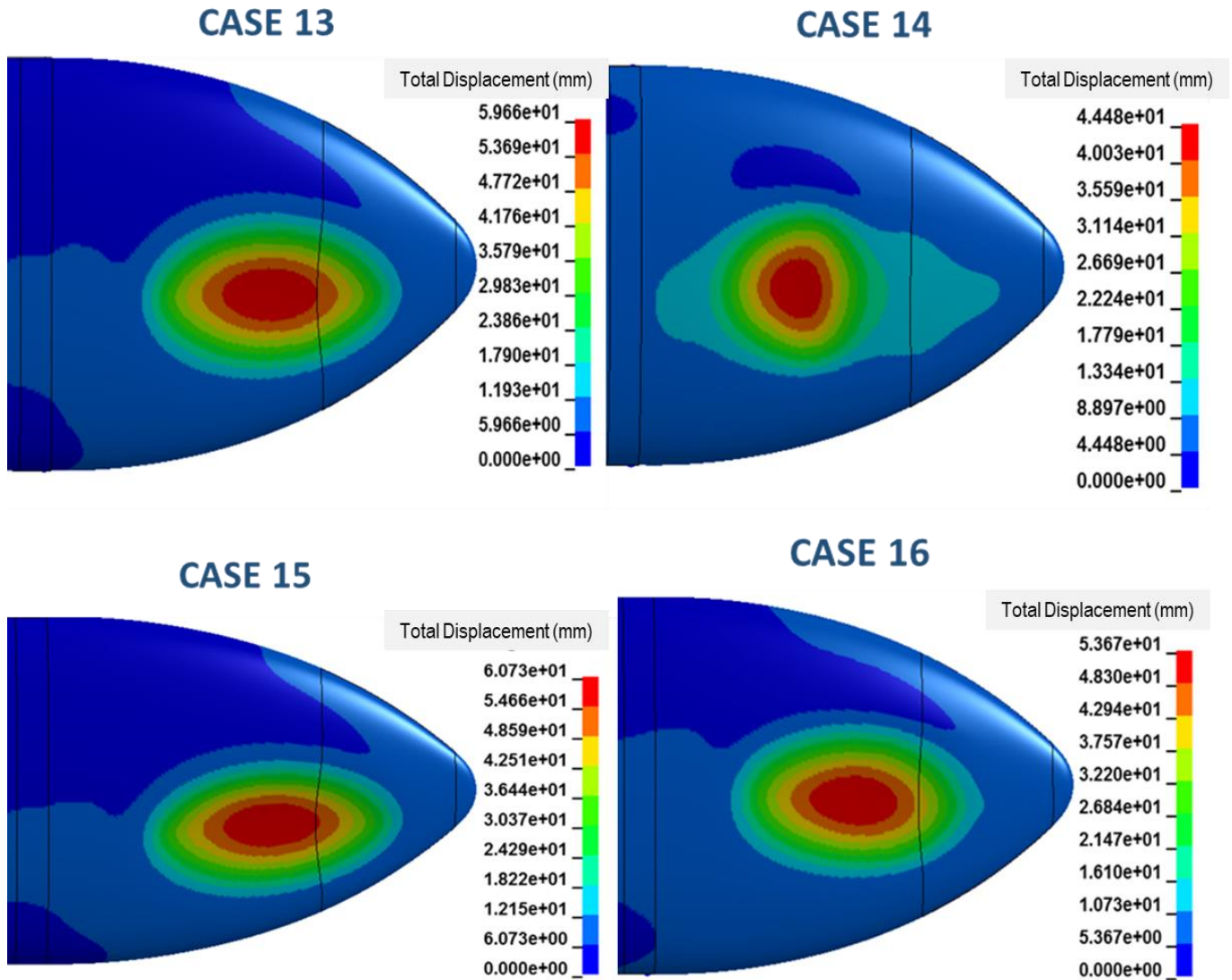


Figure 113 Displacement Results (mm) at 4.0 ms for Impactor Position 4

Displacements on Al 7075 -T6 and Al 2024-T3 are similar. Displacement values according to Piecewise Linear Plasticity material model are also similar to Johnson Cook Material model.

Displacement results at 4.5 ms for impactor position 4 is shown in Figure 114.

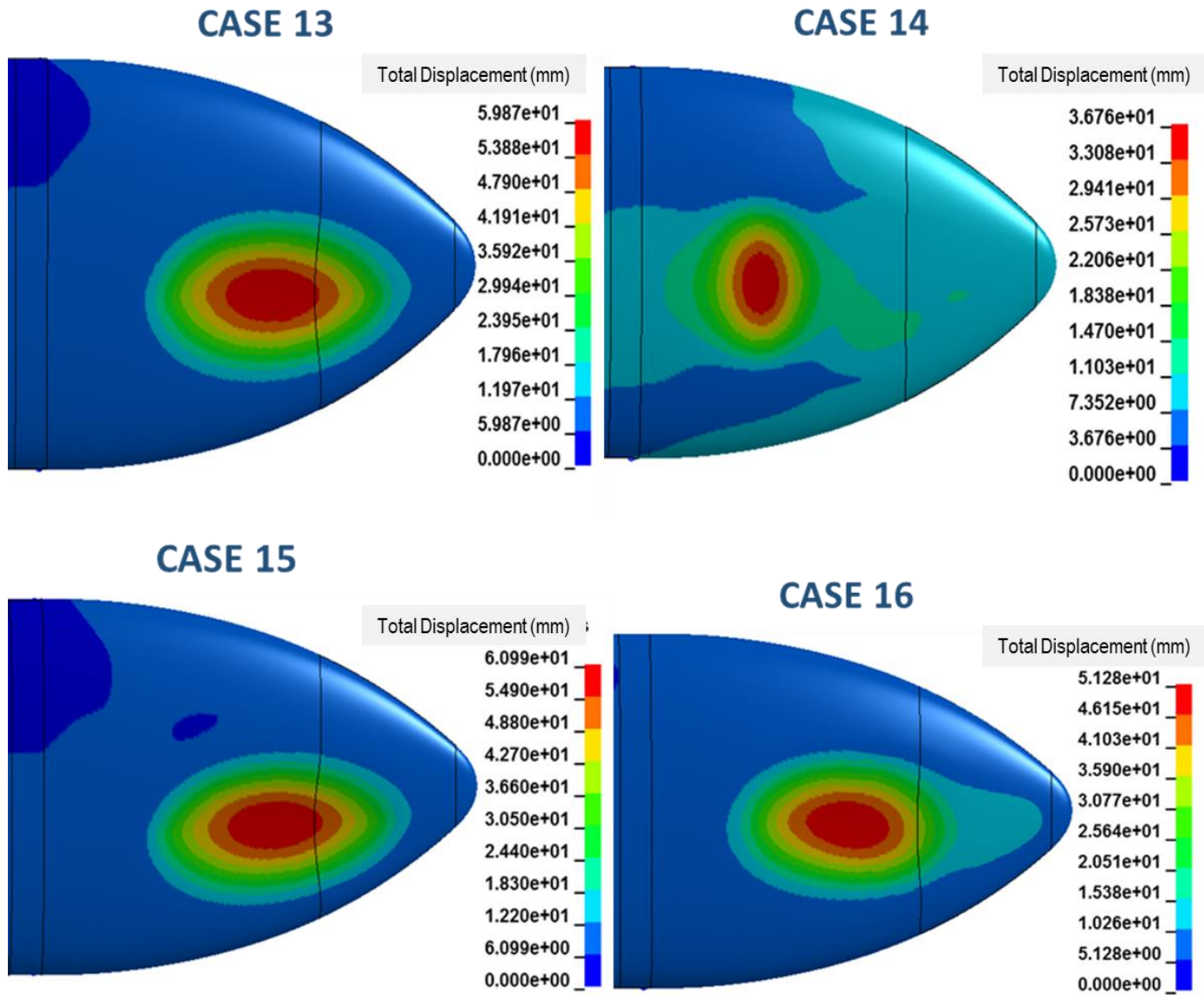


Figure 114 Displacement Results (mm) at 4.5 ms for Impactor Position 4

Displacements on Al 7075 -T6 and Al 2024-T3 are similar. Displacement values according to Piecewise Linear Plasticity material model are also similar to Johnson Cook Material model. Impact ended in 4.4 ms.

Displacement results at 5.0 ms for impactor position 4 is shown in Figure 115.



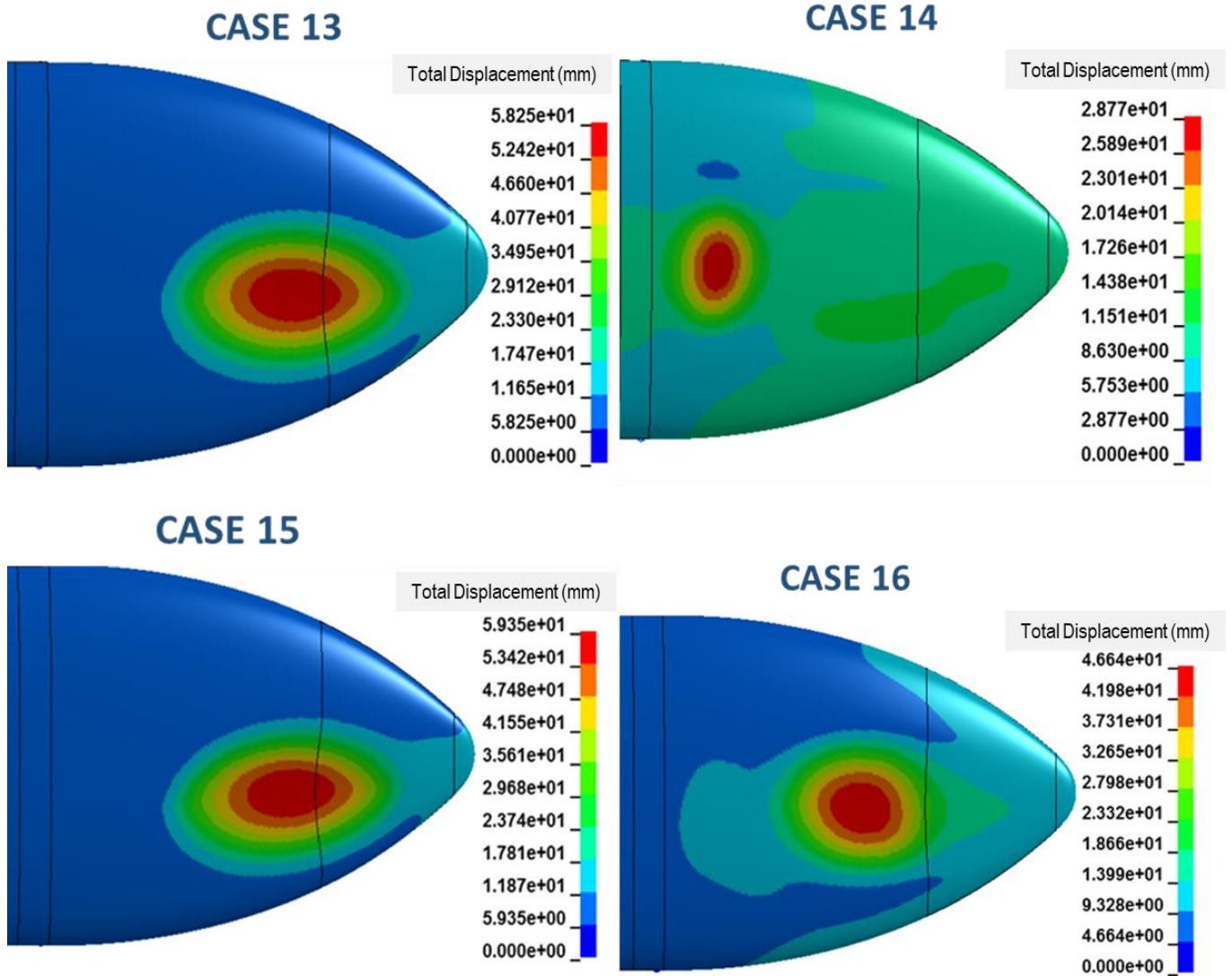


Figure 115 Displacement Results (mm) at 5.0 ms for Impactor Position 4

Displacements on Al 7075 -T6 and Al 2024-T3 are similar. Displacement values according to Piecewise Linear Plasticity material model are also similar to Johnson Cook Material model which is an expected result because of low strain rates. Impact ended in 4.4 ms.

For position 4, displacements on Al 7075 -T6 and Al 2024-T3 are similar. Displacement values according to Piecewise Linear Plasticity material model are also similar to Johnson Cook Material model.

After impact, screen shots were taken at 0.5ms intervals and the stresses are compared. Since the contact of the bird ended before 5 ms in general, the images were limited to this time period.

Von Misses Stress results at 0.5 ms for impactor position 4 is shown in Figure 116.

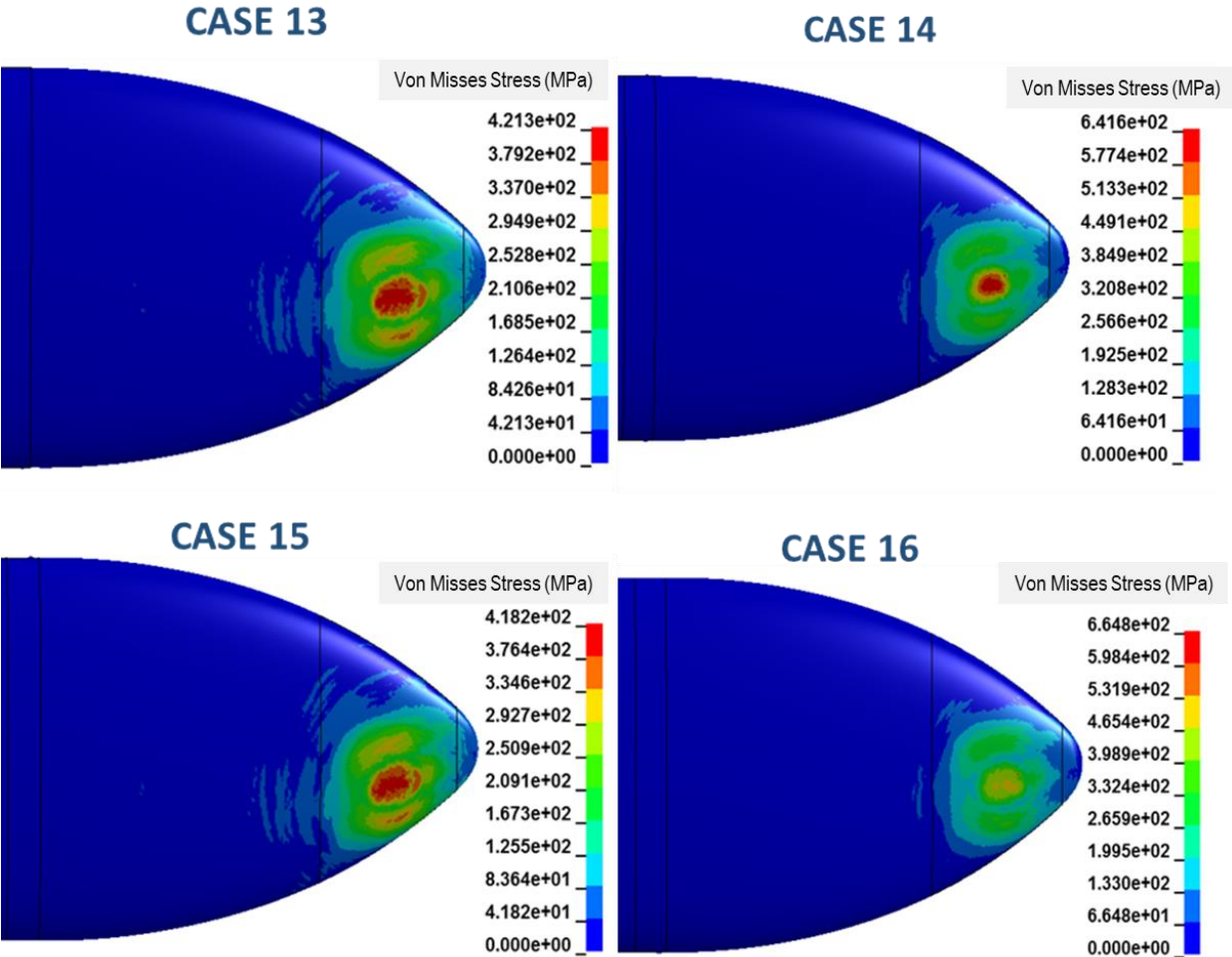


Figure 116 Von Misses Stress Results (MPa) at 0.5 ms for Impactor Position 4

The plastic deformation began at 0.5ms as shown in Figure 116. There was no tear up or penetration on the skin of EFT. The stress distributions and effective stresses on skin are similar for Piecewise Linear Plasticity material model and Johnson Cook Material model.

Von Misses Stress results at 1.0 ms for impactor position 4 is shown in Figure 117

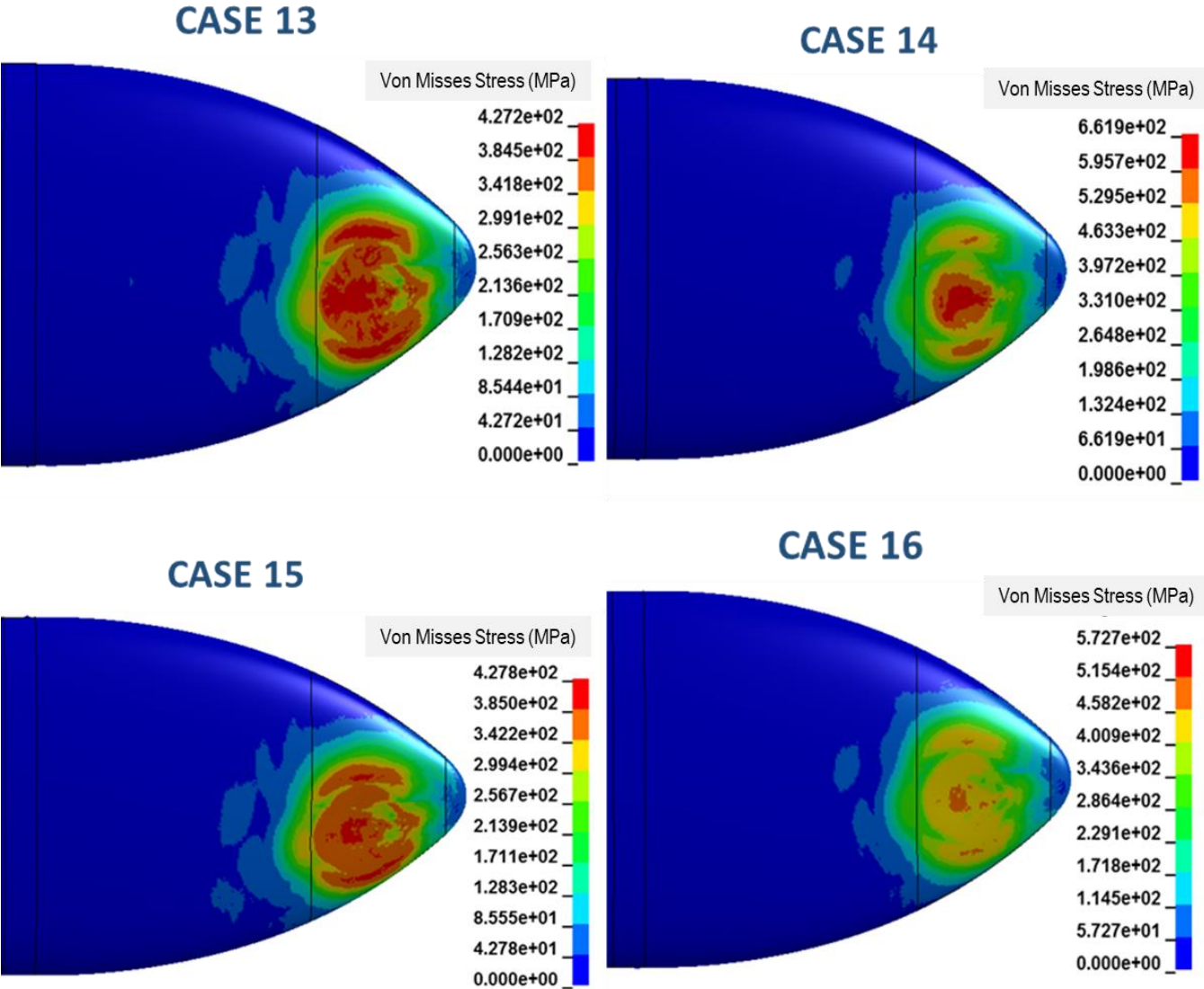


Figure 117 Von Misses Stress Results (MPa) at 1.0 ms for Impactor Position 4

There was no tear up or penetration on the skin of EFT. The stress distributions and effective stresses on skin are similar for Piecewise Linear Plasticity material model and Johnson Cook Material model.

Von Misses Stress results at 1.5 ms for impactor position 4 is shown in Figure 118.

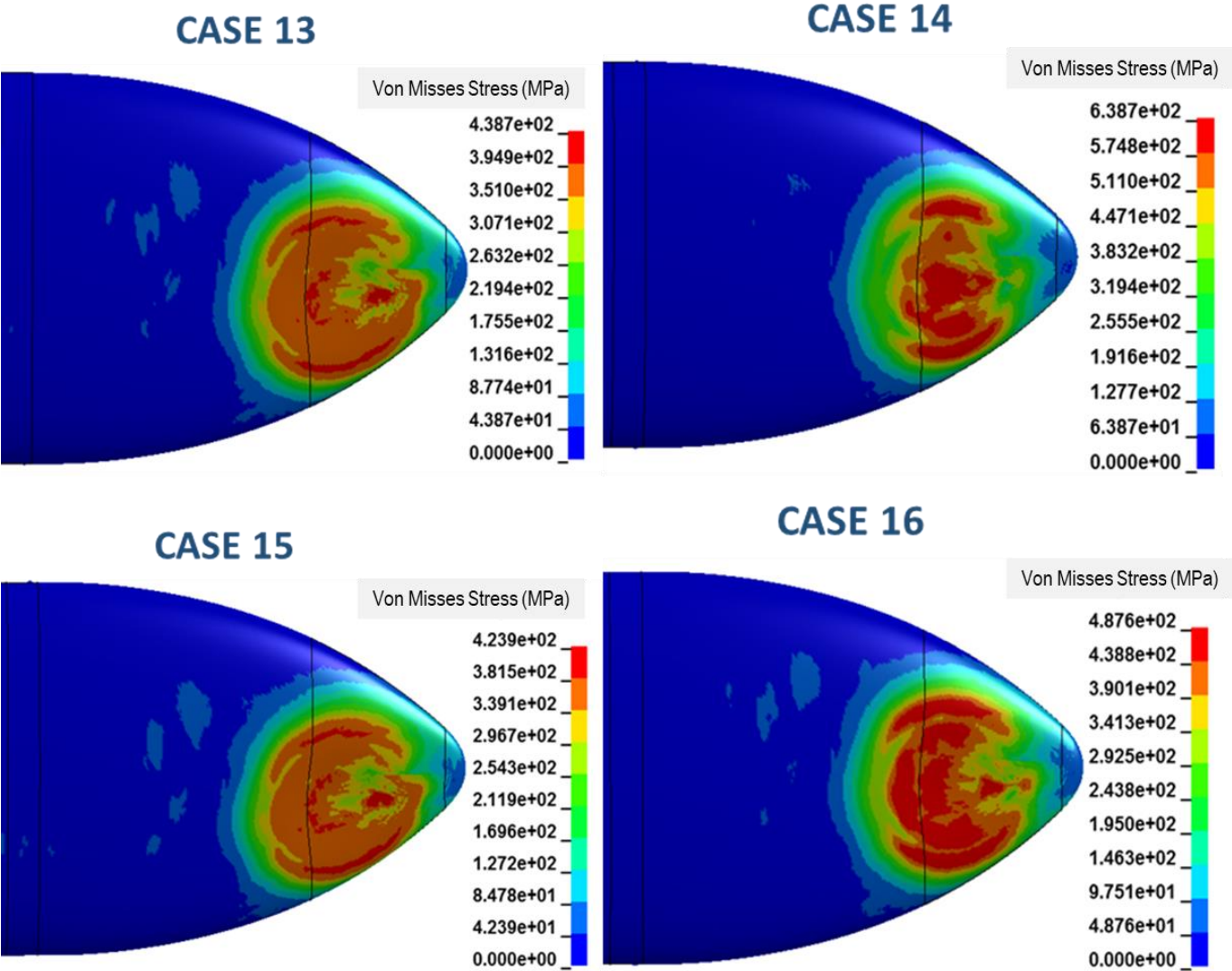


Figure 118 Von Misses Stress Results (MPa) at 1.5 ms for Impactor Position 4

There was no tear up or penetration on the skin of EFT. The stress distributions and effective stresses on skin are similar for Piecewise Linear Plasticity material model and Johnson Cook Material model.

Von Misses Stress results at 2.0 ms for impactor position 4 is shown in Figure 119.

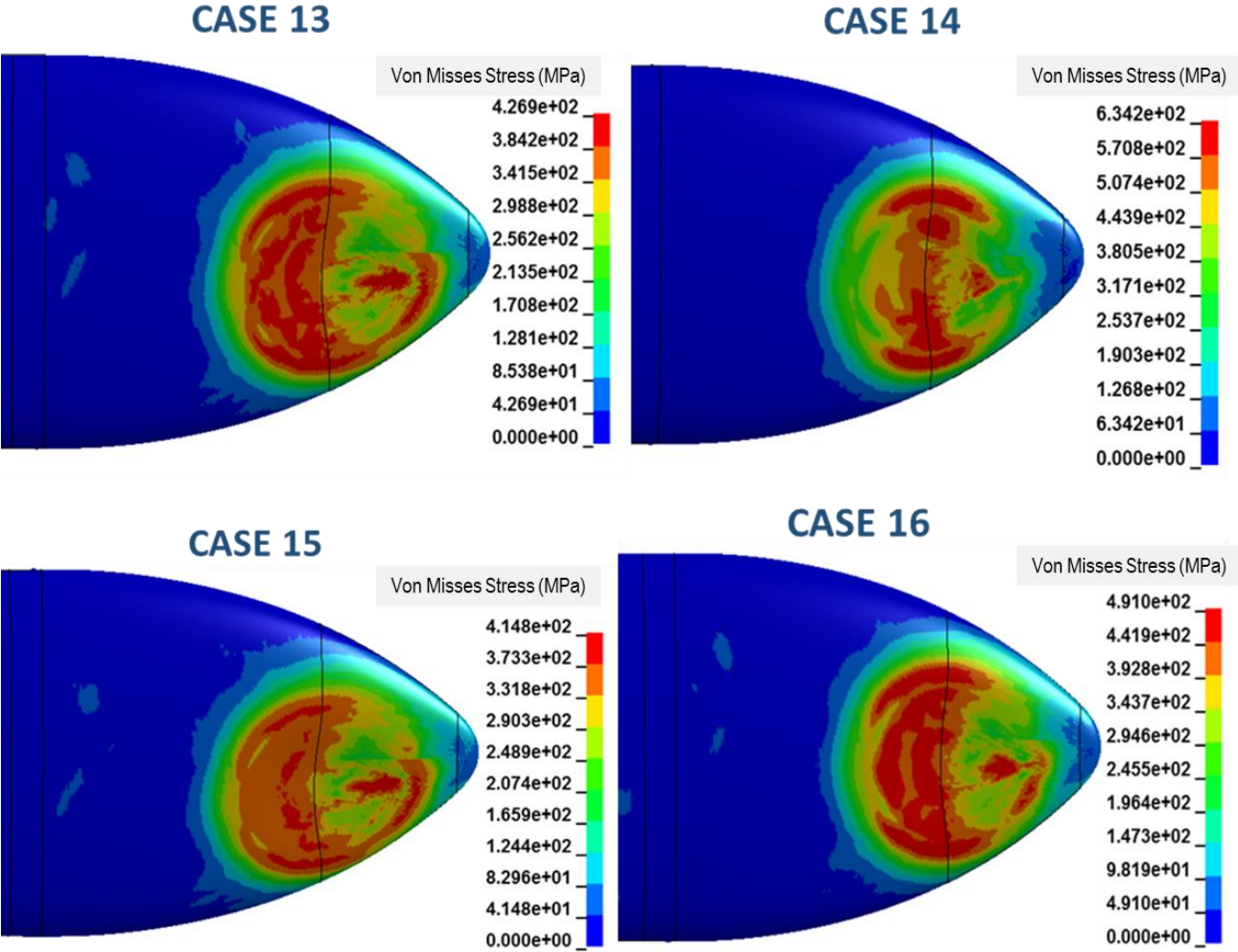


Figure 119 Von Misses Stress Results (MPa) at 2.0 ms for Impactor Position 4

There was no tear up or penetration on the skin of EFT. The stress distributions and effective stresses on skin are similar for Piecewise Linear Plasticity material model and Johnson Cook Material model.

Von Misses Stress results at 2.5 ms for impactor position 4 is shown in Figure 120.

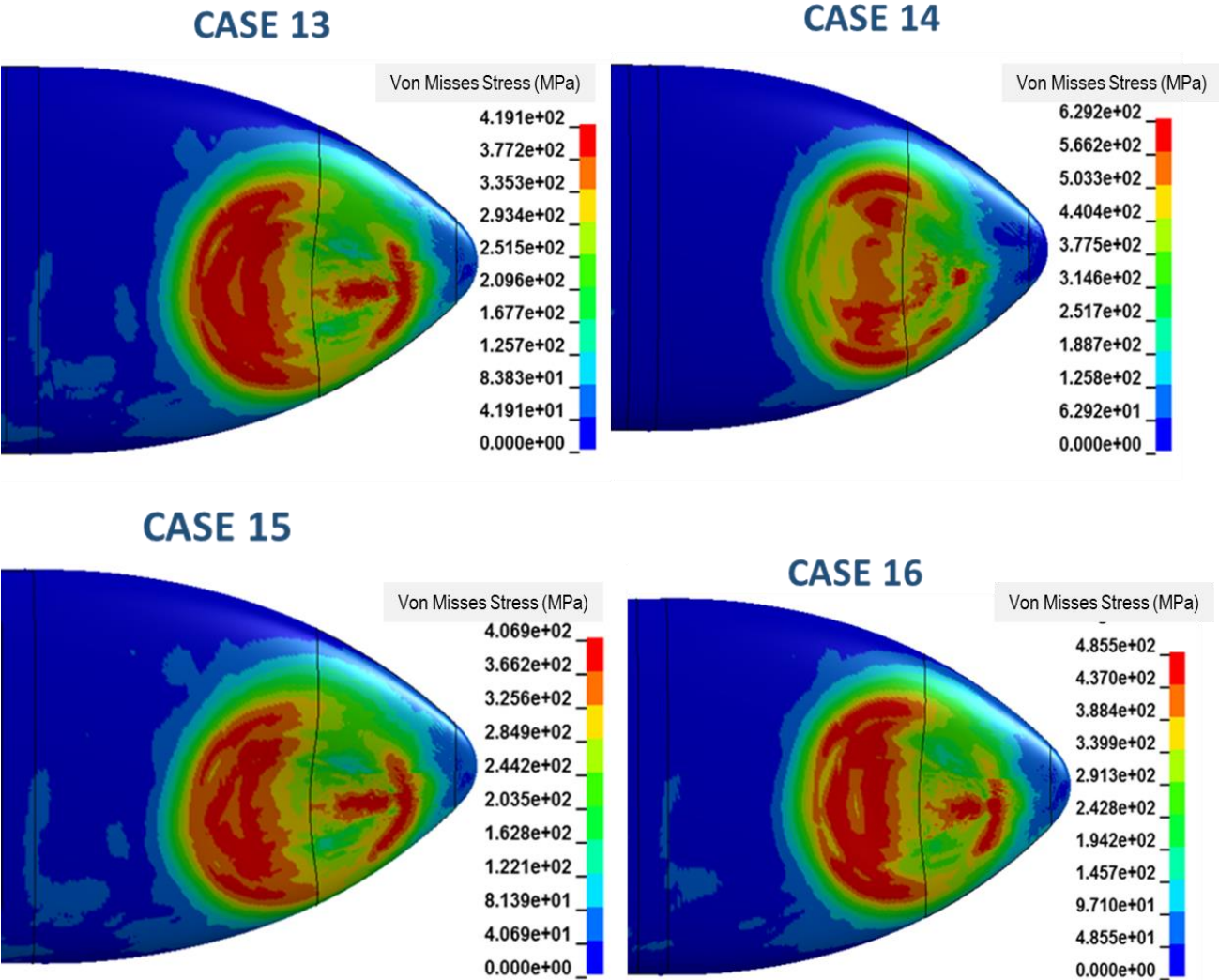


Figure 120 Von Misses Stress Results (MPa) at 2.5 ms for Impactor Position 4

There was no tear up or penetration on the skin of EFT. The stress distributions and effective stresses on skin are similar for Piecewise Linear Plasticity material model and Johnson Cook Material model.

Von Misses Stress results at 3.0 ms for impactor position 4 is shown in Figure 121.

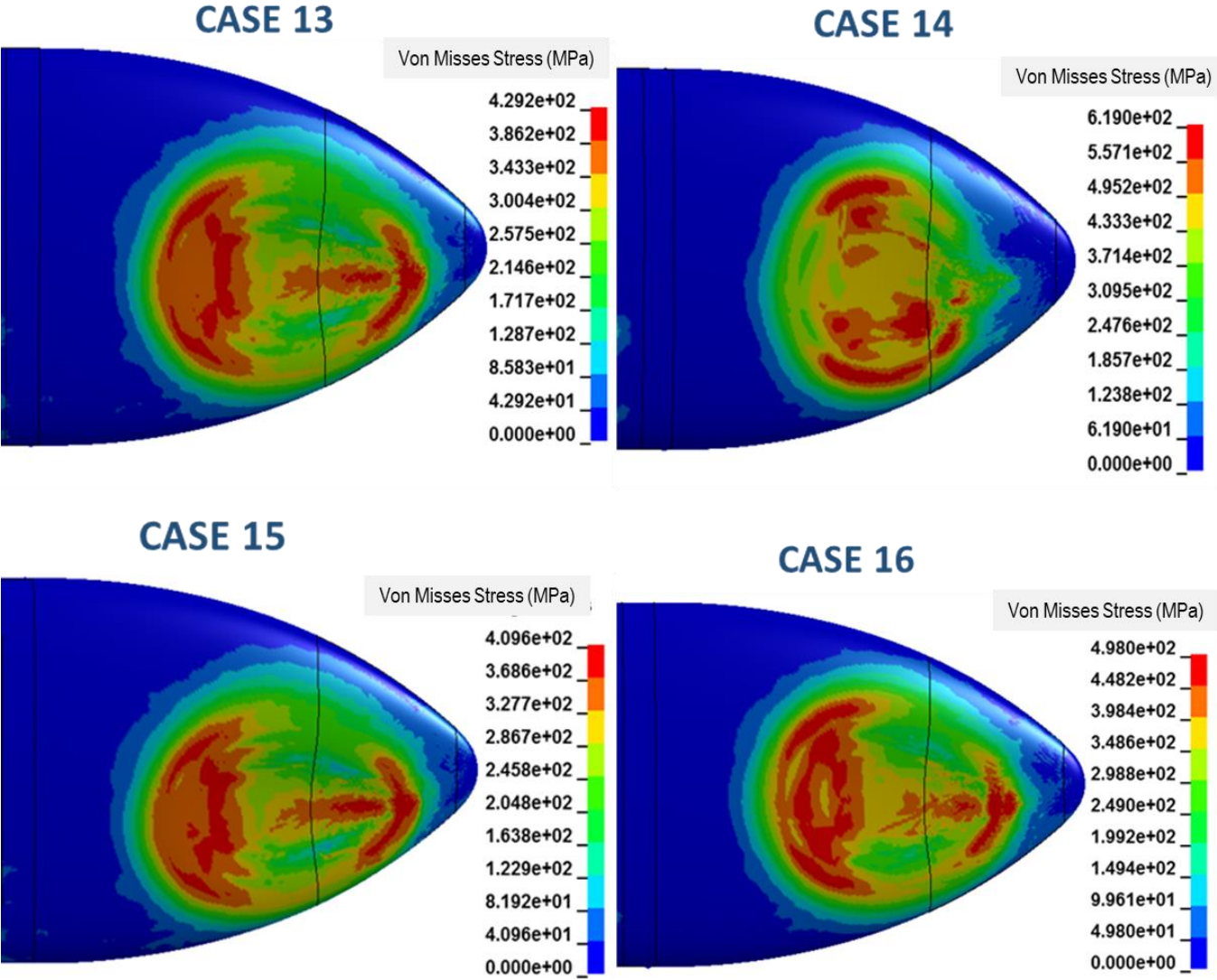


Figure 121 Von Misses Stress Results (MPa) at 3.0 ms for Impactor Position 4

There was no tear up or penetration on the skin of EFT. The stress distributions and effective stresses on skin are similar for Piecewise Linear Plasticity material model and Johnson Cook Material model.

Von Misses Stress results at 3.5 ms for impactor position 4 is shown in Figure 122.

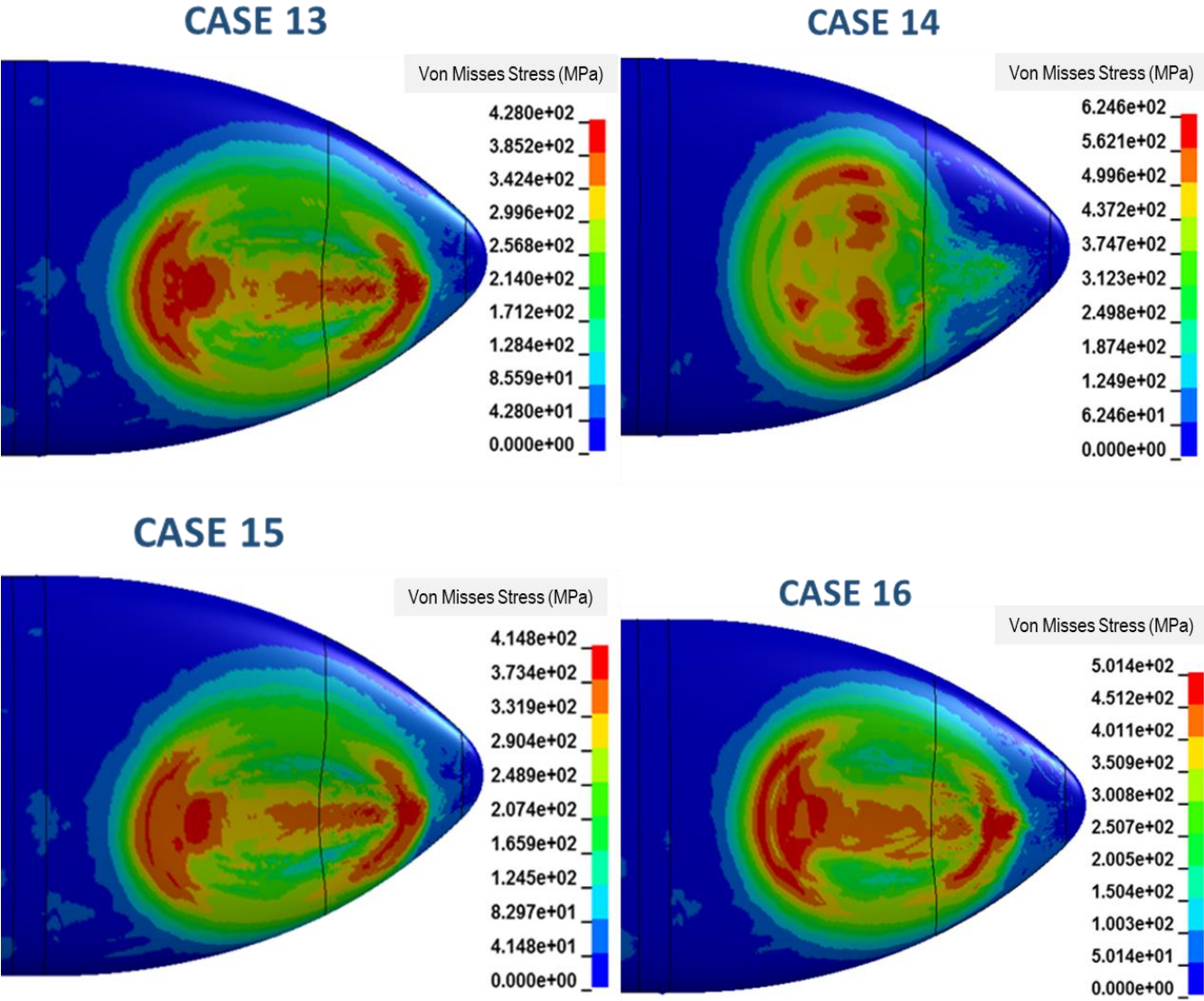


Figure 122 Von Misses Stress Results (MPa) at 3.5 ms for Impactor Position 4



There was no tear up or penetration on the skin of EFT. The stress distributions and effective stresses on skin are similar for Piecewise Linear Plasticity material model and Johnson Cook Material model.

Von Misses Stress results at 4.0 ms for impactor position 4 is shown in Figure 123.

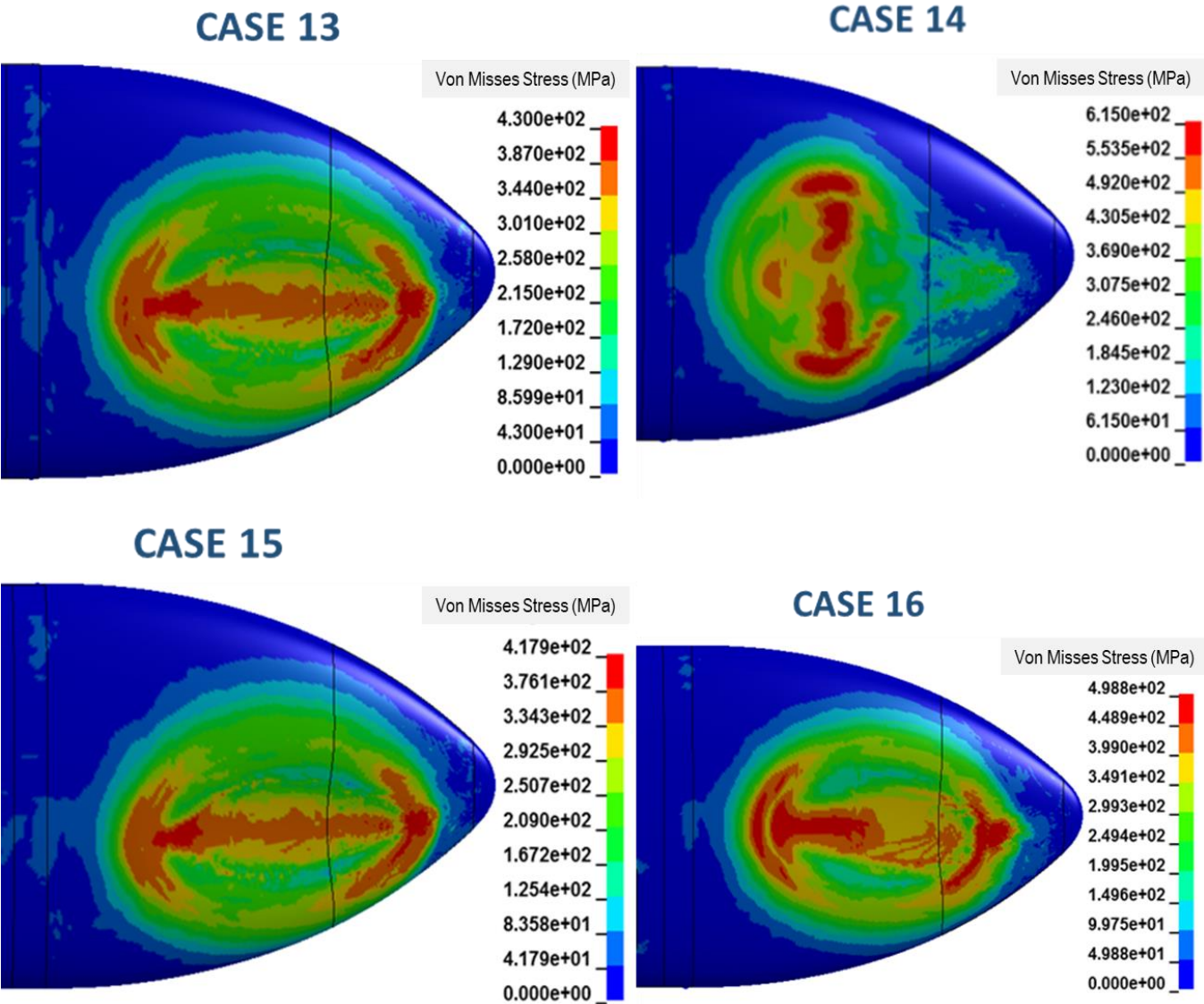


Figure 123 Von Misses Stress Results (MPa) at 4.0 ms for Impactor Position 4

There was no tear up or penetration on the skin of EFT. The stress distributions and effective stresses on skin are similar for Piecewise Linear Plasticity material model and Johnson Cook Material model.

Von Misses Stress results at 4.5 ms for impactor position 4 is shown in Figure 124.

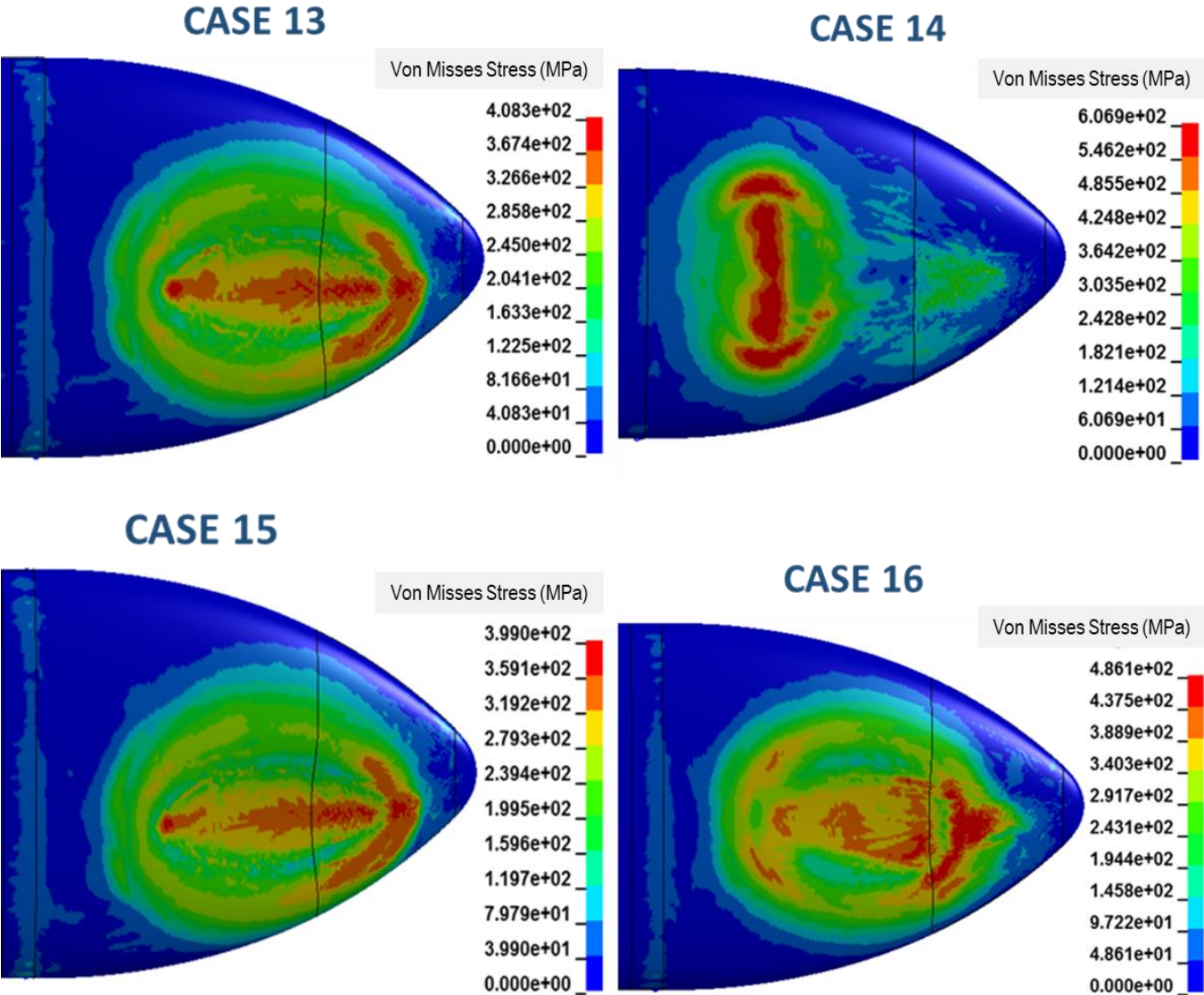


Figure 124 Von Misses Stress Results (MPa) at 4.5 ms for Impactor Position 4

There was no tear up or penetration on the skin of EFT. The stress distributions and effective stresses on skin are similar for Piecewise Linear Plasticity material model and Johnson Cook Material model. Impact ended in 4.4 ms.

Von Misses Stress results at 5.0 ms for impactor position 4 is shown in Figure 125.

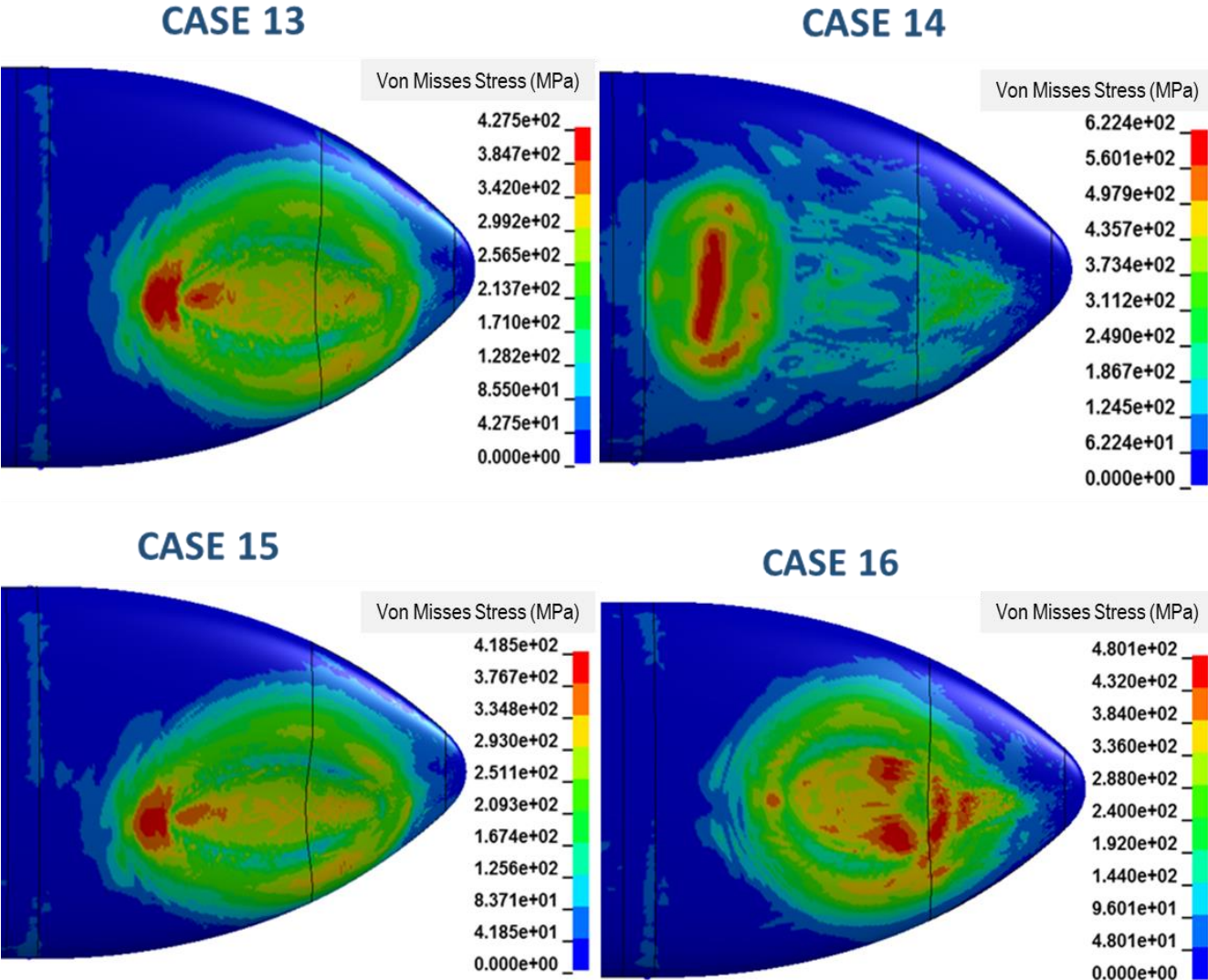


Figure 125 Von Misses Stress Results (MPa) at 5.0 ms for Impactor Position 4

There was no tear up or penetration on the skin of EFT. The stress distributions and effective stresses on skin are similar for Piecewise Linear Plasticity material model and Johnson Cook Material model. Impact ended in 4.4 ms.

The stresses and deformations on EFT skin are shown in Figure 106 to Figure 125. The plastic deformation began at 0.5ms as shown in Figure 116. There was no tear up or penetration on the skin of EFT. The stress distributions and effective stresses on skin are similar for Piecewise Linear Plasticity material model and Johnson Cook Material model.

Maximum stress on EFT skin was 439 MPa for Case 13, 662 MPa for Case 14, 428 MPa for Case 15, 665 MPa for Case 16.

Energy variations for Position 4 is given in Figure 126. While kinetic energy decreased, internal energy increased. Total energy increased for case 13, case 14, case 15 and case 16. This is because of the increase in hourglass energies. Increases in total energies for all cases are in acceptable limits.

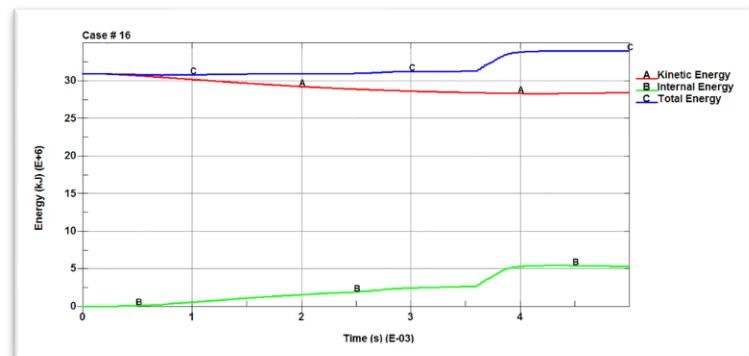
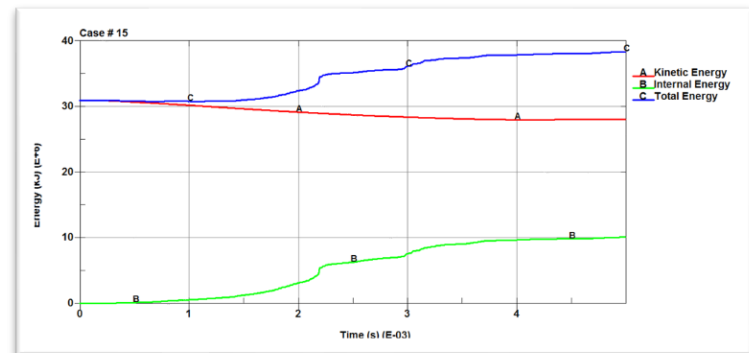
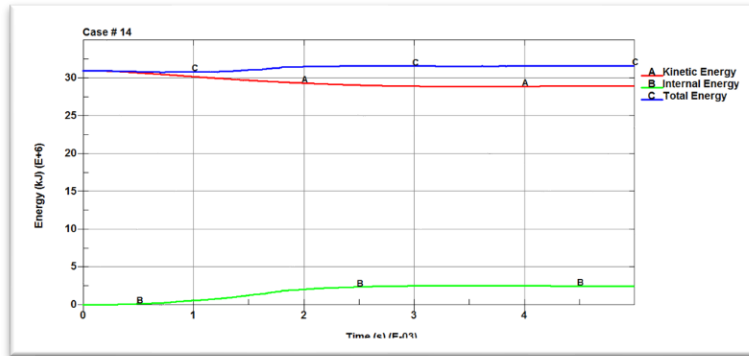
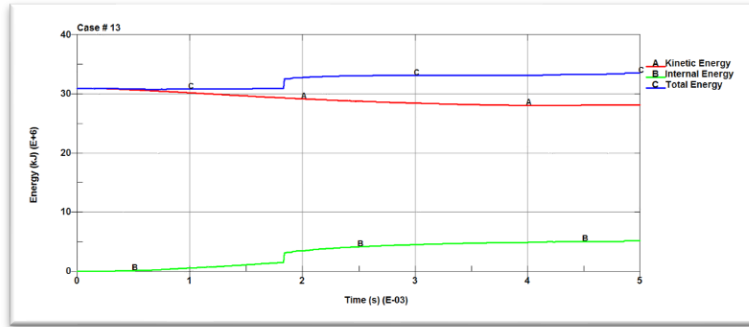


Figure 126 Energy Variation of Position 4

Energy ratios for Position 4 is given in Figure 127. Energy ratios for position 4 remained within the acceptable limits as shown for case 13, case14 and case 16. For case 15, energy ratio increased after 2 ms; however, the increase is in tha acceptable limit.

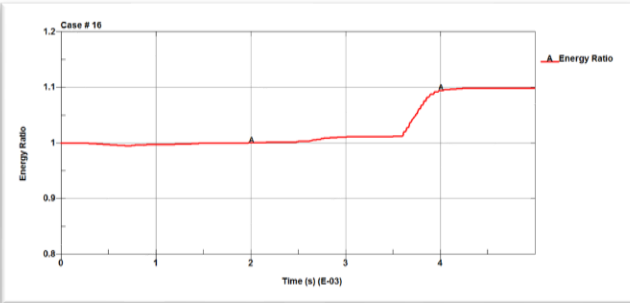
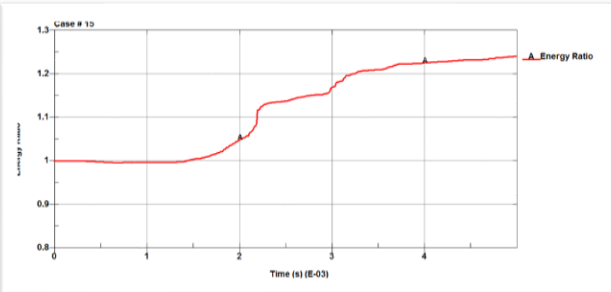
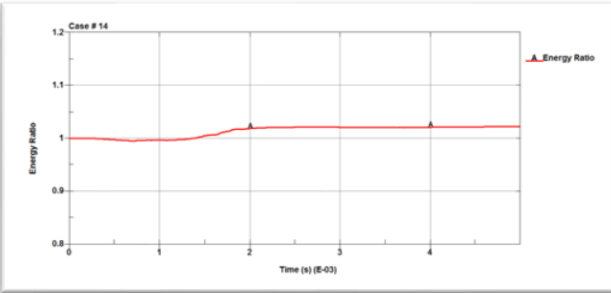
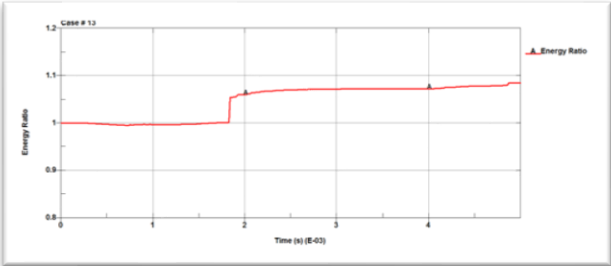


Figure 127 Energy Ratio of Position 4

Hourglass energy, damping energy and sliding energy for case 13 is given in Figure 128. Impact ended in 4.4 ms. Hourglass energy slightly increased after 1.5ms; however, the increase is in the acceptable limit. For sliding energy, peak did not occur.

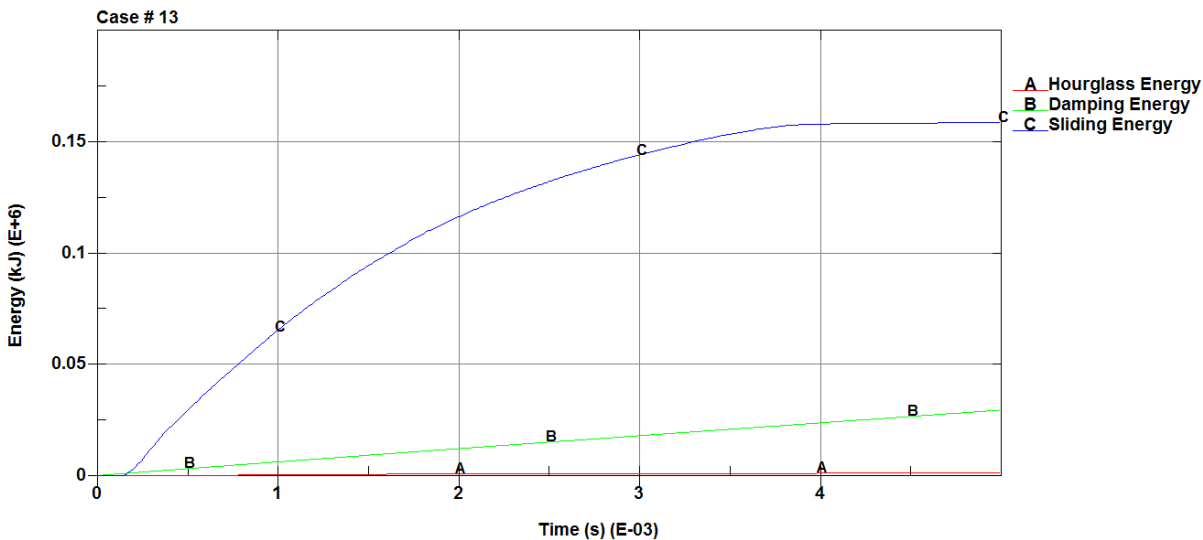


Figure 128 Hourglass, Damping and Sliding Energies Variation of Case 13

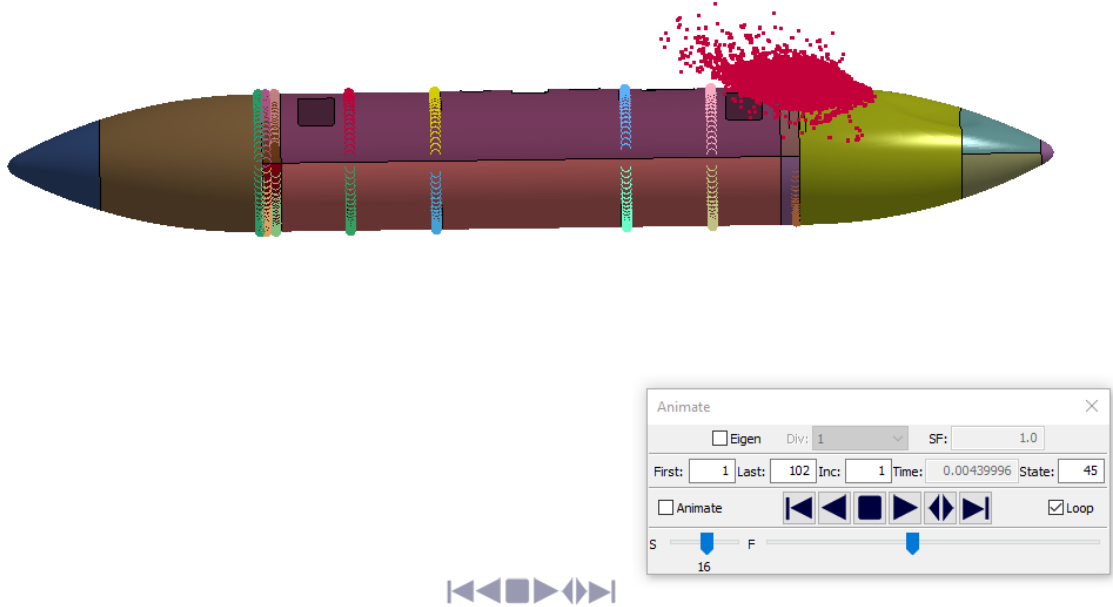


Figure 129 Bird Impact at 4 ms for Case 13

Hourglass energy, damping energy and sliding energy for case 14 is given in Figure 130. Impact ended in 4.3 ms. Hourglass energy slightly increased after 1.5ms; however, the increase is in the acceptable limit. For sliding energy, peak did not occur.

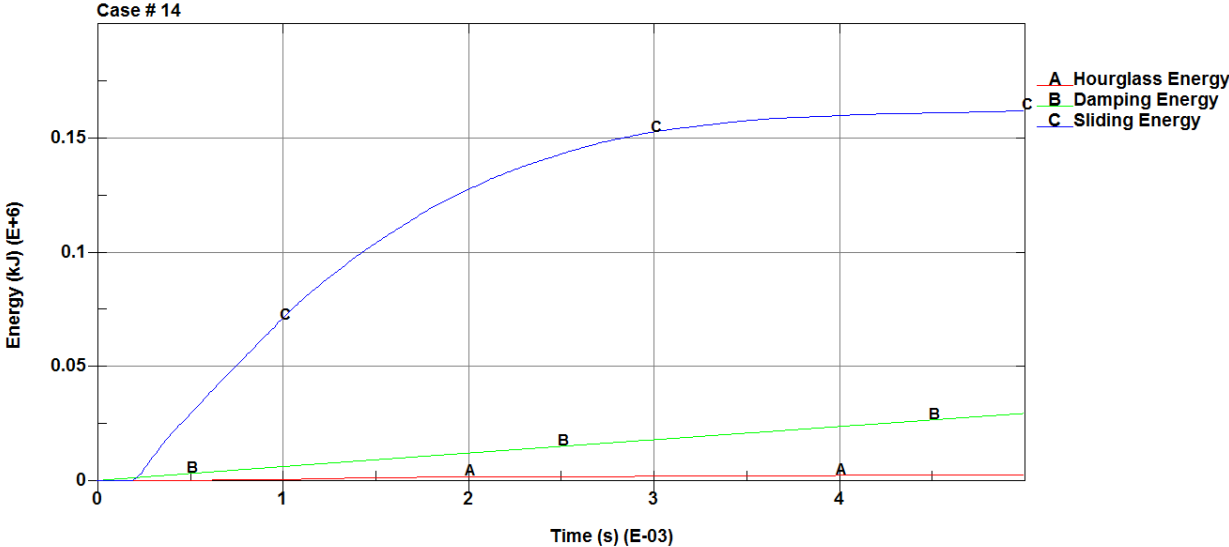


Figure 130 Hourglass, Damping and Sliding Energies Variation of Case 14

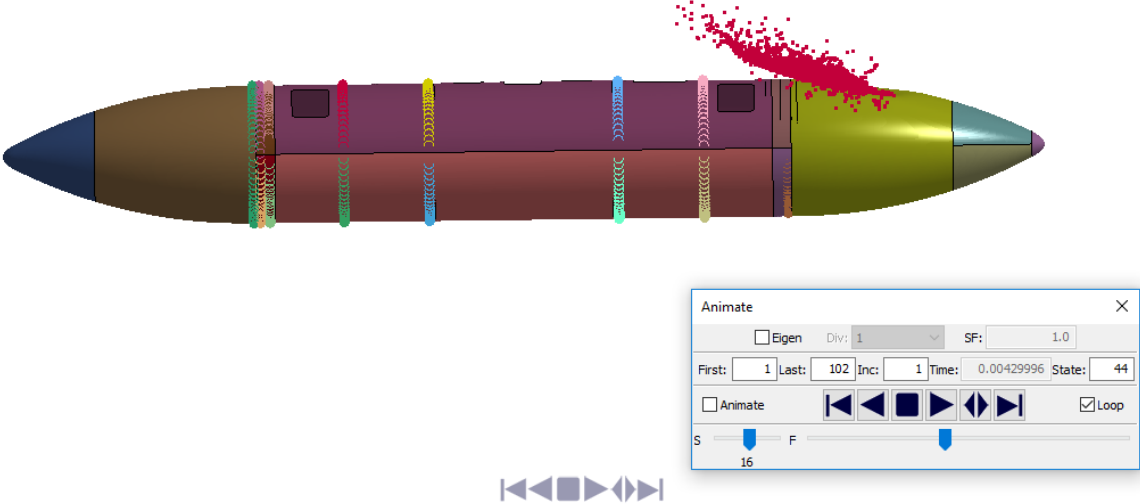


Figure 131 Bird Impact at 4 ms for Case 14

Hourglass energy, damping energy and sliding energy for case 15 is given in Figure 132. Impact ended in 5.0 ms. Hourglass energy slightly increased after 1.5ms; however, the increase is in the acceptable limit. For sliding energy, peak did not occur.



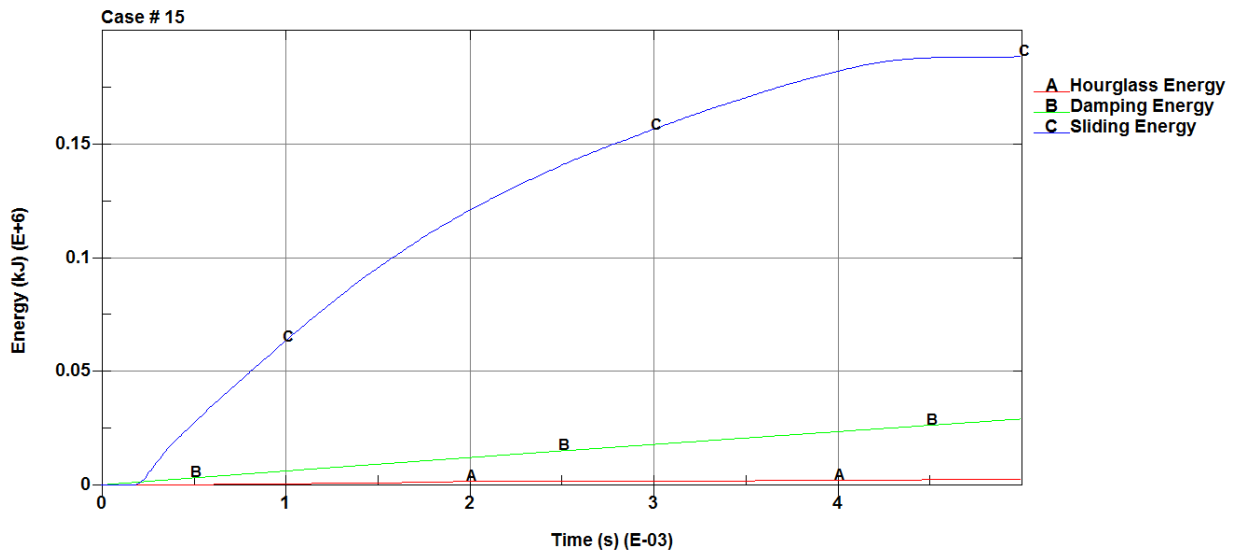


Figure 132 Hourglass, Damping and Sliding Energies Variation of Case 15

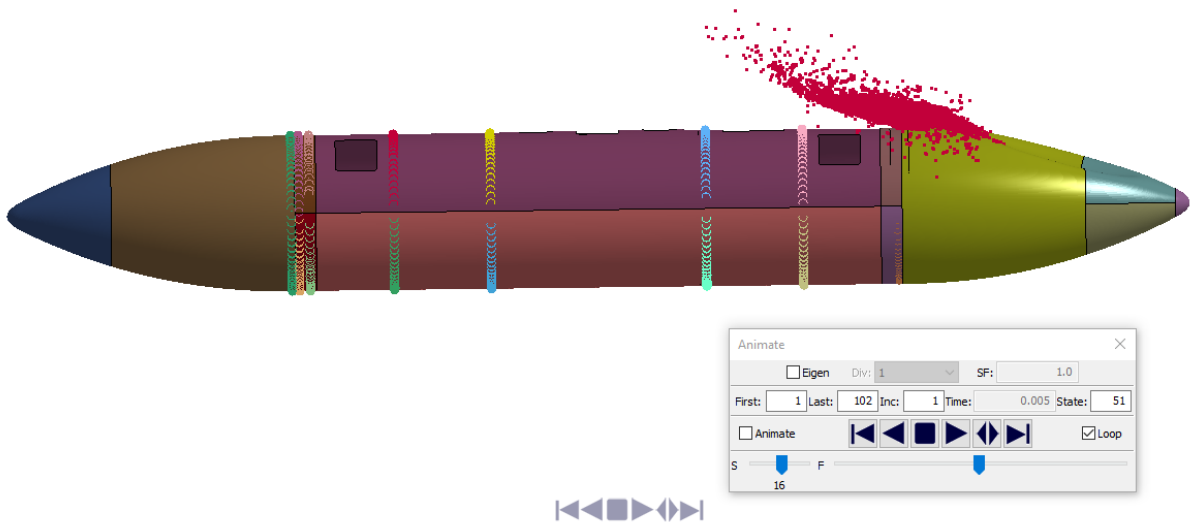


Figure 133 Bird Impact at 4 ms for Case 15

Hourglass energy, damping energy and sliding energy for case 16 is given in Figure 134. Impact ended in 5.0ms. Hourglass energy slightly increased after 1.5ms; however, the increase is in the acceptable limit. For sliding energy, peak did not occur.

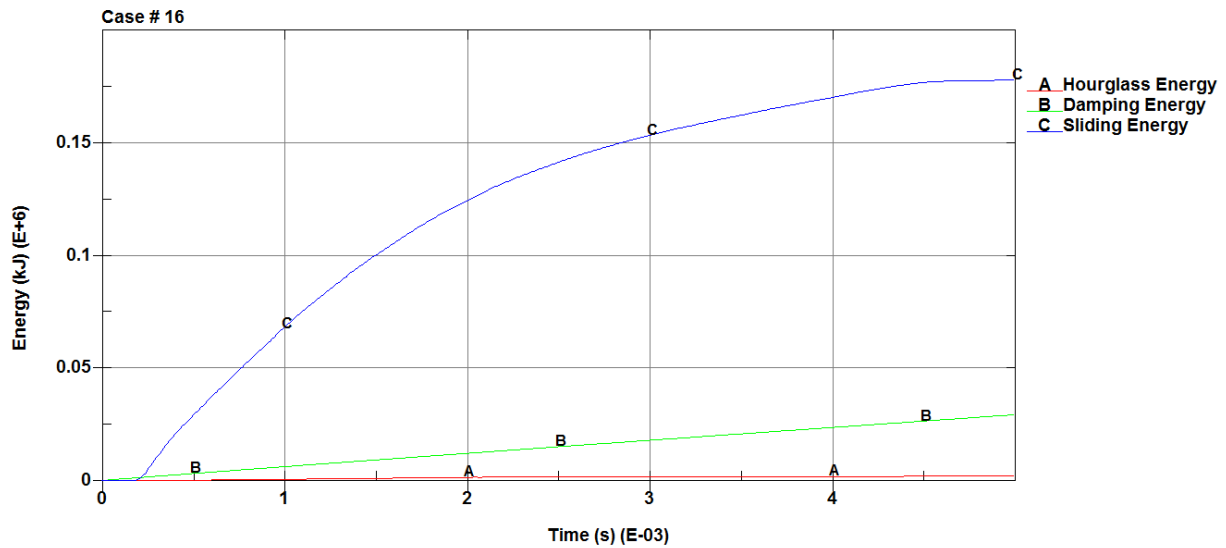


Figure 134 Hourglass, Damping and Sliding Energies Variation of Case 16

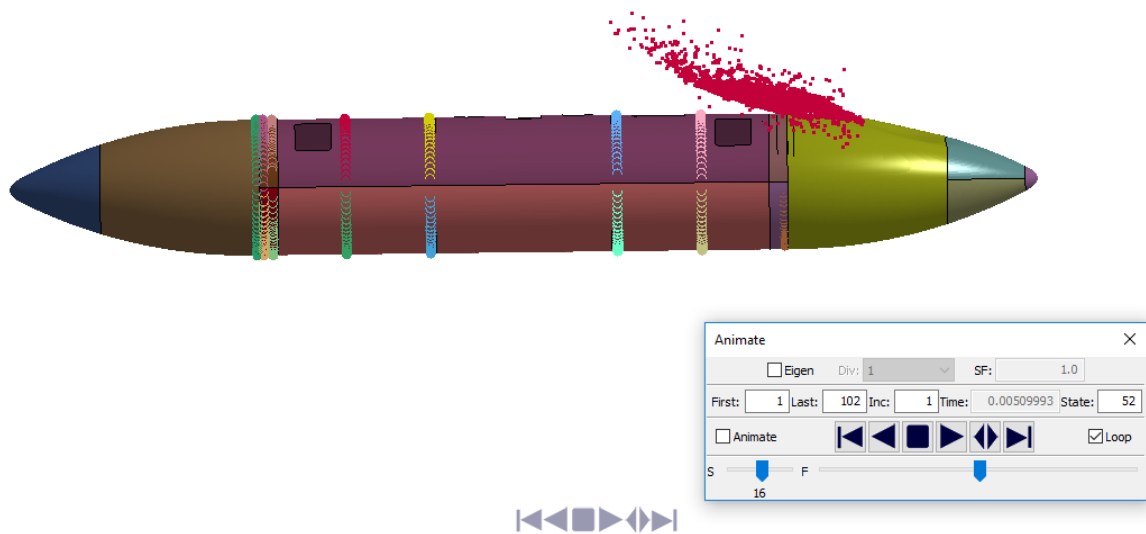


Figure 135 Bird Impact at 4 ms for Case 16

### **Analysis Results for Position 5**

An overview of the impact simulation for the position 5 was given for the general understanding. The time history was presented as a series of time step plots with explanations. The plots in Figure 136 to Figure 155 show the simulation run in several steps. Total simulation time was set to 5 ms and plots are saved in the intervals of 0.5ms.

Displacement results at 0.5 ms for impactor position 5 is shown in Figure 136.

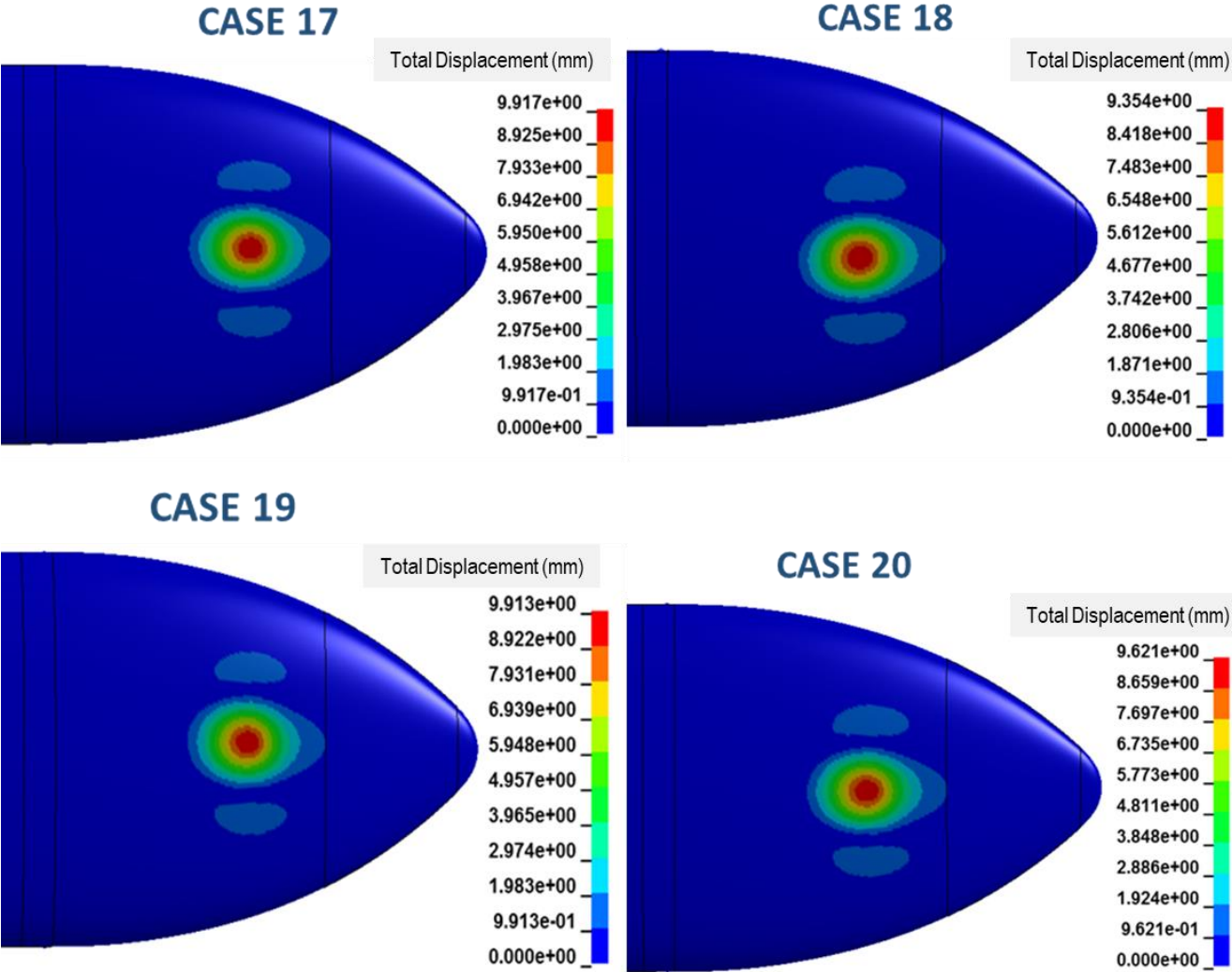


Figure 136 Displacement Results (mm) at 0.5 ms for Impactor Position 5

Displacements on Al 7075 -T6 and Al 2024-T3 are similar. Displacement values according to Piecewise Linear Plasticity material model are also similar to Johnson Cook Material model.

Displacement results at 1.0 ms for impactor position 5 is shown in Figure 137.

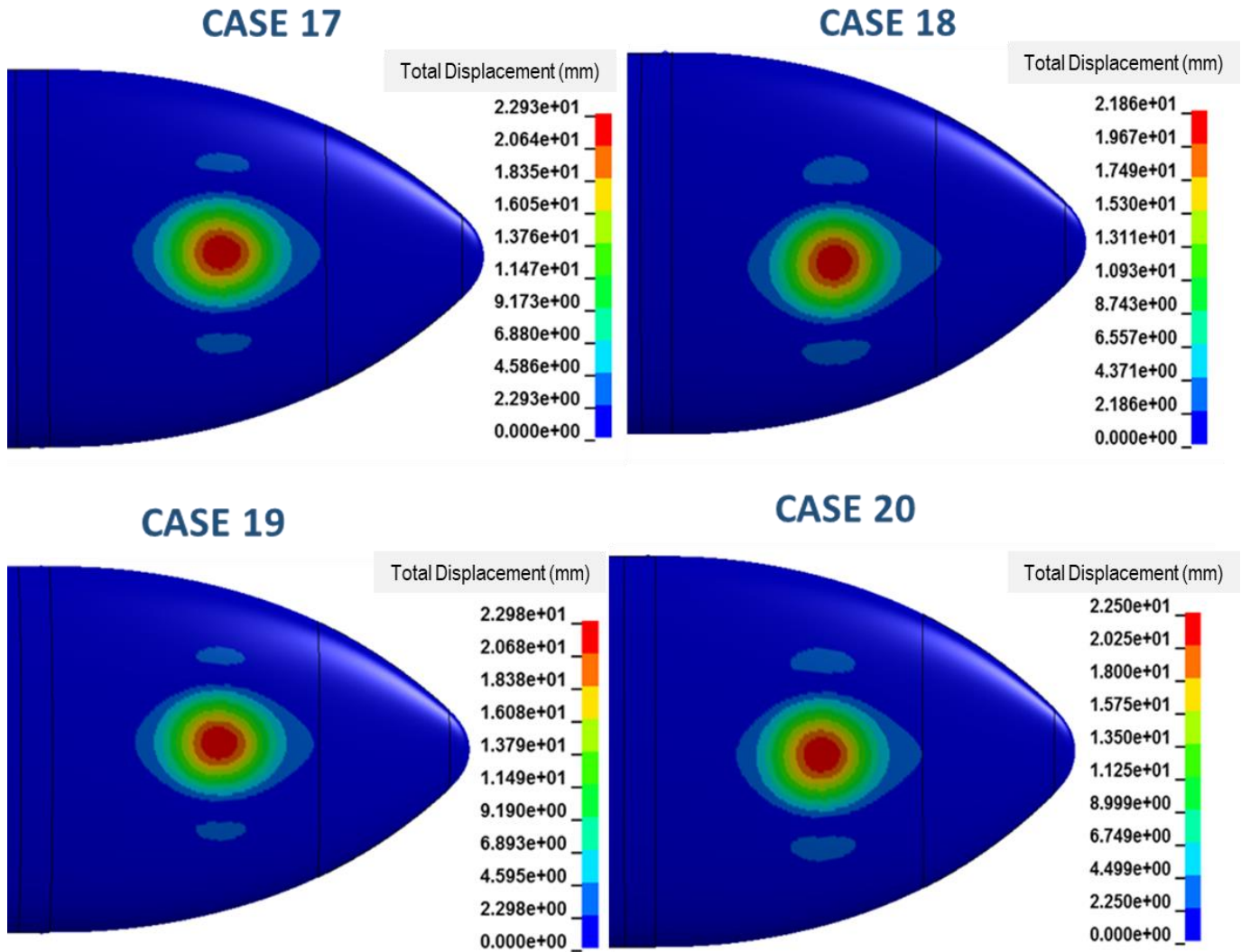


Figure 137 Displacement Results (mm) at 1.0 ms for Impactor Position 5

Displacements on Al 7075 -T6 and Al 2024-T3 are similar. Displacement values according to Piecewise Linear Plasticity material model are also similar to Johnson Cook Material model.

Displacement results at 1.5 ms for impactor position 5 is shown in Figure 138.

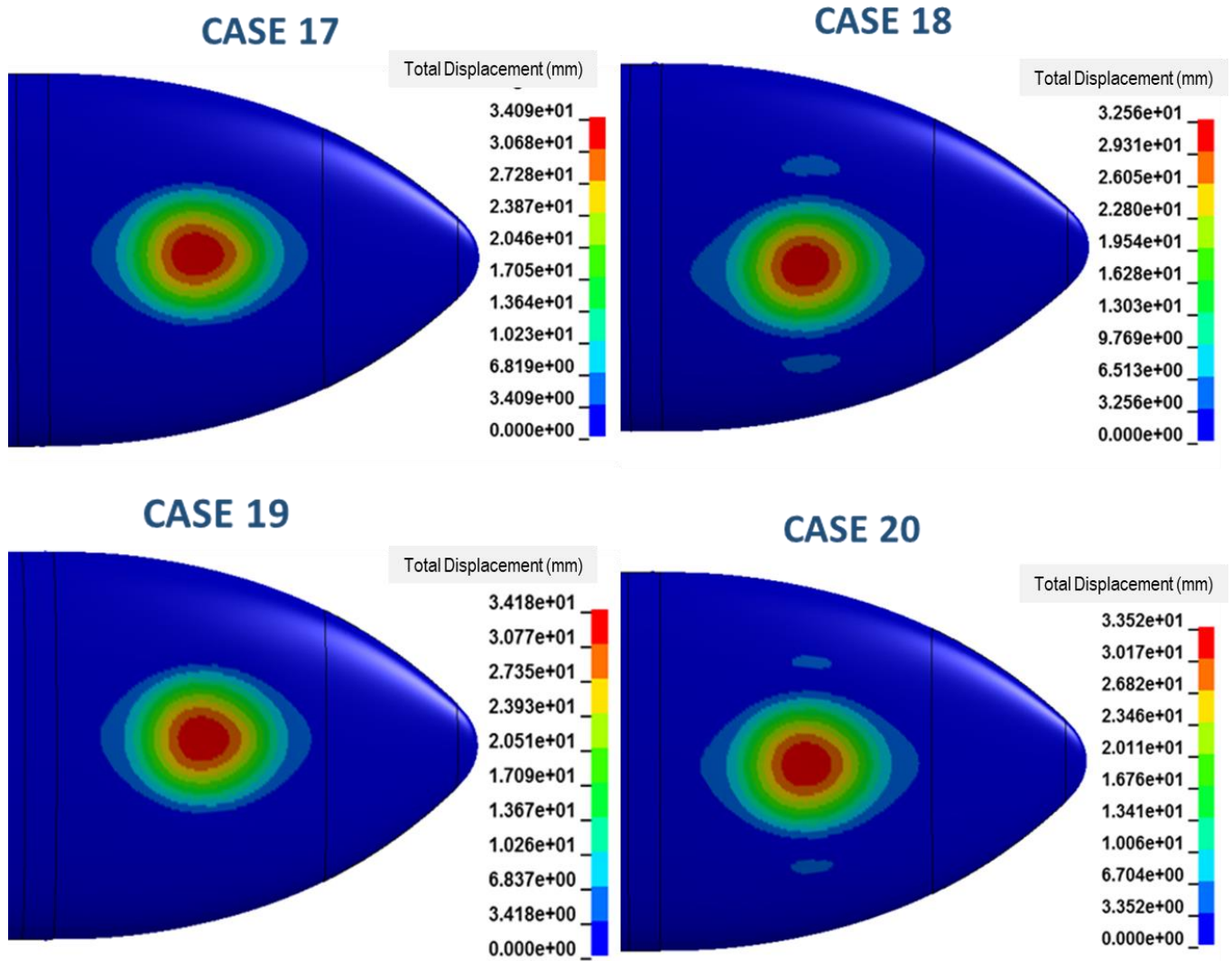


Figure 138 Displacement Results (mm) at 1.5 ms for Impactor Position 5

Displacements on Al 7075 -T6 and Al 2024-T3 are similar. Displacement values according to Piecewise Linear Plasticity material model are also similar to Johnson Cook Material model.

Displacement results at 2.0 ms for impactor position 5 is shown in Figure 139.

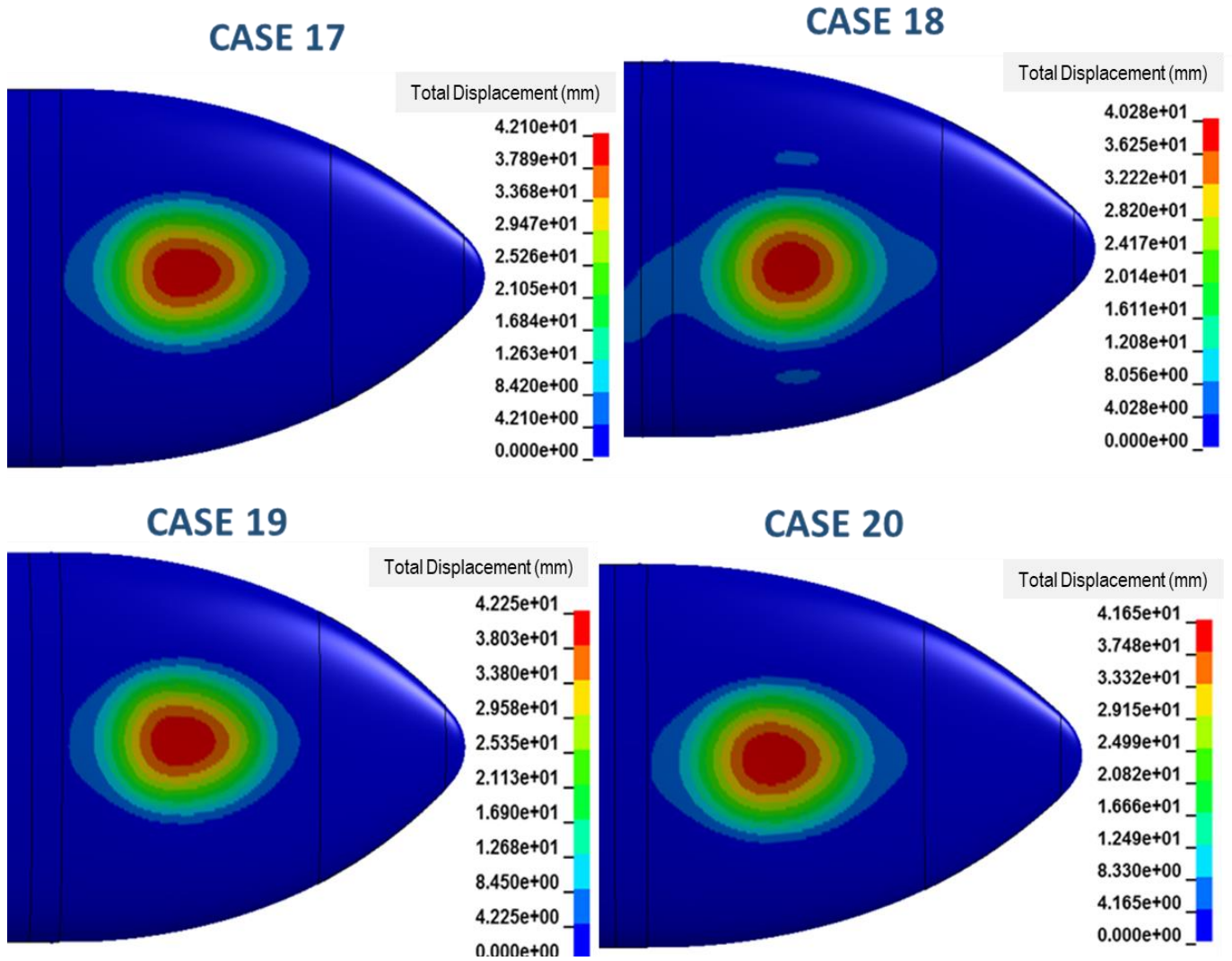


Figure 139 Displacement Results (mm) at 2.0 ms for Impactor Position 5

Displacements on Al 7075 -T6 and Al 2024-T3 are similar. Displacement values according to Piecewise Linear Plasticity material model are also similar to Johnson Cook Material model.

Displacement results at 2.5 ms for impactor position 5 is shown in Figure 140.

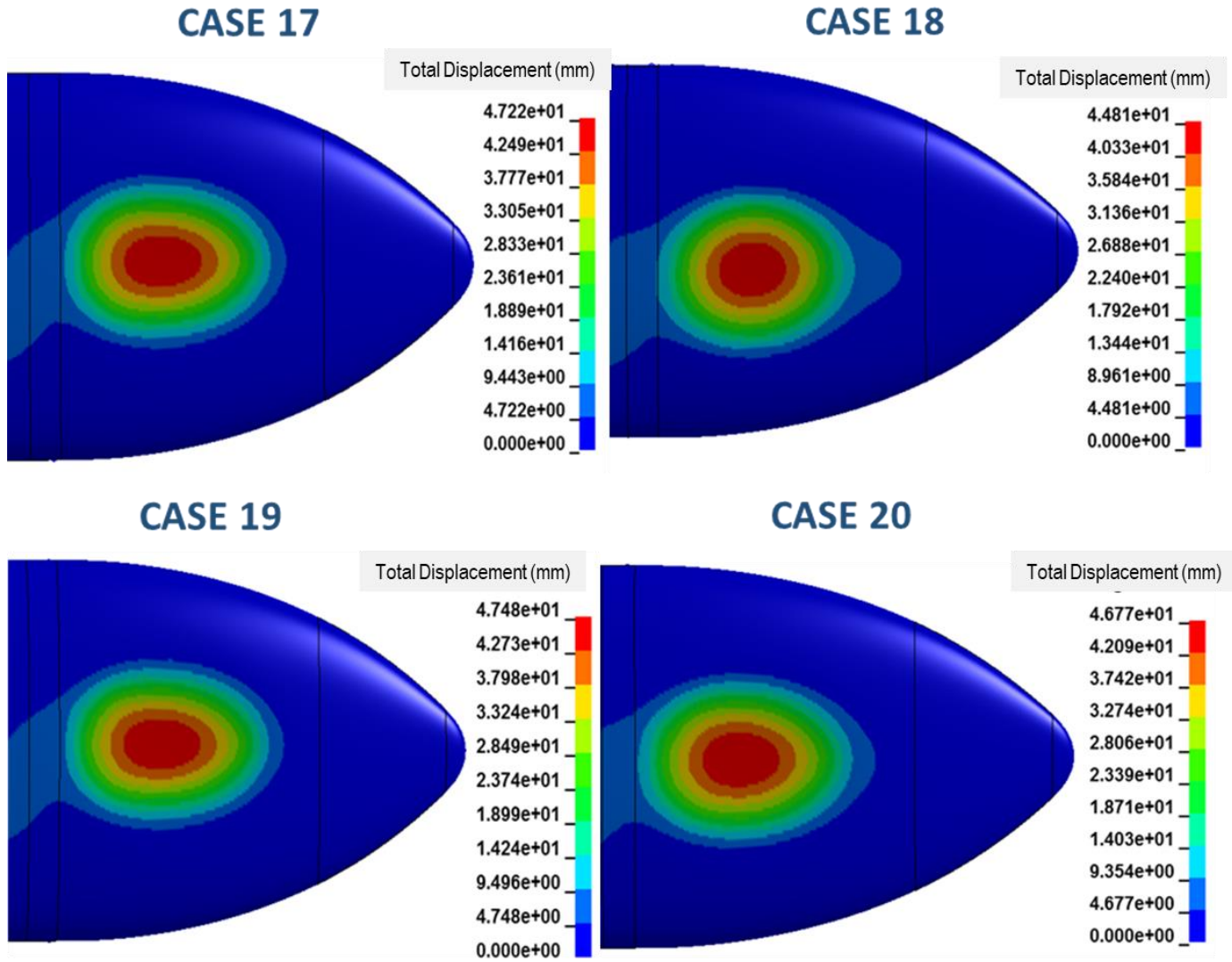


Figure 140 Displacement Results (mm) at 2.5 ms for Impactor Position 5

Displacements on Al 7075 -T6 and Al 2024-T3 are similar. Displacement values according to Piecewise Linear Plasticity material model are also similar to Johnson Cook Material model.

Displacement results at 3.0 ms for impactor position 5 is shown in Figure 141.

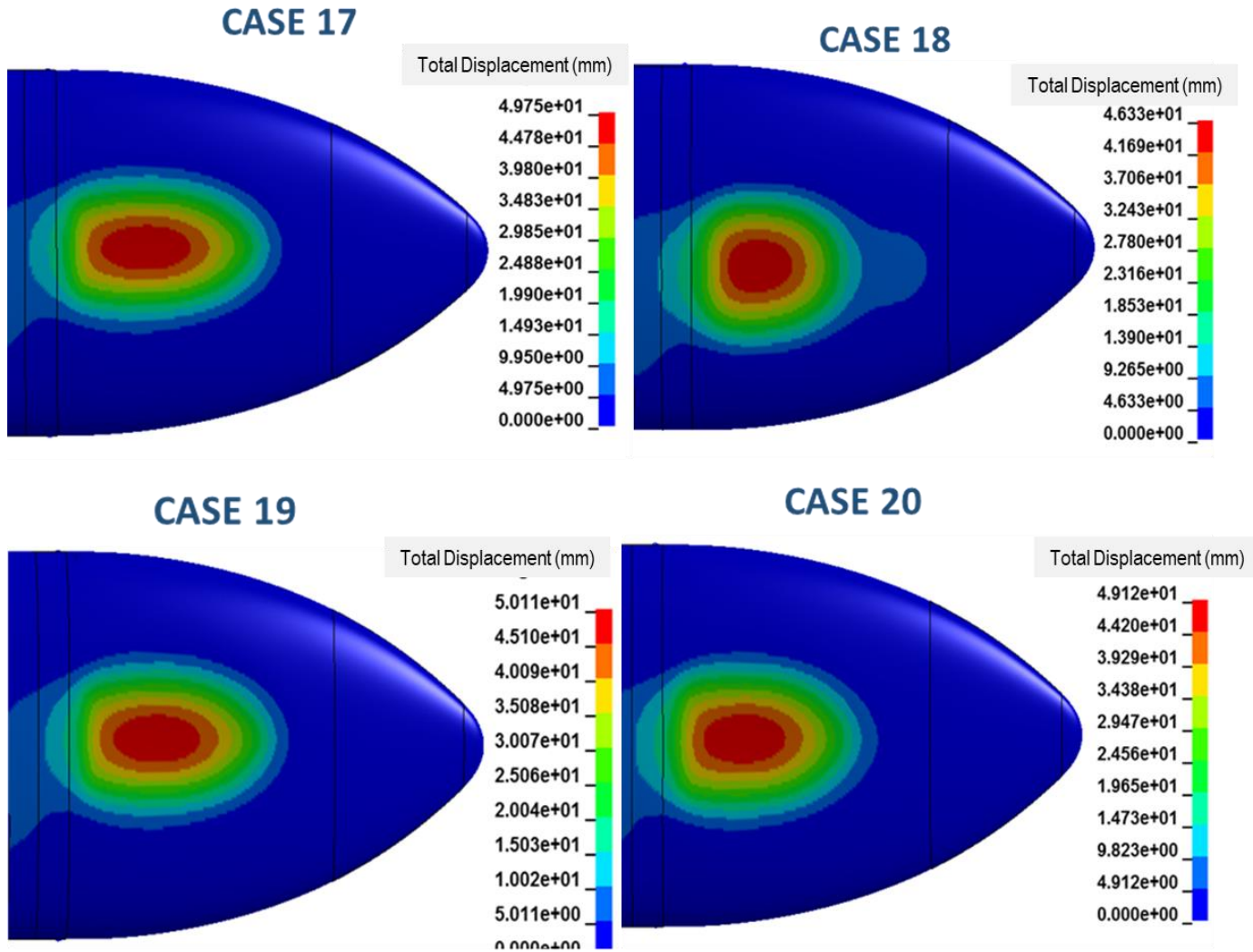


Figure 141 Displacement Results (mm) at 3.0 ms for Impactor Position 5

Displacements on Al 7075 -T6 and Al 2024-T3 are similar. Displacement values according to Piecewise Linear Plasticity material model are also similar to Johnson Cook Material model.

Displacement results at 3.5 ms for impactor position 5 is shown in Figure 142.



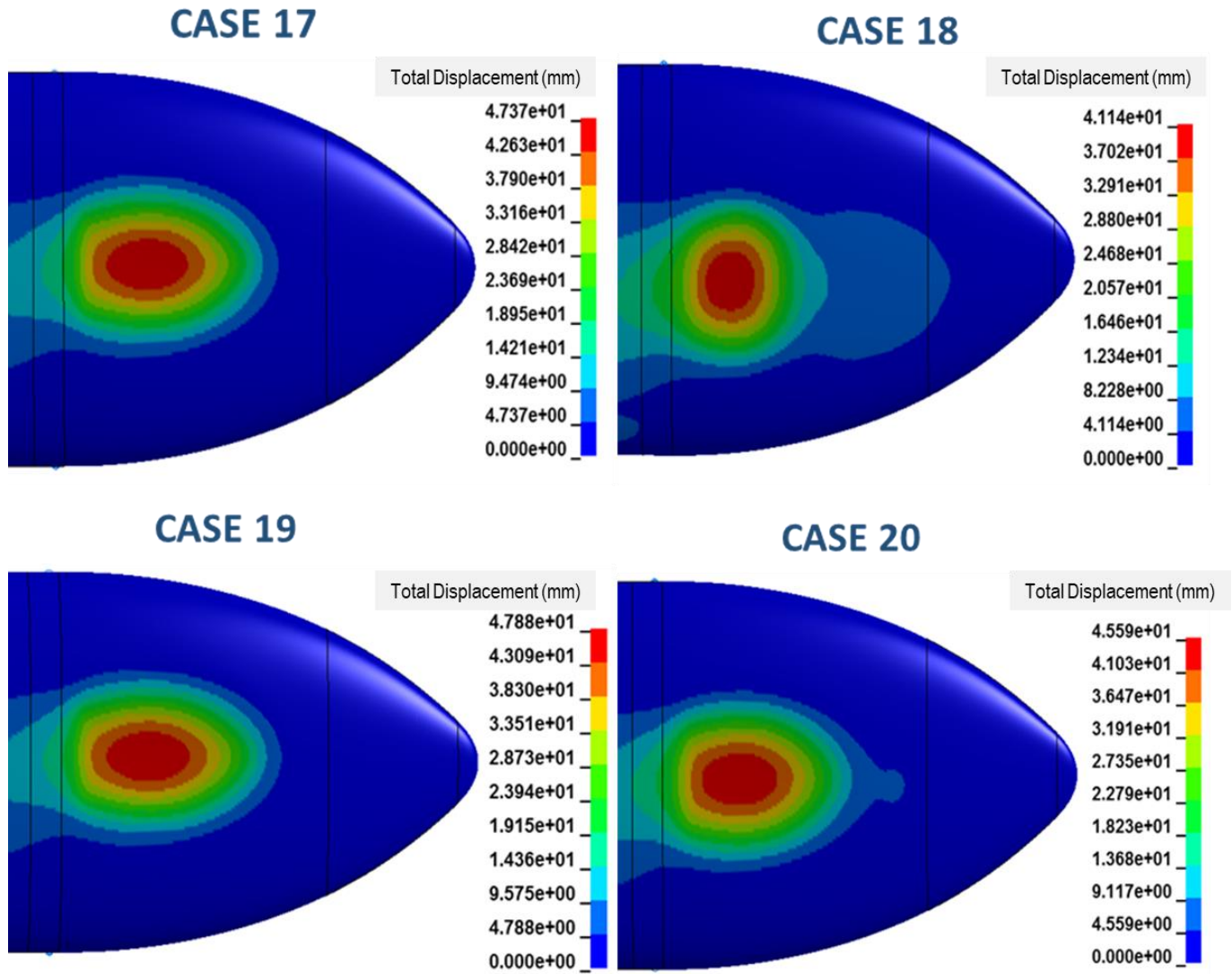


Figure 142 Displacement Results (mm) at 3.5 ms for Impactor Position 5

Displacements on Al 7075 -T6 and Al 2024-T3 are similar. Displacement values according to Piecewise Linear Plasticity material model are also similar to Johnson Cook Material model. Impact ended in 3.4 ms.

Displacement results at 4.0 ms for impactor position 5 is shown in Figure 143.

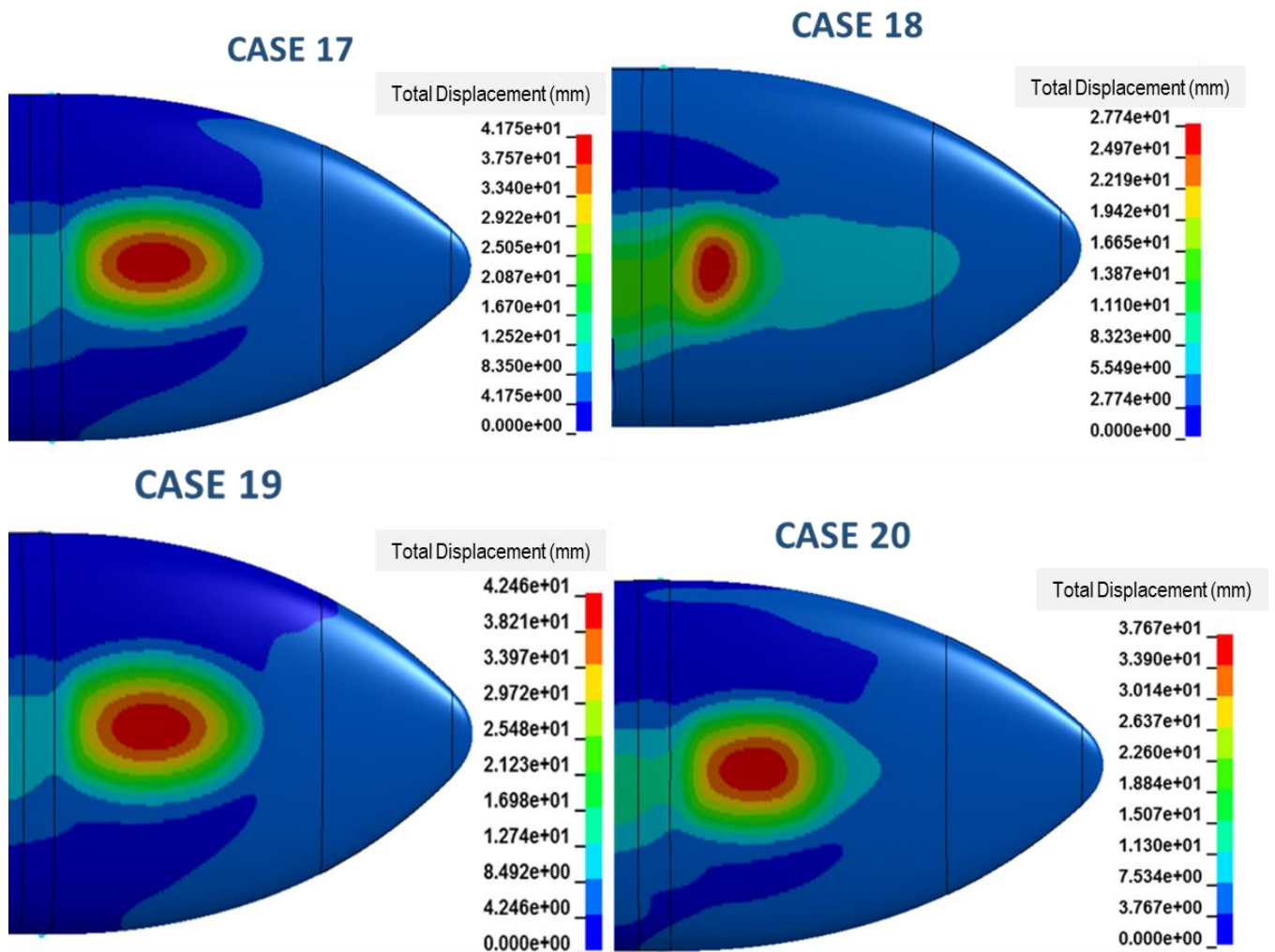


Figure 143 Displacement Results (mm) at 4.0 ms for Impactor Position 5

Displacements on Al 7075 -T6 and Al 2024-T3 are similar. Displacement values according to Piecewise Linear Plasticity material model are also similar to Johnson Cook Material model. Impact ended in 3.4 ms.

Displacement results at 4.5 ms for impactor position 5 is shown in Figure 144.

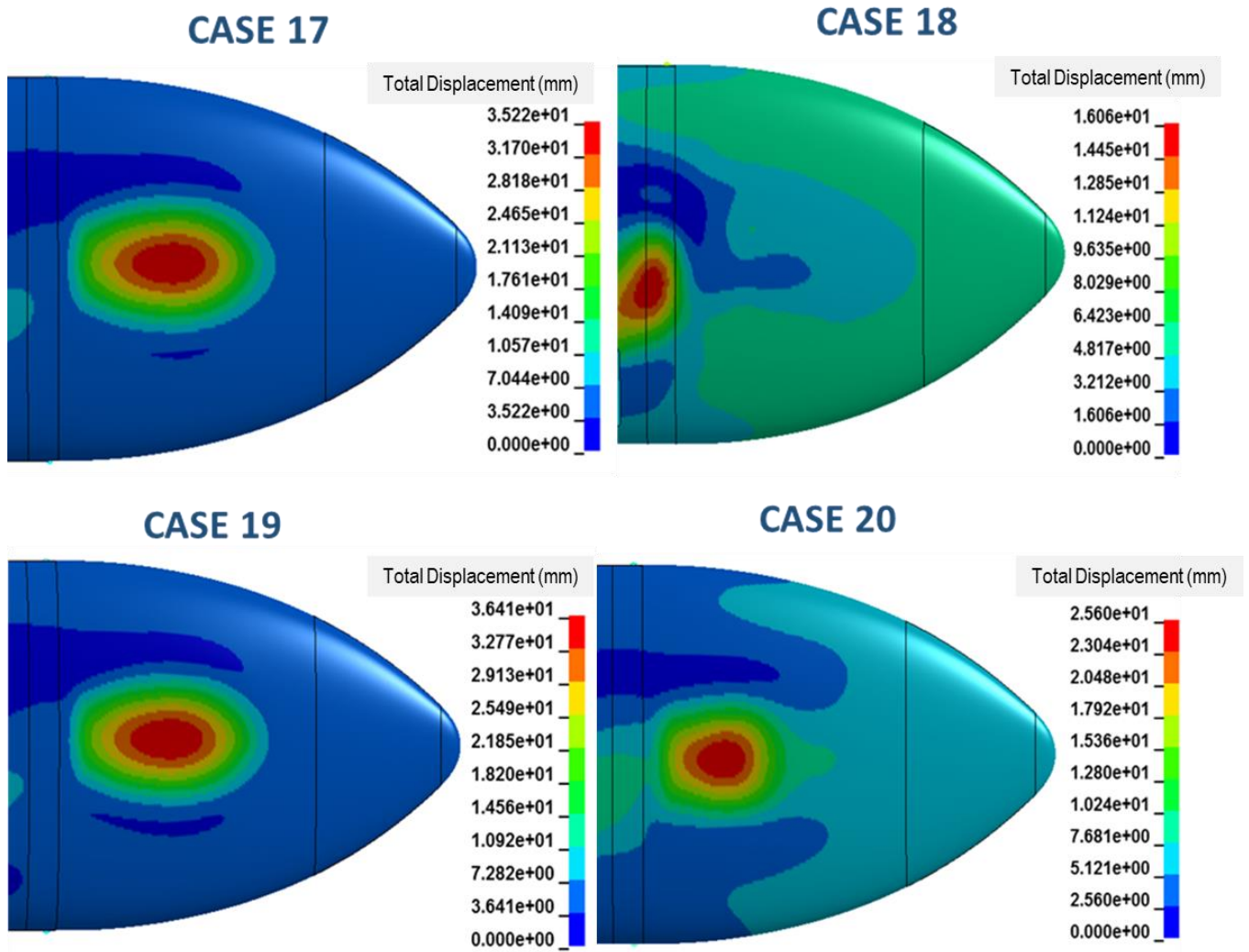


Figure 144 Displacement Results (mm) at 4.5 ms for Impactor Position 5

Displacements on Al 7075 -T6 and Al 2024-T3 are similar. Displacement values according to Piecewise Linear Plasticity material model are also similar to Johnson Cook Material model. Impact ended in 3.4 ms.

Displacement results at 5.0 ms for impactor position 5 is shown in Figure 145.

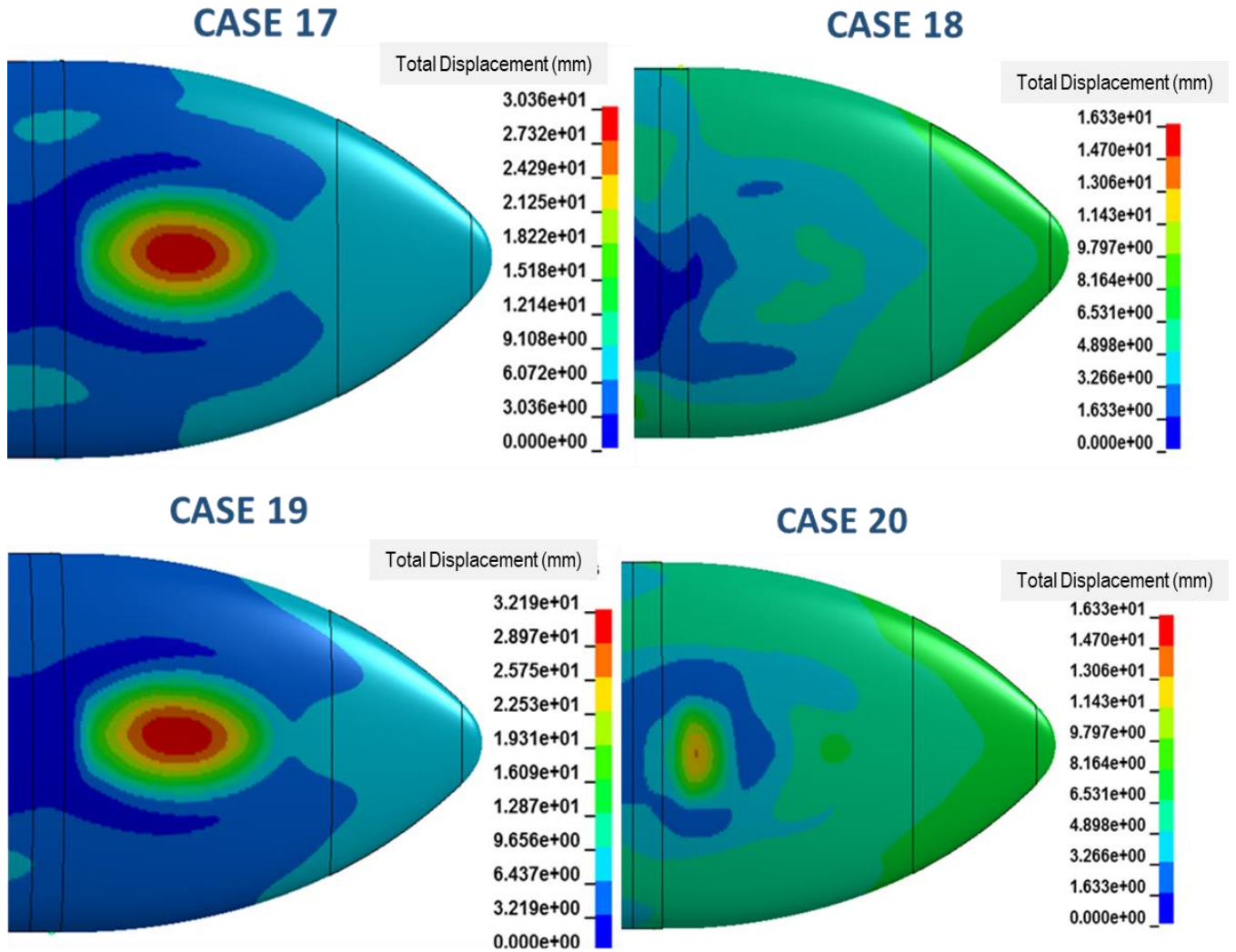


Figure 145 Displacement Results (mm) at 5.0 ms for Impactor Position 5

Displacements on Al 7075 -T6 and Al 2024-T3 are similar. Displacement values according to Piecewise Linear Plasticity material model are also similar to Johnson Cook Material model which is an expected result because of low strain rates. Impact ended in 3.4 ms.

For position 5, displacements on Al 7075 -T6 and Al 2024-T3 are similar. Displacement values according to Piecewise Linear Plasticity material model are also similar to Johnson Cook Material model.

After impact, screen shots were taken at 0.5ms intervals and the stresses are compared. Since the contact of the bird ended before 5 ms in general, the images were limited to this time period.

Von Misses Stress results at 0.5 ms for impactor position 5 is shown in Figure 146.

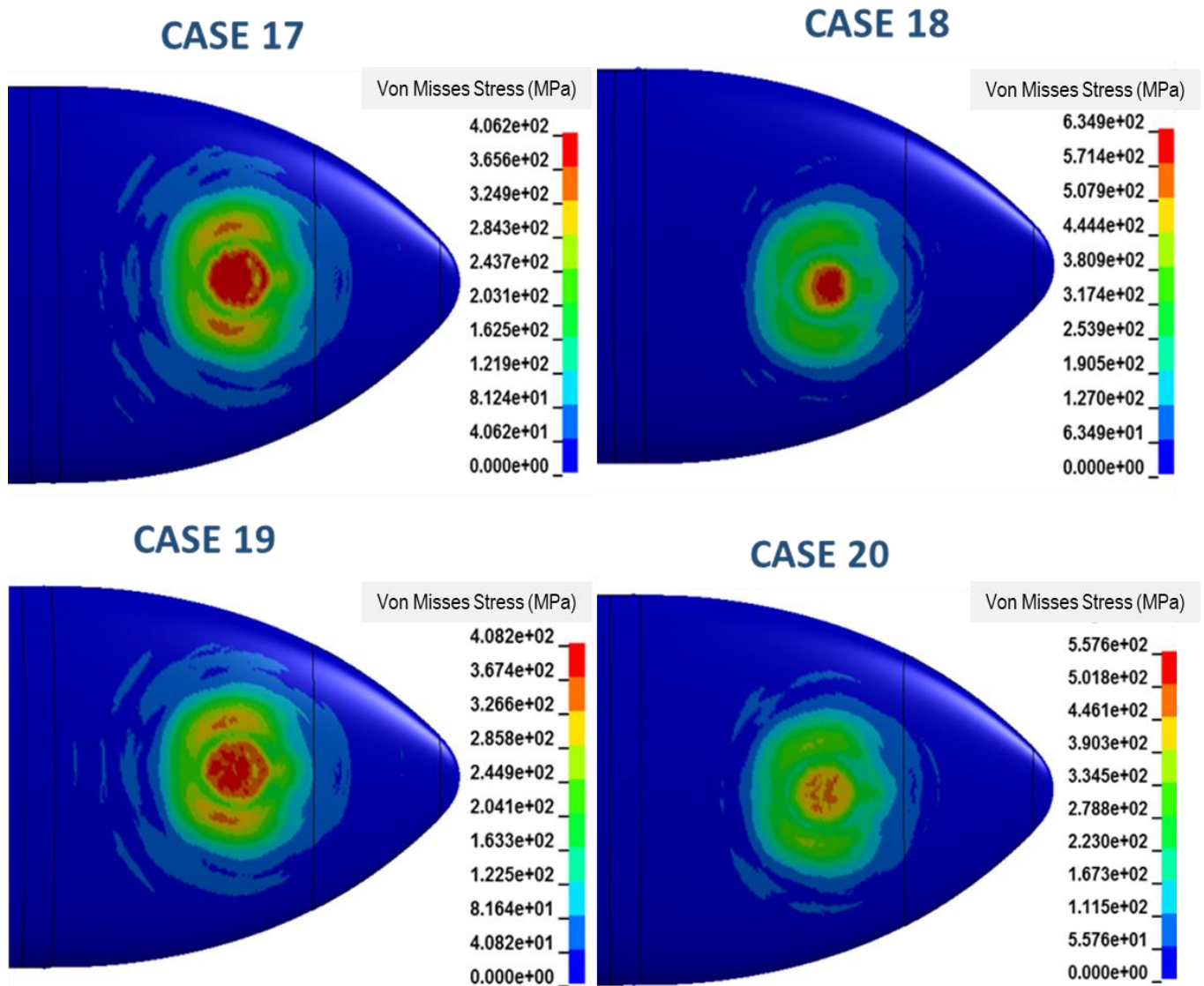


Figure 146 Von Misses Stress Results (MPa) at 0.5 ms for Impactor Position 5

The plastic deformation began at 0.5ms as shown in Figure 146. There was no tear up or penetration on the skin of EFT. The stress distributions and effective stresses on skin are similar for Piecewise Linear Plasticity material model and Johnson Cook Material model.

Von Misses Stress results at 1.0 ms for impactor position 5 is shown in Figure 147.

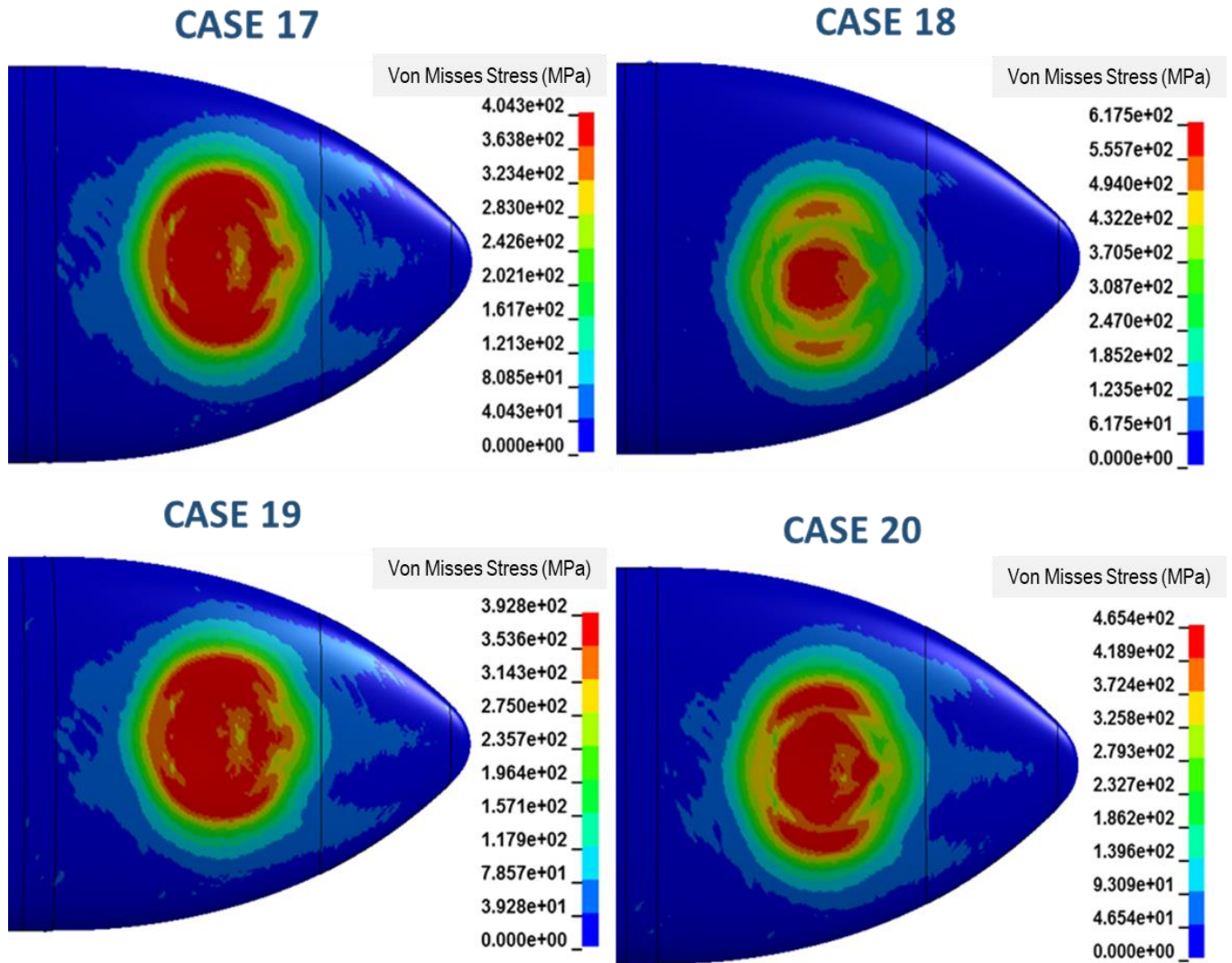


Figure 147 Von Misses Stress Results (MPa) at 1.0 ms for Impactor Position 5

There was no tear up or penetration on the skin of EFT. The stress distributions and effective stresses on skin are similar for Piecewise Linear Plasticity material model and Johnson Cook Material model.

Von Misses Stress results at 1.5 ms for impactor position 5 is shown in Figure 148.

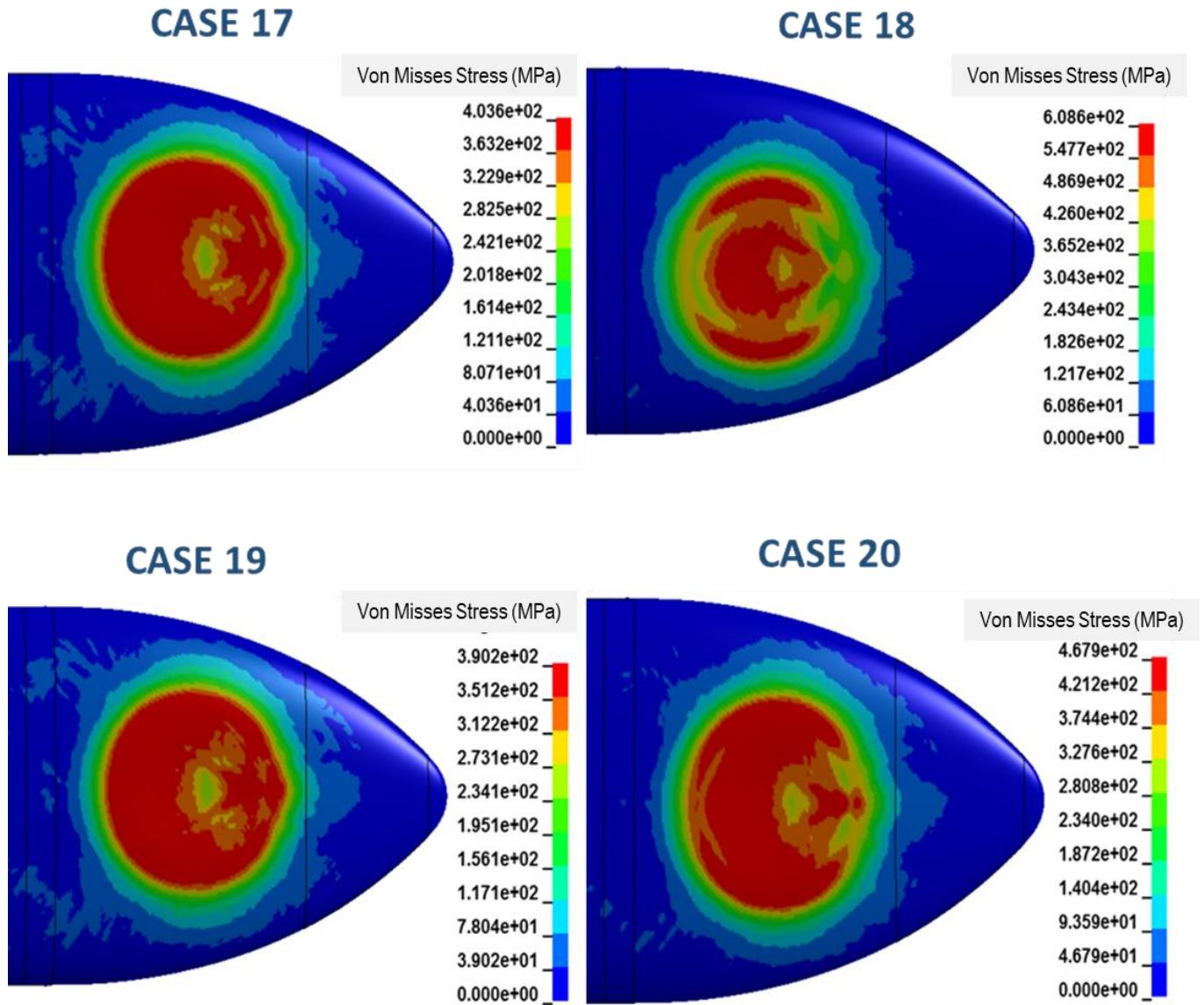


Figure 148 Von Misses Stress Results (MPa) at 1.5 ms for Impactor Position 5

There was no tear up or penetration on the skin of EFT. The stress distributions and effective stresses on skin are similar for Piecewise Linear Plasticity material model and Johnson Cook Material model.

Von Misses Stress results at 2.0 ms for impactor position 5 is shown in Figure 149.



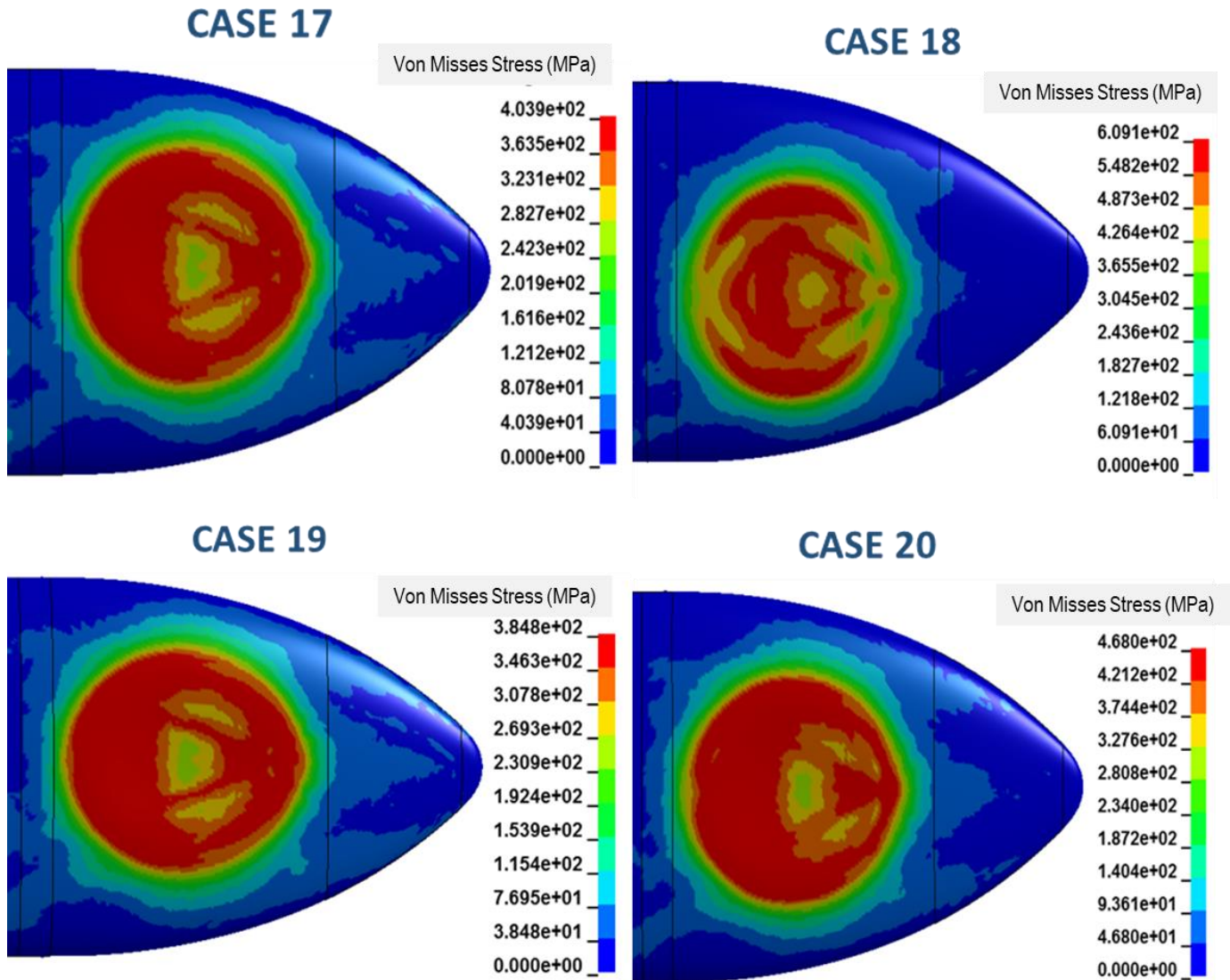


Figure 149 Von Misses Stress Results (MPa) at 2.0 ms for Impactor Position 5

There was no tear up or penetration on the skin of EFT. The stress distributions and effective stresses on skin are similar for Piecewise Linear Plasticity material model and Johnson Cook Material model.

Von Misses Stress results at 2.5 ms for impactor position 5 is shown in Figure 150.

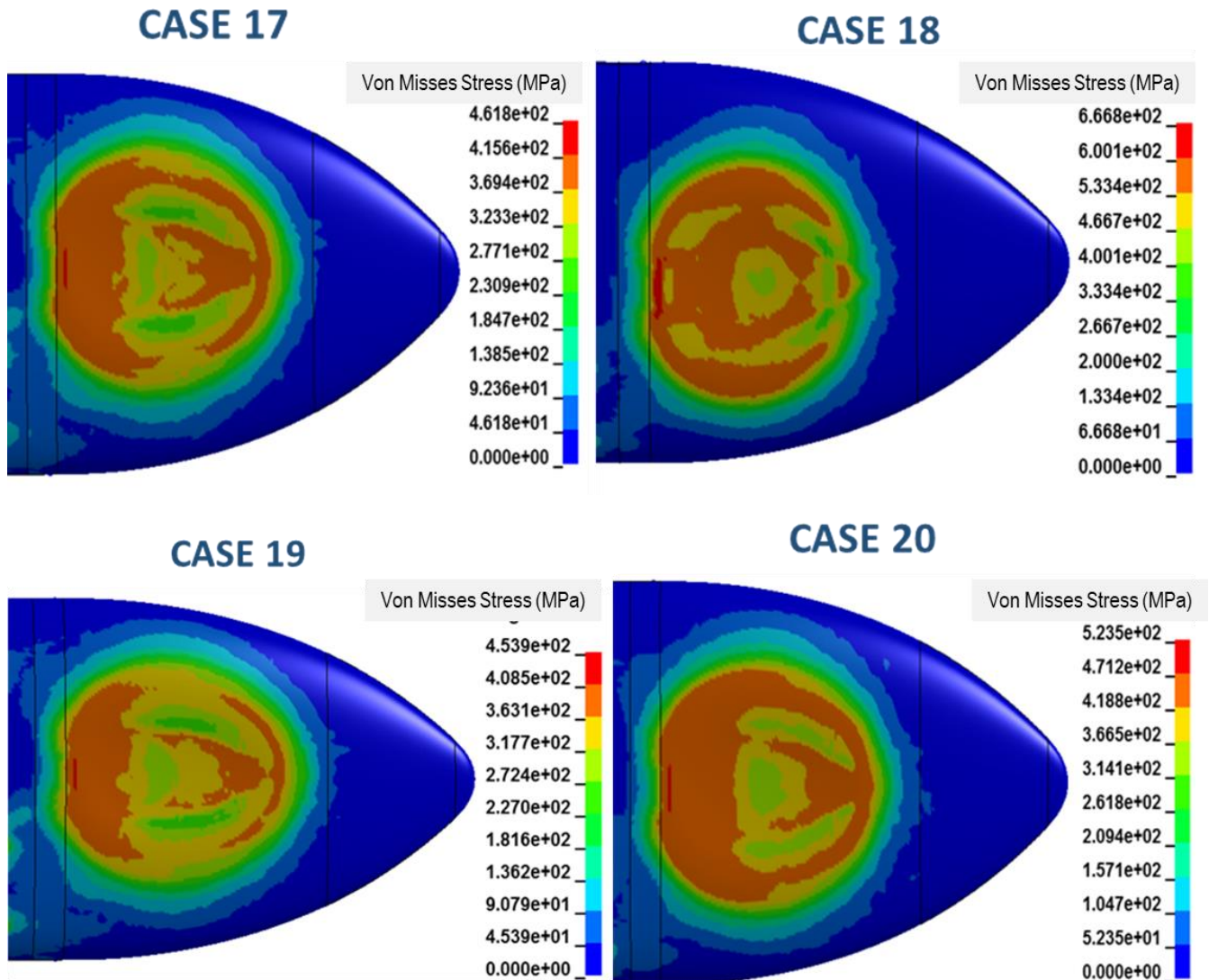


Figure 150 Von Misses Stress Results (MPa) at 2.5 ms for Impactor Position 5

There was no tear up or penetration on the skin of EFT. The stress distributions and effective stresses on skin are similar for Piecewise Linear Plasticity material model and Johnson Cook Material model.

Von Misses Stress results at 3.0 ms for impactor position 5 is shown in Figure 151.

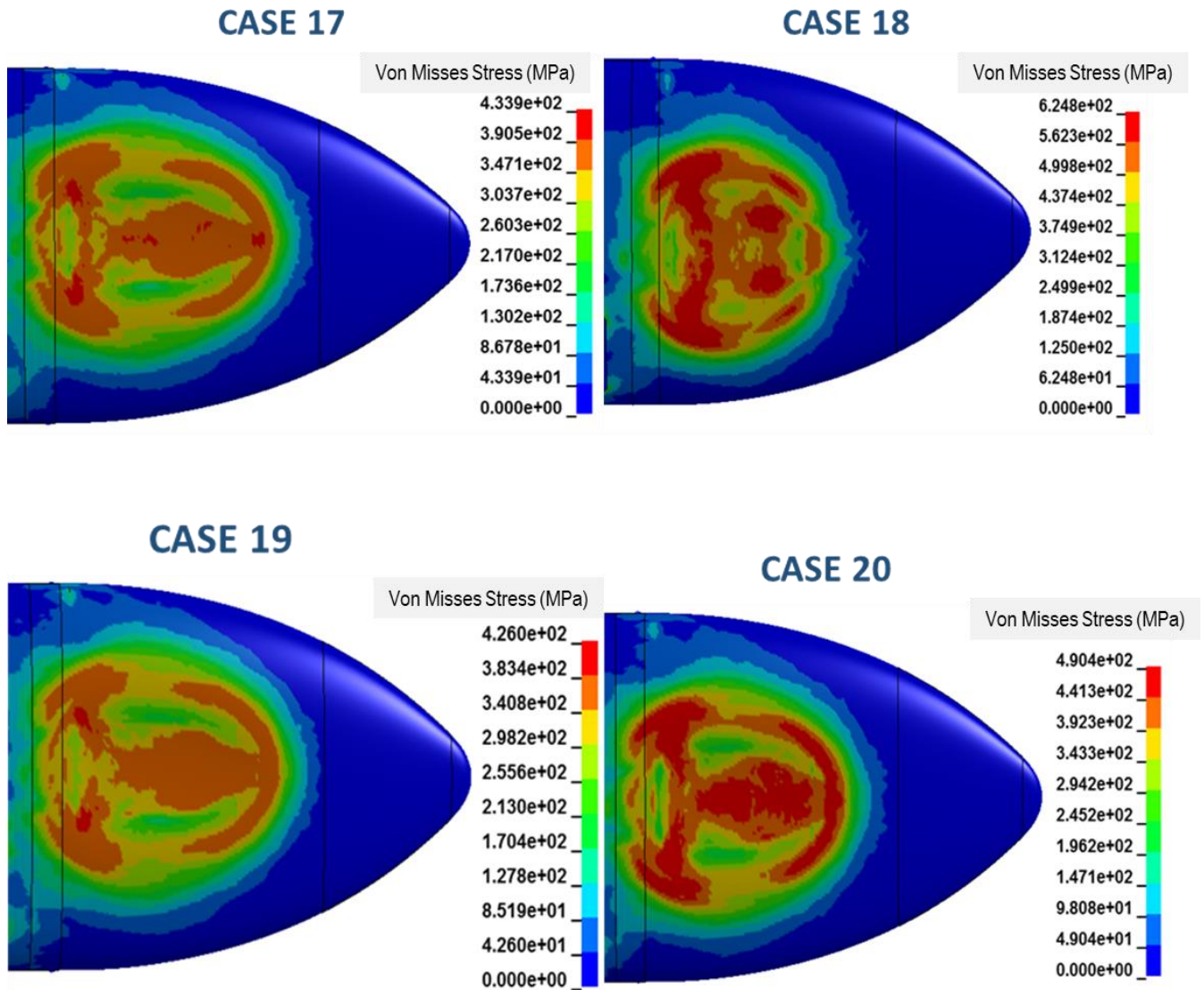


Figure 151 Von Misses Stress Results (MPa) at 3.0 ms for Impactor Position 5

There was no tear up or penetration on the skin of EFT. The stress distributions and effective stresses on skin are similar for Piecewise Linear Plasticity material model and Johnson Cook Material model.

Von Misses Stress results at 3.5 ms for impactor position 5 is shown in Figure 152.

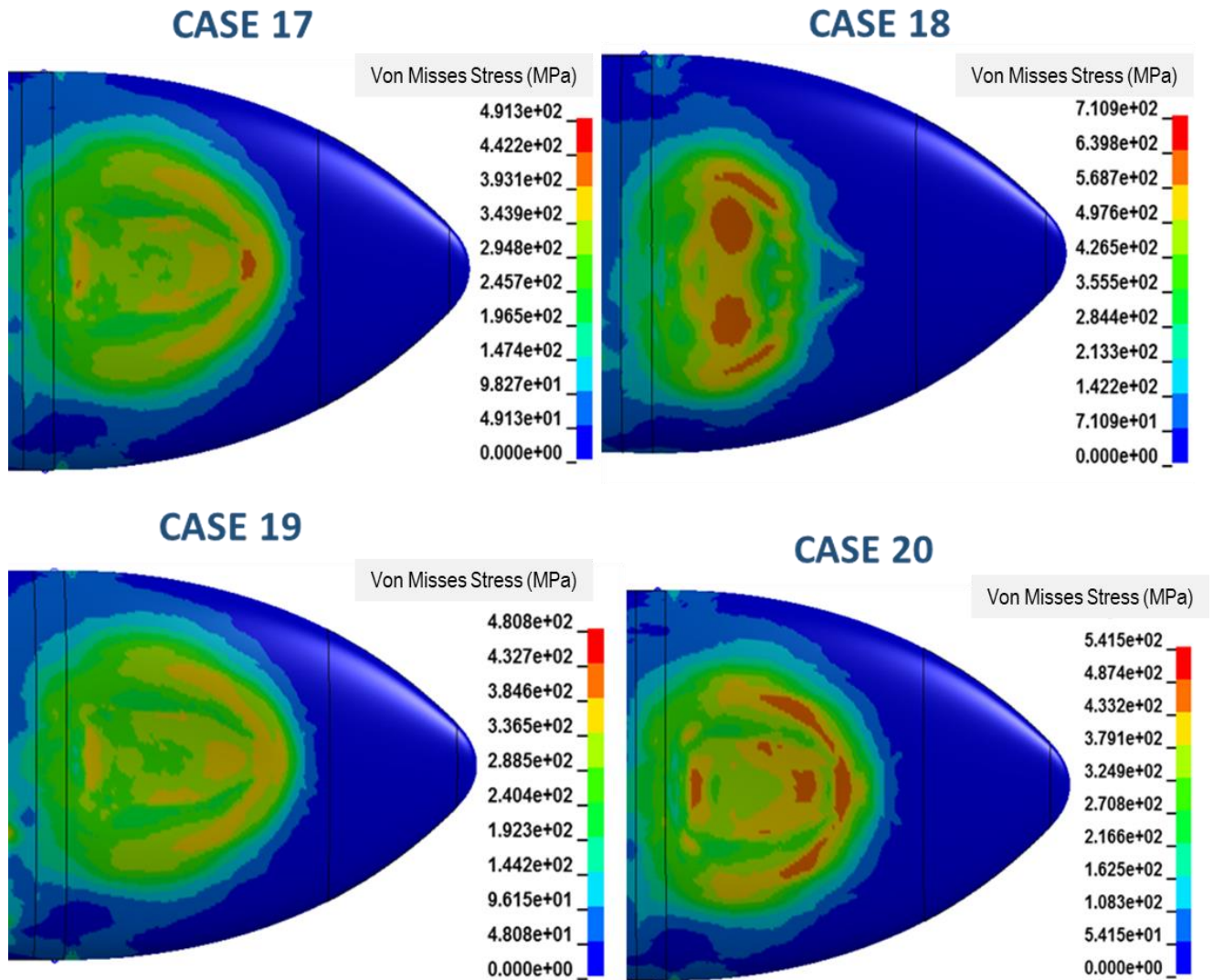


Figure 152 Von Misses Stress Results (MPa) at 3.5 ms for Impactor Position 5

There was no tear up or penetration on the skin of EFT. The stress distributions and effective stresses on skin are similar for Piecewise Linear Plasticity material model and Johnson Cook Material model. Impact ended in 3.4 ms.

Von Misses Stress results at 4.0 ms for impactor position 5 is shown in Figure 153.

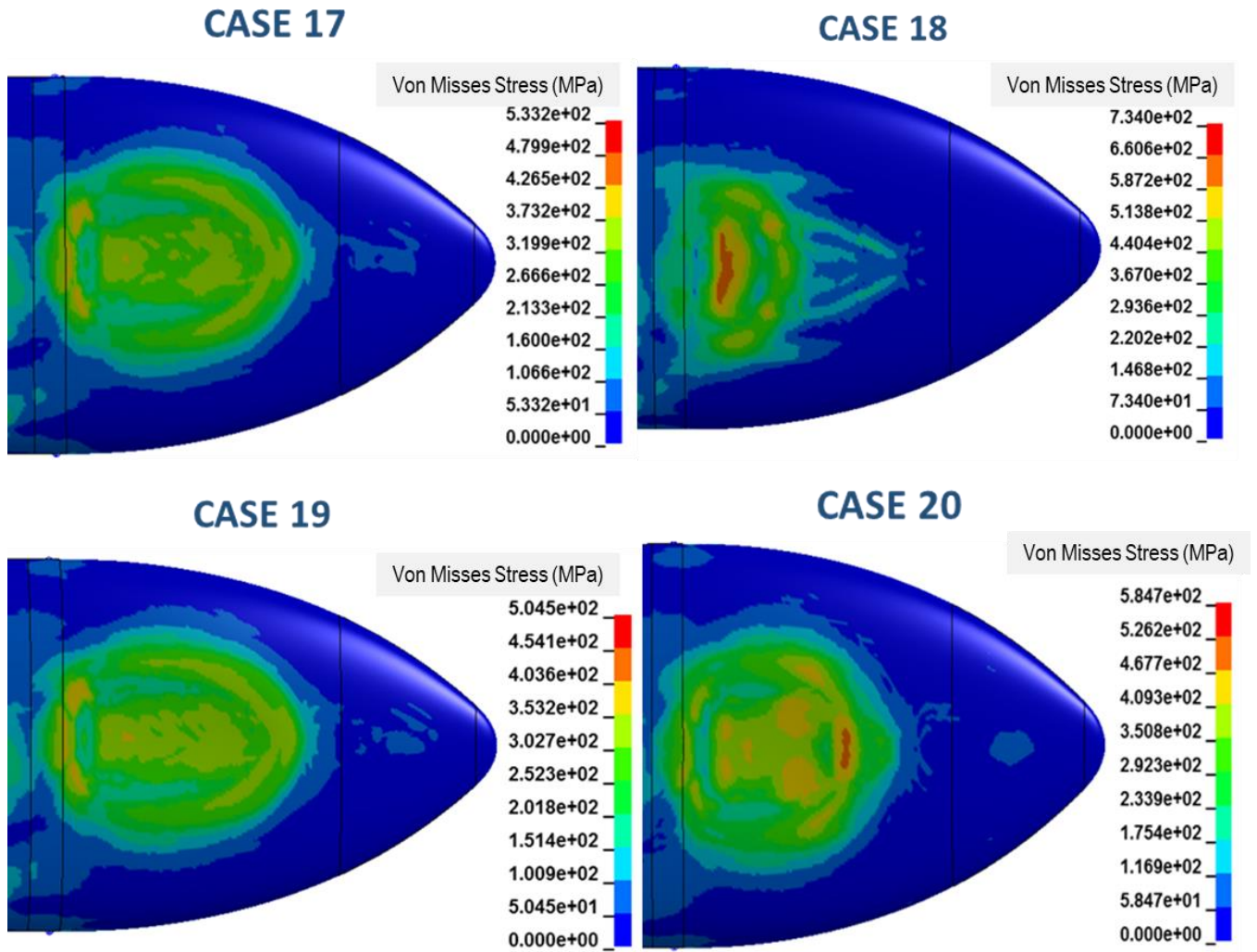


Figure 153 Von Misses Stress Results (MPa) at 4.0 ms for Impactor Position 5

There was no tear up or penetration on the skin of EFT. The stress distributions and effective stresses on skin are similar for Piecewise Linear Plasticity material model and Johnson Cook Material model. Impact ended in 3.4 ms.

Von Misses Stress results at 4.5 ms for impactor position 5 is shown in Figure 154.

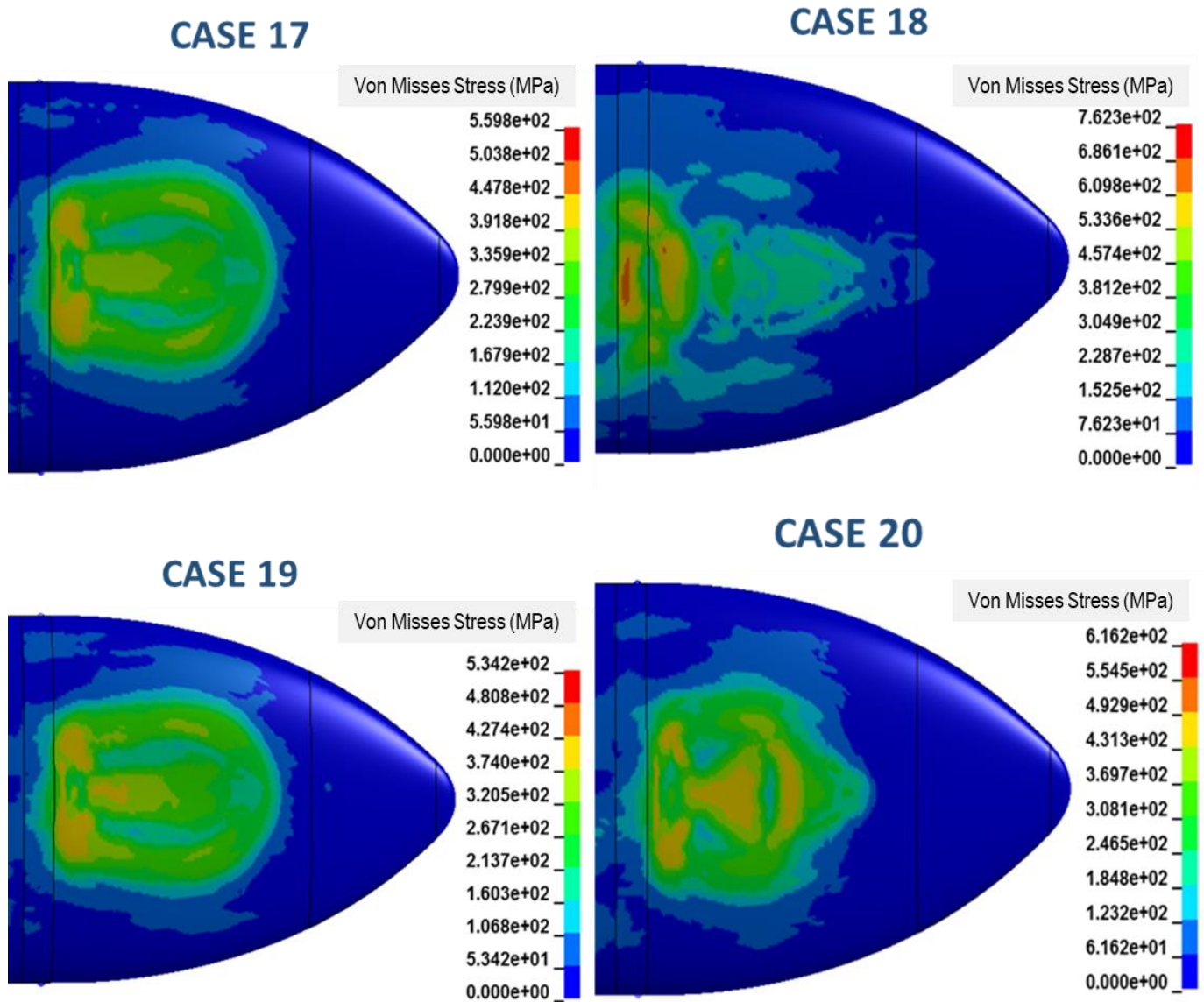


Figure 154 Von Misses Stress Results (MPa) at 4.5 ms for Impactor Position 5

There was no tear up or penetration on the skin of EFT. The stress distributions and effective stresses on skin are similar for Piecewise Linear Plasticity material model and Johnson Cook Material model. Impact ended in 3.4 ms.

Von Misses Stress results at 5.0 ms for impactor position 5 is shown in Figure 155.

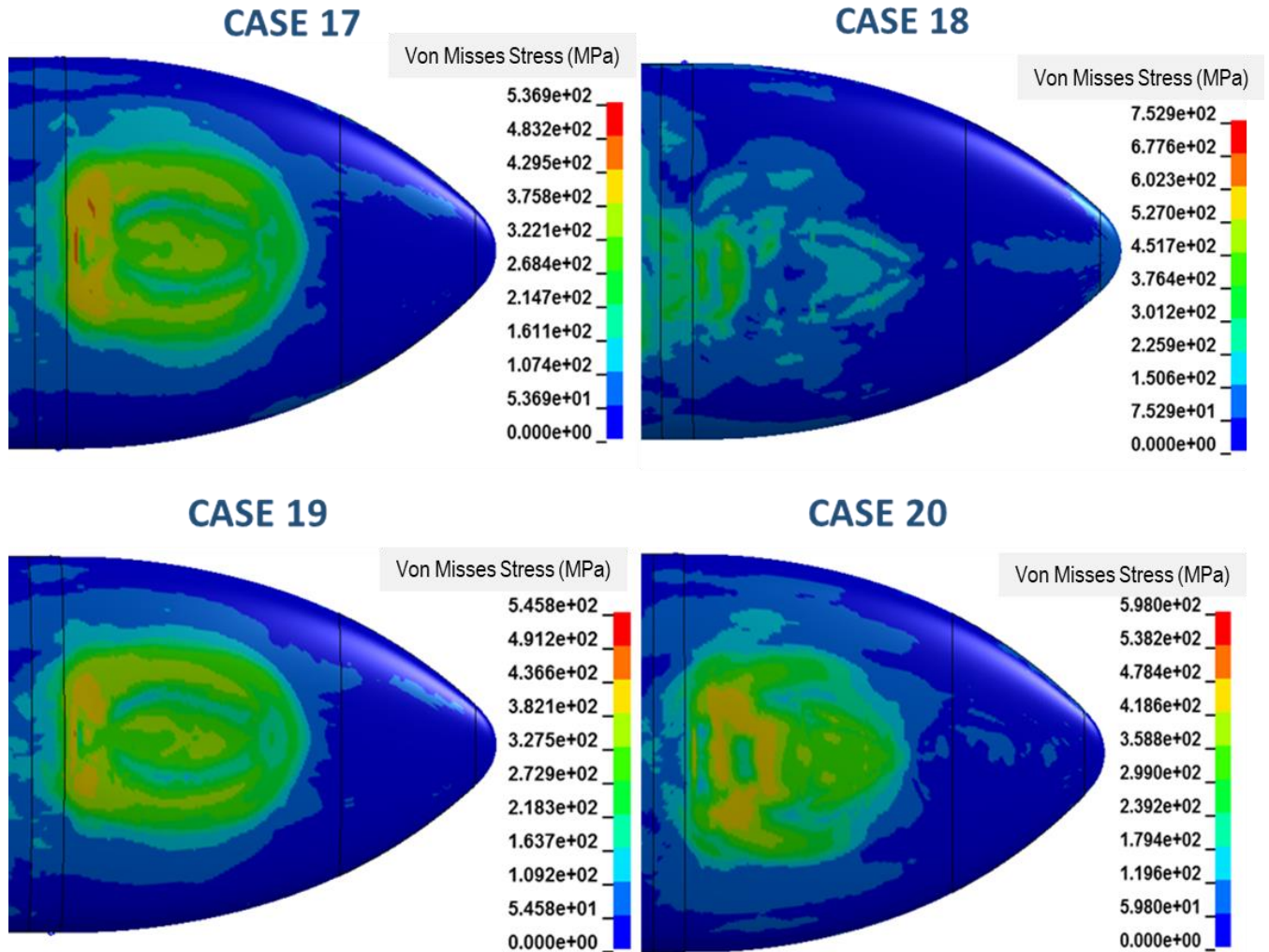


Figure 155 Von Misses Stress Results (MPa) at 5.0 ms for Impactor Position 5

There was no tear up or penetration on the skin of EFT. The stress distributions and effective stresses on skin are similar for Piecewise Linear Plasticity material model and Johnson Cook Material model. Impact ended in 3.4 ms.

The stresses and deformations on EFT skin are shown in Figure 136 to Figure 155. The plastic deformation began at 0.5ms as shown in Figure 146. There was no tear up or penetration on the skin of EFT. The stress distributions and effective stresses on skin are similar for Piecewise Linear Plasticity material model and Johnson Cook Material model.

Maximum stress on EFT skin was 560 MPa for Case 17, 762 MPa for Case 18, 546 MPa for Case 19, 616 MPa for Case 20.

Energy variations for Position 5 is given in Figure 156. While kinetic energy decreased, internal energy increased. Total energy remained almost constant for case 18 and case 20. For case 17, total energy increases after 2ms. This is because of the increase in sliding energy. Total energy increased after 3.4ms; however, since the impact ended after 3.4ms, the analysis results before 3.4ms shall be taken into account.



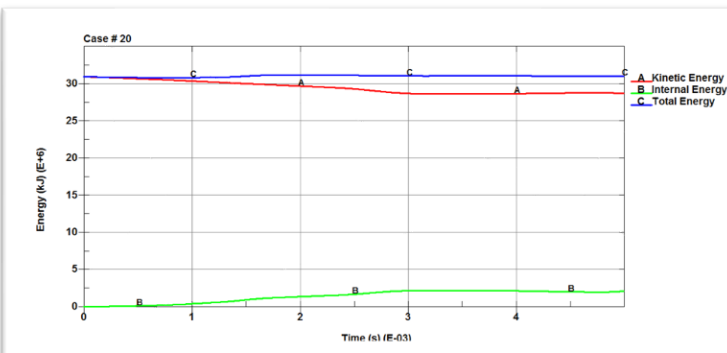
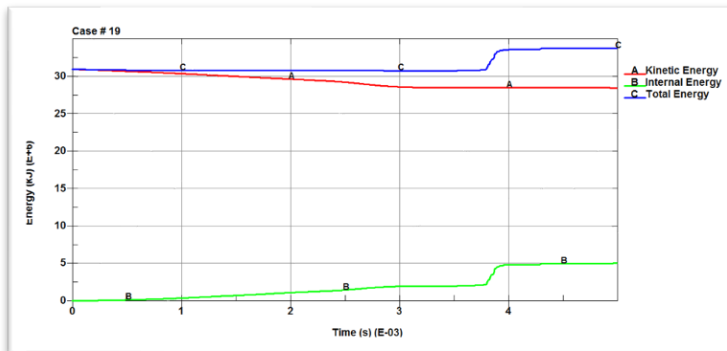
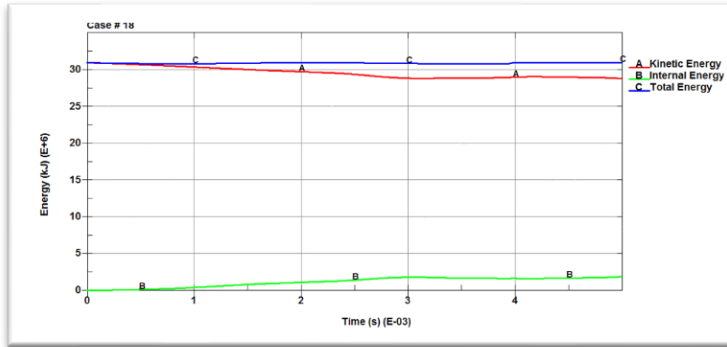
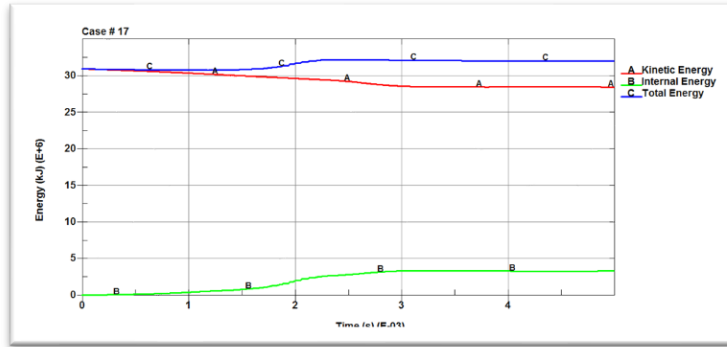


Figure 156 Energy Variation of Position 5

Energy ratios for Position 5 is given in Figure 157. Energy ratios for position 5 remained within the acceptable limits as shown.

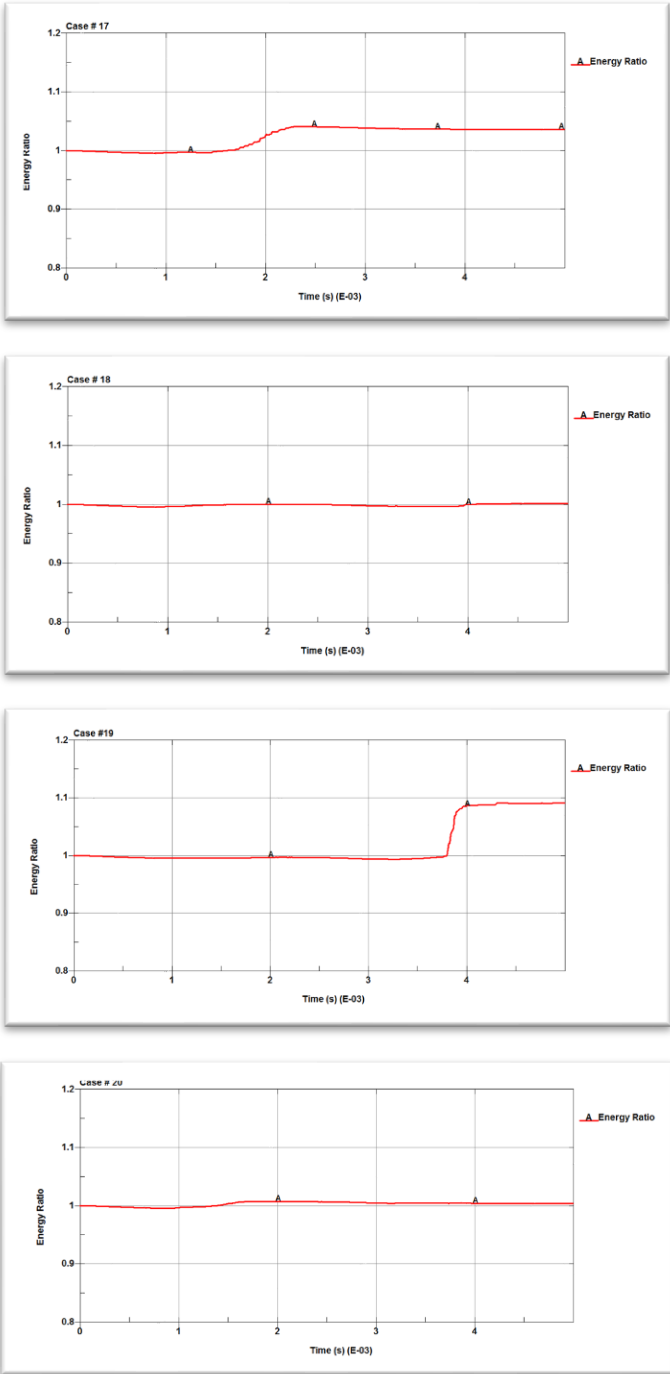


Figure 157 Energy Ratio of Position 5

Hourglass energy, damping energy and sliding energy for case 17 is given in Figure 158. Impact ended in 3.5 ms. Hourglass energy remained almost 0. Sliding energy increased between 2ms and 3ms; however, the increase is in the acceptable limit.

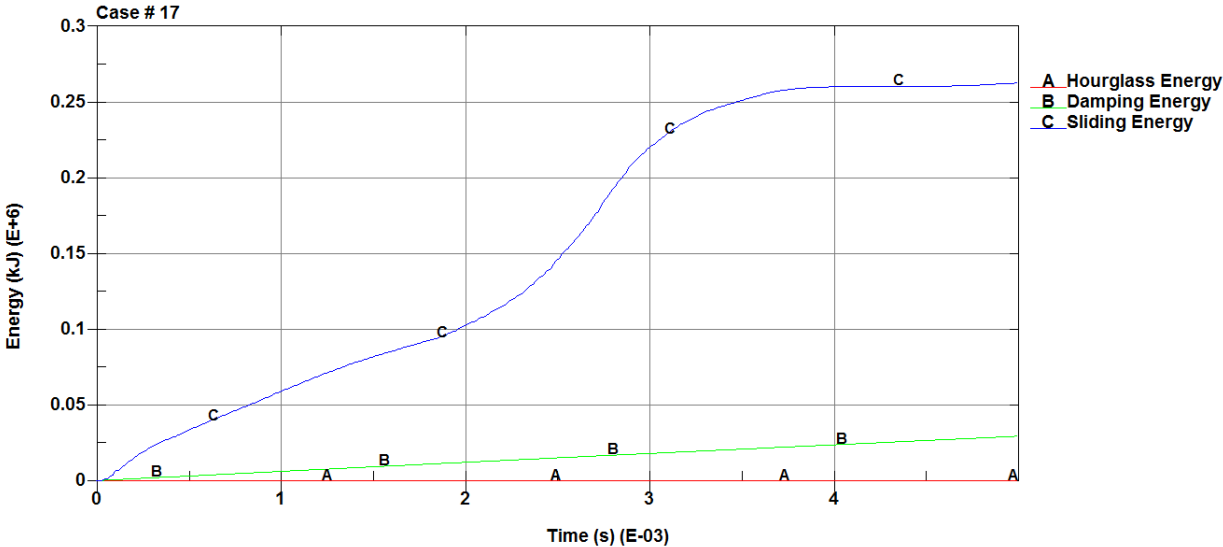


Figure 158 Hourglass, Damping and Sliding Energies Variation of Case 17

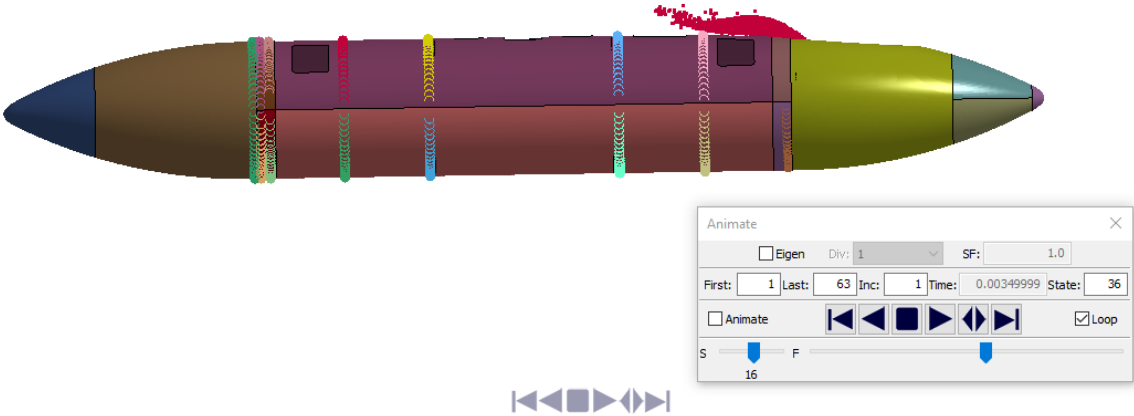


Figure 159 Bird Impact at 4 ms for Case 17

Hourglass energy, damping energy and sliding energy for case 18 is given in Figure 160. Impact ended in 3.4 ms. Hourglass energy remained almost 0. Sliding energy increased between 2ms and 3ms; however, the increase is in the acceptable limit.

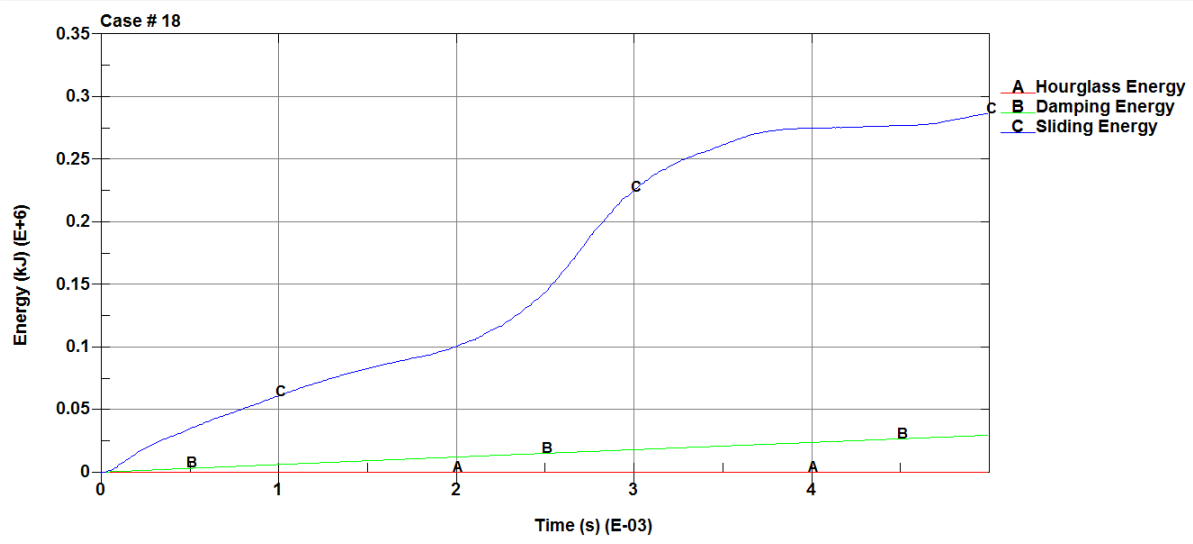


Figure 160 Hourglass, Damping and Sliding Energies Variation of Case 18

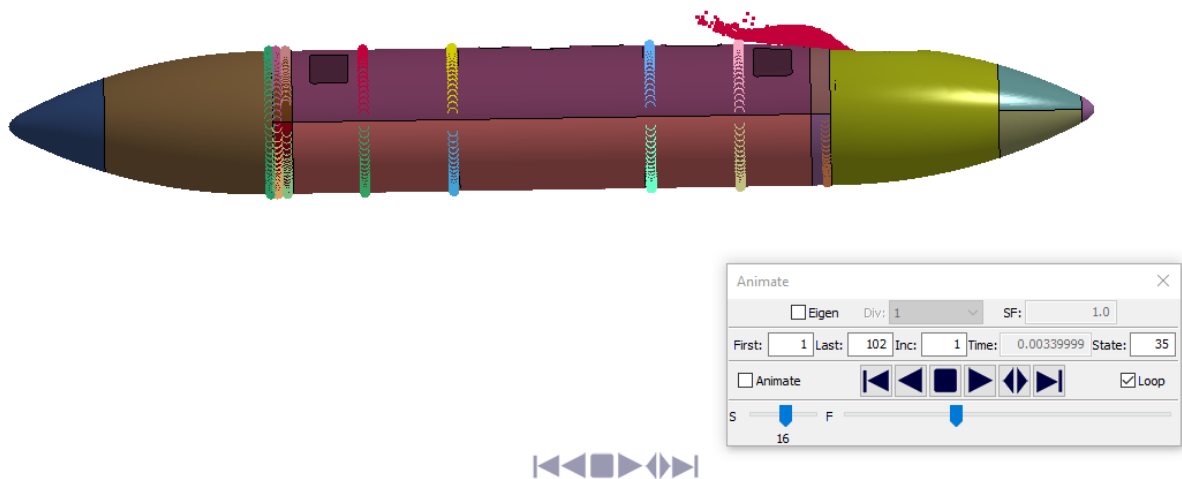


Figure 161 Bird Impact at 4 ms for Case 18

Hourglass energy, damping energy and sliding energy for case 19 is given in Figure 162. Impact ended in 3.4 ms. Hourglass energy remained almost 0. Sliding energy increased between 2ms and 3ms.

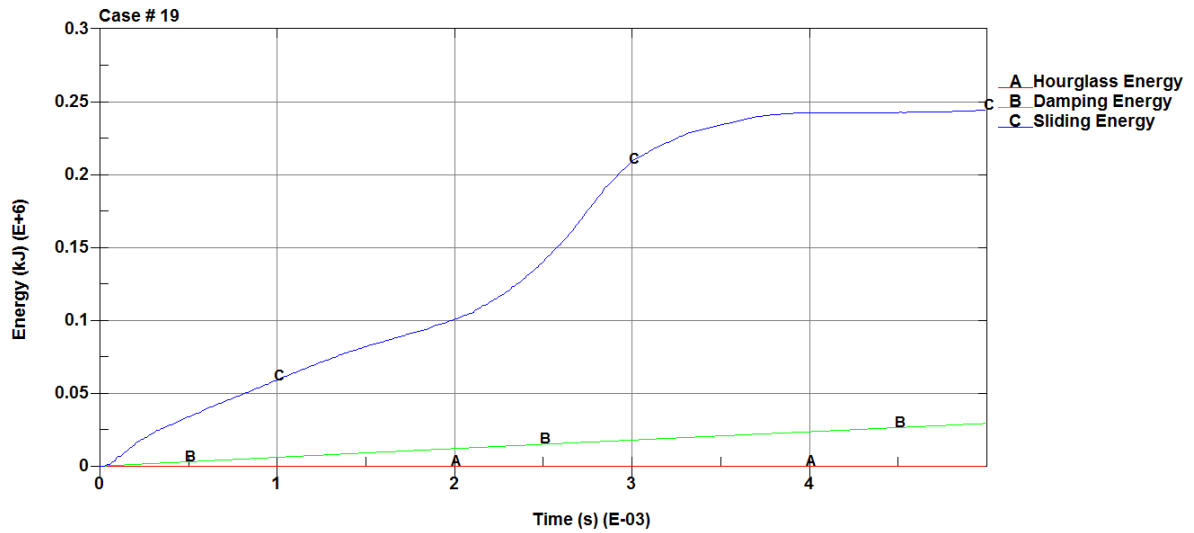


Figure 162 Hourglass, Damping and Sliding Energies Variation of Case 19

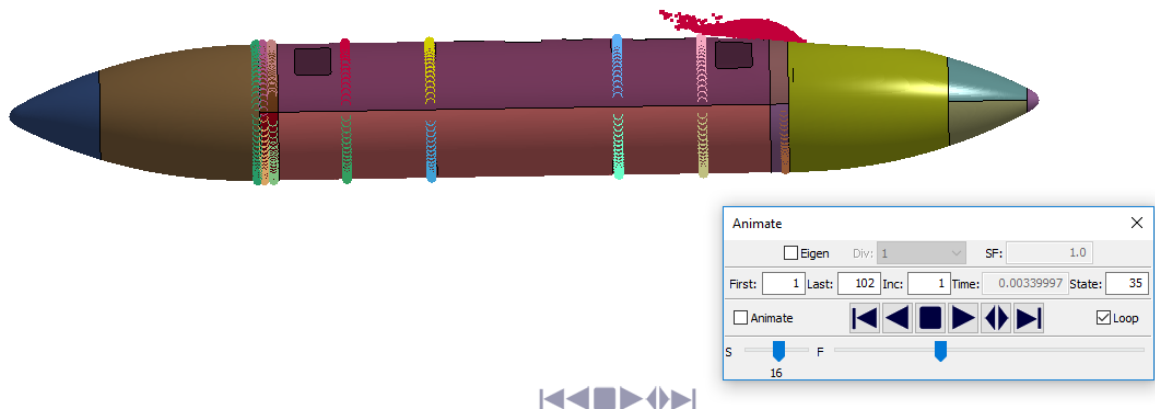


Figure 163 Bird Impact at 4 ms for Case 19

Hourglass energy, damping energy and sliding energy for case 20 is given in Figure 164. Impact ended in 3.4 ms. Hourglass energy remained almost 0. Sliding energy increased between 2ms and 3ms; however, the increase is in the acceptable limit.

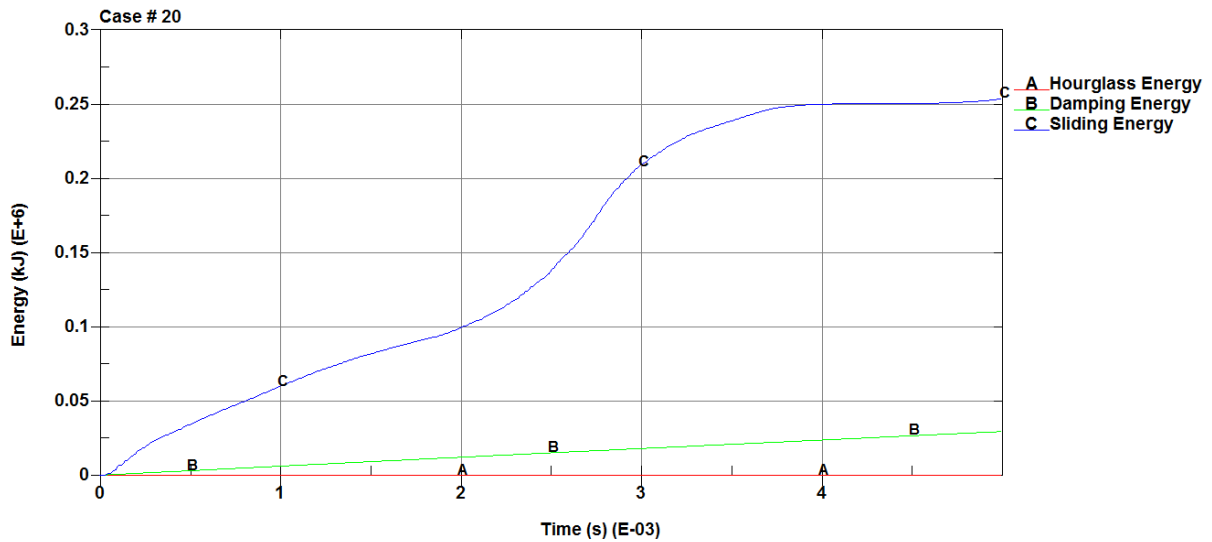


Figure 164 Hourglass, Damping and Sliding Energies Variation of Case 20

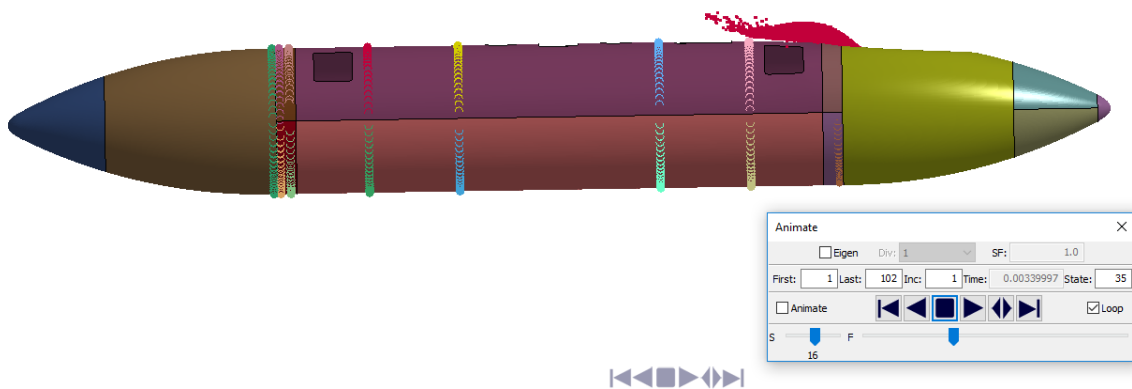


Figure 165 Bird Impact at 4 ms for Case 20

### **Analysis Results for Position 6**

An overview of the impact simulation for the position 6 was given for the general understanding. The time history was presented as a series of time step plots with explanations. The plots in Figure 166 to Figure 185 show the simulation run in several steps. Total simulation time was set to 5 ms and plots are saved in the intervals of 0.5ms.

Displacement results at 0.5 ms for impactor position 6 is shown in Figure 166.

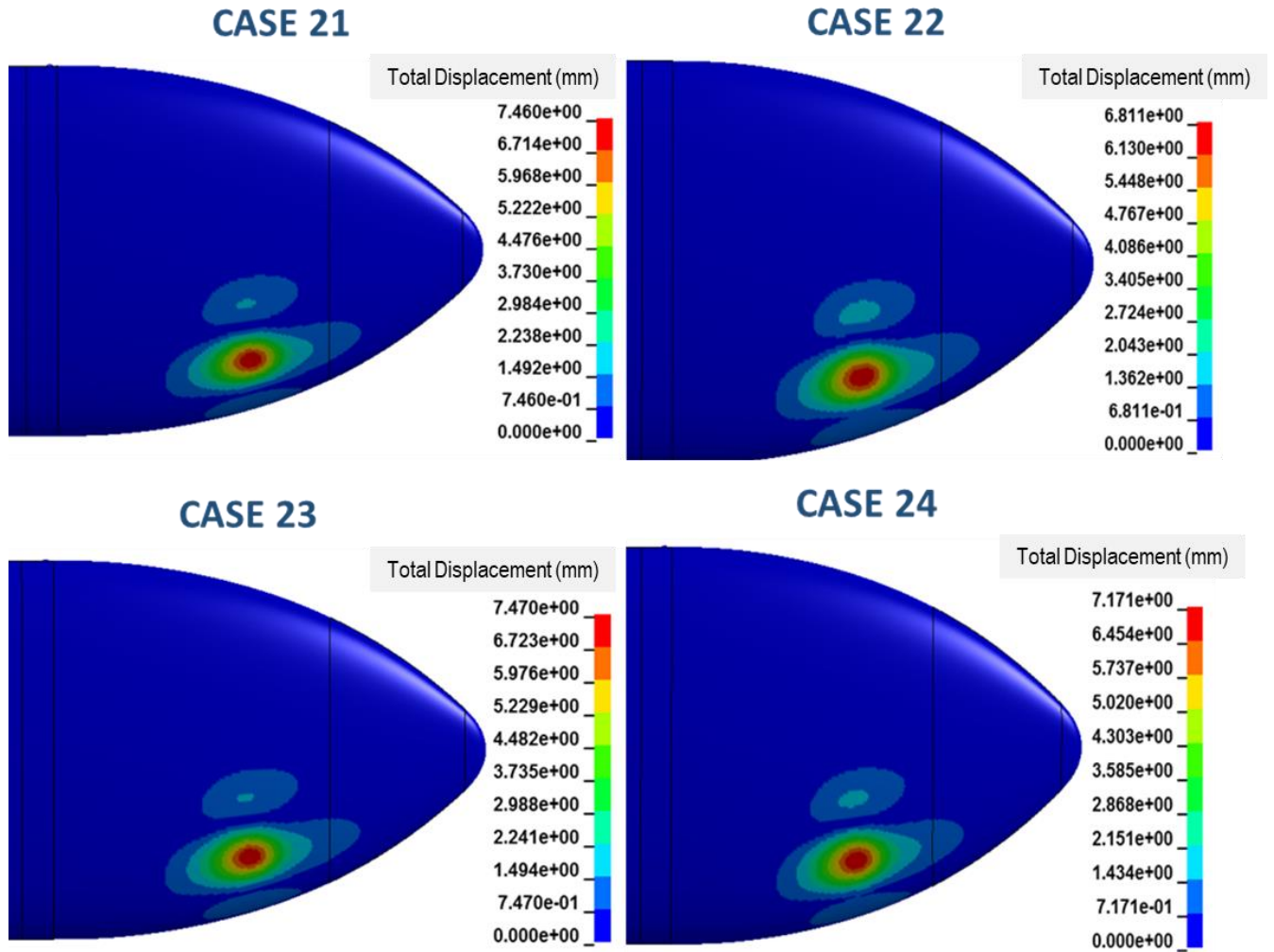


Figure 166 Displacement Results (mm) at 0.5 ms for Impactor Position 6

Displacements on Al 7075 -T6 and Al 2024-T3 are similar. Displacement values according to Piecewise Linear Plasticity material model are also similar to Johnson Cook Material model.

Displacement results at 1.0 ms for impactor position 6 is shown in Figure 167.

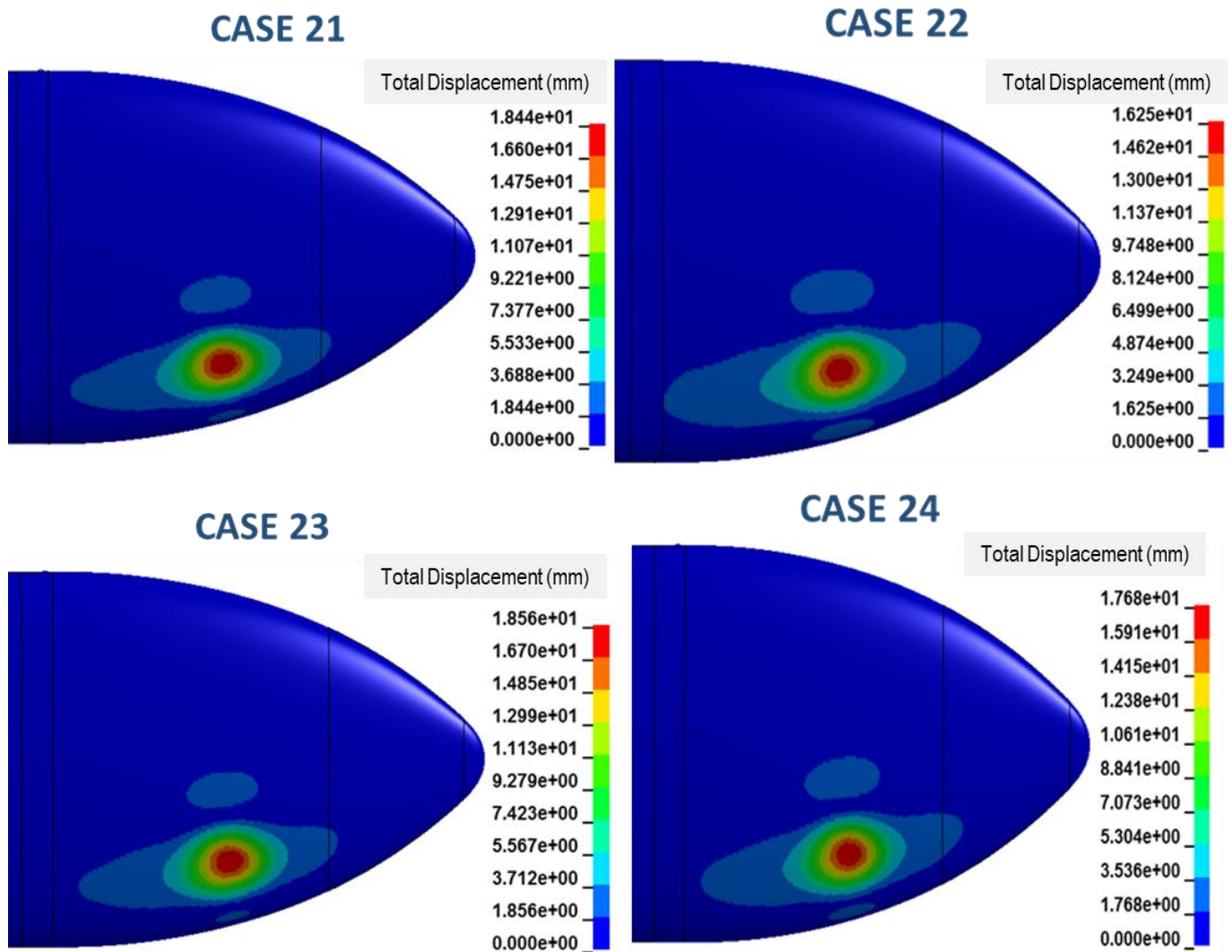


Figure 167 Displacement Results (mm) at 1.0 ms for Impactor Position 6

Displacements on Al 7075 -T6 and Al 2024-T3 are similar. Displacement values according to Piecewise Linear Plasticity material model are also similar to Johnson Cook Material model.

Displacement results at 1.5 ms for impactor position 6 is shown in Figure 168.



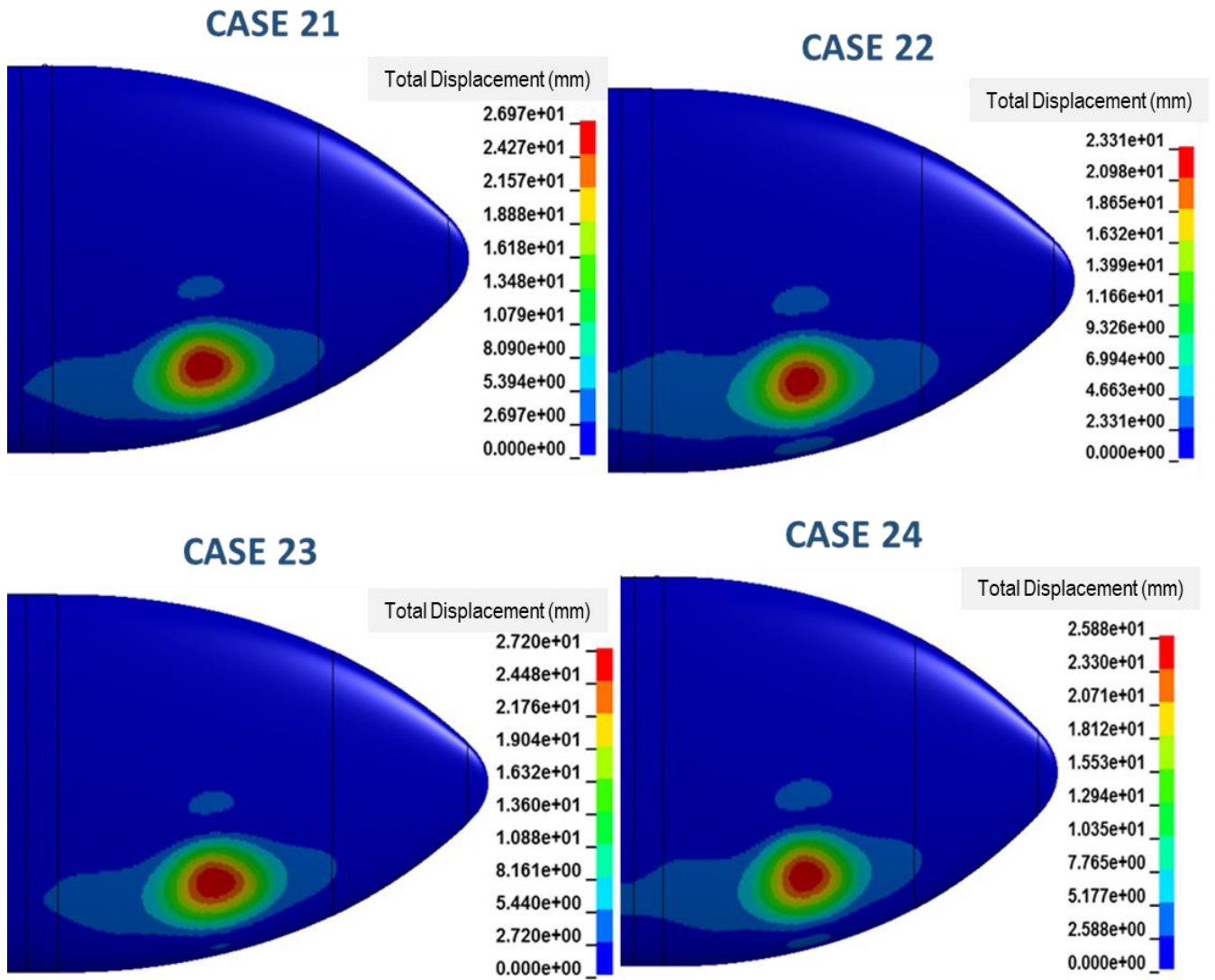


Figure 168 Displacement Results (mm) at 1.5 ms for Impactor Position 6

Displacements on Al 7075 -T6 and Al 2024-T3 are similar. Displacement values according to Piecewise Linear Plasticity material model are also similar to Johnson Cook Material model.

Displacement results at 2.0 ms for impactor position 6 is shown in Figure 169.

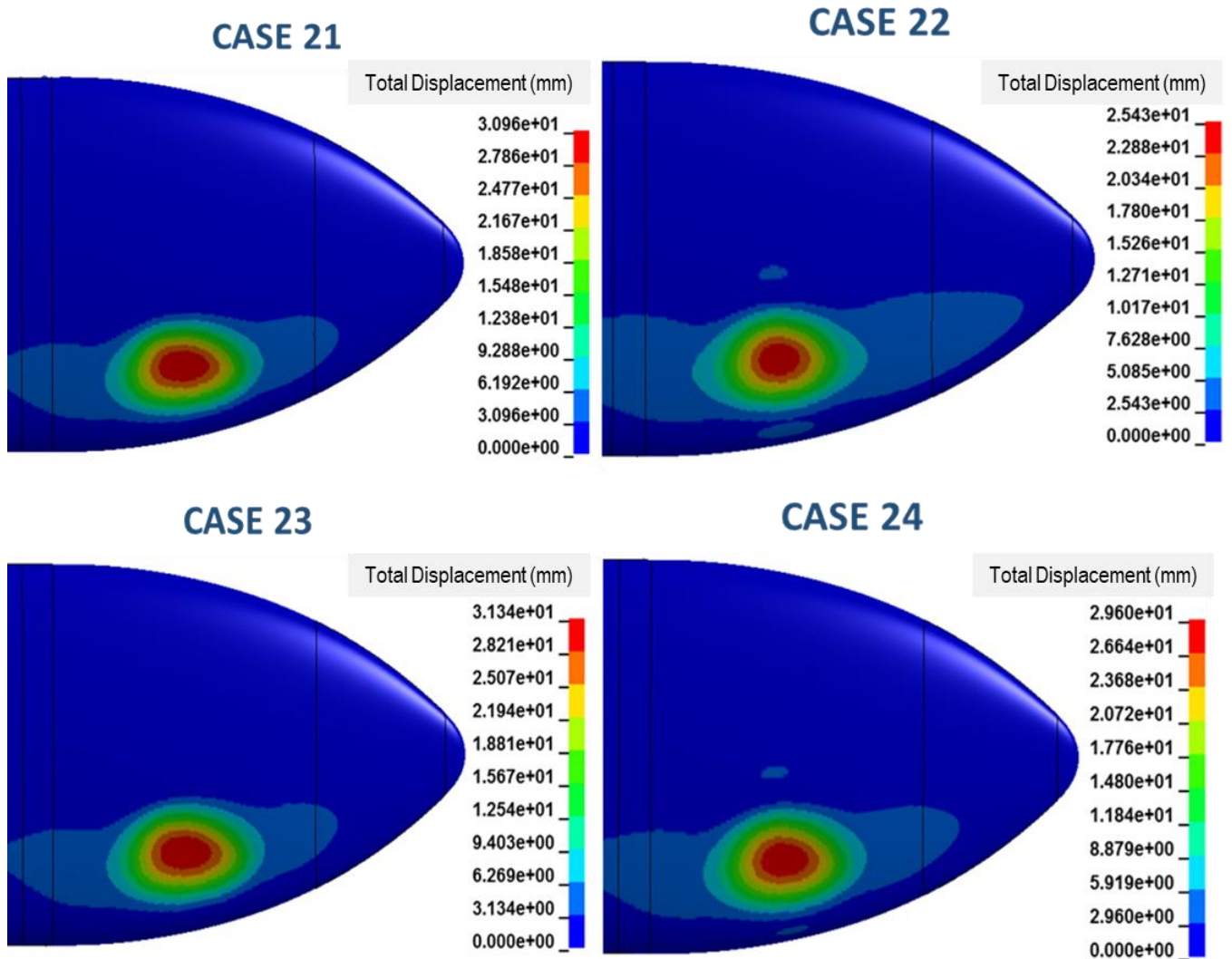


Figure 169 Displacement Results (mm) at 2.0 ms for Impactor Position 6

Displacements on Al 7075 -T6 and Al 2024-T3 are similar. Displacement values according to Piecewise Linear Plasticity material model are also similar to Johnson Cook Material model.

Displacement results at 2.5 ms for impactor position 6 is shown in Figure 170.

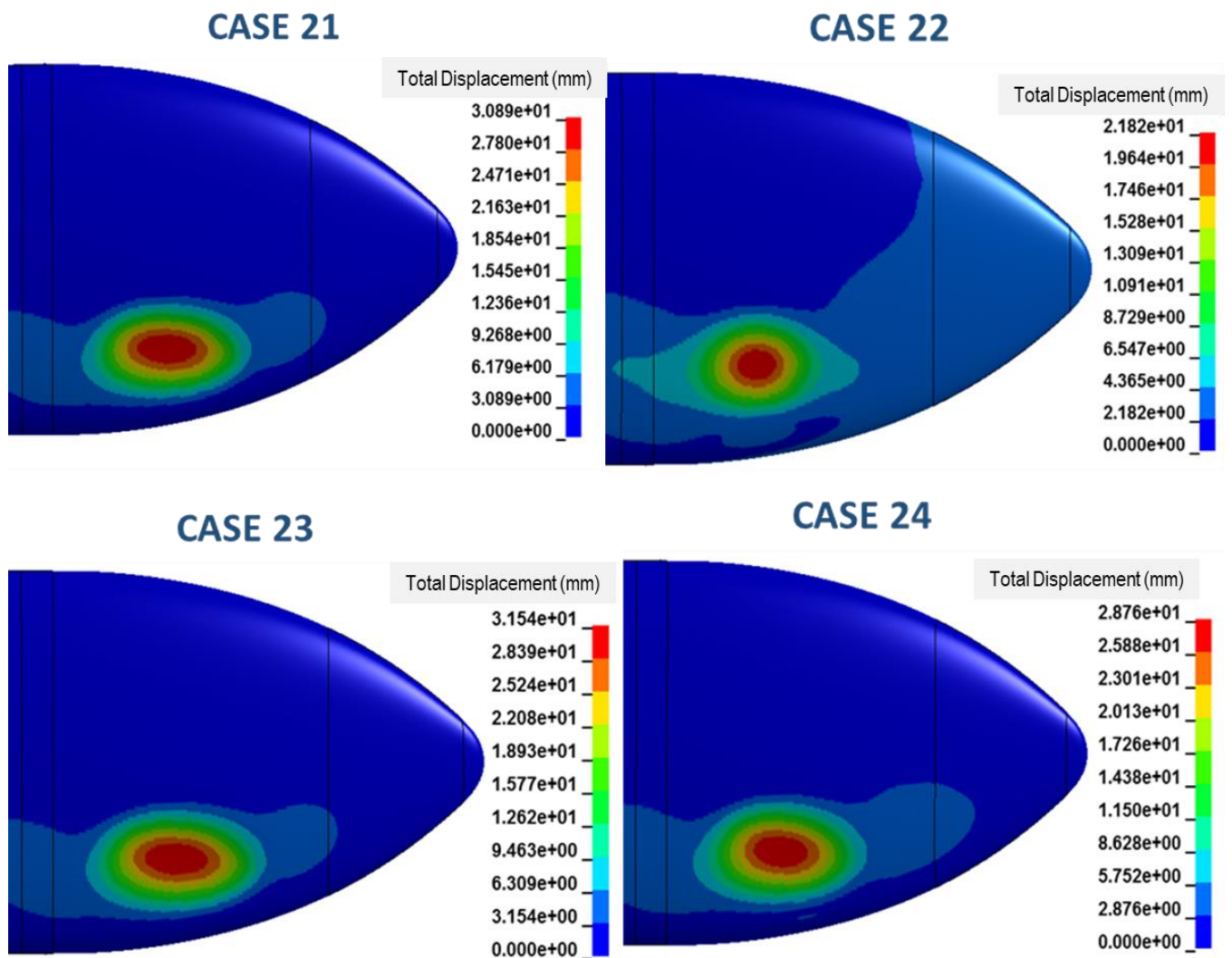


Figure 170 Displacement Results (mm) at 2.5 ms for Impactor Position 6

Displacements on Al 7075 -T6 and Al 2024-T3 are similar. Displacement values according to Piecewise Linear Plasticity material model are also similar to Johnson Cook Material model.

Displacement results at 3.0 ms for impactor position 6 is shown in Figure 171.

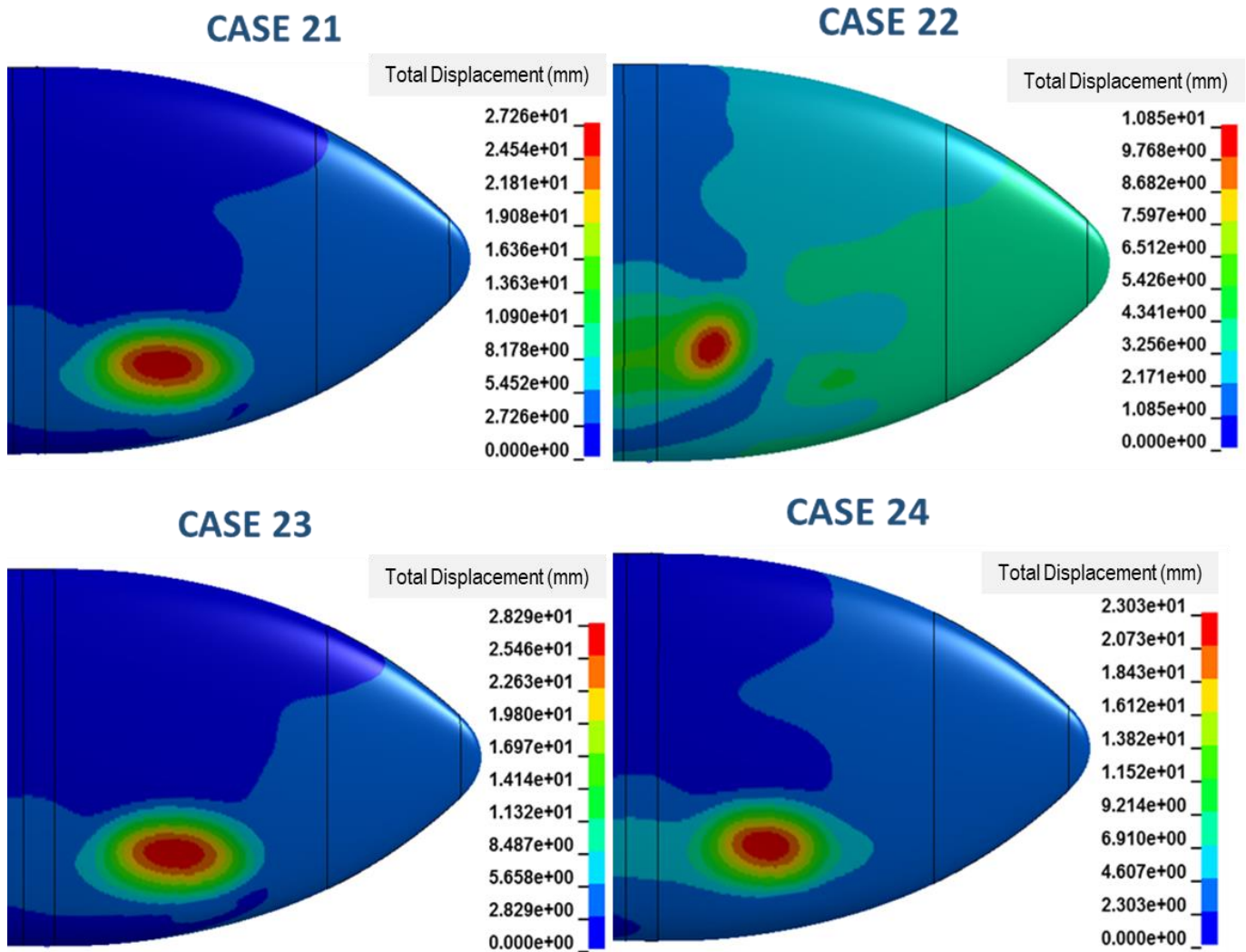


Figure 171 Displacement Results (mm) at 3.0 ms for Impactor Position 6

Displacements on Al 7075 -T6 and Al 2024-T3 are similar. Displacement values according to Piecewise Linear Plasticity material model are also similar to Johnson Cook Material model.

Displacement results at 3.5 ms for impactor position 6 is shown in Figure 172.

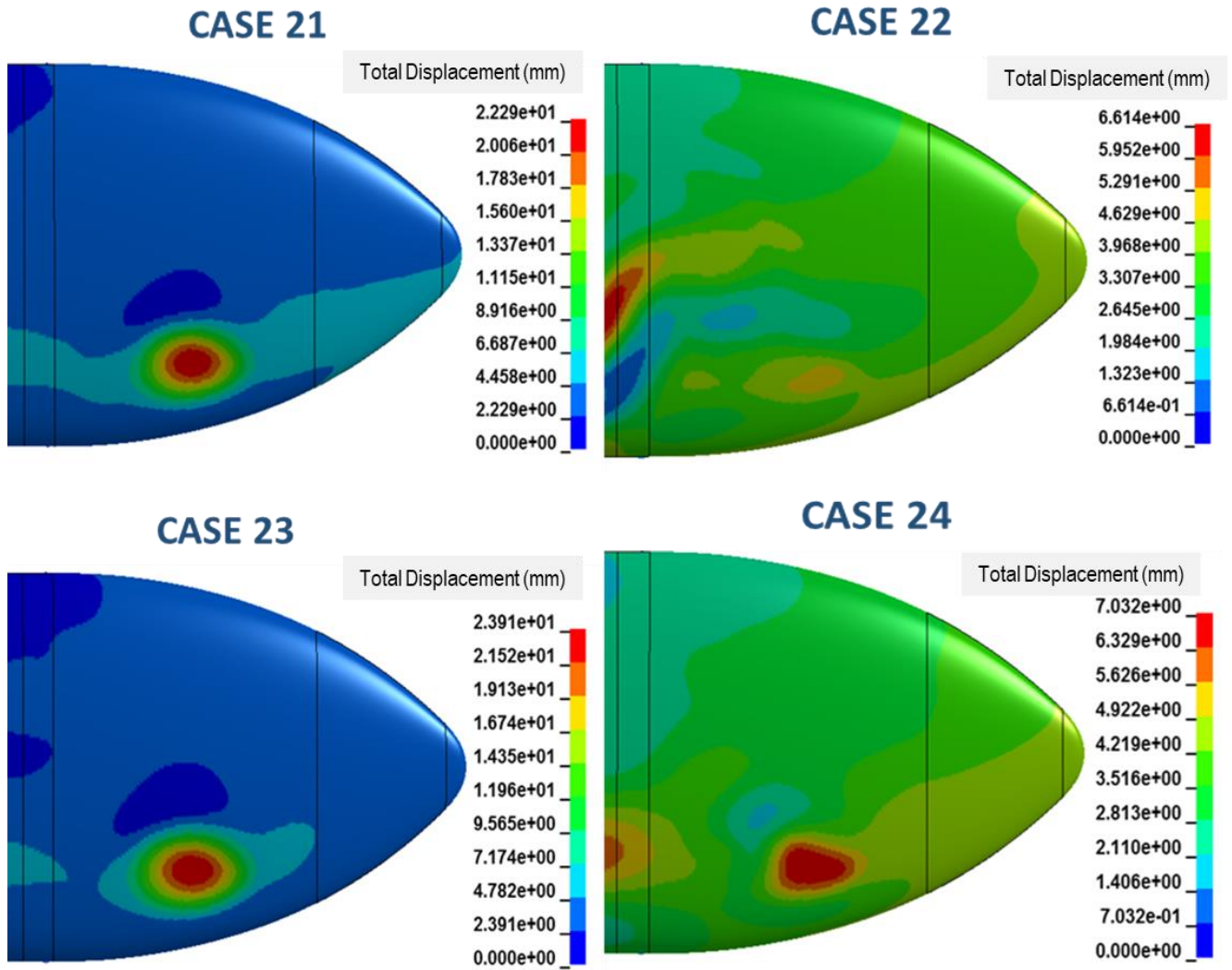


Figure 172 Displacement Results (mm) at 3.5 ms for Impactor Position 6

Displacements on Al 7075 -T6 and Al 2024-T3 are similar. Displacement values according to Piecewise Linear Plasticity material model are also similar to Johnson Cook Material model. Impact ended in 3.3 ms.

Displacement results at 4.0 ms for impactor position 6 is shown in Figure 173.

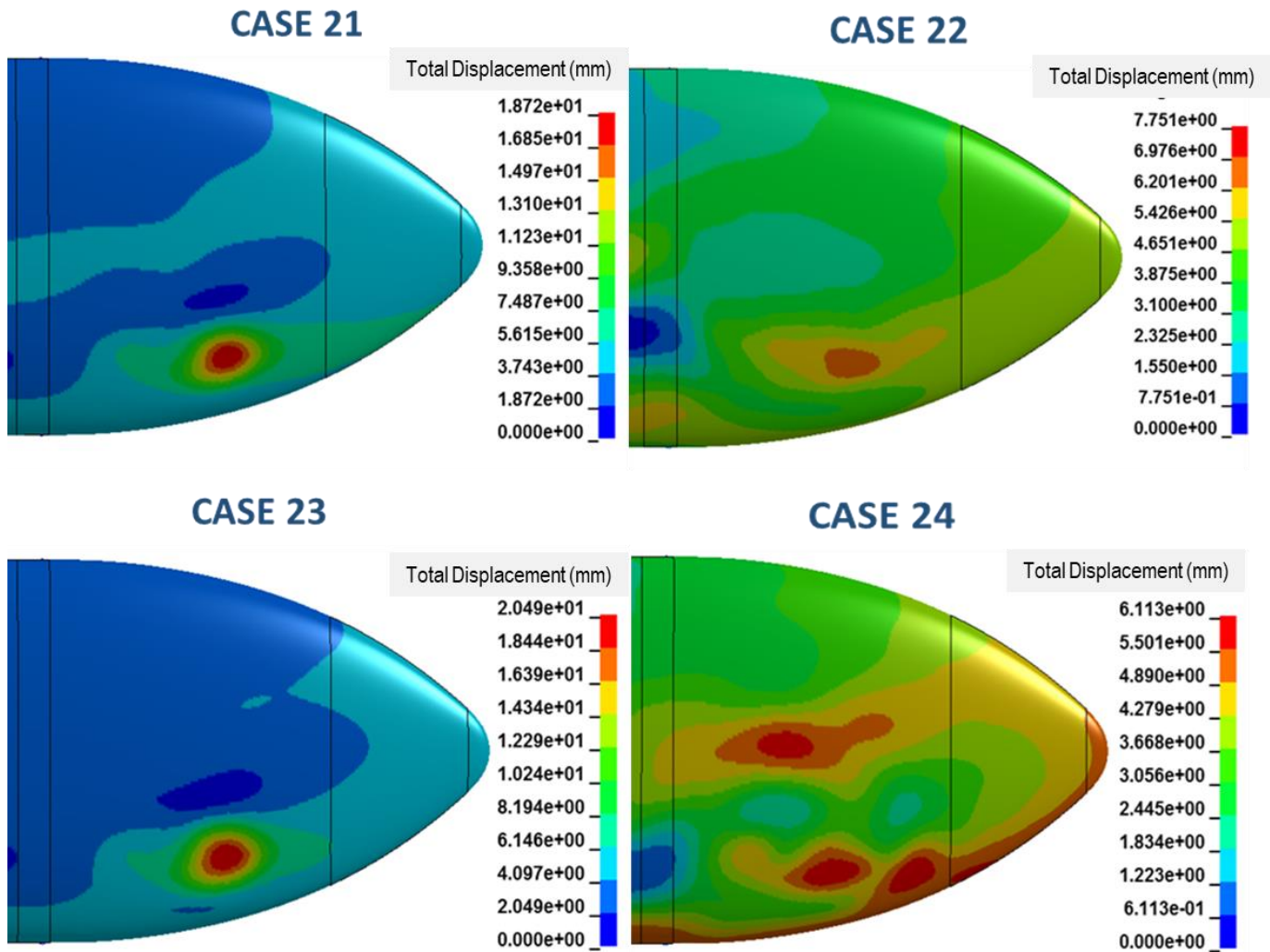


Figure 173 Displacement Results (mm) at 4.0 ms for Impactor Position 6

Displacements on Al 7075 -T6 and Al 2024-T3 are similar. Displacement values according to Piecewise Linear Plasticity material model are also similar to Johnson Cook Material model. Impact ended in 3.3 ms.

Displacement results at 4.5 ms for impactor position 6 is shown in Figure 174.

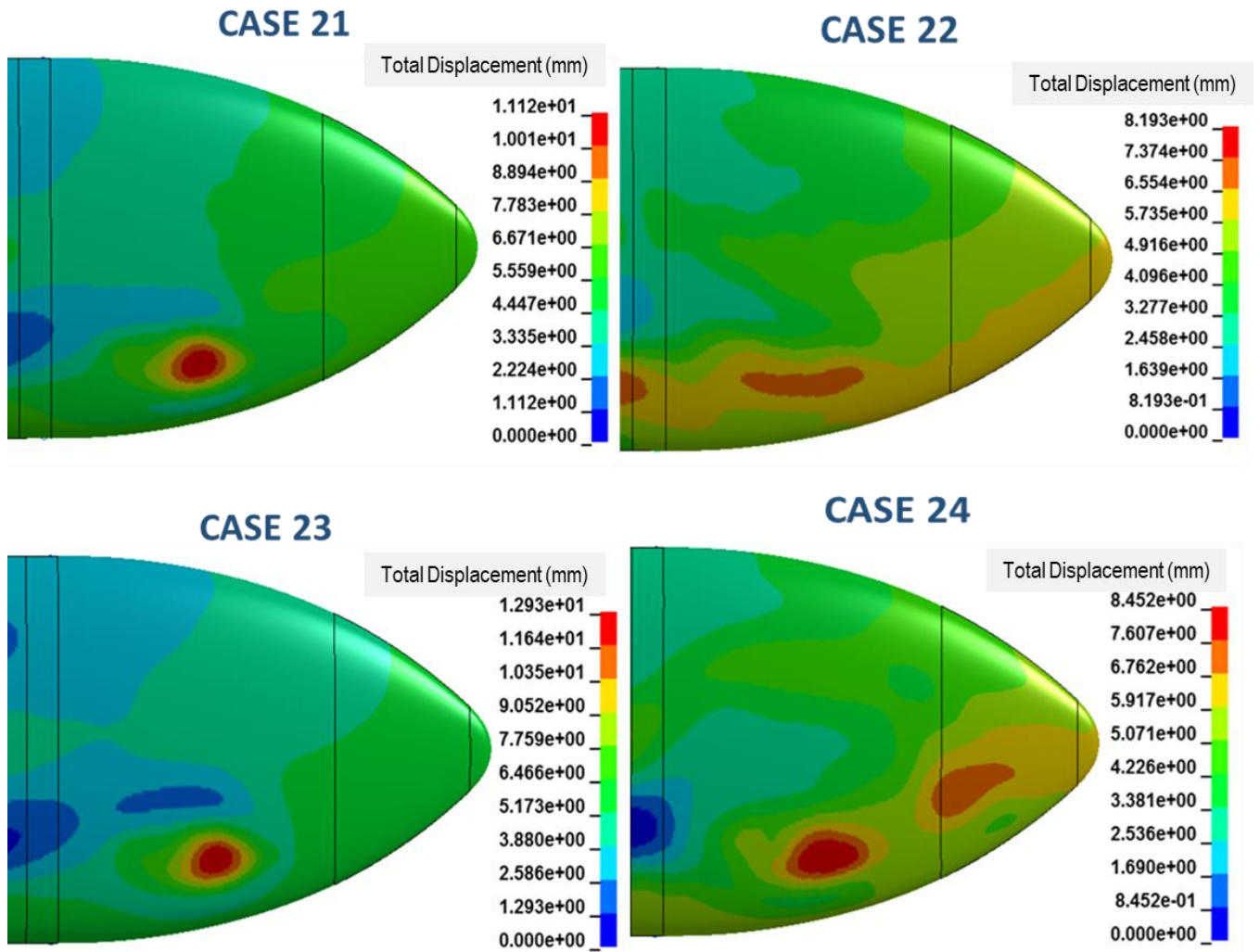


Figure 174 Displacement Results (mm) at 4.5 ms for Impactor Position 6

Displacements on Al 7075 -T6 and Al 2024-T3 are similar. Displacement values according to Piecewise Linear Plasticity material model are also similar to Johnson Cook Material model. Impact ended in 3.3 ms.

Displacement results at 5.0 ms for impactor position 6 is shown in Figure 175.

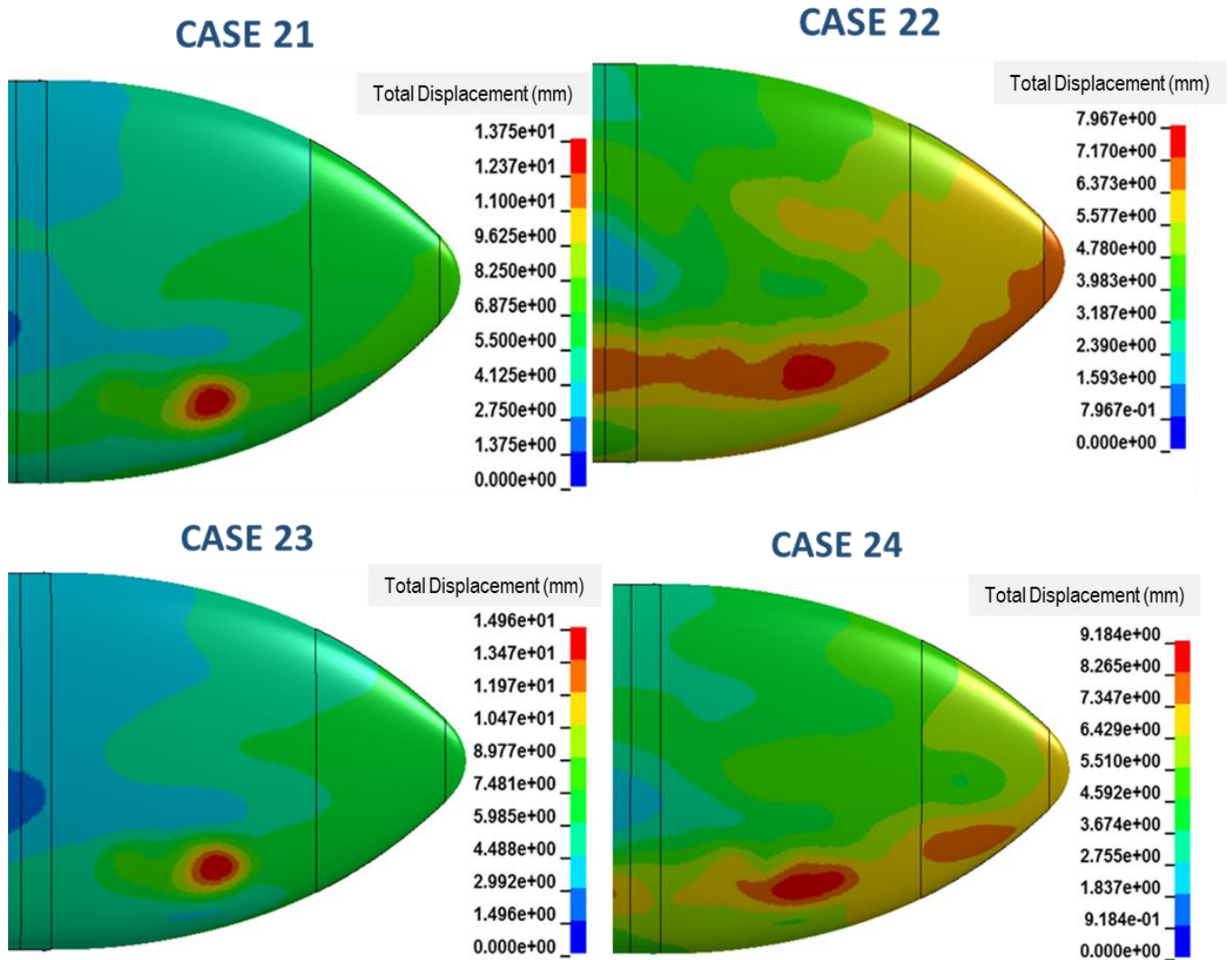


Figure 175 Displacement Results (mm) at 5.0 ms for Impactor Position 6

Displacements on Al 7075 -T6 and Al 2024-T3 are similar. Displacement values according to Piecewise Linear Plasticity material model are also similar to Johnson Cook Material model which is an expected result because of low strain rates. Impact ended in 3.3 ms.

For position 6, displacements on Al 7075 -T6 and Al 2024-T3 are similar. Displacement values according to Piecewise Linear Plasticity material model are also similar to Johnson Cook Material model.



After impact, screen shots were taken at 0.5ms intervals and the stresses are compared. Since the contact of the bird ended before 5 ms in general, the images were limited to this time period.

Von Misses Stress results at 0.5 ms for impactor position 6 is shown in Figure 176.

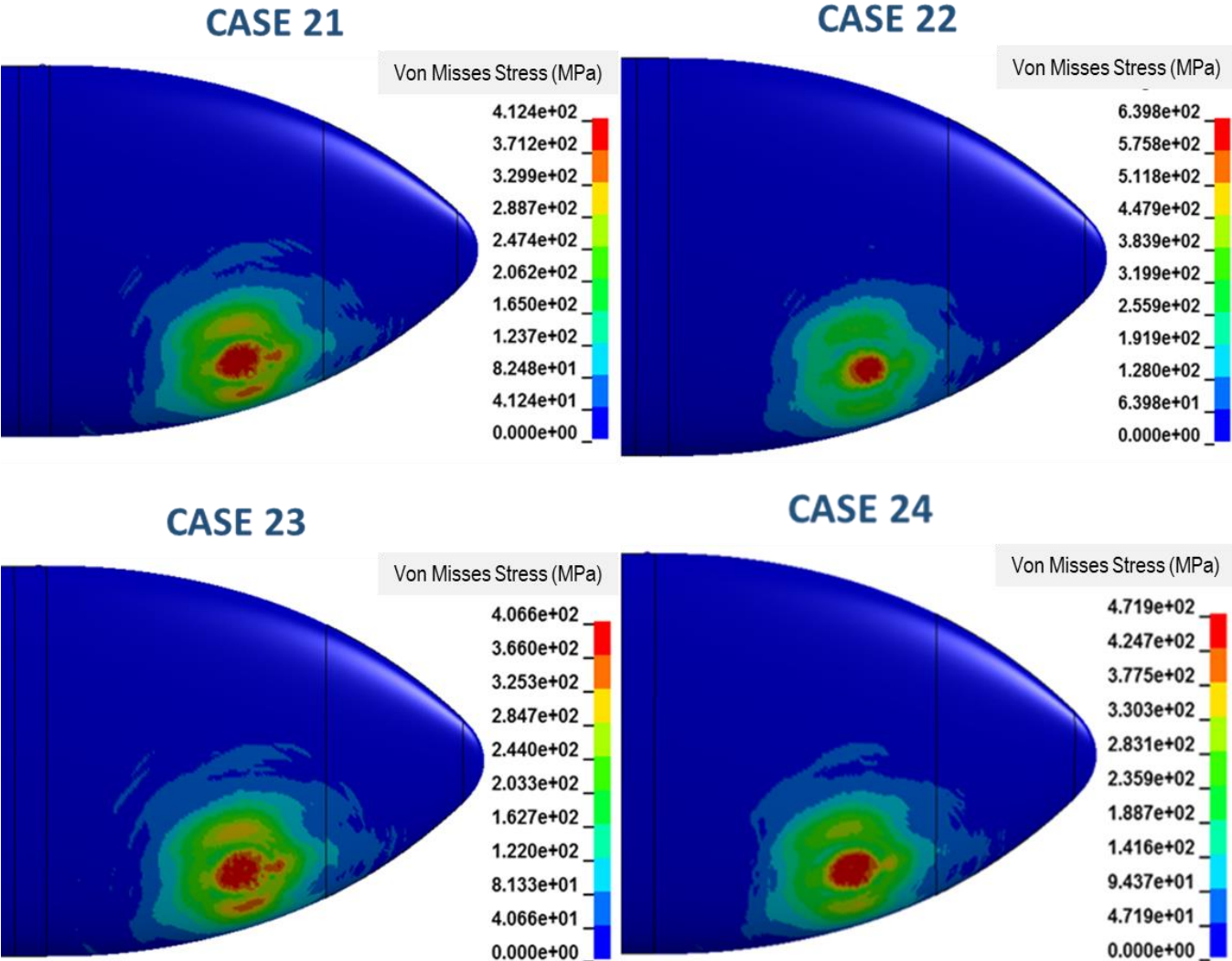


Figure 176 Von Misses Stress Results (MPa) at 0.5 ms for Impactor Position 6

The plastic deformation began at 0.5 ms as shown in Figure 176. There was no tear up or penetration on the skin of EFT. The stress distributions and effective stresses on skin are similar for Piecewise Linear Plasticity material model and Johnson Cook Material model.

Von Misses Stress results at 1.0 ms for impactor position 6 is shown in Figure 177.

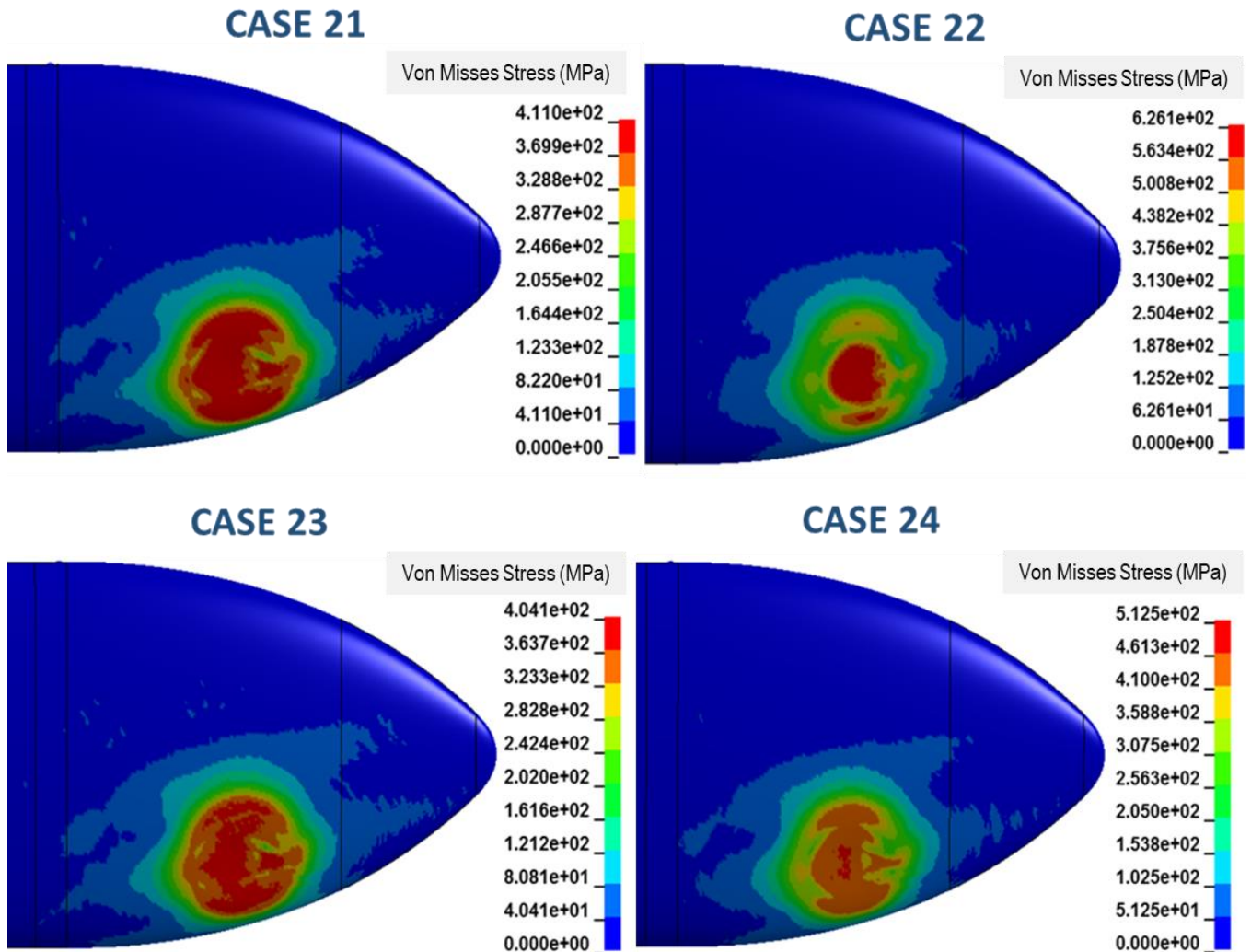


Figure 177 Von Misses Stress Results (MPa) at 1.0 ms for Impactor Position 6

There was no tear up or penetration on the skin of EFT. The stress distributions and effective stresses on skin are similar for Piecewise Linear Plasticity material model and Johnson Cook Material model.

Von Misses Stress results at 1.5 ms for impactor position 6 is shown in Figure 178.

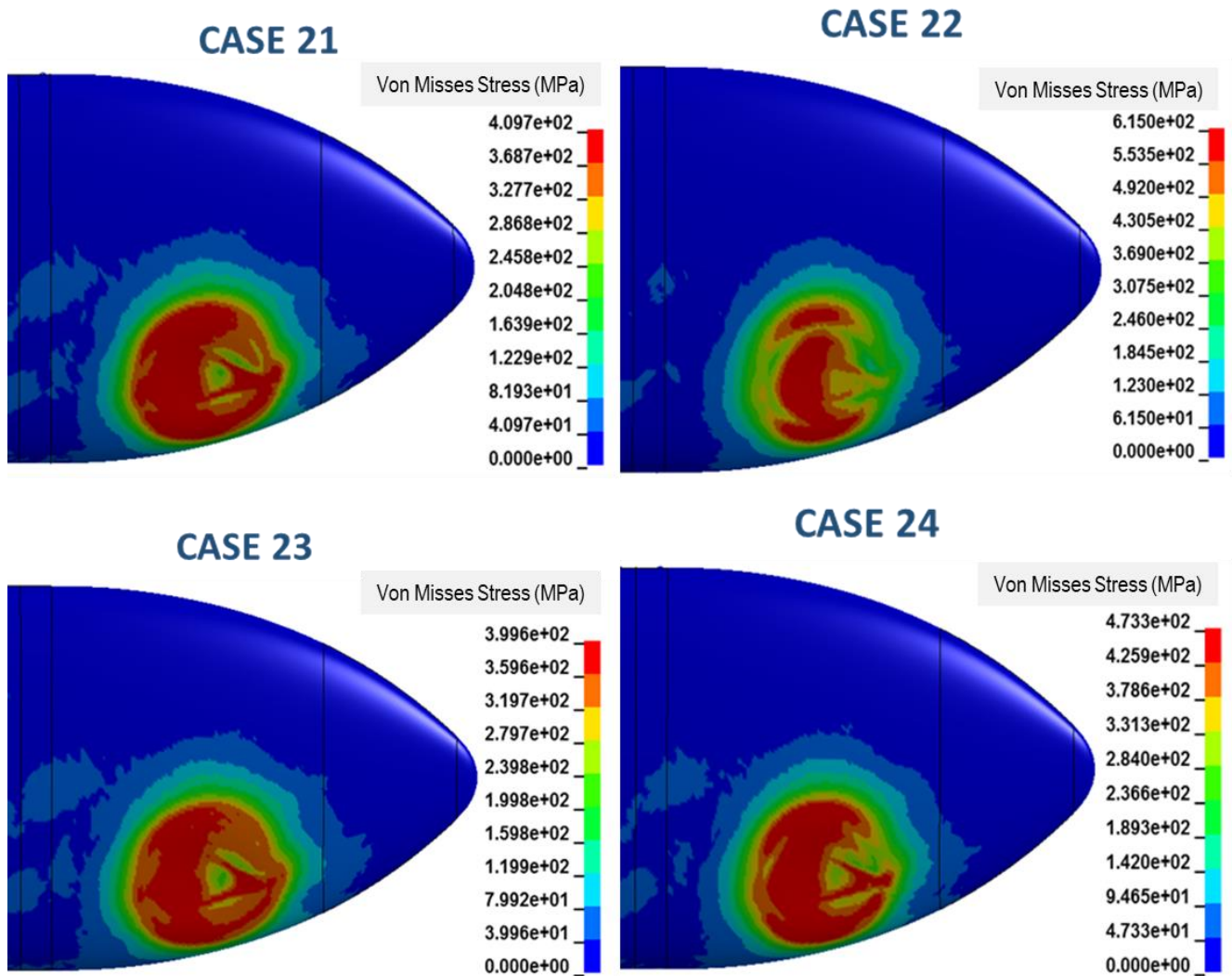


Figure 178 Von Misses Stress Results (MPa) at 1.5 ms for Impactor Position 6

There was no tear up or penetration on the skin of EFT. The stress distributions and effective stresses on skin are similar for Piecewise Linear Plasticity material model and Johnson Cook Material model.

Von Misses Stress results at 2.0 ms for impactor position 6 is shown in Figure 179.

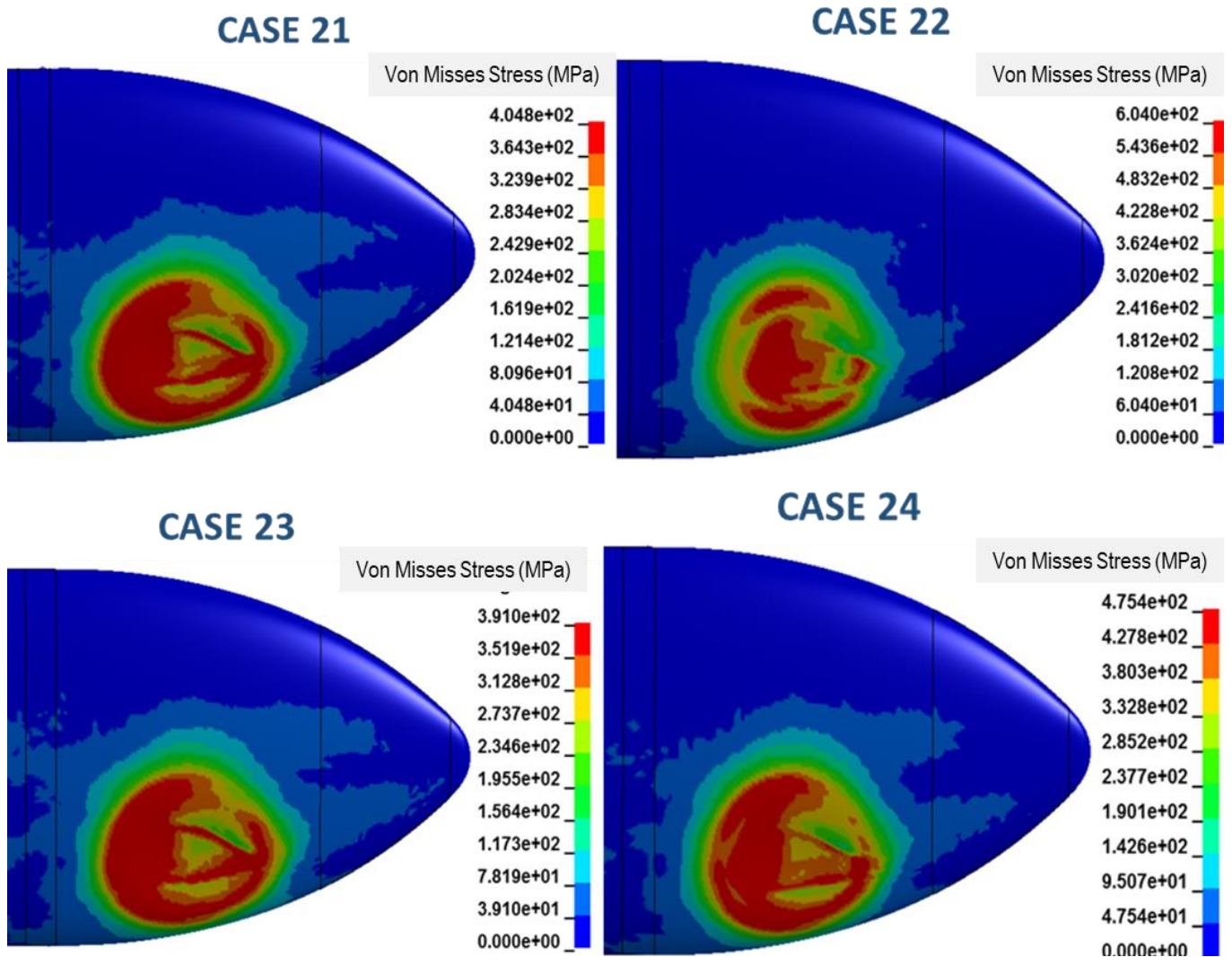


Figure 179 Von Misses Stress Results (MPa) at 2.0 ms for Impactor Position 6

There was no tear up or penetration on the skin of EFT. The stress distributions and effective stresses on skin are similar for Piecewise Linear Plasticity material model and Johnson Cook Material model.

Von Misses Stress results at 2.5 ms for impactor position 6 is shown in Figure 180.

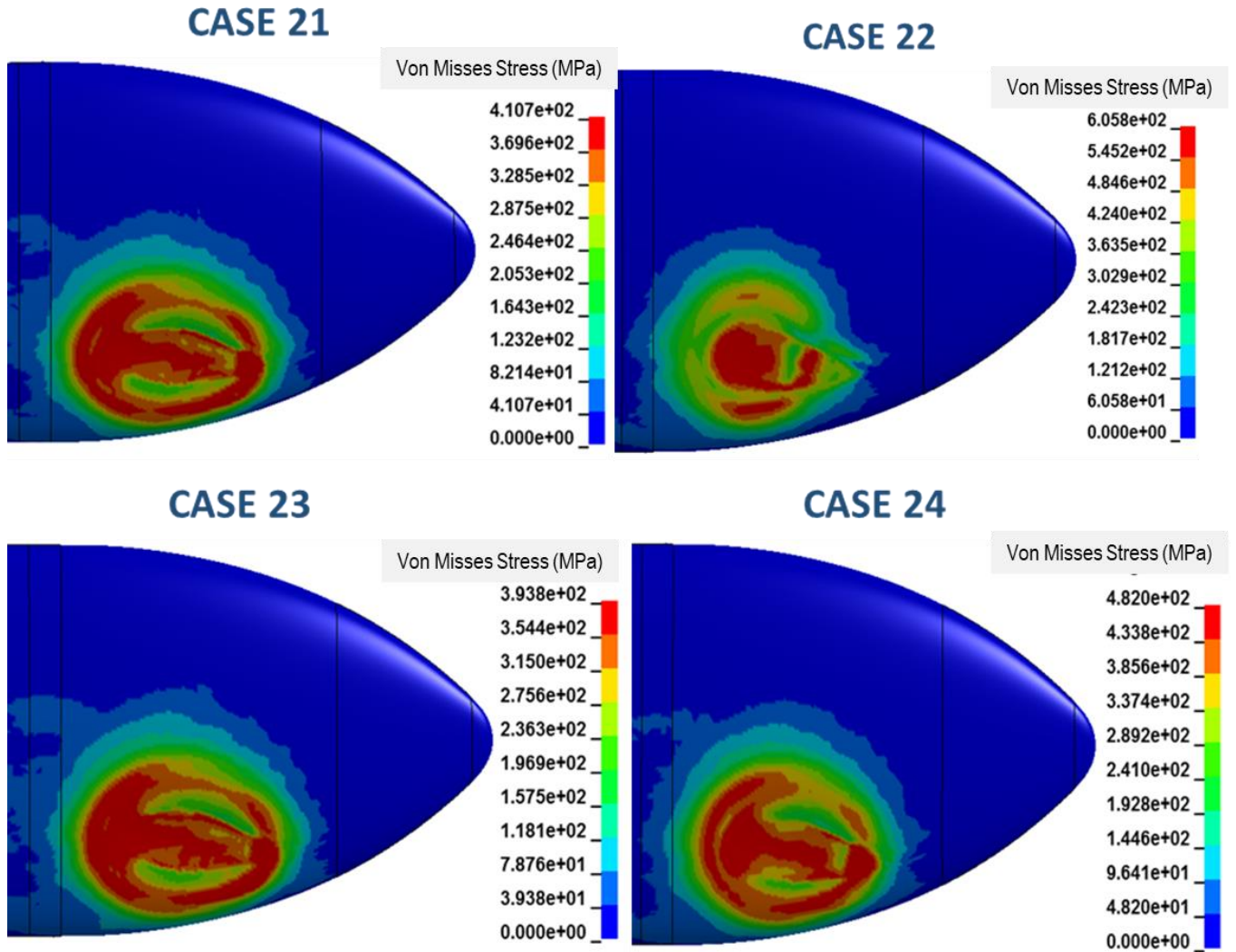


Figure 180 Von Misses Stress Results (MPa) at 2.5 ms for Impactor Position 6

There was no tear up or penetration on the skin of EFT. The stress distributions and effective stresses on skin are similar for Piecewise Linear Plasticity material model and Johnson Cook Material model.

Von Misses Stress results at 3.0 ms for impactor position 6 is shown in Figure 181.

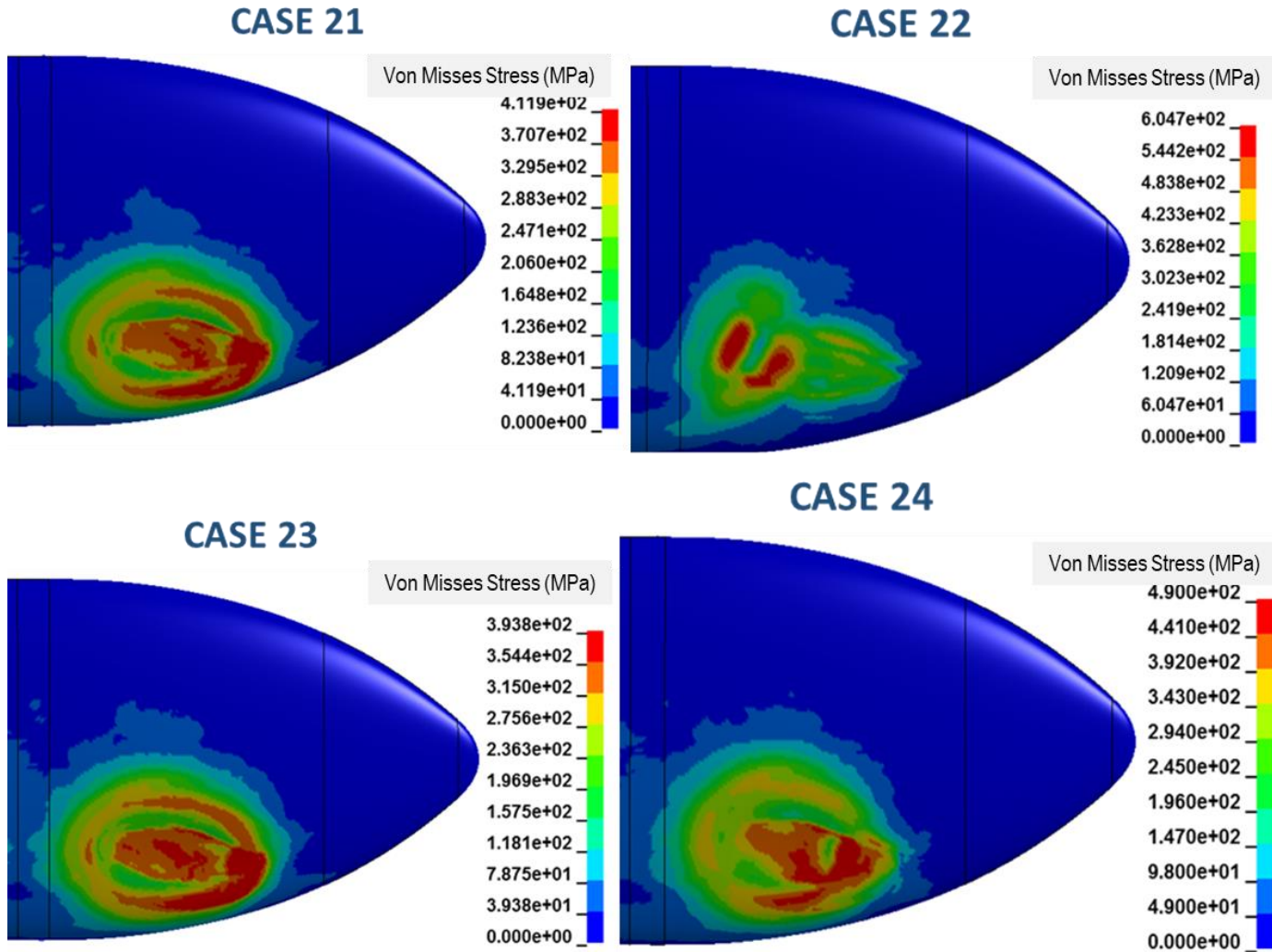


Figure 181 Von Misses Stress Results (MPa) at 3.0 ms for Impactor Position 6

There was no tear up or penetration on the skin of EFT. The stress distributions and effective stresses on skin are similar for Piecewise Linear Plasticity material model and Johnson Cook Material model.

Von Misses Stress results at 3.5 ms for impactor position 6 is shown in Figure 182.

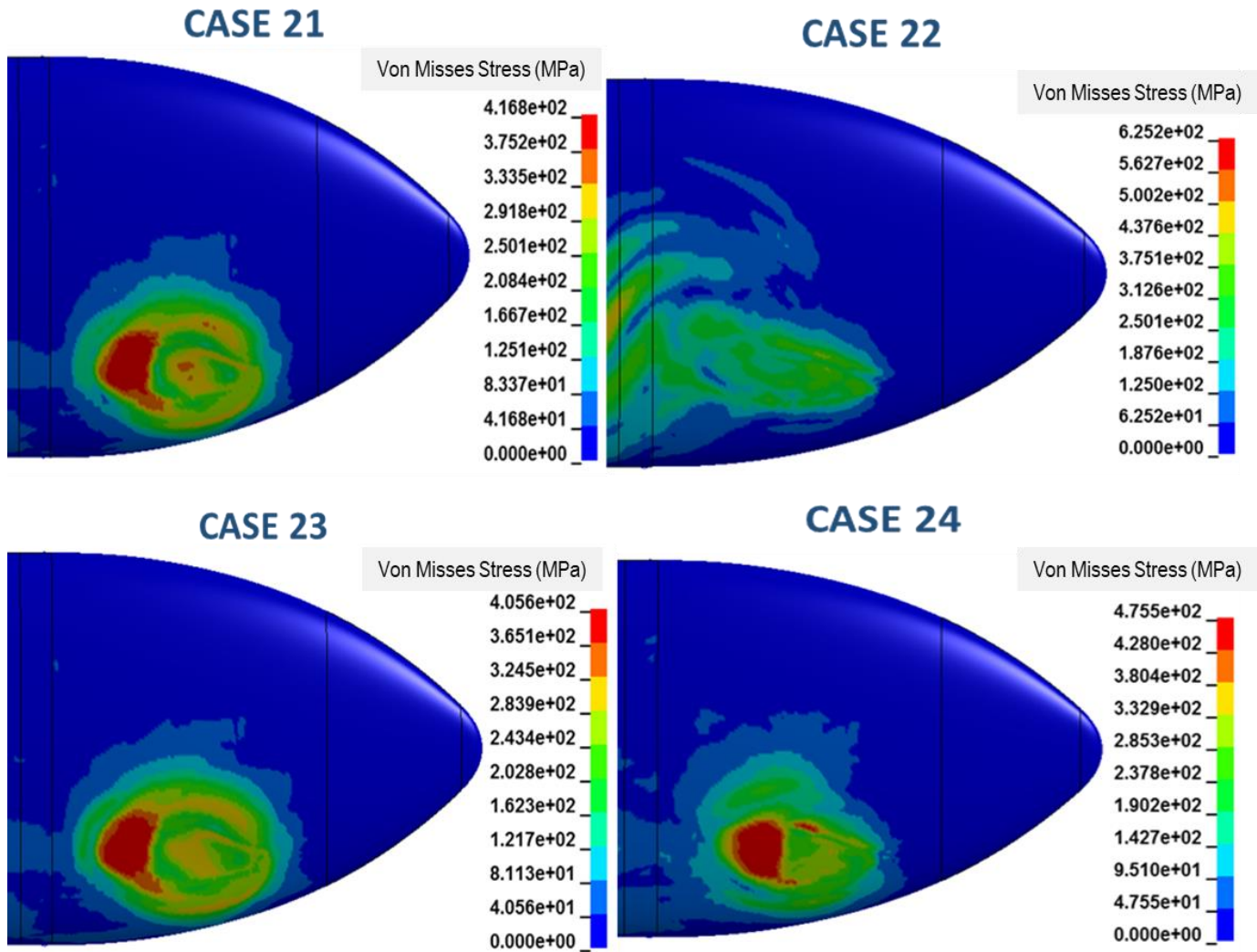


Figure 182 Von Misses Stress Results (MPa) at 3.5 ms for Impactor Position 6

There was no tear up or penetration on the skin of EFT. The stress distributions and effective stresses on skin are similar for Piecewise Linear Plasticity material model and Johnson Cook Material model. Impact ended in 3.3 ms.

Von Misses Stress results at 4.0 ms for impactor position 6 is shown in Figure 183.

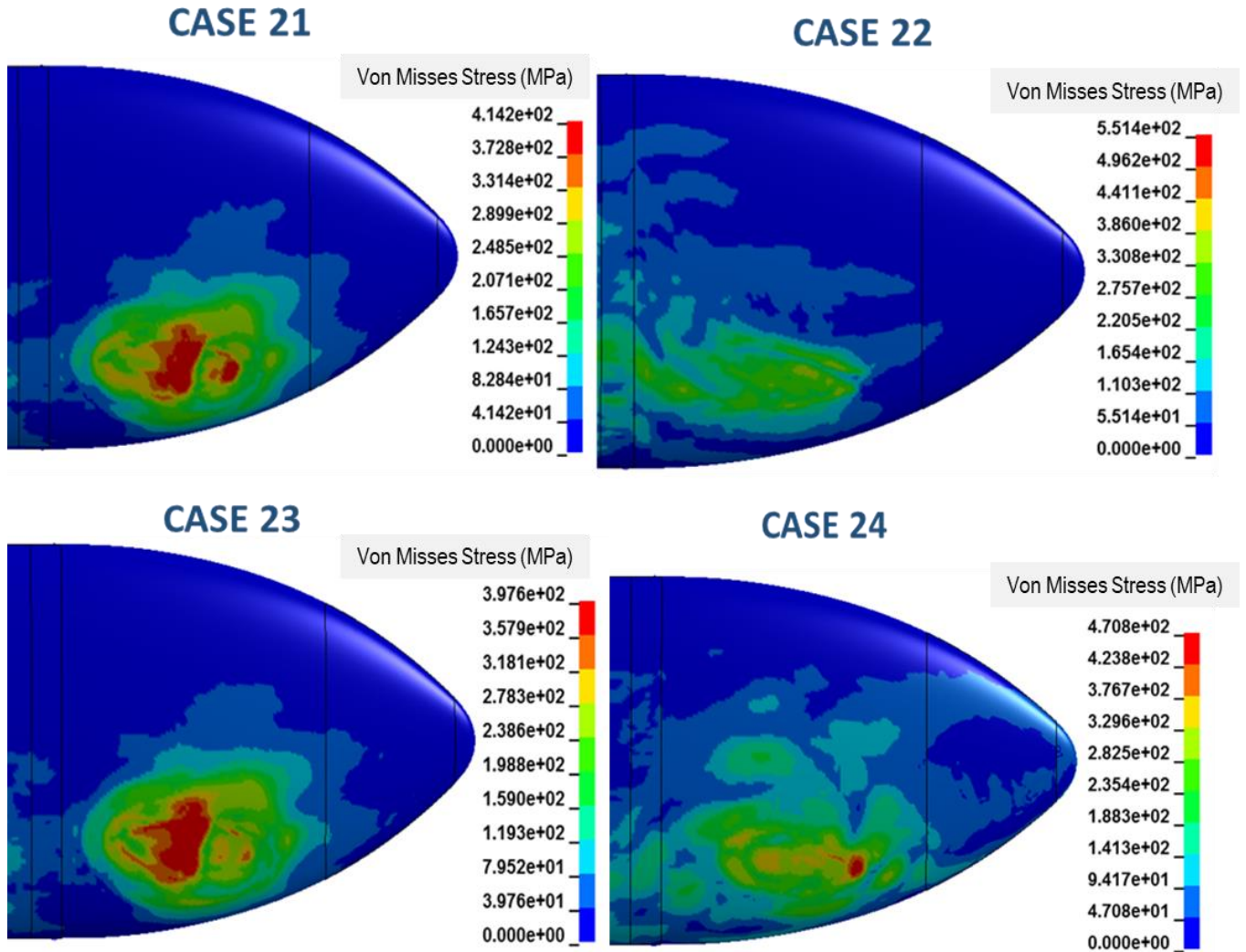


Figure 183 Von Misses Stress Results (MPa) at 4.0 ms for Impactor Position 6

There was no tear up or penetration on the skin of EFT. The stress distributions and effective stresses on skin are similar for Piecewise Linear Plasticity material model and Johnson Cook Material model. Impact ended in 3.3 ms.

Von Misses Stress results at 4.5 ms for impactor position 6 is shown in Figure 184.



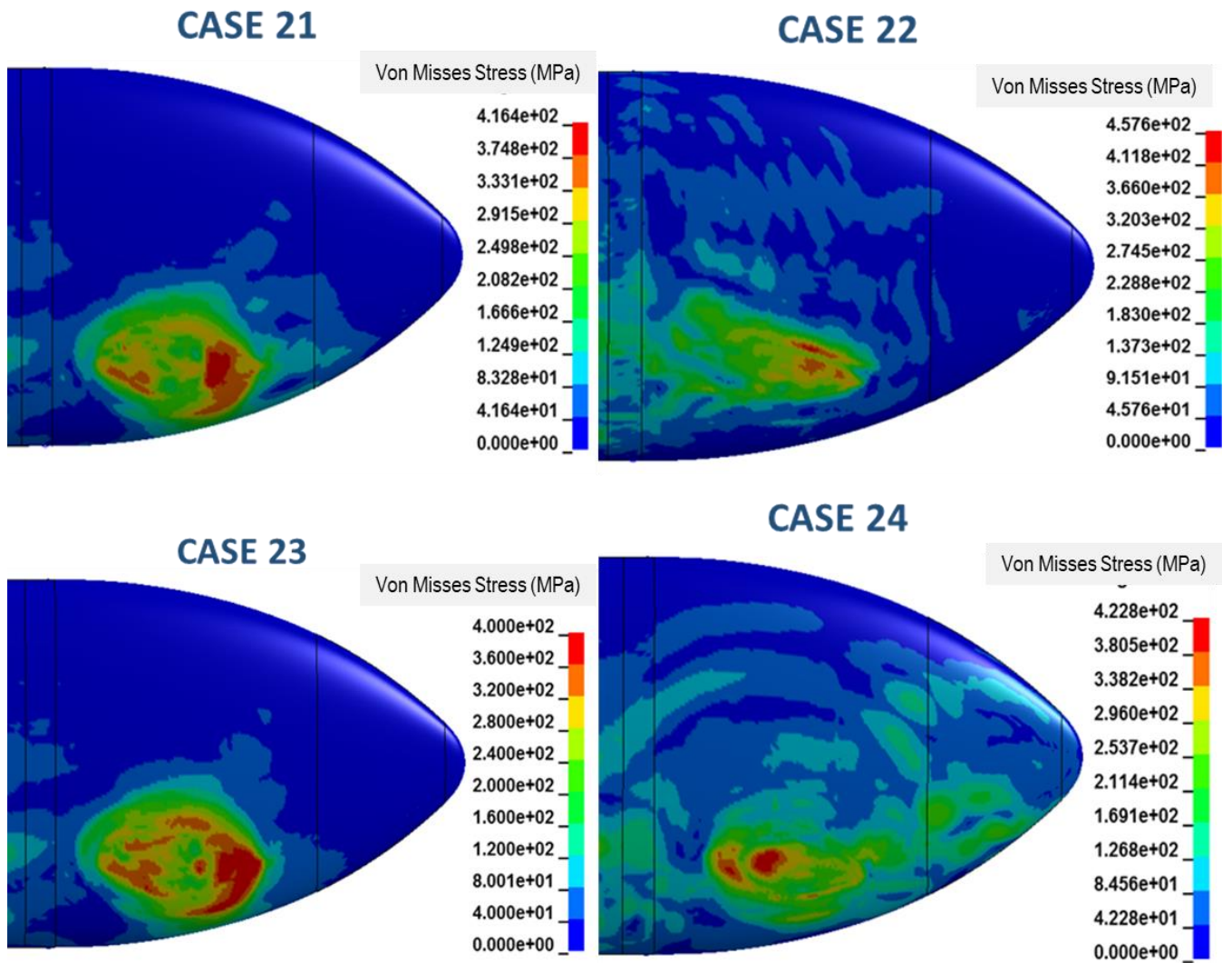


Figure 184 Von Misses Stress Results (MPa) at 4.5 ms for Impactor Position 6

There was no tear up or penetration on the skin of EFT. The stress distributions and effective stresses on skin are similar for Piecewise Linear Plasticity material model and Johnson Cook Material model. Impact ended in 3.3 ms.

Von Misses Stress results at 5.0 ms for impactor position 6 is shown in Figure 185.

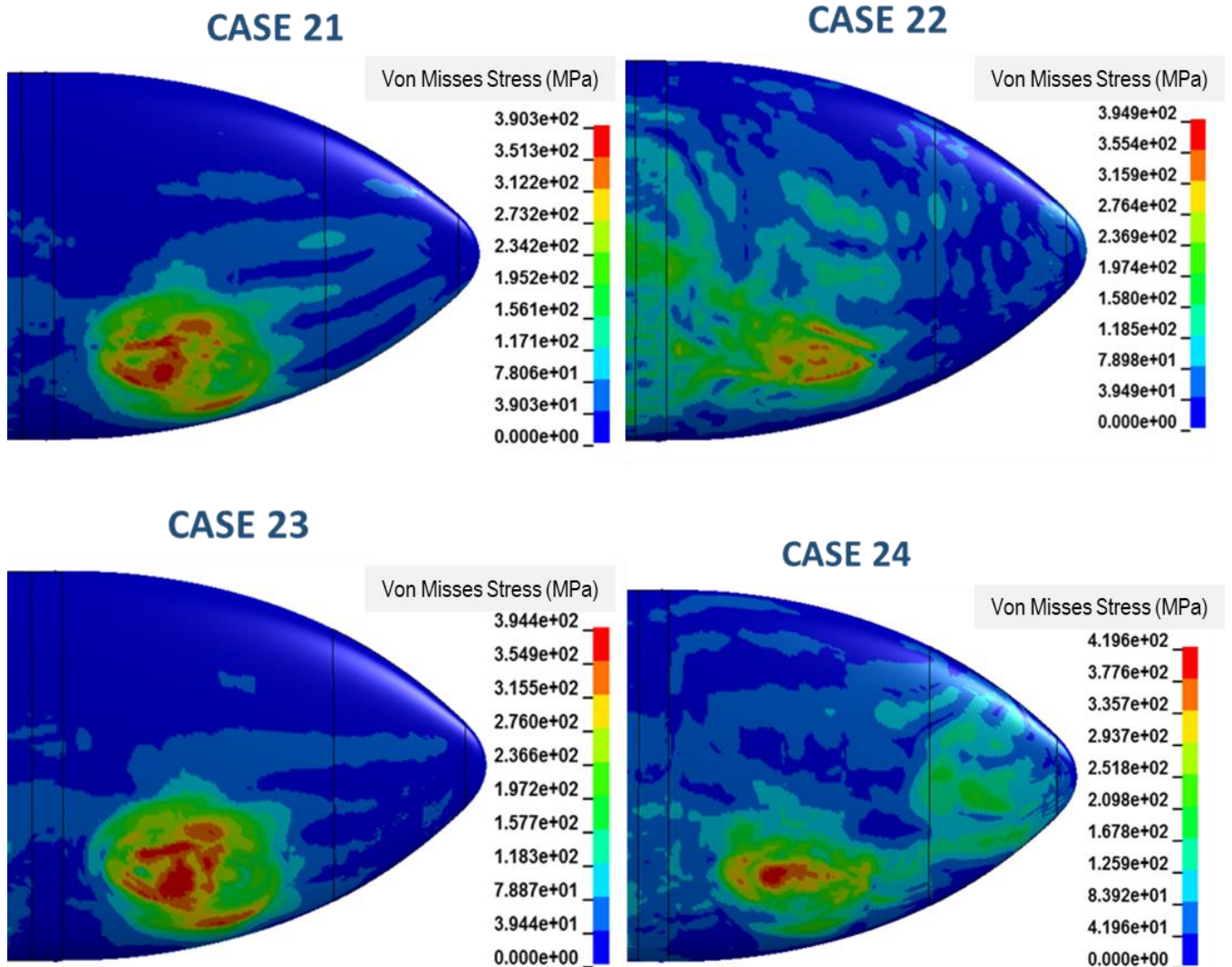


Figure 185 Von Misses Stress Results (MPa) at 5.0 ms for Impactor Position 6

There was no tear up or penetration on the skin of EFT. The stress distributions and effective stresses on skin are similar for Piecewise Linear Plasticity material model and Johnson Cook Material model. Impact ended in 3.3 ms.

The stresses and deformations on EFT skin are shown in Figure 166 to Figure 185. The plastic deformation began at 0.5 ms as shown in Figure 176. There was no tear up or penetration on

the skin of EFT. The stress distributions and effective stresses on skin are similar for Piecewise Linear Plasticity material model and Johnson Cook Material model.

Maximum stress on EFT skin was 417 MPa for Case 21, 640 MPa for Case 22, 407 MPa for Case 23, 513 MPa for Case 24.

Energy variations for Position 6 is given in Figure 186. While kinetic energy decreased, internal energy increased.

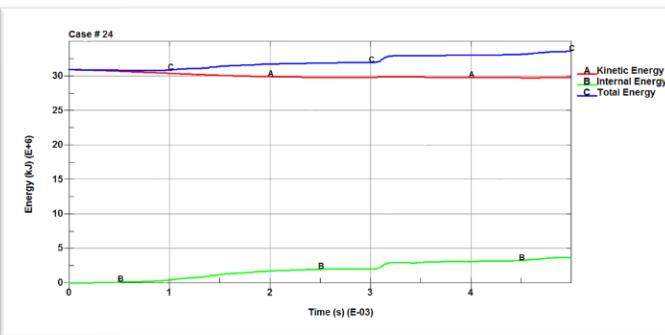
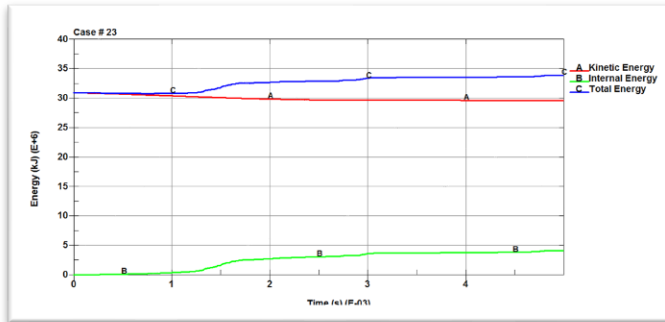
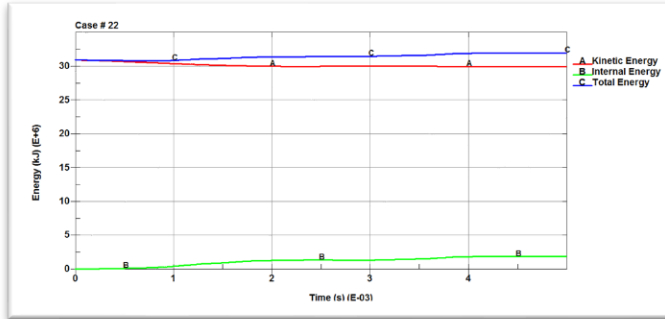
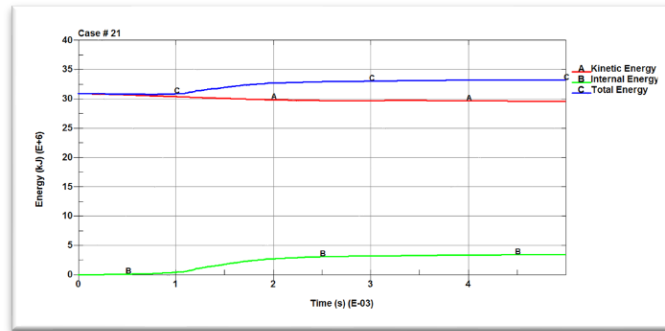


Figure 186 Energy Variation of Position 6

Energy ratios for Position 6 is given in Figure 187. Energy ratios for position 6 remained within the acceptable limits as shown.

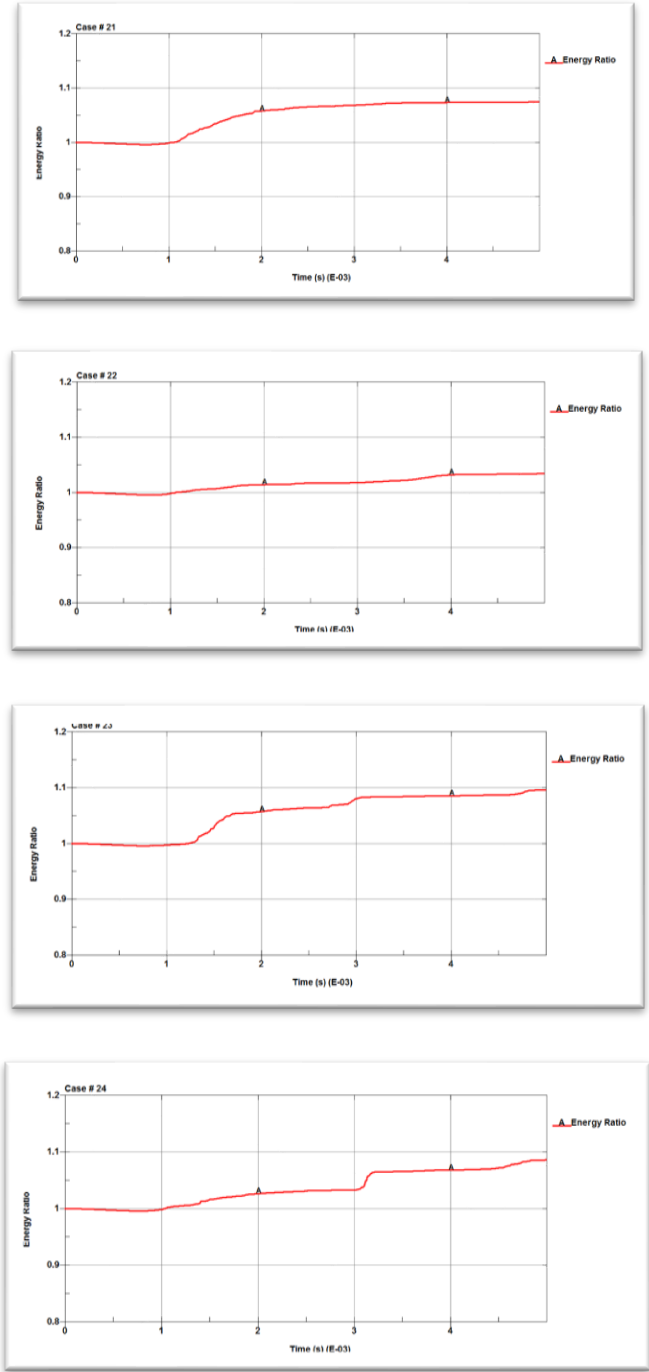


Figure 187 Energy Ratio of Position 6

Hourglass energy, damping energy and sliding energy for case 21 is given in Figure 188. Impact ended in 3.3 ms. Hourglass energy remained almost 0. For sliding energy, peak did not occur.

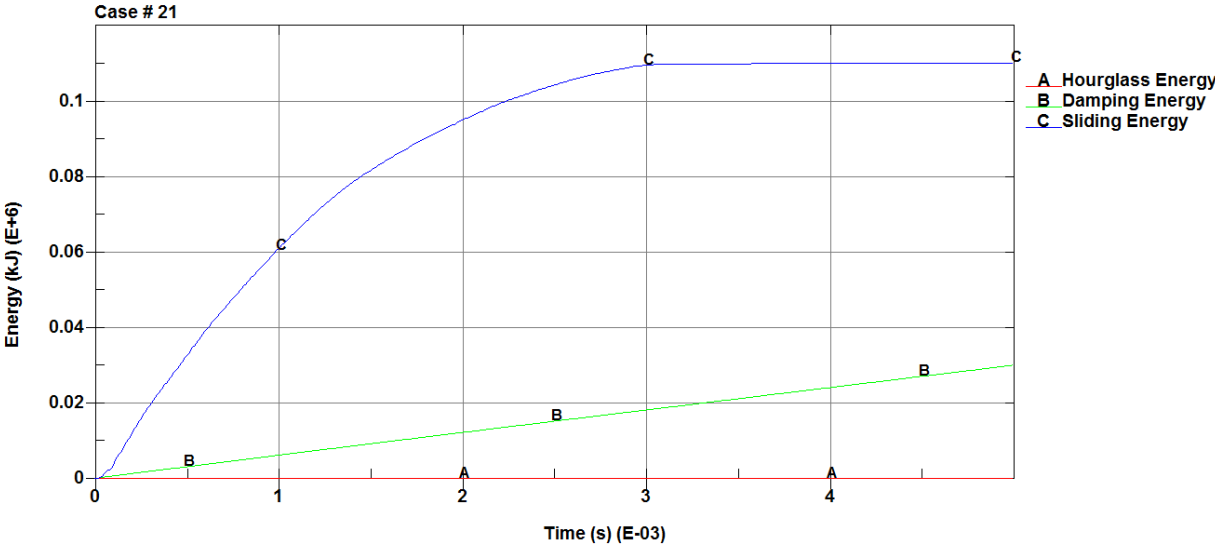


Figure 188 Hourglass, Damping and Sliding Energies Variation of Case 21

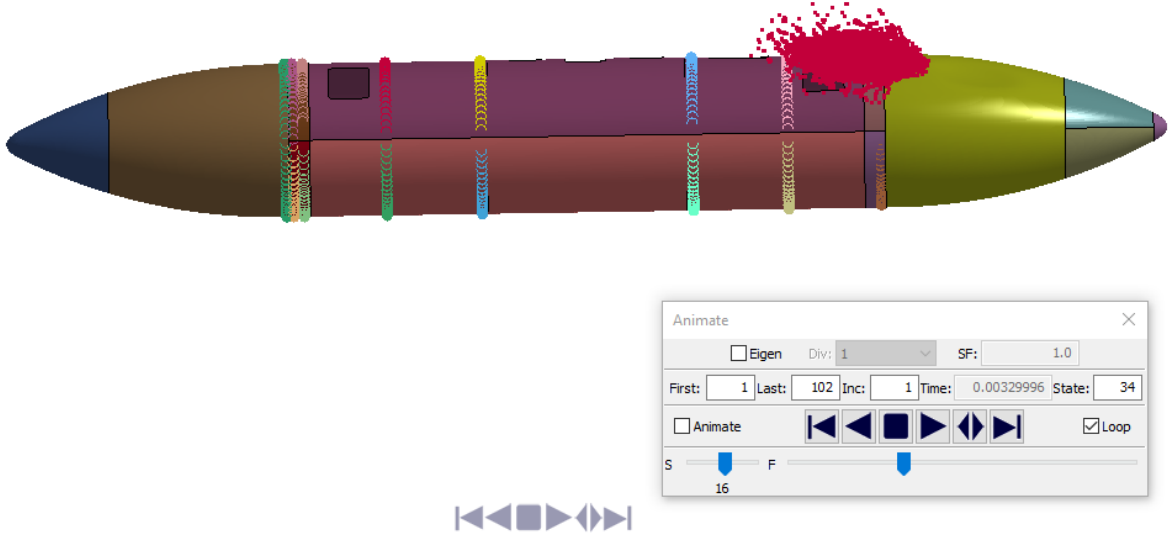


Figure 189 Bird Impact at 4 ms for Case 21

Hourglass energy, damping energy and sliding energy for case 22 is given in Figure 190. Impact ended in 3.0 ms. Hourglass energy remained almost 0. For sliding energy, peak did not occur.

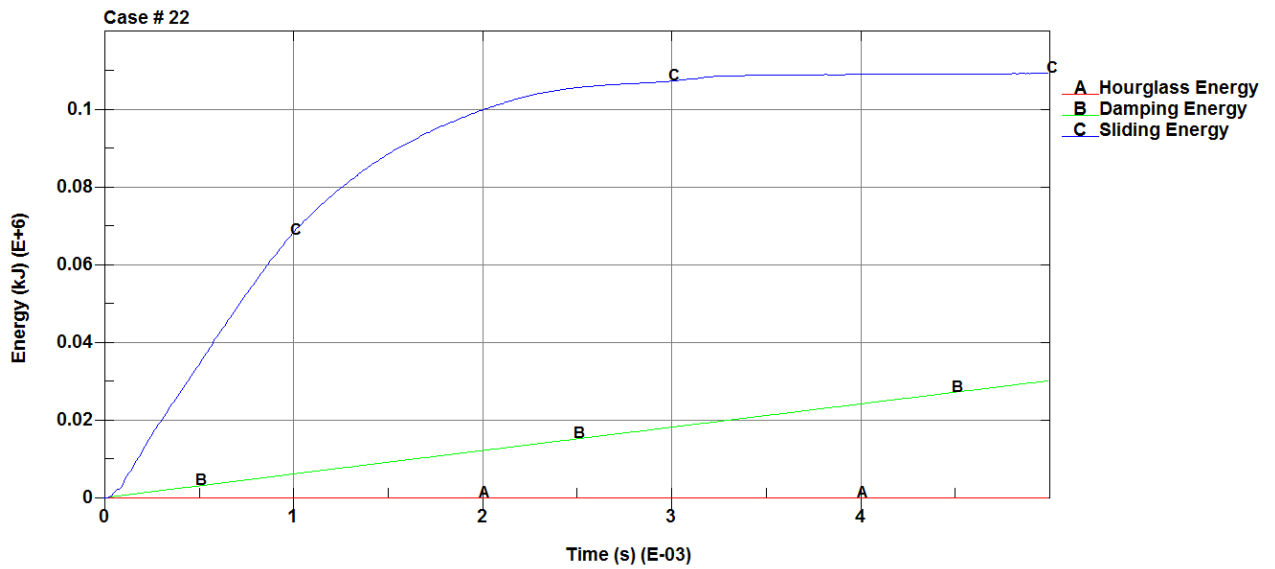


Figure 190 Hourglass, Damping and Sliding Energies Variation of Case 22

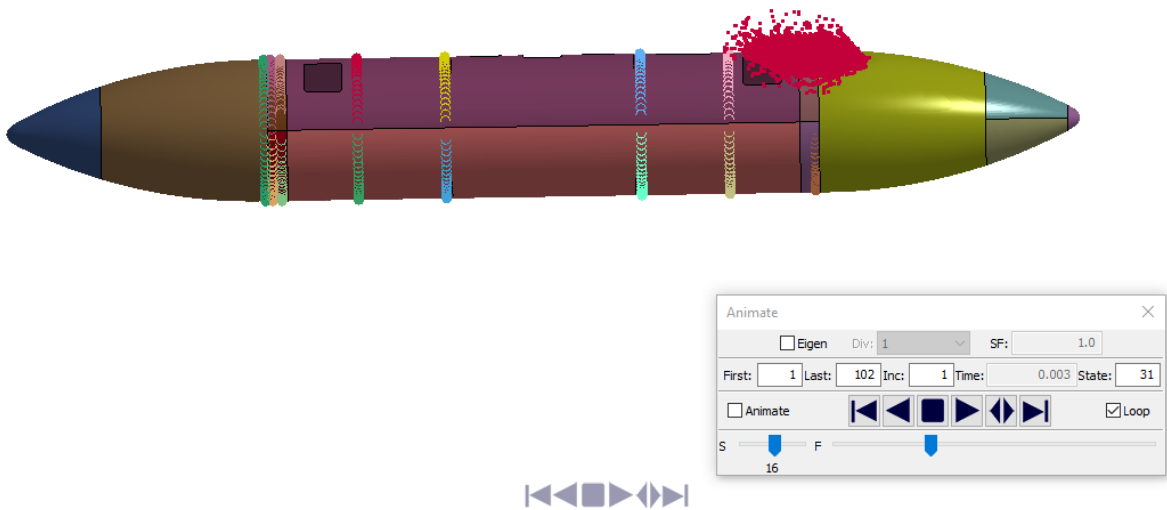


Figure 191 Bird Impact at 4 ms for Case 22

Hourglass energy, damping energy and sliding energy for case 23 is given in Figure 192. Impact ended in 3.3 ms. Hourglass energy remained almost 0. For sliding energy, peak did not occur.

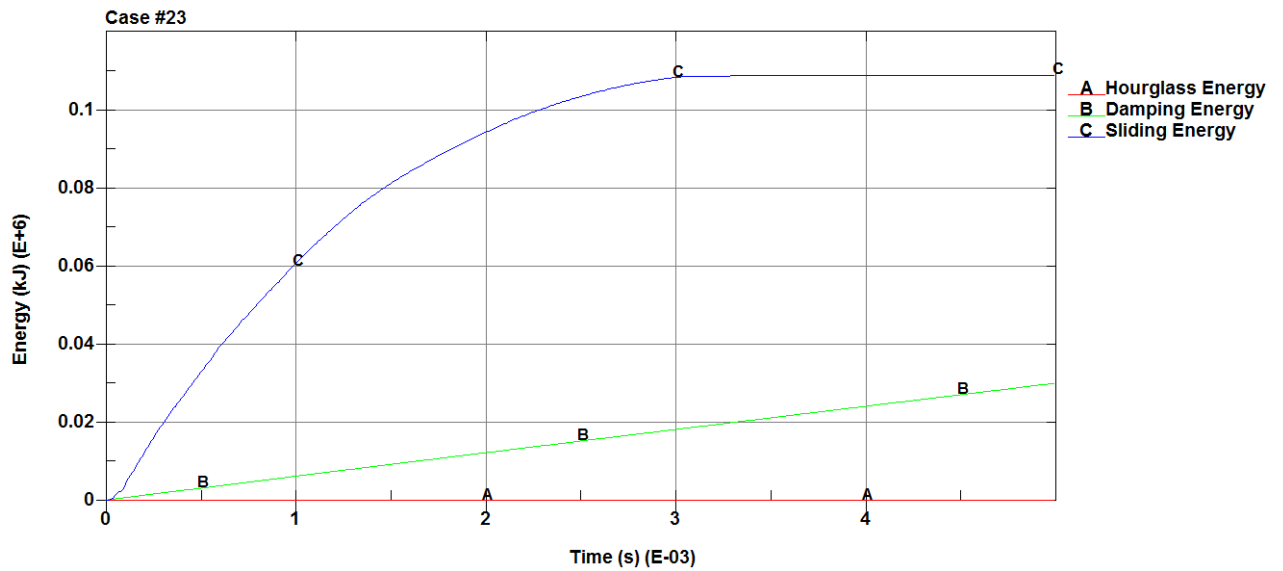


Figure 192 Hourglass, Damping and Sliding Energies Variation of Case 23

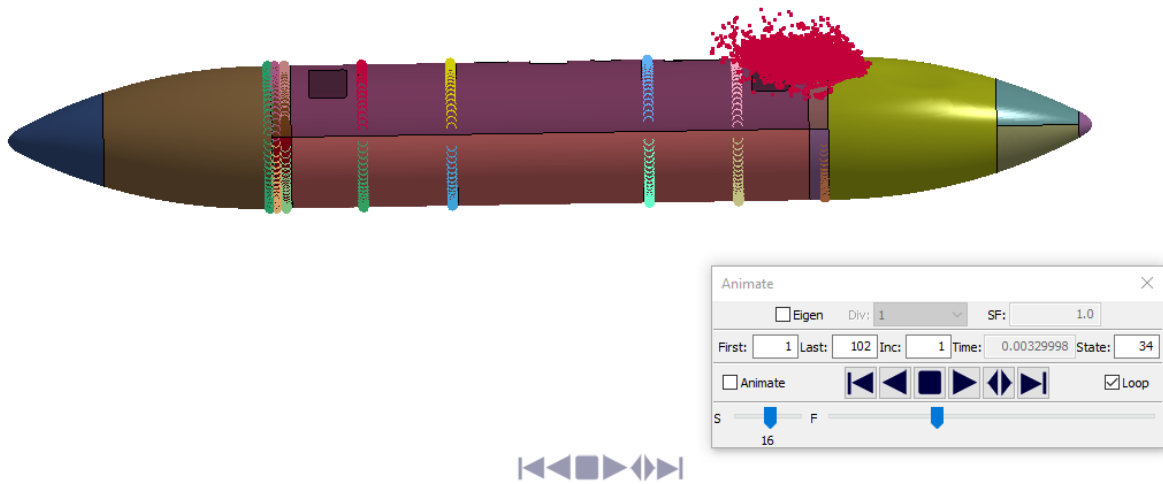


Figure 193 Bird Impact at 4 ms for Case 23

Hourglass energy, damping energy and sliding energy for case 24 is given in Figure 194. Impact ended in 3.3 ms. Hourglass energy remained almost 0. For sliding energy, peak did not occur.



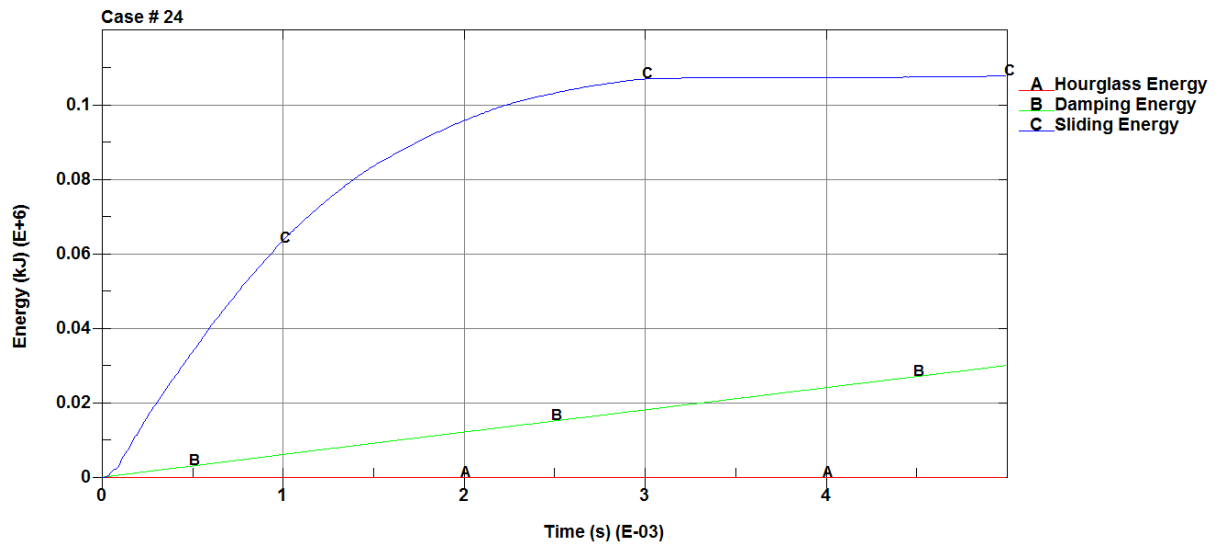


Figure 194 Hourglass, Damping and Sliding Energies Variation of Case 24

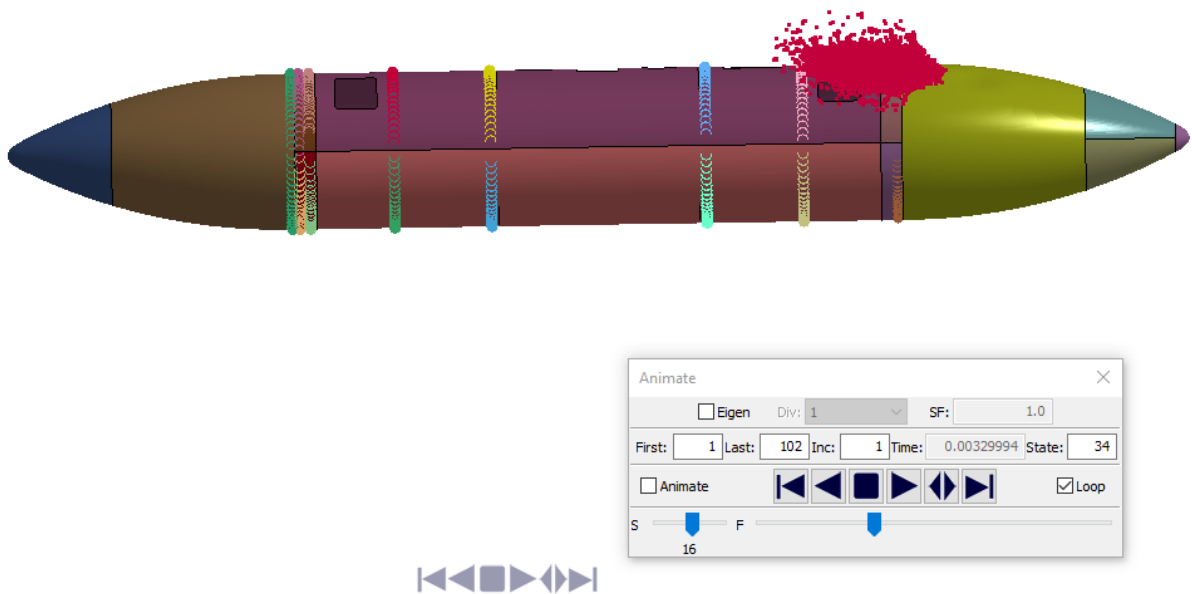


Figure 195 Bird Impact at 4 ms for Case 24

From the analysis results, following conclusions are stated:

Main concern in EFT bird strike impact analysis is to have no penetration on skin and to maintain the structural integrity of the impacted EFT. None of the impact positions resulted in

damage on the skin of EFT, the impact energy absorption of structure is sufficient in general for bird strike requirements.

No tearing of external fuel tank skin was observed for all cases. Maximum resultant displacement for skin for the cases were generally in between 62 mm to 25 mm and most critical position was found as position 2.

For position 6, less damage occurred compared to other positions.

Energy ratios remained within the acceptable limits during impact.

## 8 CONCLUSION

Bird strike issues may cause catastrophic damages for air vehicles during take-off, level flight and landing. [1]

All forward facing components of the aircraft, such as; wing leading edge, empennage leading edge, windshield, canopy, nose radome should be evaluated about bird strike endurance point of view. The methodology is mainly performing the bird strike analysis at the beginning of design; and after production, carrying out bird strike tests [9].

The aim of this study was to perform bird strike analysis on an external fuel tank of a jet trainer aircraft and provide an example study to the literature of our country. In this study, 4lb bird strike on an external fuel tank of a jet trainer aircraft was analyzed. First of all, the EFT model was created using CATIA V5 R28 software. Fuel carrying capacity of the external fuel tank was 1000lb. The geometry was designed with elliptical cross-section in order not to crash with floor during landing.

Hypermesh software was used for post processes of the analysis. The structure was modelled as shell elements consisting of 393862 nodes and 391032 elements. Figure 148 shows finite element model of external fuel tank.

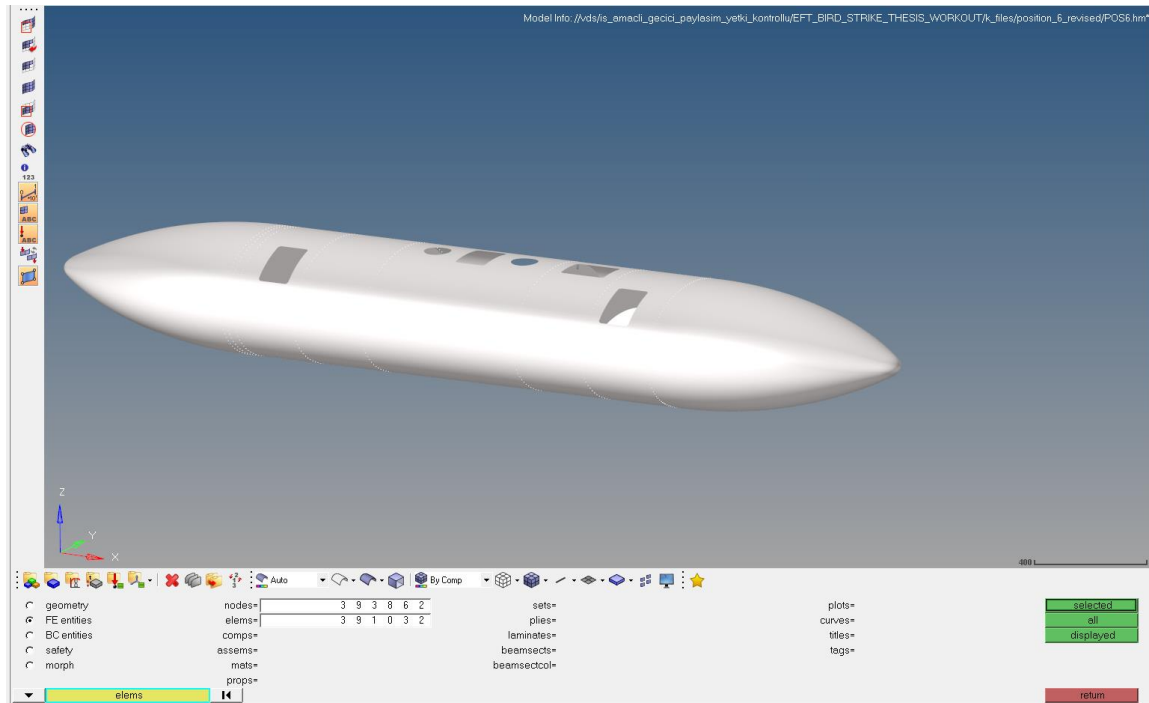


Figure 196 FEM Model of External Fuel Tank

LS Dyna software was used for impact analysis and Smoothed Particle Hydrodynamics method was chosen for impactor model. Analyses were performed using cylindrical with hemispherical ends bird geometry according to speed and mass given in literature. The density of the impactor was  $950\text{kg/m}^3$ .

Twenty-four cases were performed including six impactor positions, two different materials which are Johnson Cook material model (MAT\_15) and Piecewise Linear Plasticity material model (MAT\_24) and two different material models which are Al 2024-T3 and Al 7075-T6.

Leakage on the external fuel tank may cause fire, the loss of aircraft and death of crew. For the survivability of the aircraft, external fuel tank shall resist bird strike without penetration. Therefore, the external fuel tank was decided to be designed as impact resistant without penetration.

An overview of the impact simulation for the positions were evaluated for the general understanding. The time history was presented as a series of time step plots with explanations. Total simulation time was set to 5 ms and plots were saved in the intervals of 0.5ms.

Using numerical analysis, stress and displacement distributions, the maximum stresses and the maximum displacement were calculated. As a result, the robustness of the external fuel tank was verified due to the regulations of aviation authorities.

Energy ratios were checked and verified for 24 cases. Acceptable limits for energy ratio is between 0.9 to 1.1.

## 9 REFERENCES

1. [1] R. Hedayati and M. Sadighi, *Bird strike: an experimental, theoretical and numerical investigation*. Woodhead Publishing, 2015.
2. [2] R. Hedayati and S. Ziaei-Rad, "A new bird model and the effect of bird geometry in impacts from various orientations" *Internal Journal of Vehicle Structures and Systems*, 2011.
3. [3] S. Heimbs, "Computational methods for bird strike simulations: A review," *Computers & Structures*, 2011.
4. [4] M.Souli and L.O.I.DO, "ALE and fluid-structure interaction capabilities in LS-DYNA," 7<sup>th</sup> *International LS-DYNA Users Conference*, 2002.
5. [5] V.K.Goyal, C.A.Huertas, T.R.Leutwiler and J.R.Borrero, "Robust bird-strike modeling based on SPH formulation using LS-DYNA," 47<sup>th</sup> *AIAA/ASME/ASCE/AHS/ASC Structures, Structural Dynamics, and Materials Conference*, 2006.
6. [6] H.Sandberg and O.Rydholm, "Evaluation of material models to predict material failure in LS-DYNA," *Division of Solid Mechanics*, 2006.
7. [7] S.C.McCallum and C.Constantinou, "The influence of bird-shape in bird-strike analysis," *The 5<sup>th</sup> European LS-DYNA Users Conference*, 2005.
8. [8] LS-DYNA Aerospace Working Group, "Modeling guidelines document," *Modeling Guidelines Document Version 18-2*, 2018.
9. [9] H.-G. Kim and S. C. Kim, "A numerical study on the influence of the amount of internal fuel in a bird strike test for the external auxiliary fuel tank of rotorcraft," *International journal of crashworthiness*, 2019.

# 10 APPENDIX

## APPENDIX 1 - Resultant Forces

